

~~CONFIDENTIAL~~

RM A54LO8

NACA RM A54LO8



RESEARCH MEMORANDUM

THE LONGITUDINAL CHARACTERISTICS AT MACH NUMBERS UP TO
0.92 OF SEVERAL WING-FUSELAGE-TAIL COMBINATIONS
HAVING SWEEPBACK WINGS WITH NACA FOUR-DIGIT
THICKNESS DISTRIBUTIONS

By Fred B. Sutton and Jerald K. Dickson

Ames Aeronautical Laboratory
Moffett Field, Calif.

CLASSIFICATION CHANGED

To UNCLASSIFIED

By authority of NACA Rec Also. effective
YRN-123 Date Dec 13, 1957
LANGLEY FIELD, VIRGINIA

AMT 1-20-58

CLASSIFIED DOCUMENT

This material contains information affecting the National Defense of the United States within the meaning of the espionage laws, Title 18, U.S.C., Secs. 793 and 794, the transmission or revelation of which in any manner to an unauthorized person is prohibited by law.

NATIONAL ADVISORY COMMITTEE FOR AERONAUTICS

WASHINGTON

March 24, 1955

~~CONFIDENTIAL~~



NATIONAL ADVISORY COMMITTEE FOR AERONAUTICS

RESEARCH MEMORANDUMTHE LONGITUDINAL CHARACTERISTICS AT MACH NUMBERS UP TO
0.92 OF SEVERAL WING-FUSELAGE-TAIL COMBINATIONS
HAVING SWEEPBACK WINGS WITH NACA FOUR-DIGIT
THICKNESS DISTRIBUTIONS


By Fred B. Sutton and Jerald K. Dickson

SUMMARY

A wind-tunnel investigation has been conducted to determine the effects of various wing-fence arrangements upon the longitudinal characteristics of several wing-fuselage and wing-fuselage-tail combinations having sweptback wings with NACA four-digit thickness distributions. Tests were made with the wing swept back 40° , 45° , and 50° and with a horizontal tail at several tail heights. The tests were conducted through an angle-of-attack range at Mach numbers of 0.165 and 0.25 at a Reynolds number of 8 million, and at Mach numbers varying from 0.25 to 0.92 at a Reynolds number of 2 million.

The addition of multiple fences to the wings with the tail off eliminated large changes in longitudinal stability up to lift coefficients in excess of 1.0 at low speeds, an improvement of as much as 80 percent over the values obtained with the fences off. At high subcritical speeds, the fences eliminated large changes in the stability of the wing-fuselage-tail combinations up to lift coefficients of at least 0.80, an improvement of as much as 60 percent over the lift coefficients for instability without fences. The fences had little effect on the tail contribution to the stability. The fences increased the drag of the wing-fuselage combinations moderately at low lift coefficients, but reduced the drag and increased the lift-drag ratios at the higher lift coefficients. The Mach numbers for drag divergence were increased slightly by the fences; however, the corresponding drag coefficients were higher than those at the divergence Mach numbers without fences.

The effectiveness of the all-movable stabilizer as a longitudinal control was little affected by Mach number. Raising the horizontal tail above the fuselage center line as much as 20 percent of the wing semispan had little effect on the tail contribution to stability, but did increase its effectiveness as a longitudinal control at low values of lift.



INTRODUCTION

The aerodynamic characteristics of wings suitable for long-range airplanes designed to fly at relatively high subsonic speeds have been the subject of an investigation in the Ames 12-foot pressure wind tunnel. A series of twisted and cambered wings of relatively high aspect ratio were tested with several angles of sweepback and the results are presented in reference 1. All these wings experienced a severe decrement in longitudinal stability at moderate lift coefficients due to the onset of stalling over the outer portions of the span. The results in reference 2 indicate that the stability characteristics of such wings could be improved by the use of chordwise fences. Therefore, the present phase of the investigation was directed toward the development of wing fences which would delay stalling to higher lift coefficients and would possibly eliminate the instability which usually accompanied the stall. The wings of reference 1, with NACA four-digit sections perpendicular to the quarter-chord line, were tested with sweepback angles of 40° , 45° , and 50° in combination with a fuselage and various fence configurations. The fences were systematically varied in spanwise position, number, and chordwise extent to establish for the various wing-fuselage combinations the fence configuration which afforded the greatest improvement in stability.

The wing-fuselage combinations with and without their most satisfactory fences were then tested with a horizontal tail to determine the effects of the wing fences on the tail contribution to stability. The angle of incidence and the height of the horizontal tail, which was all-movable, were varied for the combination employing wing fences and the 40° sweptback wing to evaluate the longitudinal characteristics of the configuration and the control effectiveness of the horizontal tail at each height. The effects of varying tail height on the stability of the configurations using wing fences and wings with 45° and 50° of sweepback were also determined.

The tests to determine the most satisfactory fence configurations were conducted primarily at a Mach number of 0.417 and a Reynolds number of approximately 4 million. The longitudinal characteristics of the various combinations with the best fences were then measured at Mach numbers of 0.165 and 0.25 at a Reynolds number of 8 million and at Mach numbers from 0.25 to 0.92 at a Reynolds number of 2 million. The lift and pitching moment of the isolated horizontal tail were also measured over most of these Mach and Reynolds number ranges.

NOTATION

A	aspect ratio, $\frac{b^2}{2S}$
a	mean-line designation, fraction of chord over which design load is uniform
a_t	lift-curve slope of the isolated horizontal tail, per deg
a_{w+f}	lift-curve slope of the wing-fuselage combinations, per deg
a_{w+f+t}	lift-curve slope of the wing-fuselage-tail combinations, per deg
$\frac{b}{2}$	wing semispan perpendicular to the plane of symmetry
C_D	drag coefficient, $\frac{\text{drag}}{qS}$
C_L	lift coefficient, $\frac{\text{lift}}{qS}$
C_{L_i}	inflection lift coefficient, lowest positive lift coefficient at which $\frac{dC_m}{dC_L} = 0.10$
C_m	pitching-moment coefficient about the quarter point of the wing mean aerodynamic chord, $\frac{\text{pitching moment}}{qS\bar{c}}$
c	local wing chord parallel to the plane of symmetry
c_r	wing root chord
c_t	wing tip chord
c'	local wing chord perpendicular to the wing sweep axis

\bar{c}	mean aerodynamic chord, $\frac{\int_0^{b/2} c^2 dy}{\int_0^{b/2} c dy}$
c_{l_1}	section design lift coefficient
i_t	incidence of the horizontal tail with respect to the root chord of the wing with 40° of sweepback
$\frac{L}{D}$	lift-drag ratio
l_t	tail length, longitudinal distance between the quarter points of the mean aerodynamic chords of the wing and the horizontal tail
M	free-stream Mach number
q	free-stream dynamic pressure
R	Reynolds number based on the mean aerodynamic chord
S	area of semispan wing
S_t	area of semispan horizontal tail
t	maximum thickness of section
\bar{V}_t	horizontal-tail volume, $\frac{S_t l_t}{S \bar{c}}$
x	distance from the intersection of the leading edges of the wings and the plane of symmetry to the moment center, measured parallel to fuselage center line
y	lateral distance from the plane of symmetry
z	wing height from the quarter point of the mean aerodynamic chord to the fuselage center line, measured in a plane parallel to the plane of symmetry

α	angle of attack, measured with respect to a reference plane through the leading edge and the root chord of the wing with 40° of sweepback
α_t	angle of attack of the isolated horizontal tail
ϵ	effective average downwash angle
ϕ	angle of twist, the angle between the local wing chord and the reference plane through the leading edge and the root chord of the wing with 40° of sweepback (positive for washin and measured in planes parallel to the plane of symmetry)
η	fraction of semispan, $\frac{y}{b/2}$
$\eta_t \left(\frac{q_t}{q} \right)$	tail efficiency factor (ratio of the lift-curve slope of the horizontal tail when mounted on the fuselage in the flow field of the wing to the lift-curve slope of the isolated horizontal tail)
Λ	angle of sweepback of the line through the quarter-chord points of the reference sections
λ	taper ratio

Subscripts

div	divergence
f	fuselage
r	wing root
t	horizontal tail
w	wing

MODEL

The wing-fuselage and wing-fuselage-tail combinations investigated (fig. 1(a)) employed the twisted and cambered wing of reference 1 which

had NACA four-digit thickness distributions. These distributions of thickness were combined with an $a = 0.8$ modified mean line having an ideal lift coefficient of 0.4 to form the sections perpendicular to the quarter-chord line of the unswept wing panel. The thickness-chord ratios of these sections varied from 14 percent at the root to 11 percent at the tip.

The wing was constructed of solid steel and the surfaces were polished smooth. The angle of sweepback of the wing could be adjusted to 40° , 45° , and 50° without changing the longitudinal position of the quarter point of the mean aerodynamic chords, thus maintaining constant tail length. At 40° of sweepback, the wing had an aspect ratio of 7.0; at 45° and 50° of sweepback, the aspect ratio decreased to approximately 6 and 5, respectively. Twist was introduced by rotating the streamwise sections of the wing at 40° of sweepback about the leading edge while maintaining the projected plan form. The variations of twist and thickness ratio along the semispan are shown in figure 1(b) for angles of sweepback of 40° , 45° , and 50° . A more complete description of the wing is given in reference 1. The wing-fuselage combinations using the wing at the various angles of sweepback are regarded as three individual configurations and are referred to herein as the 40° combination, the 45° combination, and the 50° combination.

The fuselage employed for these tests consisted of a cylindrical mid-section with simple fairings fore and aft. Coordinates of the fuselage are listed in table I. The fuselage had a fineness ratio of 12.6 and was located with respect to the wing so that the upper surface of the wing was nearly tangent to the top of the fuselage at the plane of symmetry. (See fig. 2.) The angle of incidence of the wing root with respect to the fuselage center line was approximately 3° . The fuselage was constructed of aluminum bolted to a heavy steel structural member.

The model was tested with several combinations of streamwise boundary-layer fences on the upper surface of the wing at each angle of sweepback. The fences were varied in spanwise position, number, and chordwise extent. The forward portions of the fences which extended from the lower surface around the leading edge of the wing to 0.10 chord and the rear portion of the fences which extended from 0.75 chord to the trailing edge of the wing could be removed to effect the change in the chordwise extent of the fences. Details of the fences and their locations on the wings are shown in figure 2.

The all-movable horizontal tail had an aspect ratio of 3.0, a taper ratio of 0.5, and 40° of sweepback. The reference sweep line was the line joining the quarter-chord points of the sections which were inclined 40° to the plane of symmetry. The horizontal tail had no dihedral and its incidence axis (53.4 percent of the tail root chord) was not swept. This hinge axis was either at the intersection of the fuselage center line and the plane of the wing root chord and leading edge or above this intersection

as shown in figure 1(a). Tail volume varied from 0.497 for the configuration with 40° of sweepback to 0.436 for the configuration with 50° of sweepback. The tail was constructed of solid steel and the surfaces were polished smooth.

A photograph of the model mounted in the wind tunnel is shown in figure 3. The turntable upon which the model was mounted was directly connected to the balance system. Figure 3 also shows the manner in which roughness was applied on the upper surface of the wing at 0.10 chord with a band of 60 grit carborundum particles.

CORRECTIONS TO DATA

The data have been corrected for constriction effects due to the presence of the tunnel walls, for tunnel-wall interference originating from lift on the model, and for drag tares caused by aerodynamic forces on the turntable upon which the model was mounted. The constriction and tunnel-wall interference corrections to the data for the tests of the isolated horizontal tail were calculated and found to be negligible.

The dynamic pressures were corrected for constriction effects due to the presence of the tunnel walls by the method of reference 3. These corrections and the corresponding corrected Mach numbers are listed in the following table:

Corrected Mach number	Uncorrected Mach number	$\frac{q_{\text{corrected}}}{q_{\text{uncorrected}}}$
0.165	0.165	1.002
.25	.25	1.003
.60	.59	1.006
.70	.696	1.007
.80	.793	1.010
.83	.821	1.012
.86	.848	1.015
.88	.866	1.017
.90	.883	1.020
.92	.899	1.024

Corrections for the effects of tunnel-wall interference originating from the lift on the model were calculated by the method of reference 4. The corrections to the angle of attack and to the drag coefficient showed insignificant variations with Mach number and wing sweepback. The corrections added to the data were as follows:

~~CONFIDENTIAL~~

$$\Delta\alpha = 0.455 C_L$$

$$\Delta C_D = 0.00662 C_L^2$$

The correction to the pitching-moment coefficient was relatively unaffected by changes in the angle of wing sweepback; however, this correction had significant variations with Mach number. The following corrections were added to the pitching-moment coefficients:

$$\Delta C_m(\text{tail off}) = K_1 C_{L_{\text{tail off}}}$$

$$\Delta C_m(\text{tail on}) = K_1 C_{L_{\text{tail off}}} - \left[\left(K_2 C_{L_{\text{tail off}}} - \Delta\alpha \right) \frac{\partial C_m}{\partial i_t} \right]$$

The values of K_1 and K_2 for each Mach number were calculated by the method of reference 4 and are given in the following table:

M	K_1	K_2
0.165	0.0025	0.72
.25	.0027	.72
.60	.0038	.74
.70	.0043	.76
.80	.0049	.79
.83	.0050	.80
.86	.0053	.83
.88	.0054	.84
.90	.0056	.86
.92	.0057	.88

Since the turntable upon which the model was mounted was directly connected to the balance system, a tare correction to drag was necessary. This correction was determined by measuring the drag force on the turntable with the model removed from the wind tunnel.

TESTS

The wing-fuselage and wing-fuselage-tail combinations were investigated with the wing swept back 40° , 45° , and 50° . Tests were conducted at a Mach number of 0.417 and a Reynolds number of approximately 4 million of the wing-fuselage combinations without fences and with various fence arrangements to determine the most satisfactory fence configuration for each wing-fuselage combination. The longitudinal characteristics of the wing-fuselage and wing-fuselage-horizontal-tail combinations were then

~~CONFIDENTIAL~~

measured with the best fences at Mach numbers of 0.165 and 0.25 at a Reynolds number of 8 million and at Mach numbers from 0.25 to 0.92 at a Reynolds number of 2 million. The angle of incidence and the height of the all-movable horizontal tail were varied for the 40° combination. Tests were also conducted with various tail heights on the 45° and 50° wing-fuselage combinations. A limited number of tests were made with the wing fences removed from the wing-fuselage-tail combinations and the lift and pitching-moment characteristics of the isolated horizontal tail were also determined.

RESULTS

Results of tests to determine the most satisfactory fence configuration for each of the wing-fuselage combinations are presented in figures 4 through 16. Figures 17 through 21 show the results of tests of each wing-fuselage combination with its most satisfactory fences. Summary plots showing the effects of Mach number on the inflection lift coefficients C_{L_i} , the slopes of the lift and pitching-moment curves, and the drag coefficients of the wing-fuselage combinations with and without fences are presented in figures 22, 23, and 24, respectively. Figures 25 through 27 compare the effects of Reynolds number on the wing-fuselage combinations with and without fences. The effects of applying surface roughness on the wings are shown in figures 28, 29, and 30.

The effects of the most satisfactory wing fences on the longitudinal characteristics of the various combinations with a horizontal tail are shown in figures 31 to 34. Figures 35 to 37 show the effects of Mach number on the inflection lift coefficients, the slopes of the lift and pitching-moment curves, and the drag coefficients of the wing-fuselage-tail combinations with and without fences. The longitudinal characteristics of the 40° combination with its best fences and a horizontal tail at several heights and angles of incidence are presented in figures 38 through 41. The lift and pitching-moment characteristics of the isolated horizontal tail are shown in figure 42. Figure 43 shows the variation with angle of attack of the factors affecting the stability contribution of the horizontal tail of the 40° combination. The variations with Mach number of the lift-curve slope of the isolated horizontal tail, the tail-effectiveness parameter $\partial C_m / \partial i_t$, and the factors affecting the stability contribution of the horizontal tail are shown in figures 44 to 46. The effects of varying tail height on the lift and pitching-moment characteristics of the 45° and 50° wing-fuselage-tail combinations are shown in figures 47 and 48, and the effect of the horizontal tail on longitudinal characteristics of these combinations are shown in figures 49, 50, and 51 for a range of Mach numbers.

~~CONFIDENTIAL~~

DISCUSSION

Fence Development

The design and location of the boundary-layer fences were based on the flow studies shown in reference 1 and the results of the fence investigation reported in reference 2. The fences were designed to act as physical barriers to prevent the spanwise flow of the boundary-layer air indicated by the flow studies. Tests to determine the most satisfactory fences were conducted with the tail off since the results in reference 5 indicated that reductions in longitudinal stability with increasing lift for a comparable configuration were primarily due to changes in the static longitudinal stability of the wing-fuselage combination.

Figures 4 through 16 show, mostly at a Mach number of 0.417, the effects of varying the number of fences, the spanwise location of the fences, and the chordwise extent of the fences on the longitudinal characteristics of the wing-fuselage combinations. The effect of the fences on the inflection lift coefficients¹ (fig. 22) of the various wing-fuselage combinations was more a function of the number than of the chordwise extent of the fences. The inflection lift coefficients of the wing-fuselage combinations were increased only slightly by the addition of single fences (figs. 4, 9, and 13). The largest inflection lift coefficients for the three wing-fuselage combinations were with multiple fences on the wings. Four fences provided the most satisfactory stability characteristics for the 40° and 45° combinations (figs. 7 and 11), whereas the largest improvements in stability for the 50° combination were with three fences (figs. 14 and 15).

Varying the chordwise extent of the fences on the 40° combination did not significantly change the effectiveness of the fences (fig. 8). This was anticipated, since the flow studies reported in reference 1 indicated that separation on the wings usually started behind the forward end (0.10 chord) of the partial-chord fence. Slightly higher maximum lift coefficients were generally attained with the fences which extended around the leading edge; however, the inflection lift coefficients were

¹Inflection lift coefficient is defined herein as the lift coefficient at which the slope of the pitching-moment curve equaled 0.10. This value was selected because the fuselage was so destabilizing that, even in the absence of separated flow, the aerodynamic center of the wing-fuselage combinations was very near the quarter-chord point of the wing mean aerodynamic chord. Since it was not considered desirable to use a more forward moment center for the computation of pitching-moment coefficient, the inflection lift coefficient was arbitrarily defined as the lift coefficient at which $dC_m/dC_L = 0.10$. The values of inflection lift coefficient so obtained correspond very closely to those that would exist if the moment center were at 0.15 \bar{c} and C_{L_1} had its more conventional definition as the lift coefficient at which $dC_m/dC_L = 0$.

~~CONFIDENTIAL~~

approximately the same with both types of fences (fig. 22). Removing the rear portions of the fences (from 0.75 chord to the trailing edge) also resulted in only small changes in the effectiveness of the fences, at least for the 40° combination at a Mach number of 0.417. The effects of the fences on the inflection lift coefficients of the combinations are summarized in figure 22.

The fence development program indicated that the installation of several partial-chord fences (extending from 0.10 chord to the trailing edge) resulted in the largest improvements in stability without excessive drag penalties. For the 40° combination it was determined that partial-chord fences at 33, 50, 70, and 85 percent of the semispan provided the best results; for the 45° combination, partial-chord fences at 25, 45, 65, and 85 percent were best; and for the 50° combination, partial-chord fences at 30, 55, and 80 percent of the semispan were best. It is believed that these fence configurations, while possibly not the optimum for each combination, were at least representative of the most effective arrangement for improvement in the stability characteristics.

Wing-Fuselage Combinations

Effects of fences at low speed.— Each wing-fuselage combination with its best fences was tested at a Mach number of 0.165 and a Reynolds number of 8 million. The results are shown in figure 17. The addition of fences increased the lift and reduced drag at high lift coefficients; however, at low lift coefficients the fences increased drag moderately.

Large improvements in stability resulted from the use of fences. For the 40° combination the inflection lift coefficient without fences was approximately 0.93; with fences a lift coefficient of 1.34 was reached without any significant changes in stability. Similar results were obtained with the 45° combination; the inflection lift coefficient without fences was approximately 0.80, while with fences, a lift coefficient of 1.24 was attained without instability. The 50° combination was tested at low speed with both full-chord and partial-chord fences since the flow studies of reference 1 indicated the possibility of the leading-edge type of flow separation. Large improvements in inflection lift coefficient resulted from the use of either fence configuration. The addition of partial-chord fences increased the inflection lift coefficient from approximately 0.63 to approximately 1.08.

Effects of fences at high speed.— The lift characteristics of the various wing-fuselage combinations with and without fences are shown in figure 18 for Mach numbers varying from 0.25 to 0.92 at a constant Reynolds number of 2 million. The addition of fences usually resulted in increased lift at moderately high angles of attack. The effect of Mach number on the lift-curve slopes of the combinations with and without fences is shown

in figure 23. At the selected lift coefficient (0.40) the fences increased the lift-curve slopes of the 40° combination at Mach numbers greater than 0.80. The lift-curve slopes of the 45° and 50° combinations were increased at all Mach numbers by the addition of fences.

The drag characteristics of the combinations with and without fences are shown in figure 19 for the range of Mach numbers at which the tests were conducted. Use of the fences resulted in moderate increases in drag at low lift coefficients and appreciable reductions in drag at the higher lift coefficients. These effects of fences are also shown in figure 21 which compares the lift-drag ratios of the configurations with and without fences at several Mach numbers, and in figure 24 which shows the effect of the fences on the variation of drag coefficient with Mach number for several constant lift coefficients. The Mach numbers for drag divergence of the combinations (defined as $dC_D/dM = 0.10$) were increased slightly by the addition of fences; however, the corresponding drag coefficients were usually higher than those at the divergence Mach numbers of the combinations without fences (fig. 24). These values are shown for the various wing-fuselage combinations in the following table:

CL	$\Lambda = 40^\circ$				$\Lambda = 45^\circ$				$\Lambda = 50^\circ$			
	M for drag divergence		$C_{D_{div}}$		M for drag divergence		$C_{D_{div}}$		M for drag divergence		$C_{D_{div}}$	
	Fences off	Fences on	Fences off	Fences on	Fences off	Fences on	Fences off	Fences on	Fences off	Fences on	Fences off	Fences on
0.40	0.860	0.866	0.0235	0.0258	0.880	0.890	0.0247	0.0280	---	---	---	---
.50	.831	.846	.0288	.0321	.850	.865	.0314	.0350	0.865	0.885	0.0385	0.0388
.60	.800	.801	.0361	.0381	.763	.819	.0422	.0442	.831	.868	.0660	.0584

There is a possibility that at least part of the drag due to the fences at the lower lift coefficients was due to the exposed flange used in mounting the fences.

Figure 20 shows the effect of fences on the pitching-moment characteristics of the combinations at Mach numbers from 0.25 to 0.92. The effects of fences on the variations with Mach number of the inflection lift coefficients and the slopes of the pitching-moment curves are shown in figures 22 and 23, respectively. These data indicate that large changes in longitudinal stability with increasing lift coefficient were eliminated up to lift coefficients of at least 0.60 at practically all Mach numbers. The largest improvements in stability occurred at the lower Mach numbers. The degree of improvement in stability due to fences generally decreased with increasing Mach number. The fences had only small effect on the variations of the slopes of the pitching-moment curves with Mach number of the 40° and 45° combinations at subcritical speeds. With further increase in Mach number there was an abrupt increase in the stability of the combinations with fences. Fences eliminated the decrease in stability with increasing Mach number indicated for the 50° combination without fences at

Mach numbers below about 0.73. At the higher Mach numbers the effects of the fences were similar to those shown for the 40° and 45° combinations.

Effects of Reynolds number.- The effect of increasing Reynolds number from 2 million to 8 million at a Mach number of 0.25 is shown in figures 25 through 27 for the wing-fuselage combinations with and without fences. The longitudinal characteristics of the combinations with fences were less affected by increases in Reynolds number than those for the combinations without fences. This effect is also evident in figure 22 which shows that an approximate doubling of Reynolds number at a Mach number of 0.417 did not significantly affect the inflection lift coefficient of the wing-fuselage combinations with fences. In comparison, inflection lift coefficients for the combinations without fences were increased as much as 25 percent by this increase in Reynolds number.

An effort was made to simulate the effects of Reynolds number at higher speeds by applying surface roughness at 0.10 chord on the upper surfaces of the wings (fig. 3), and the results are presented in figures 28 through 30. Roughness did not effect any significant change in the effective Reynolds numbers of the tests. The roughness resulted in increases in the pitching moments for low and moderate lift coefficients. This may have been due to applying roughness to only the upper surfaces of the wings. As expected, drag was increased considerably by the roughness.

Wing-Fuselage-Tail Combinations

Effects of wing fences.- The effects of fences on the longitudinal characteristics of the wing-fuselage-tail combinations are shown in figures 31 through 33 which compare for several test conditions the fence-on data of figures 38, 49, 50, and 51 with the data obtained without wing fences. This comparison shows that large changes in the stability of the wing-fuselage-tail combination were eliminated by the addition of fences up to lift coefficients of at least 0.80 at Mach numbers up to 0.80. The pitching-moment contribution of the horizontal tail was not changed significantly by the addition of the wing fences (fig. 34) which indicates that adding fences caused little or no change in either the average effective downwash angle or the tail efficiency factor. The improvements in the tail-on pitching-moment characteristics due to the fences were primarily due to improvements of the longitudinal characteristics of the wing-fuselage combination.

Figures 35 through 37 summarize the longitudinal characteristics of the wing-fuselage-tail combinations with and without fences. The curves shown for the fence-on condition are cross plots of the data presented in figures 38, 49, 50, and 51. The variations with Mach number of the inflection lift coefficients of the combinations are shown in figure 35. Figure 36 presents for a lift coefficient of 0.40 the variations with

Mach number of the lift-curve and pitching-moment-curve slopes, and figure 37 shows for several lift coefficients the variation of drag coefficient with Mach number. At subcritical speeds, inflection lift coefficients of at least 0.80 are shown for all the wing-fuselage-tail combinations with fences. At supercritical speeds, the addition of the fences resulted in increases of the lift-curve slopes and the stability. The effect of the fences on the drag characteristics was small. Drag at constant lift increased moderately as was expected; however, the drag-divergence Mach numbers were not significantly affected.

Longitudinal characteristics of the 40° combination with a horizontal tail.— Since the data in reference 1 indicate that the over-all characteristics of the wing with 40° of sweepback were superior to the wings with 45° or 50° of sweepback, a more extensive investigation was conducted with the 40° combination than with the 45° or 50° combinations. The longitudinal characteristics of the 40° combination with its best fences were determined with the horizontal tail at several angles of incidence at each of several tail heights to establish the effectiveness of the tail as a longitudinal control for the configuration.

The results of these tests are shown by the lift, drag, and pitching-moment data in figures 38 through 41. These data show that the addition of a horizontal tail to the 40° combination had only small effect on the lift and drag characteristics of the combination at most Mach numbers and tail heights. However, the pitching-moment curves were more nearly linear with the tail on than with the tail off, and the inflection lift coefficients were usually higher with the tail on than with it off.

The tail contribution to stability can be expressed by the following equation:

$$\left[\left(\frac{dC_m}{dC_L} \right)_t \right]_{w+f} = -V_t \frac{a_t}{a_{w+f}} \left[\eta_t \frac{q_t}{q} \left(1 - \frac{d\epsilon}{d\alpha} \right) + \alpha_t \frac{\partial \left(\eta_t \frac{q_t}{q} \right)}{\partial \alpha} \right]$$

where the expression $(dC_m/dC_L)_t$ represents the variation of pitching-moment coefficient due to the tail with the lift coefficient of the wing-fuselage combinations. This parameter is related to the increment due to the tail in the stability of the complete model by the expression:

$$\left[\left(\frac{dC_m}{dC_L} \right)_t \right]_{w+f+t} = \frac{a_{w+f}}{a_{w+f+t}} \left[\left(\frac{dC_m}{dC_L} \right)_t \right]_{w+f}$$

The effective downwash angle ϵ , the tail efficiency factor $\eta_t(q_t/q)$, and the ratio of the isolated tail lift-curve slope to the lift-curve slopes of the wing-fuselage combinations a_t/a_{w+f} , were computed by the method of

reference 6 using the wing-fuselage force data presented in figures 38 through 41 and the isolated tail force data presented in figure 42. The results are shown for several Mach numbers and tail heights in figure 43 as functions of angle of attack. It was assumed for the computation of downwash angle and tail efficiency factor that the Mach number at the tail was the same as free-stream Mach number. The results of these calculations show that the higher inflection lift coefficients attained with the tail on were mostly due to an increase in the factor a_t/a_{w+f} with increasing lift coefficient in a manner which tended to offset the reduction in stability which occurred for the wing-fuselage combination. This was generally true at all Mach numbers. The variations with Mach number of the isolated tail lift-curve slope, the tail control-effectiveness parameter $\partial C_m / \partial i_t$, and the various factors affecting the stability contribution of the tail are shown in figures 44, 45, and 46, respectively.

Effects of tail height.- The longitudinal characteristics of the 40° combination are shown for several tail heights in figures 38 through 41. The effects of tail height on the lift and pitching-moment characteristics of the 45° and 50° combinations are shown in figures 47 and 48, respectively. Increasing the height of the horizontal tail from 0 b/2 to 0.07 b/2 usually resulted in small reductions in the inflection lift coefficients of the various combinations. There were no significant effects on inflection lift coefficient with further increases (up to about 0.20 b/2) in tail height. At comparatively low lift coefficients, both longitudinal stability and the lift coefficient for balance were increased slightly by raising the tail. These effects were probably due to increases in tail efficiency factor $\eta_t(q_t/q)$ resulting from moving the tail from the fuselage center line to a position above the fuselage. The effects of raising the tail of the 40° combination on the factors affecting the stability contribution of the tail are shown in figure 43. Raising the tail resulted in increases in the rate of change of downwash with angle of attack; however, this destabilizing effect of increased tail height was more than compensated for by increases in tail-efficiency factor $\eta_t(q_t/q)$. Figure 45, which shows the tail control-effectiveness factor $\partial C_m / \partial i_t$ as a function of Mach number, indicates at a Mach number of 0.80 and an angle of attack of 4° about a 33 percent increase in control effectiveness resulting from an increase in tail height of 0.20 b/2.

Longitudinal characteristics of the 45° and 50° combinations with a horizontal tail.- The longitudinal characteristics of the 45° and 50° combinations with the best fences and a horizontal tail are presented in figures 49 through 51. A comparison of these data with the tail-off data (figs. 18 through 20) shows that the horizontal tail had about the same effect on the 45° and 50° combinations as on the 40° combination. The addition of the horizontal tail had only small effect on the lift and drag characteristics of the combinations at most Mach numbers. The pitching-moment curves were more nearly linear with the tail on than with the tail off, and the inflection lift coefficients were usually higher with the tail on than off. Figures 35 through 37 summarize the results of the tail-on tests on these combinations.

CONCLUSIONS

A wind-tunnel investigation has been made of three-wing-fuselage combinations, with and without a horizontal tail, having sweptback wings with NACA four-digit thickness distributions. Tests were conducted with the wings swept back 40° , 45° , and 50° . The following conclusions were indicated:

1. The addition of multiple wing fences to the wing-fuselage and wing-fuselage-tail combinations eliminated large changes in longitudinal stability up to lift coefficients in excess of 1.0 at low speeds, an improvement of as much as 80 percent over the values with the fences off. At high subcritical speeds, the addition of fences eliminated large changes in the stability of the wing-fuselage-tail combinations up to lift coefficients of at least 0.80, an improvement of as much as 60 percent over the lift coefficients for instability without fences.
2. The fences had little effect on the tail contribution to stability.
3. Adding fences to the wings increased the drag of the combinations moderately at low lift coefficients, but reduced the drag and increased the lift-drag ratios at the higher lift coefficients.
4. The Mach numbers for drag divergence of the combinations were increased slightly by the addition of fences; however, the corresponding drag coefficients were higher than those at the divergence Mach numbers of the combinations without fences.
5. Increasing the height of the horizontal tail as much as 20 percent of the wing semispan above the fuselage center line had only small effect on the tail contribution to stability.
6. The all-movable horizontal tail had nearly constant control effectiveness throughout the lift range at most Mach numbers and its effectiveness at a lift coefficient of about 0.40 was not significantly affected by increasing Mach number.
7. Increasing the height of the all-movable horizontal tail of the 40° combination from the fuselage center line to about 20 percent of the wing semispan above the fuselage center line increased its effectiveness as a longitudinal control as much as 33 percent at low values of lift.

Ames Aeronautical Laboratory
National Advisory Committee for Aeronautics
Moffett Field, Calif., Dec. 8, 1954

REFERENCES

1. Sutton, Fred B., and Dickson, Jerald K.: A Comparison of the Longitudinal Aerodynamic Characteristics at Mach Numbers Up to 0.94 of Sweptback Wings Having NACA 4-Digit or NACA 64A Thickness Distributions. NACA RM A54F18, 1954.
2. Edwards, George G., Tinling, Bruce E., and Ackerman, Arthur C.: The Longitudinal Characteristics at Mach Numbers Up to 0.92 of a Cambered and Twisted Wing Having 40° of Sweepback and an Aspect Ratio of 10. NACA RM A52F18, 1952.
3. Herriot, John G.: Blockage Corrections for Three-Dimensional-Flow Closed-Throat Wind Tunnels, With Consideration of the Effect of Compressibility. NACA Rep. 995, 1950. (Formerly NACA RM A7B28)
4. Sivells, James C., and Salmi, Rachel M.: Jet-Boundary Corrections for Complete and Semispan Swept Wings in Closed Circular Wind Tunnels. NACA TN 2454, 1951.
5. Tinling, Bruce E.: The Longitudinal Characteristics at Mach Numbers Up to 0.9 of a Wing-Fuselage-Tail Combination Having a Wing With 40° of Sweepback and an Aspect Ratio of 10. NACA RM A52I19, 1952.
6. Edwards, George G., and Buell, Donald A.: Analysis of Wind-Tunnel Tests at Low Speeds of a Four-Engine Propeller-Driven Airplane Configuration Having a Wing With 40° of Sweepback. NACA RM A54F14, 1954.

~~CONFIDENTIAL~~

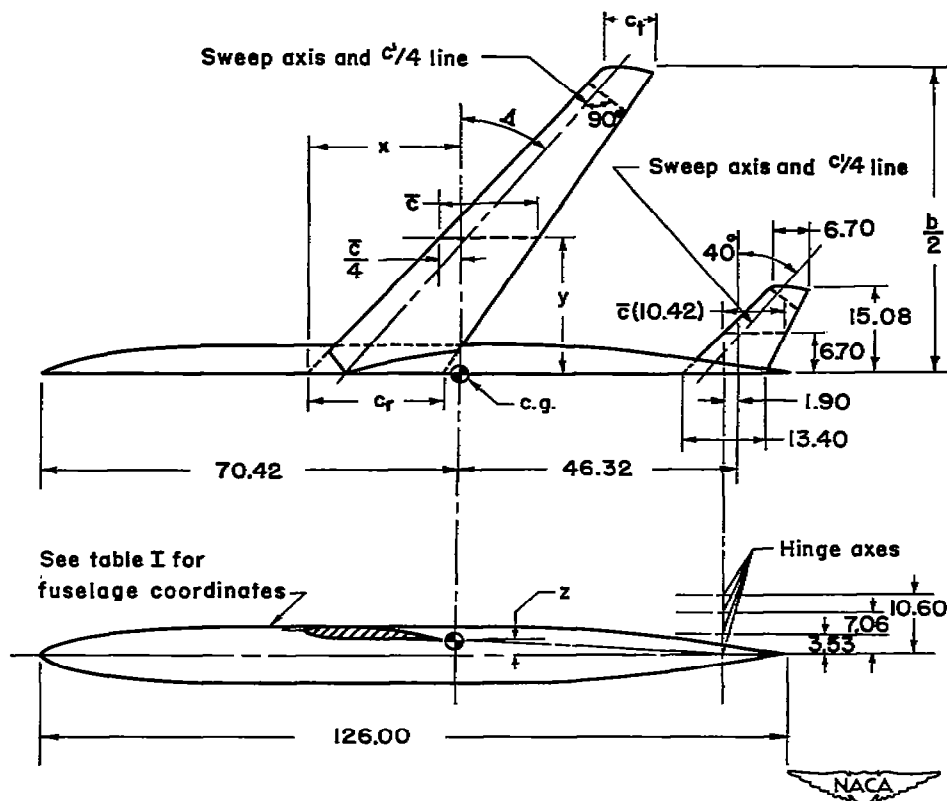
NACA RM A54108

TABLE I.- FUSELAGE COORDINATES

Distance from nose, in.	Radius, in.
0	0
1.27	1.04
2.54	1.57
5.08	2.35
10.16	3.36
20.31	4.44
30.47	4.90
39.44	5.00
50.00	5.00
60.00	5.00
70.00	5.00
76.00	4.96
82.00	4.83
88.00	4.61
94.00	4.27
100.00	3.77
106.00	3.03
126.00	0

NACA

~~CONFIDENTIAL~~



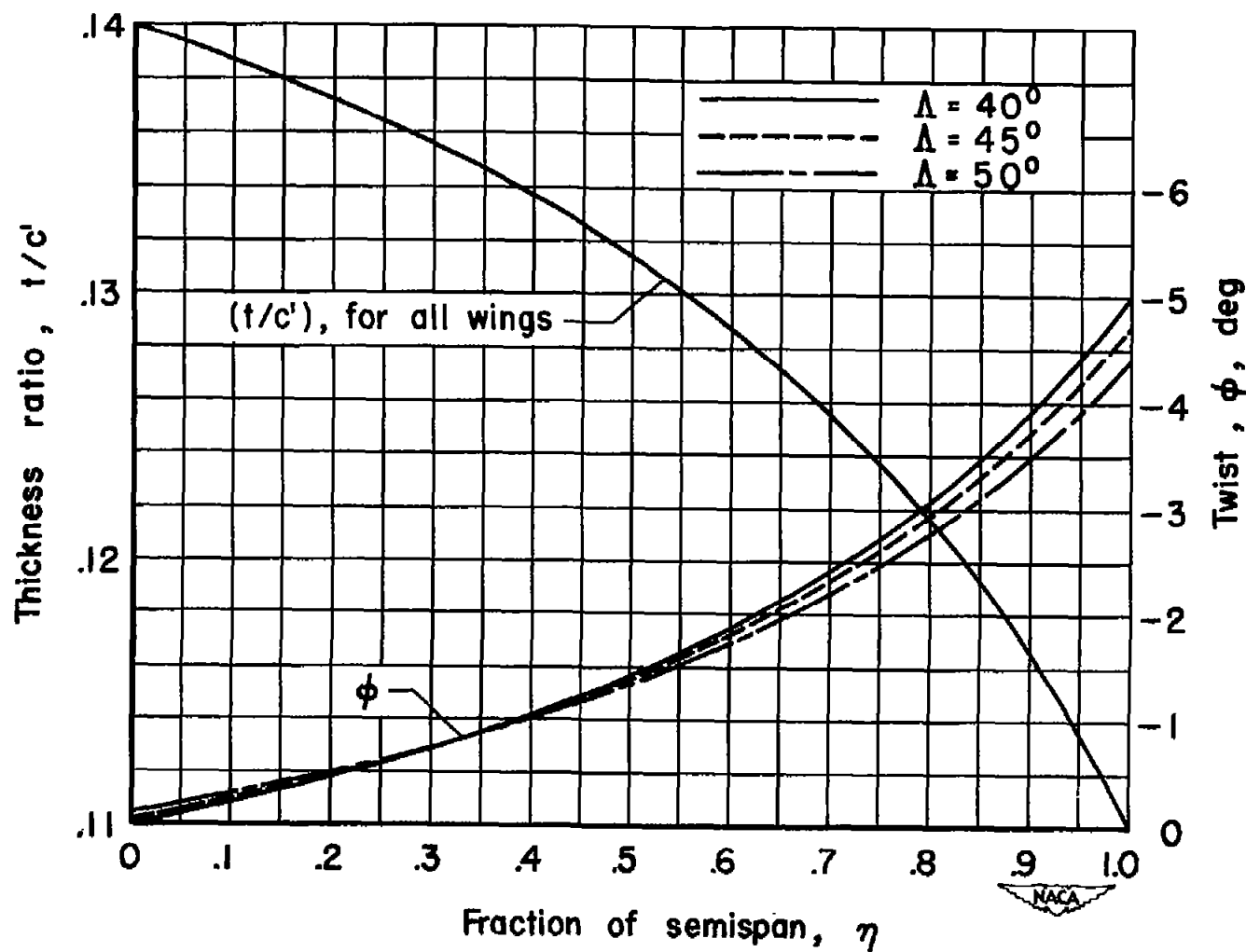
Geometry of the wings											
A	A	λ	b/2	c_r	c_f	\bar{c}	x	y	z	S	α_r for $\alpha=0^\circ$
40°	7.00	0.4	54.61	22.29	8.92	16.56	25.35	23.40	2.28	5.92	0°
45°	6.03	0.4	50.41	23.90	9.56	17.76	27.76	21.60	2.28	5.86	-0.05°
50°	5.04	0.4	45.82	25.98	10.39	19.30	30.13	19.64	2.28	5.79	-1.10°

Notes:

- (1) Wing sections perpendicular to the sweep axis have NACA OOX thickness distributions combined with an NACA $a = 0.8$ (modified) mean line, $c_{li} = 0.4$.
- (2) Horizontal tail sections perpendicular to the sweep axis have NACA OOIO thickness distributions.
- (3) All dimensions in inches and areas in square feet.

(a) Dimensions

Figure 1.- Geometry of the model.



(b) Distribution of twist and thickness ratio.

Figure 1.- Concluded.

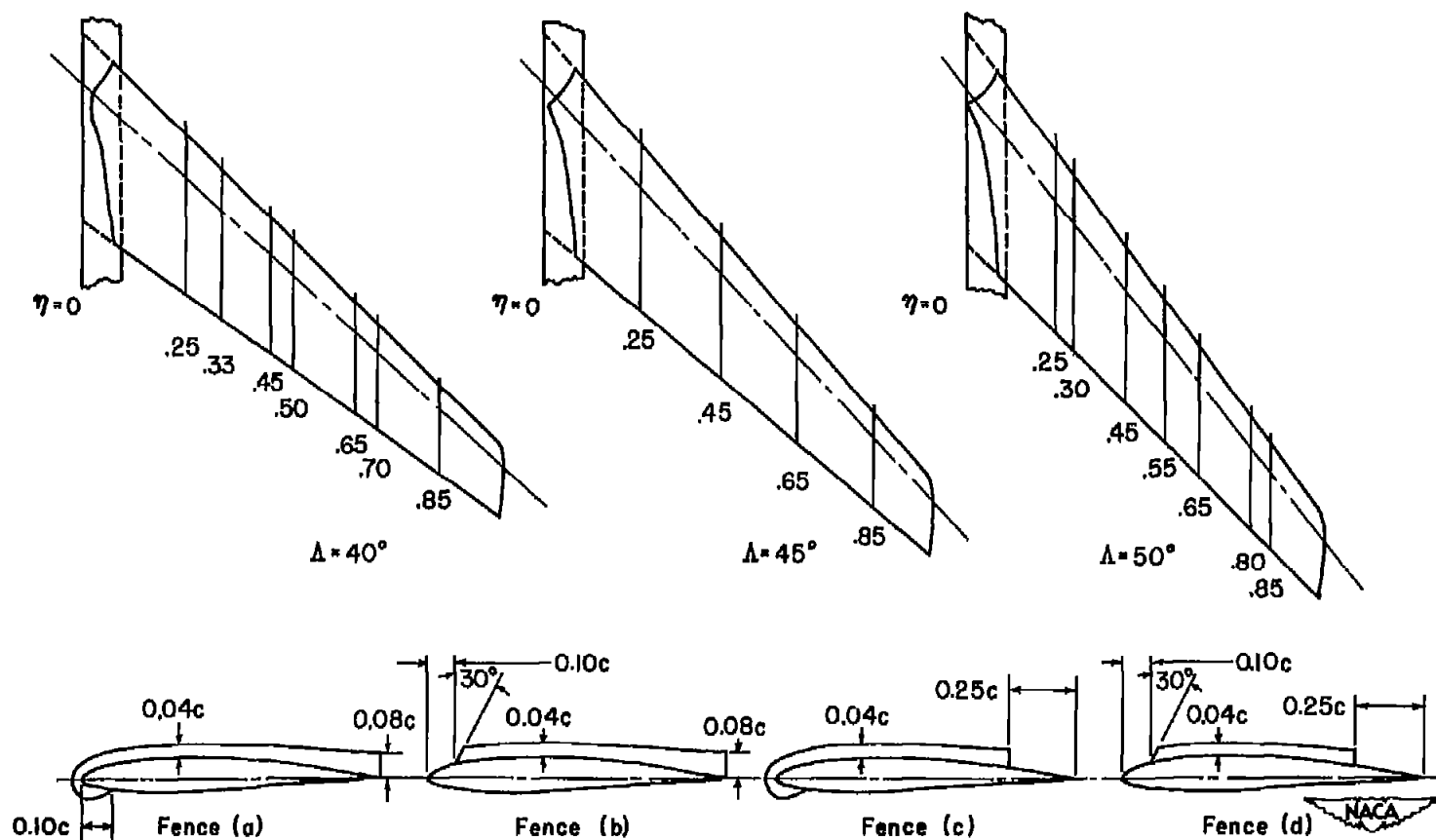


Figure 2.— The spanwise locations and the chordwise extent of the wing fences.



(a) Model mounted in tunnel. A-19214



(b) Roughness at 0.10 chord. A-19215

Figure 3.- Photographs of the model.

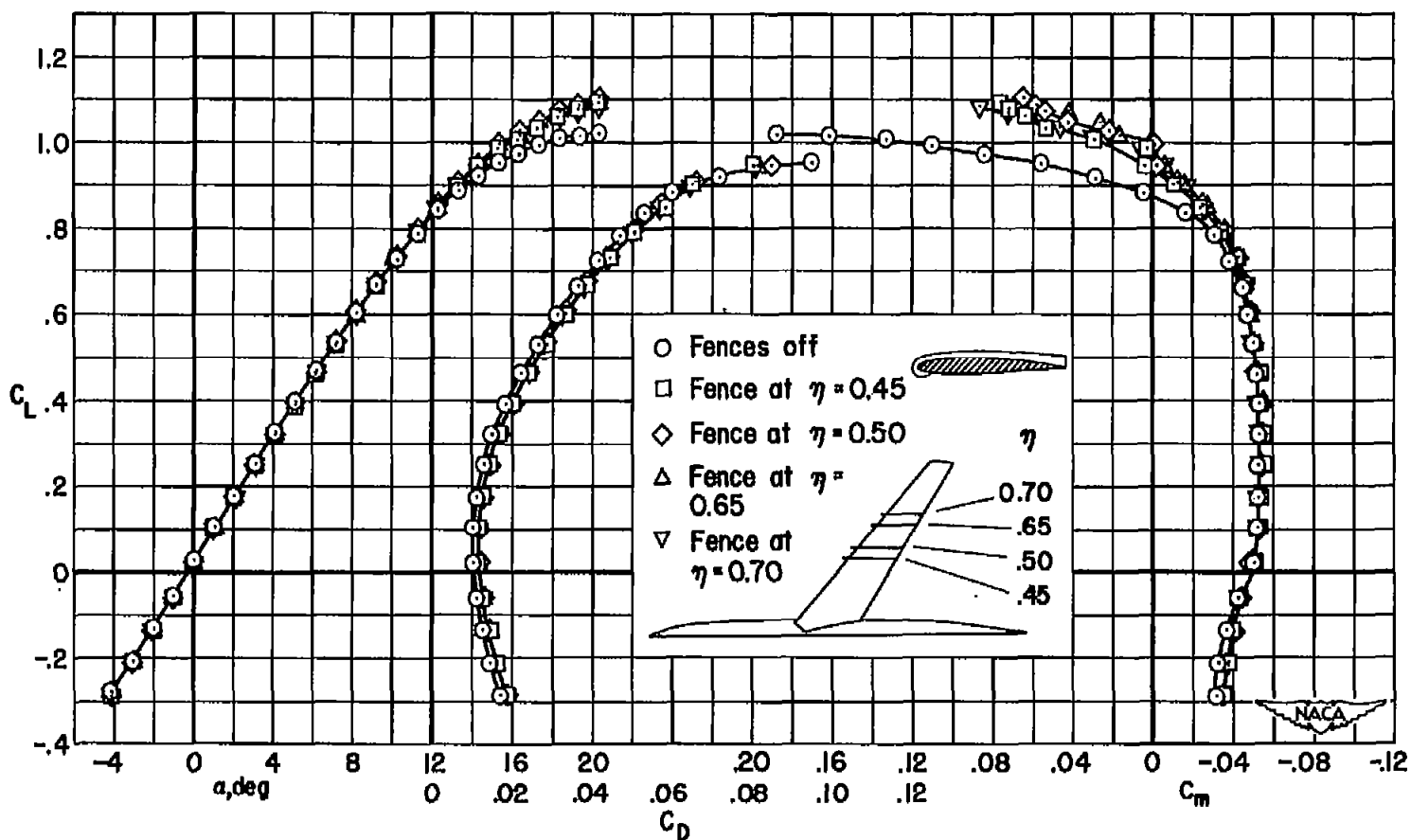


Figure 4.- The effect of a single wing fence at various spanwise locations on the longitudinal characteristics of a wing-fuselage combination having a wing with 40° of sweepback and an aspect ratio of 7.00; $M = 0.417$; $R = 3,600,000$.

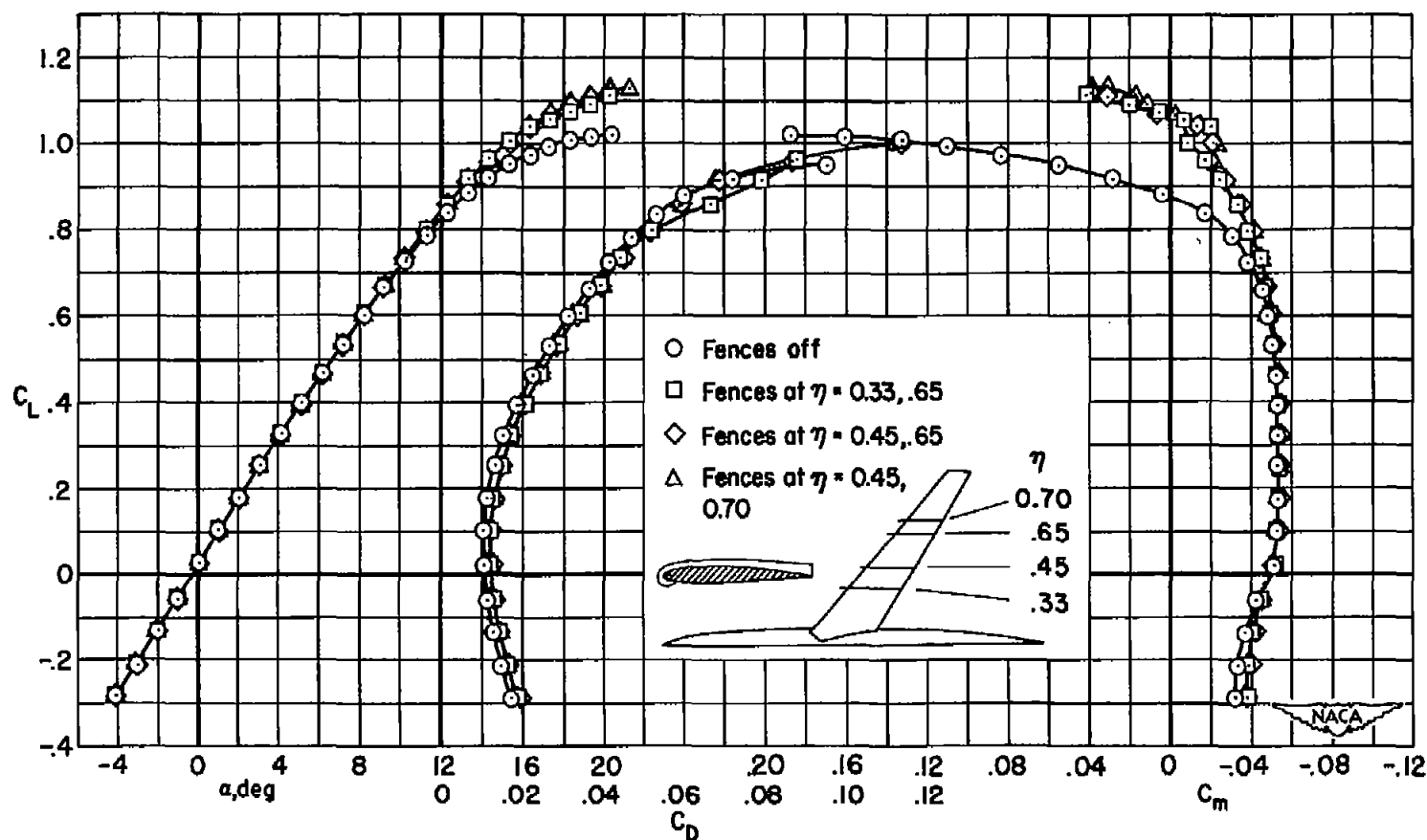


Figure 5.— The effect of two fences at various spanwise locations on the longitudinal characteristics of a wing-fuselage combination having a wing with 40° of sweepback and an aspect ratio of 7.00; $M = 0.417$; $R = 3,600,000$.

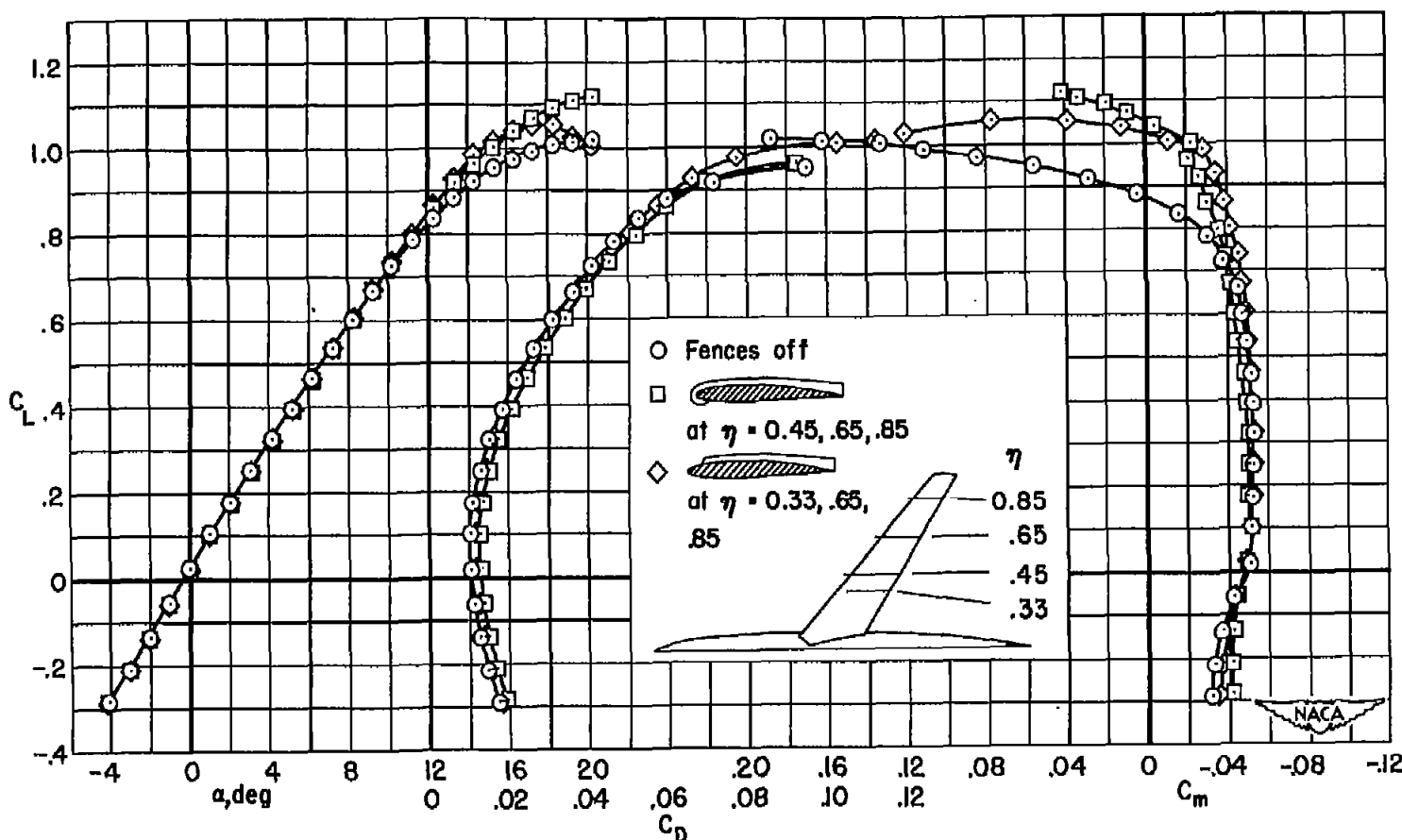
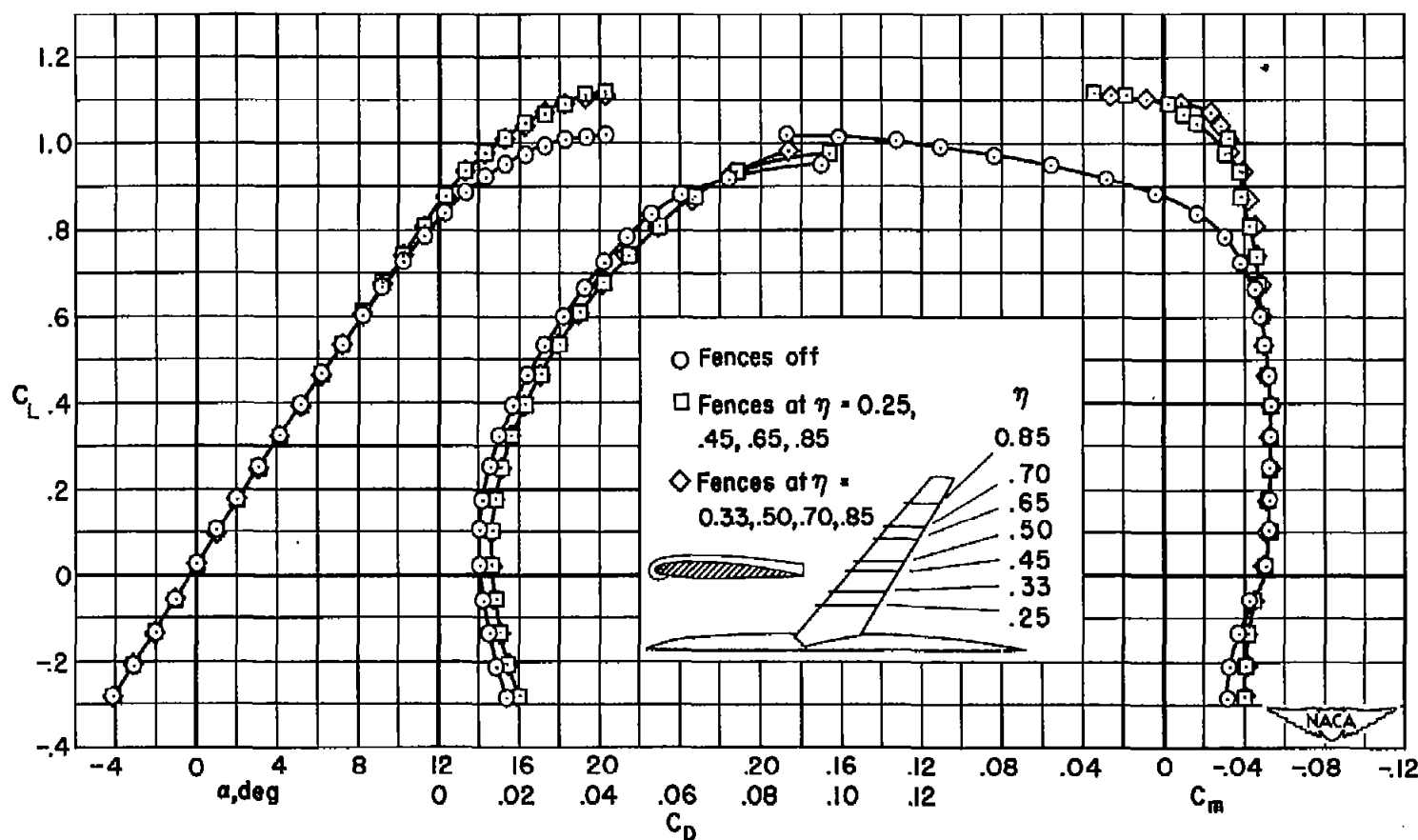
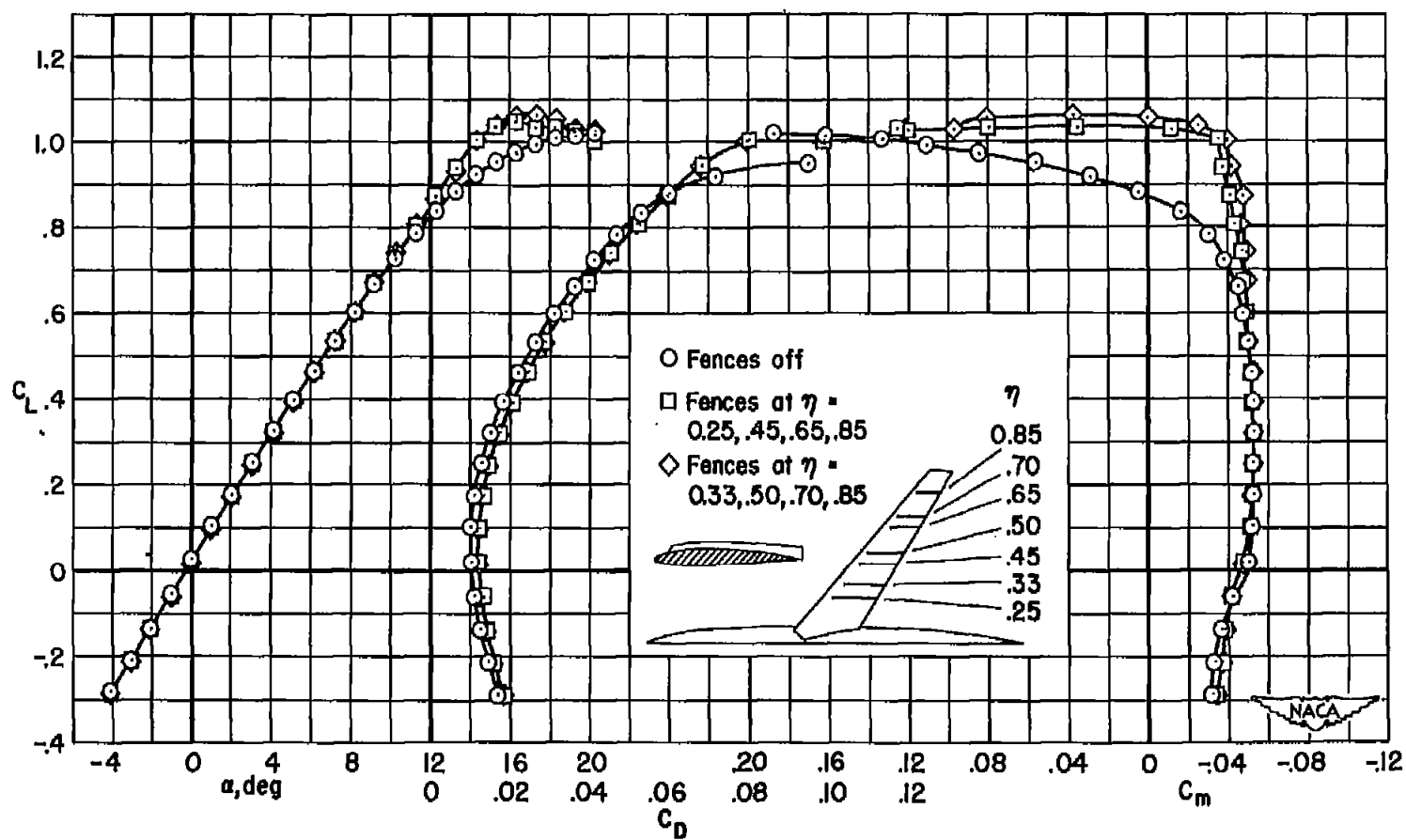


Figure 6.- The effect of three complete and three partial-chord fences on the longitudinal characteristics of a wing-fuselage combination having a wing with 40° of sweepback and an aspect ratio of 7.00; $M = 0.417$; $R = 3,600,000$.



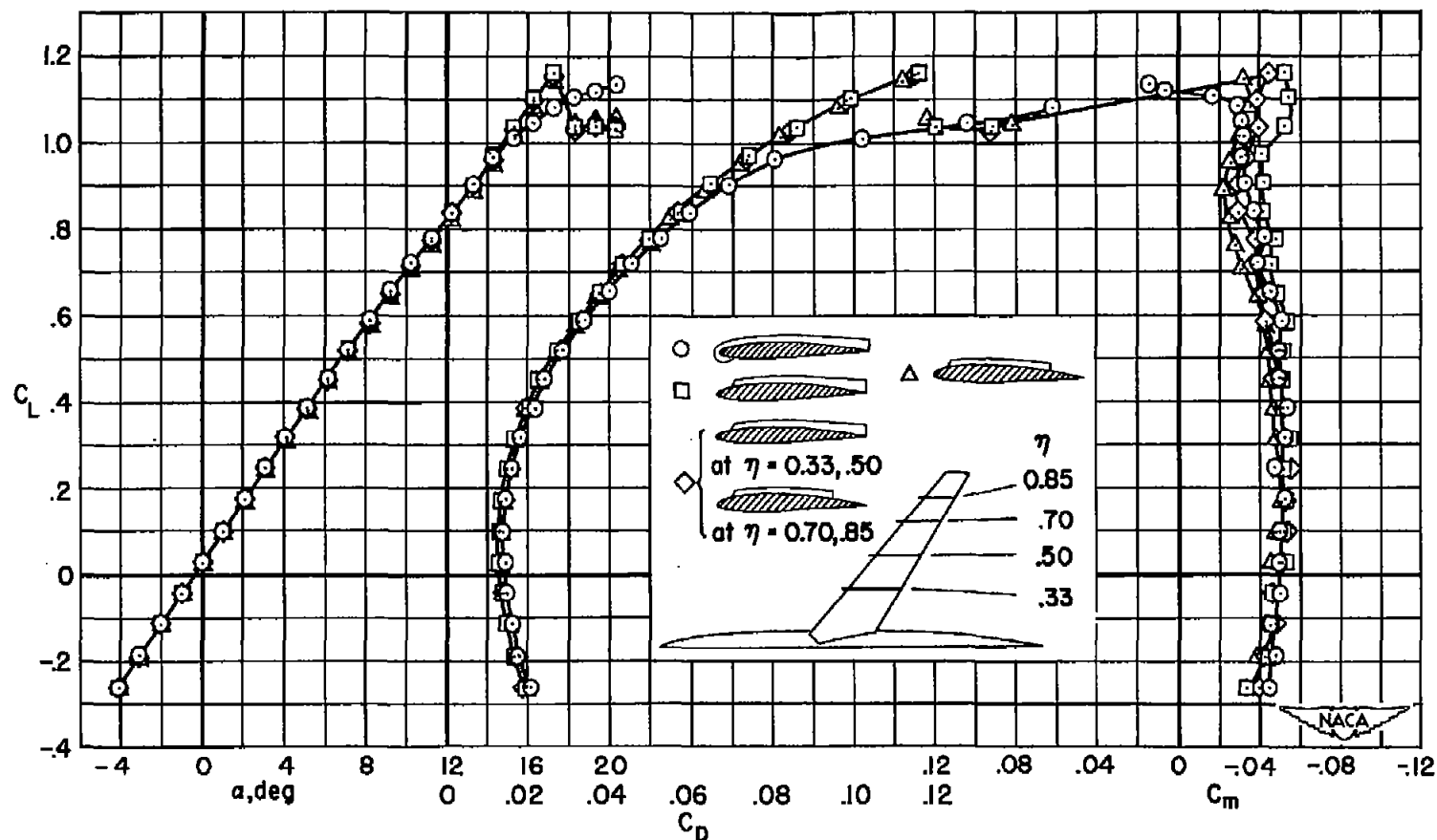
(a) Complete-chord fences.

Figure 7.- The effect of four complete-chord fences and four partial-chord fences on the longitudinal characteristics of a wing-fuselage combination having a wing with 40° of sweepback and an aspect ratio of 7.00; $M = 0.417$; $R = 3,600,000$.



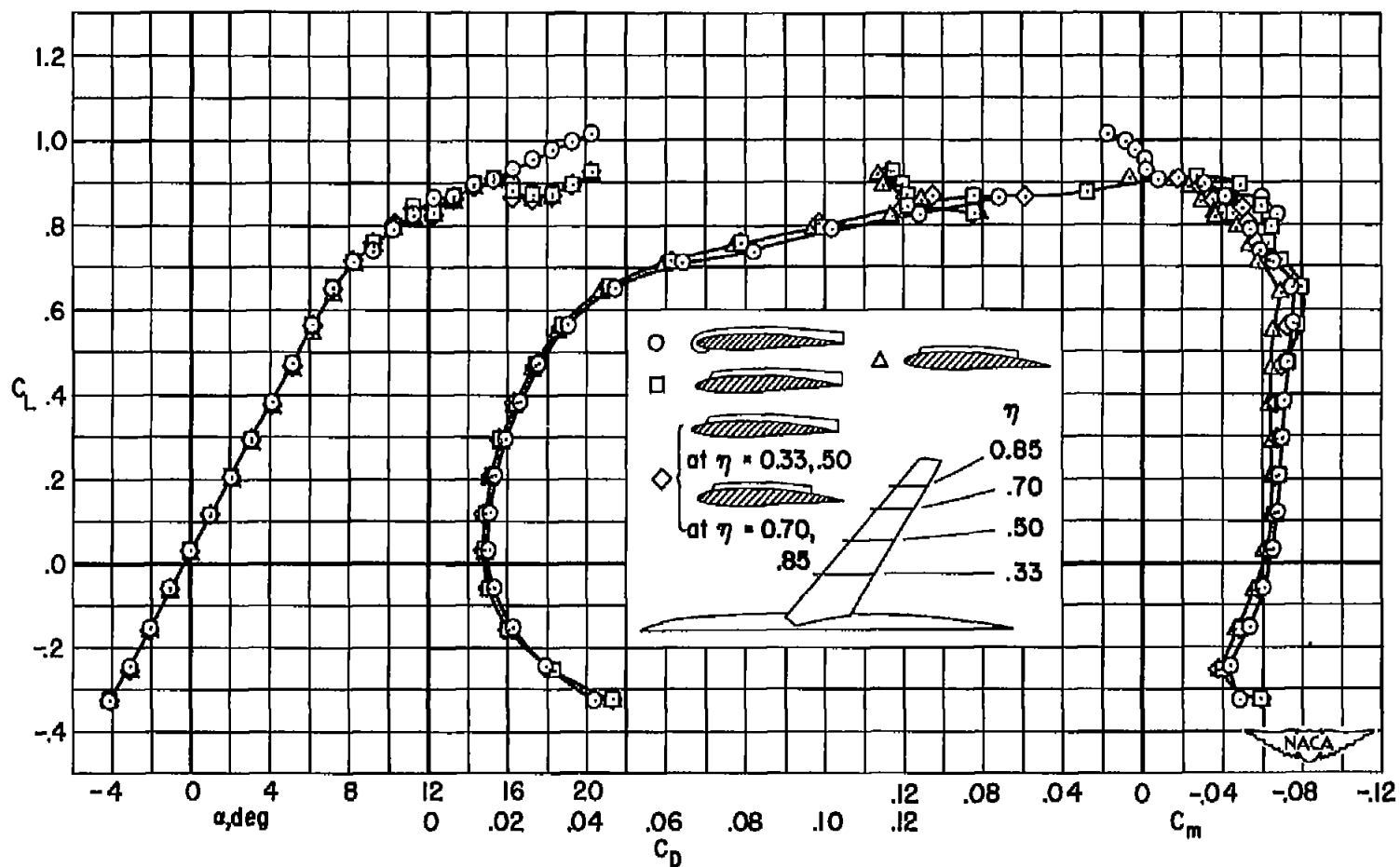
(b) Partial-chord fences.

Figure 7.- Concluded.



(a) $M = 0.25$; $R = 2,000,000$

Figure 8.- The effect of four fences of varying chordwise extent on the longitudinal characteristics of a wing-fuselage combination having a wing with 40° of sweepback and an aspect ratio of 7.00.



(b) $M = 0.80$; $R = 2,000,000$.

Figure 8.- Concluded.

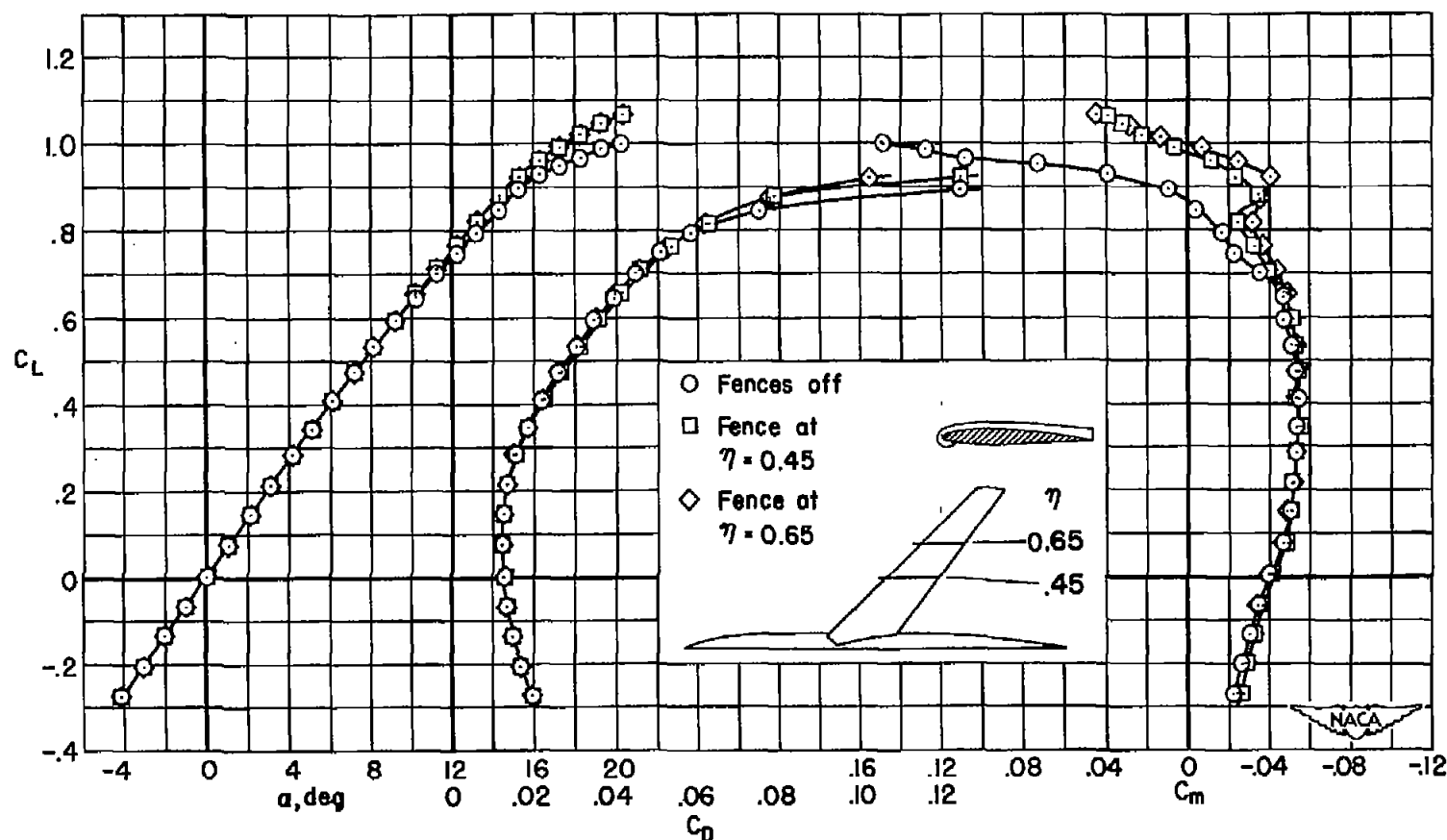


Figure 9.- The effect of a single fence at various spanwise locations on the longitudinal characteristics of a wing with 45° of sweepback and an aspect ratio of 6.03; $M = 0.417$; $R = 3,900,000$.

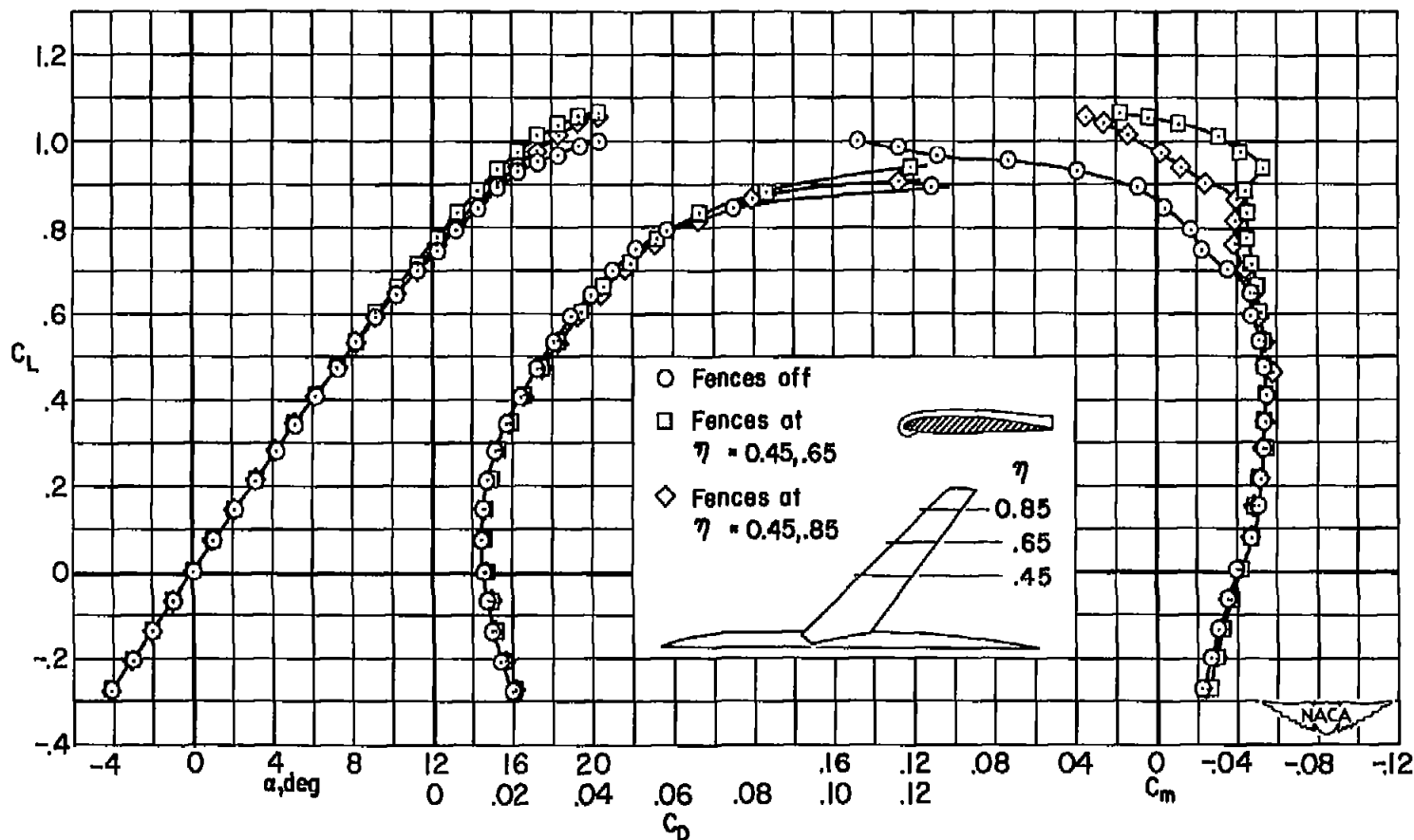


Figure 10.- The effect of two fences at various spanwise locations on the longitudinal characteristics of a wing-fuselage combination using a wing with 45° of sweepback and an aspect ratio of 6.03; $M = 0.417$; $R = 3,900,000$.

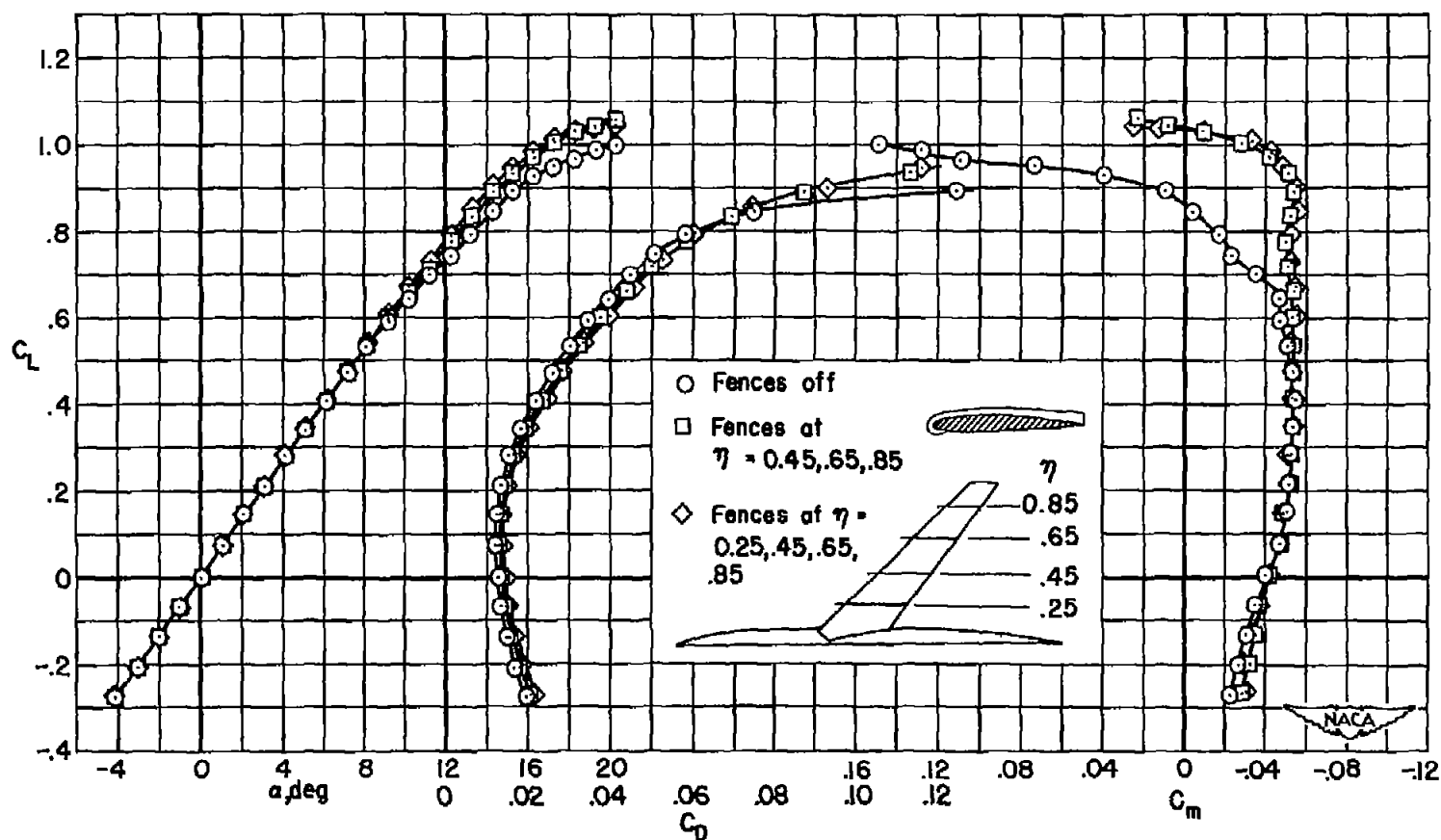


Figure 11.— The effect of three and four fences on the longitudinal characteristics of a wing-fuselage combination using a wing with 45° of sweepback and an aspect ratio of 6.03; $M = 0.417$; $R = 3,900,000$.

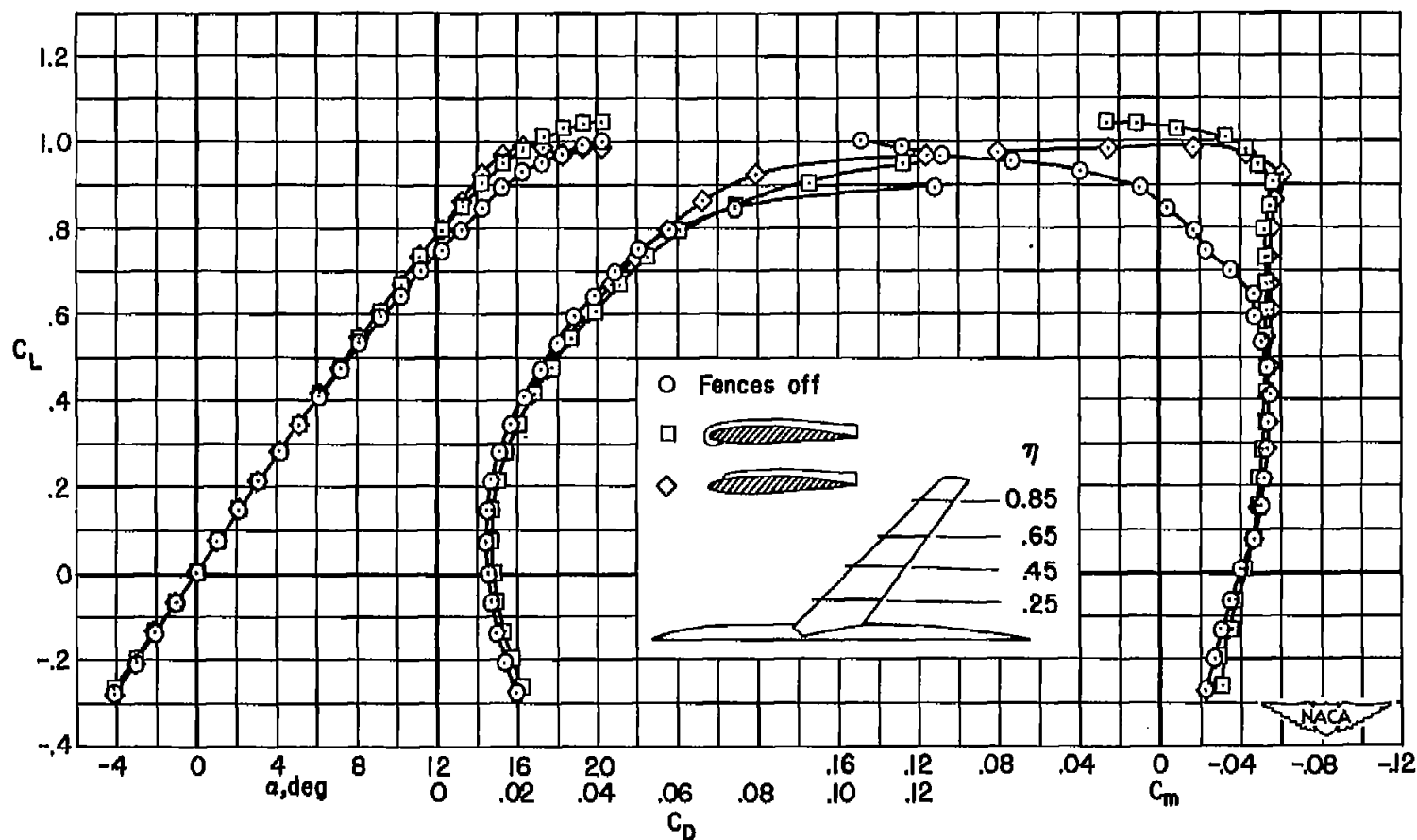


Figure 12.- The effect of four complete and four partial-chord fences on the longitudinal characteristics of a wing-fuselage combination using a wing with 45° of sweepback and an aspect ratio of 6.03; $M = 0.417$; $R = 3,900,000$.

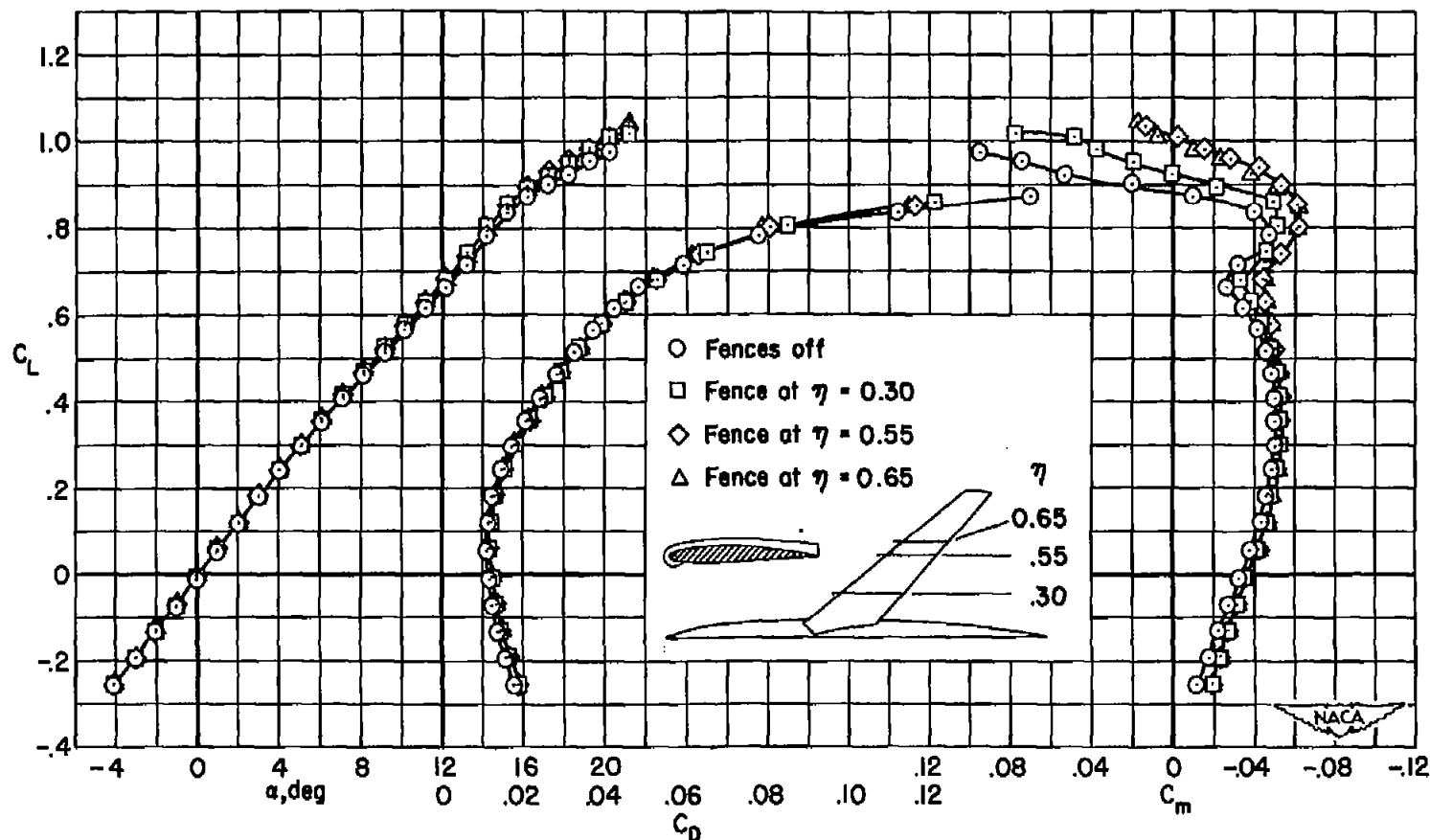


Figure 13.— The effect of a single fence at various spanwise locations on the longitudinal characteristics of a wing-fuselage combination having a wing with 50° of sweepback and an aspect ratio of 5.04; $M = 0.417$; $R = 4,300,000$.

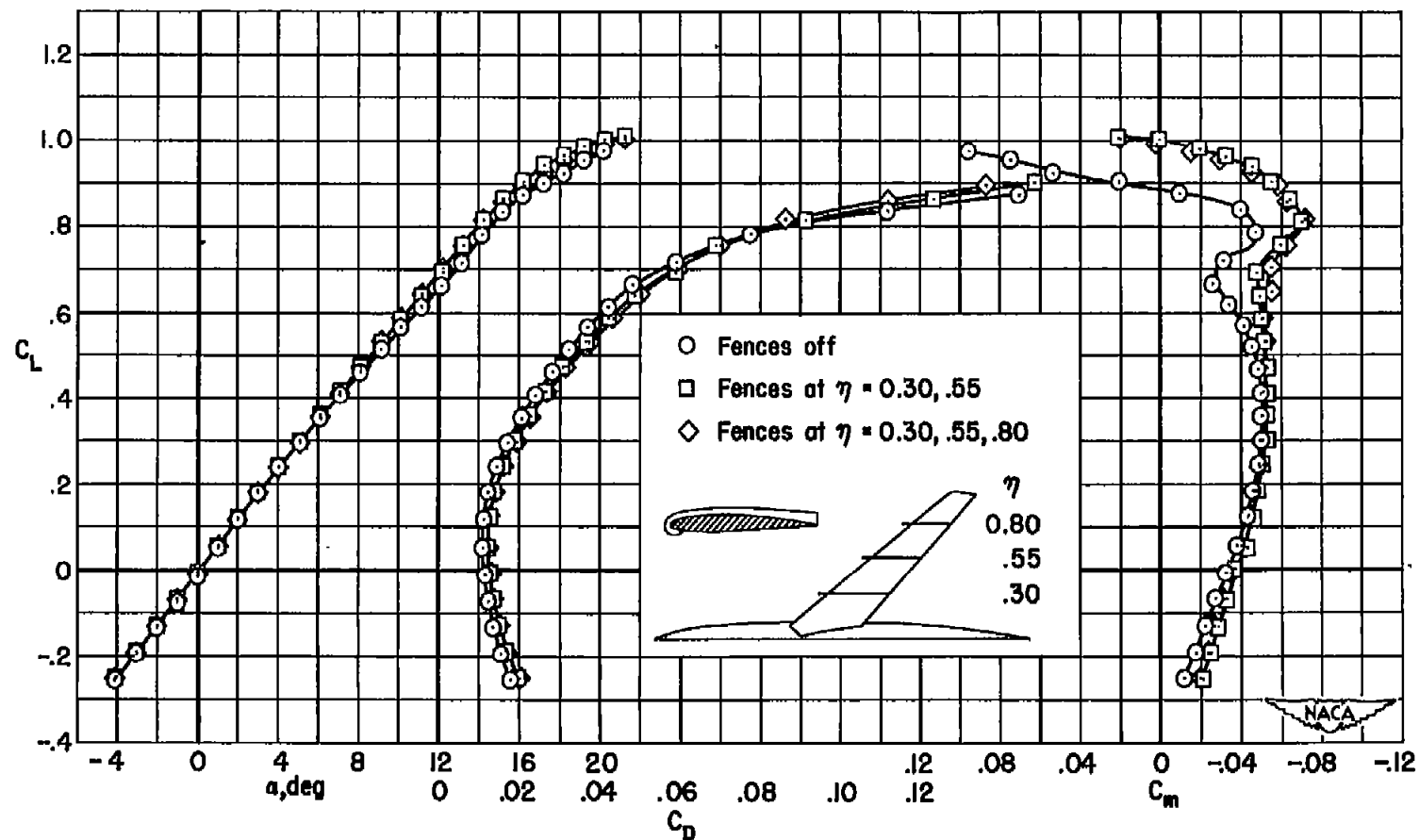


Figure 14.- The effect of two and three fences on the longitudinal characteristics of a wing-fuselage combination having a wing with 50° of sweepback and an aspect ratio of 5.04; $M = 0.417$; $R = 4,300,000$.

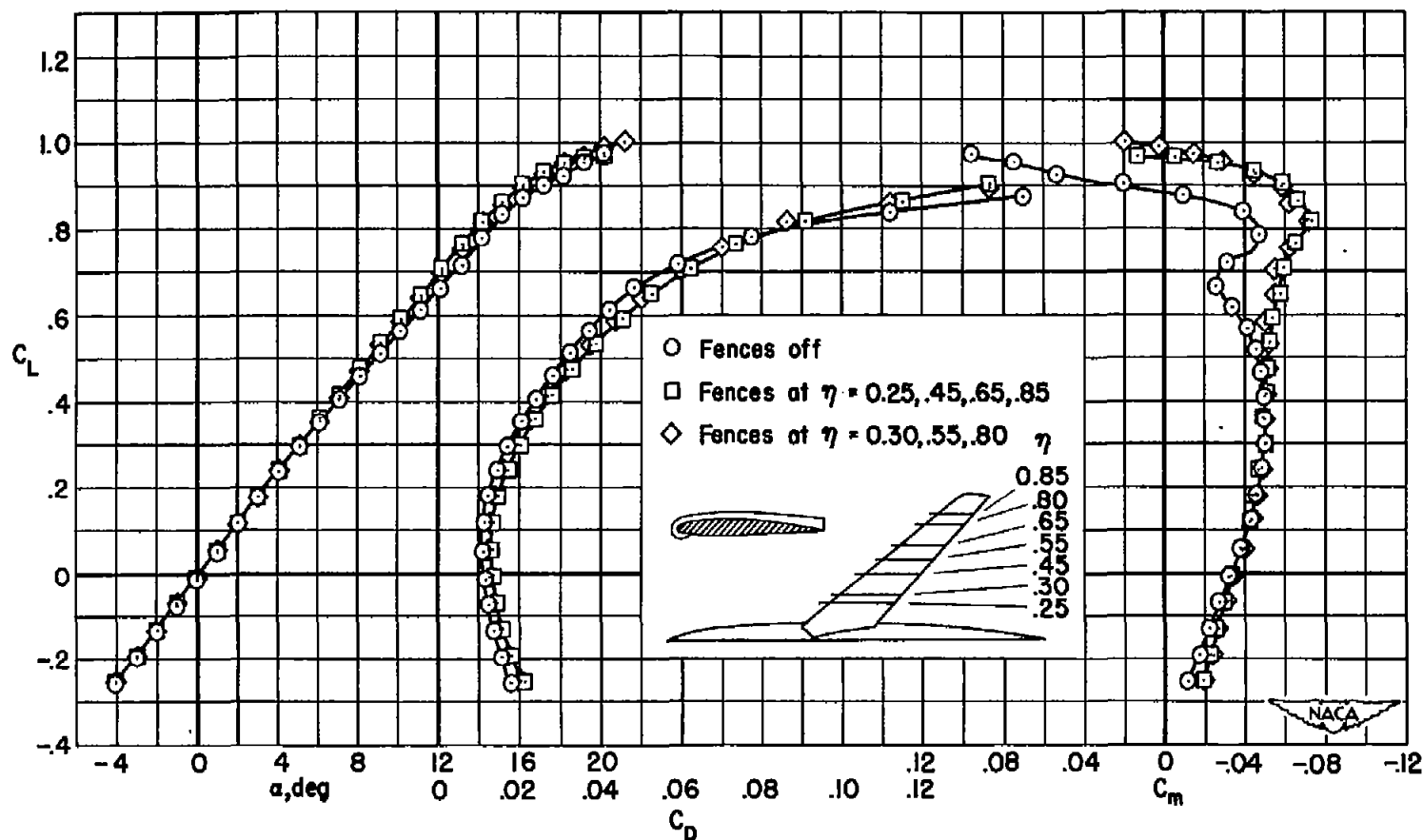


Figure 15.- The effect of three and four fences on the longitudinal characteristics of a wing-fuselage combination having a wing with 50° of sweepback and an aspect ratio of 5.04; $M = 0.417$; $R = 4,300,000$.

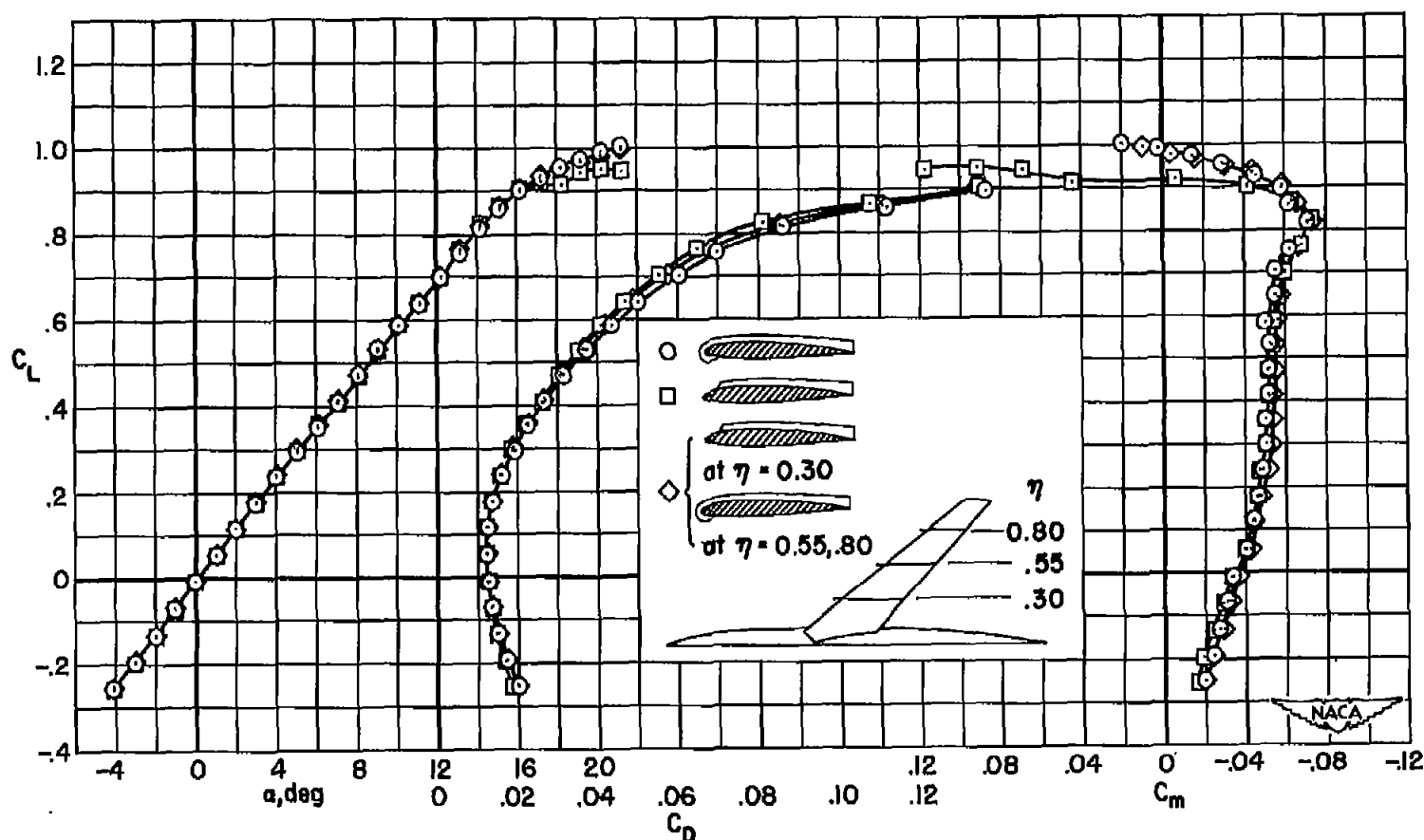
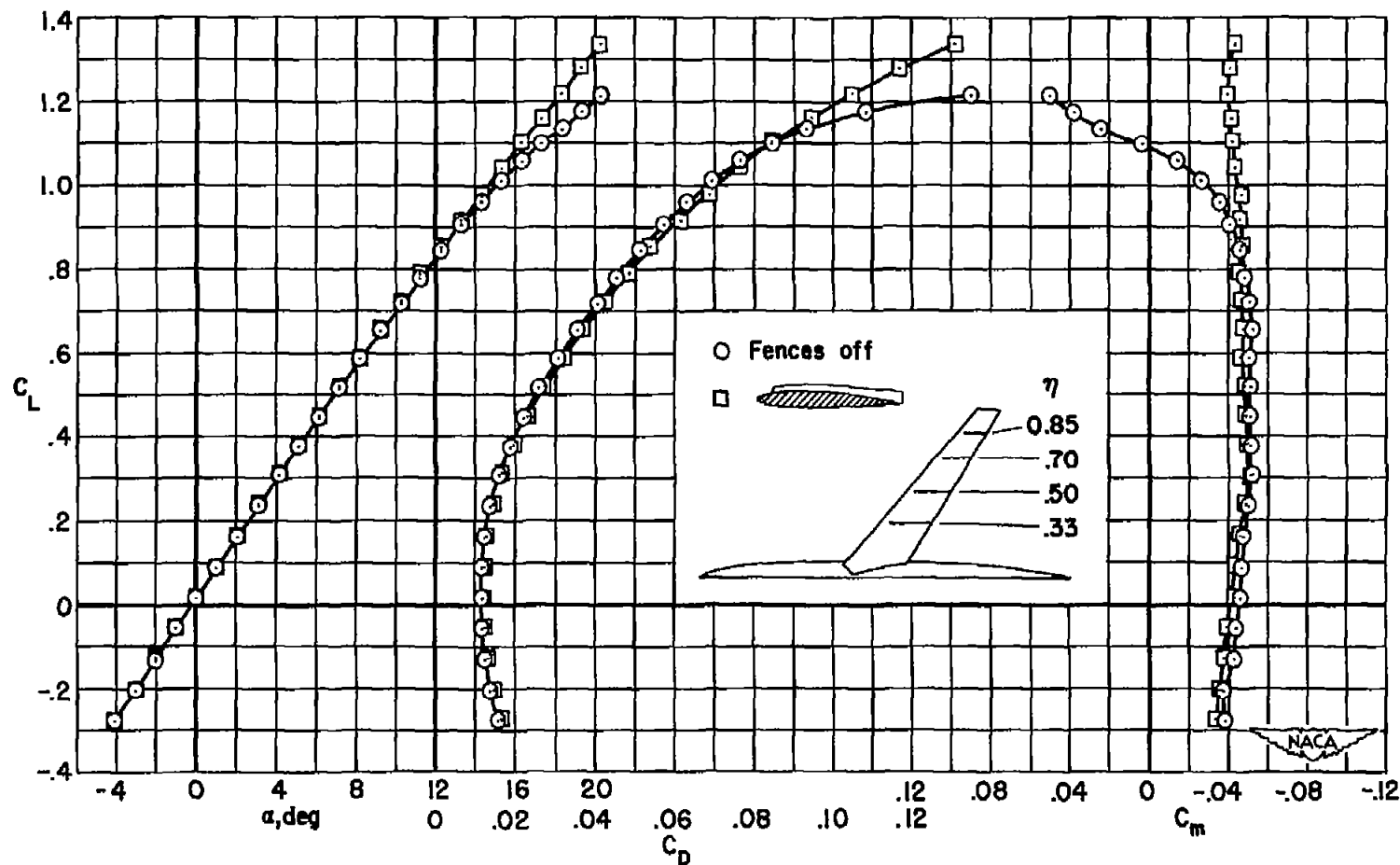


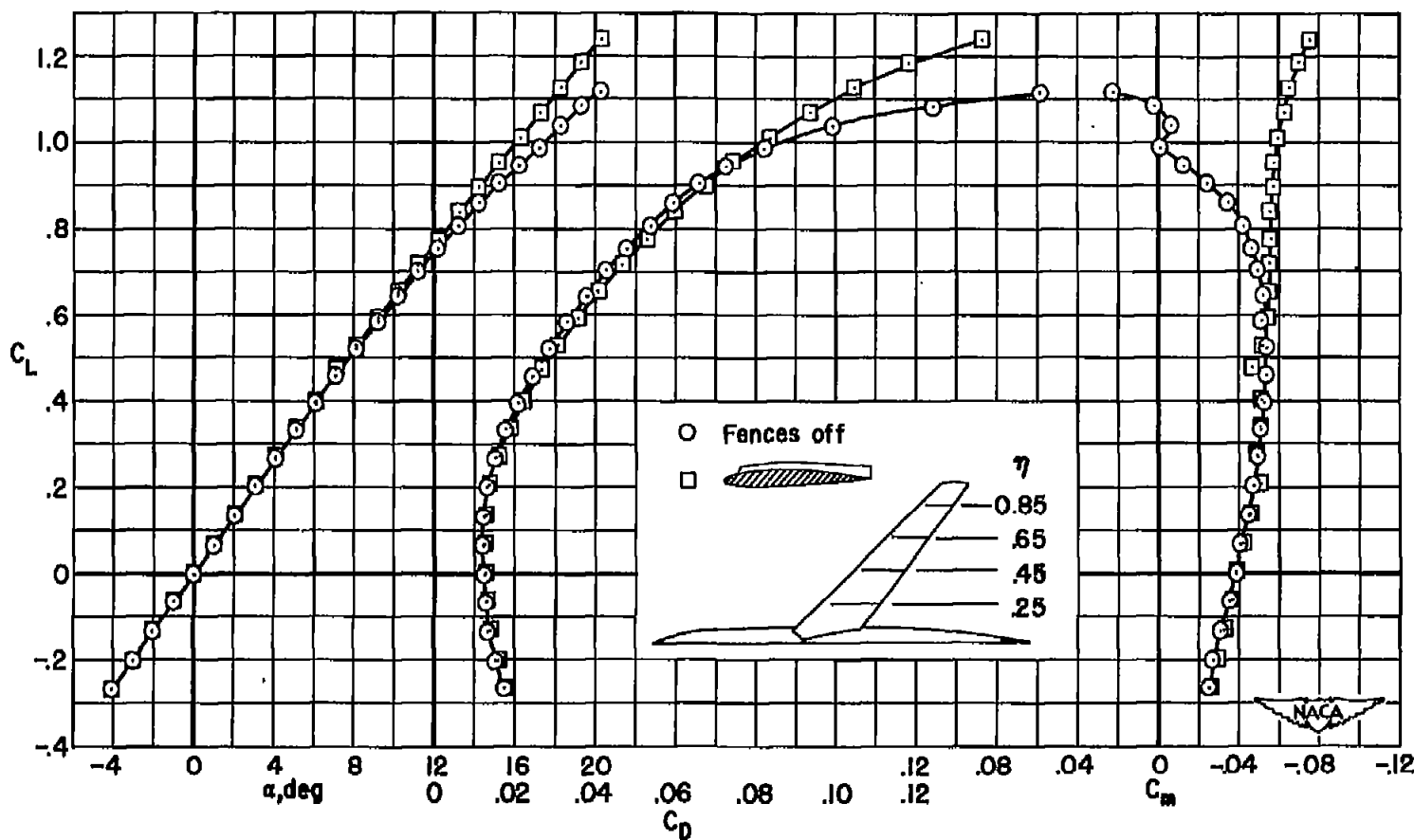
Figure 16.- The effect of three complete and partial-chord fences on the longitudinal characteristics of a wing-fuselage combination having a wing with 50° of sweepback and an aspect ratio of 5.04; $M = 0.417$; $R = 4,300,000$.



(a) $\Lambda = 40^\circ$

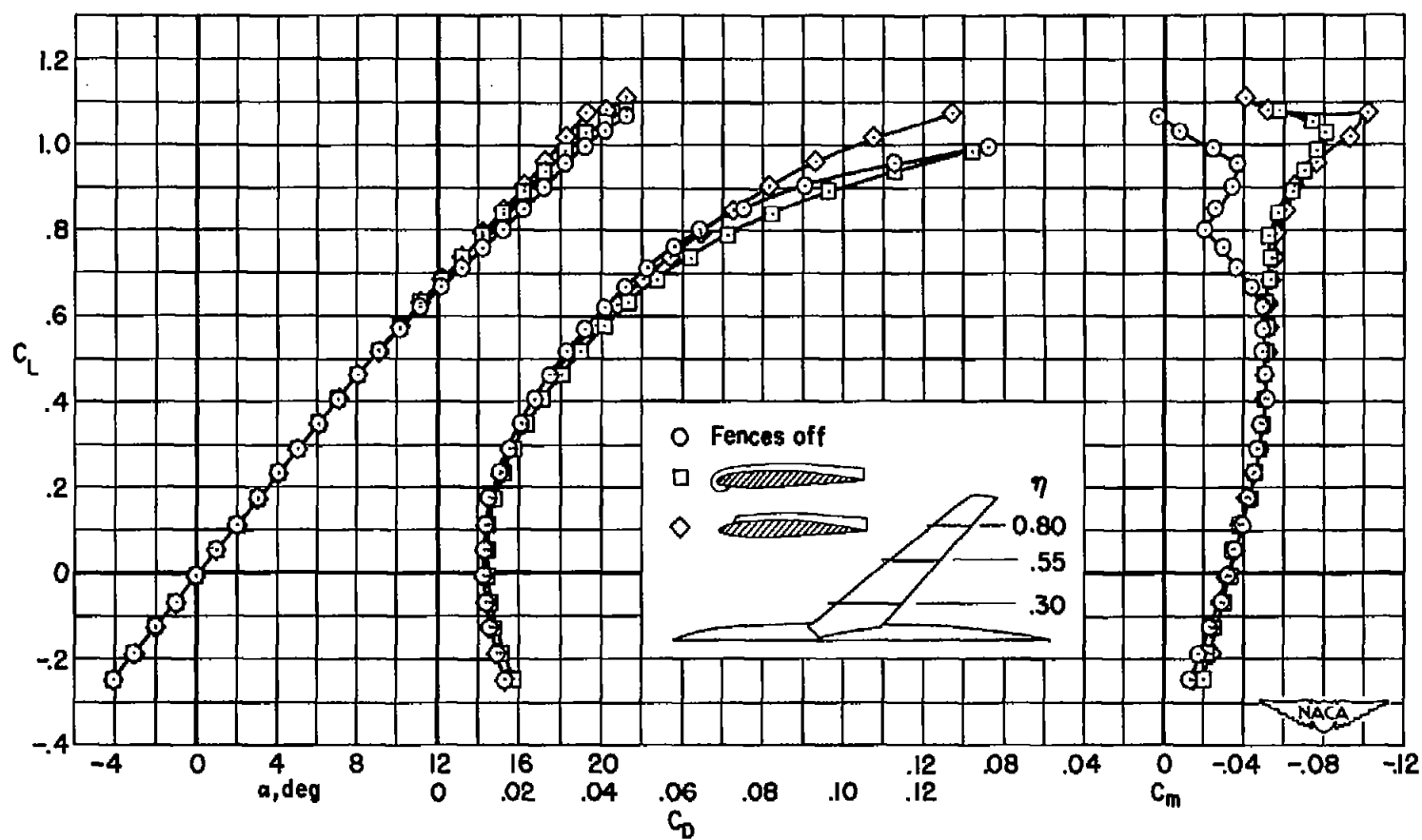
Figure 17.- The effect of fences at low speed on the longitudinal characteristics of the wing-fuselage combinations; $M = 0.165$; $R = 8,000,000$.

CONFIDENTIAL



(b) $\Lambda = 45^\circ$

Figure 17.- Continued.



(c) $\Lambda = 50^\circ$

Figure 17.- Concluded.

CONFIDENTIAL

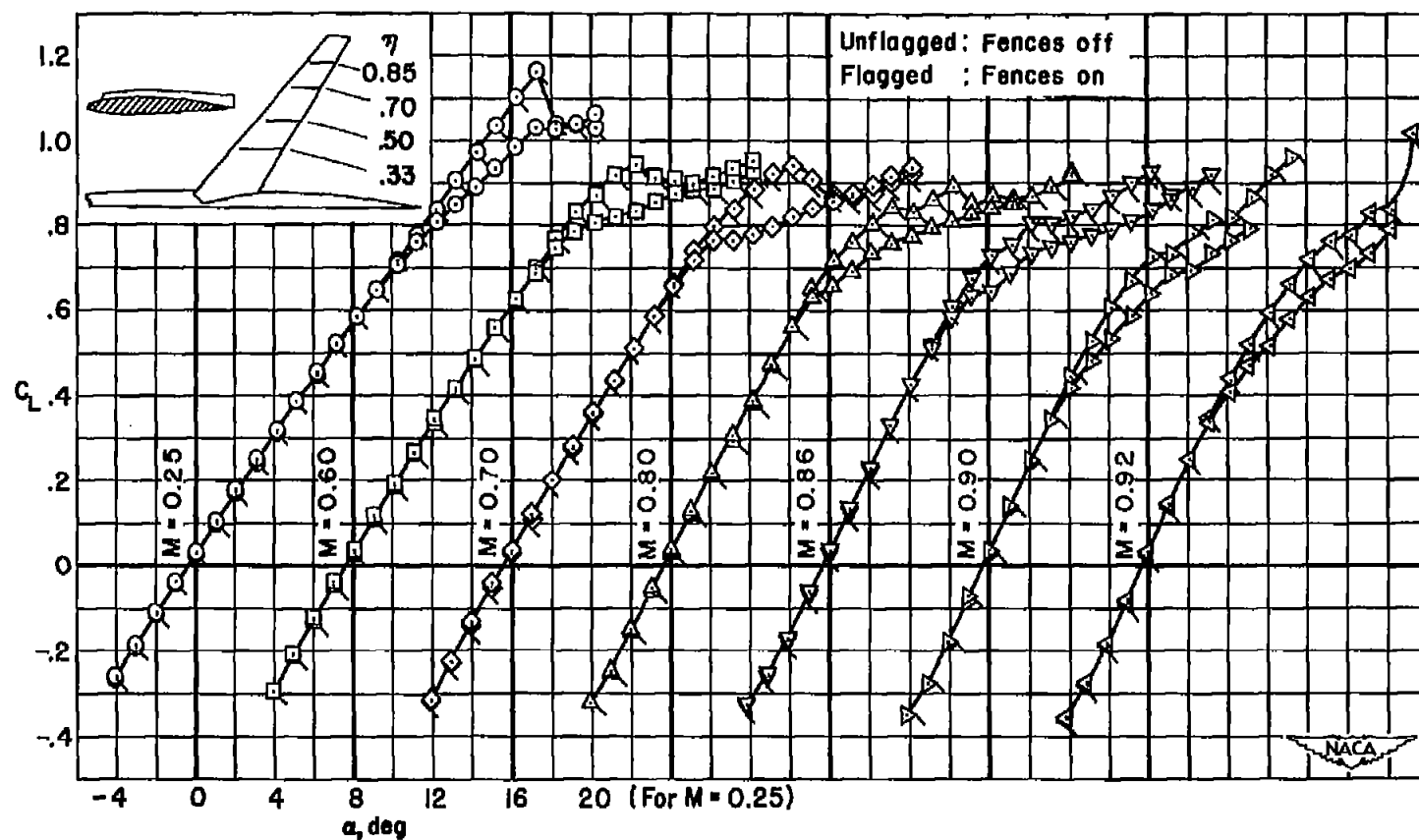
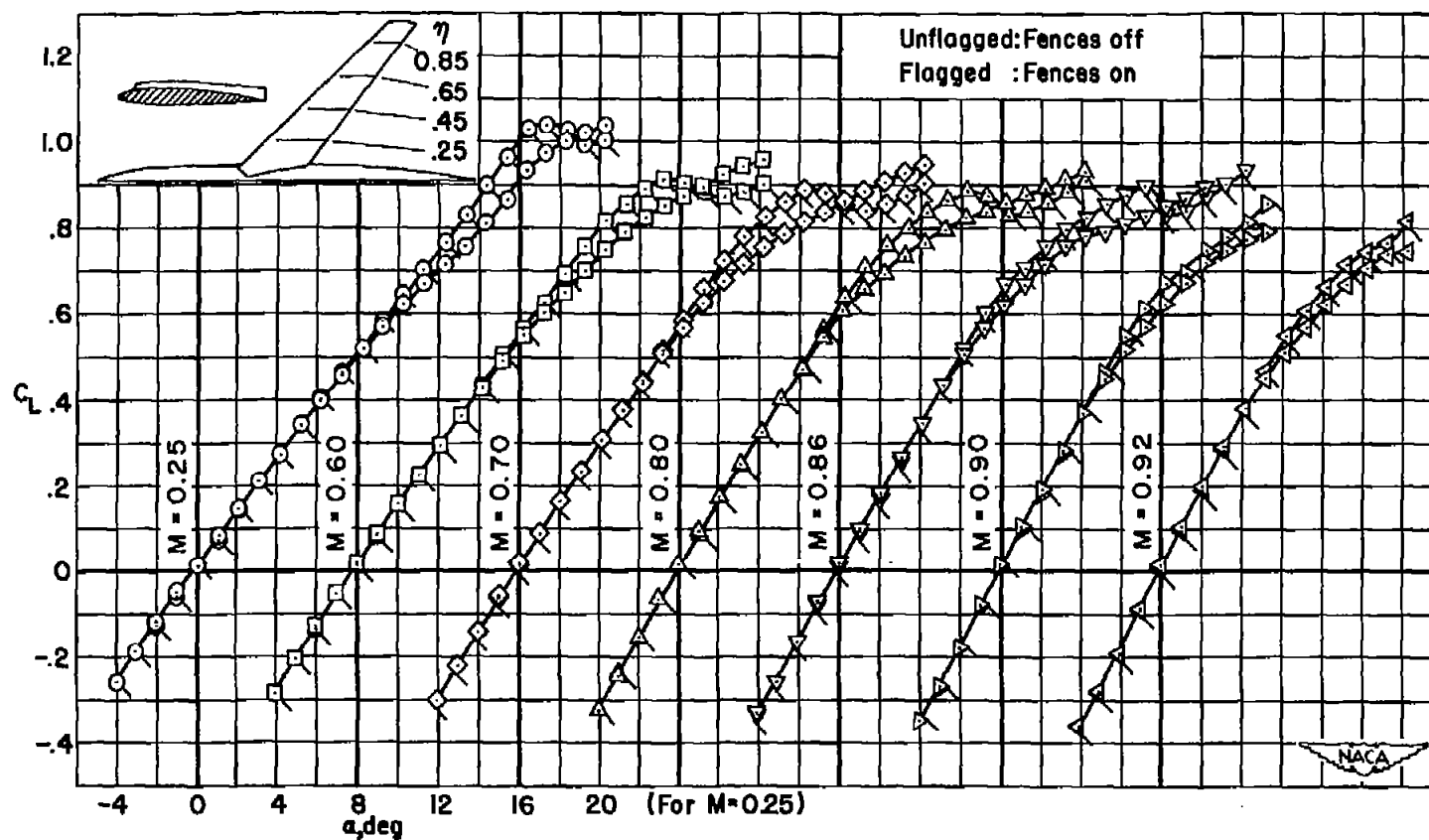
(a) $\Lambda = 40^\circ$

Figure 18.- The effect of wing fences at several Mach numbers on the lift characteristics of the wing-fuselage combinations; $R = 2,000,000$.



(b) $\Lambda = 45^\circ$

Figure 18.- Continued.

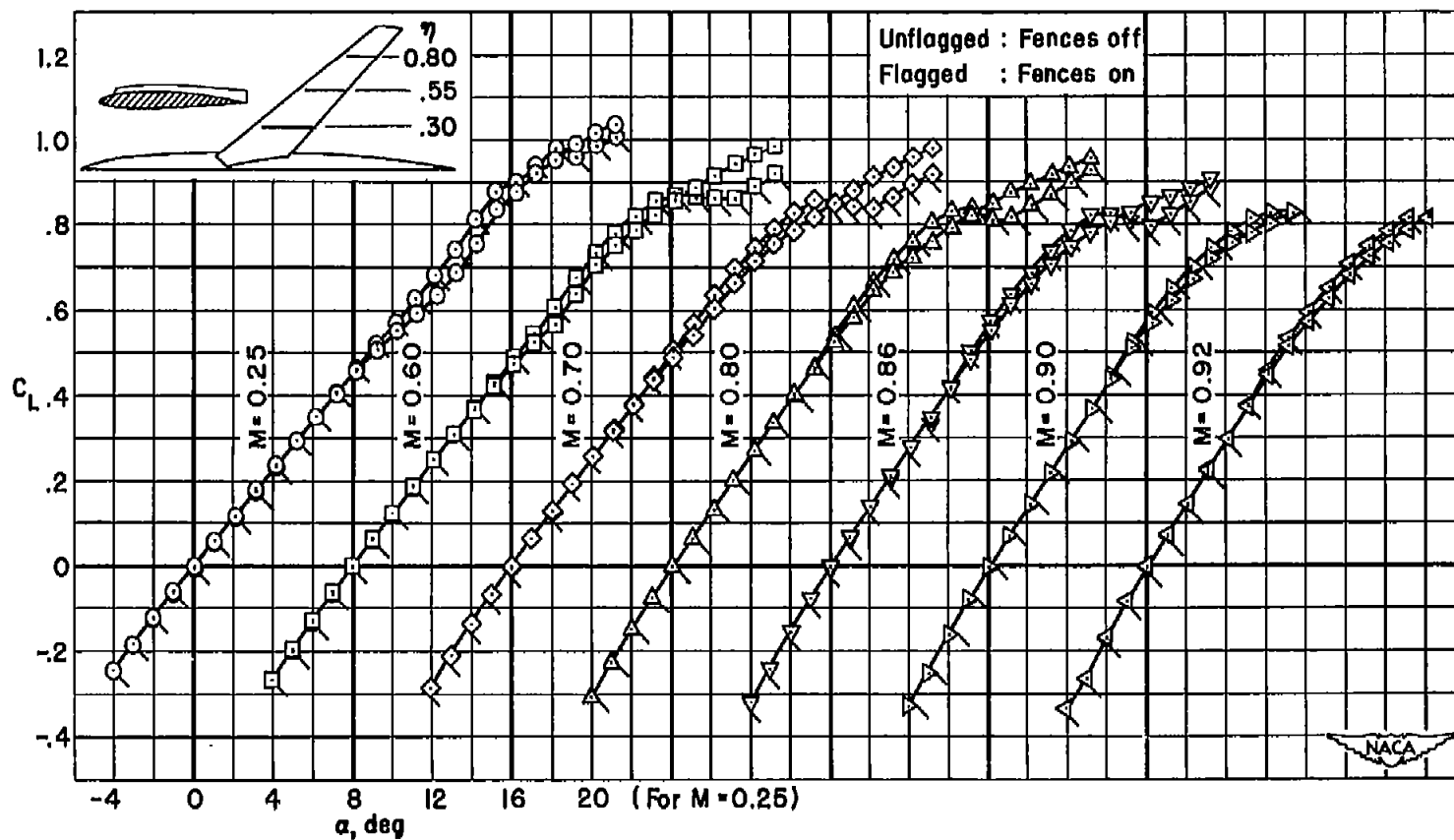
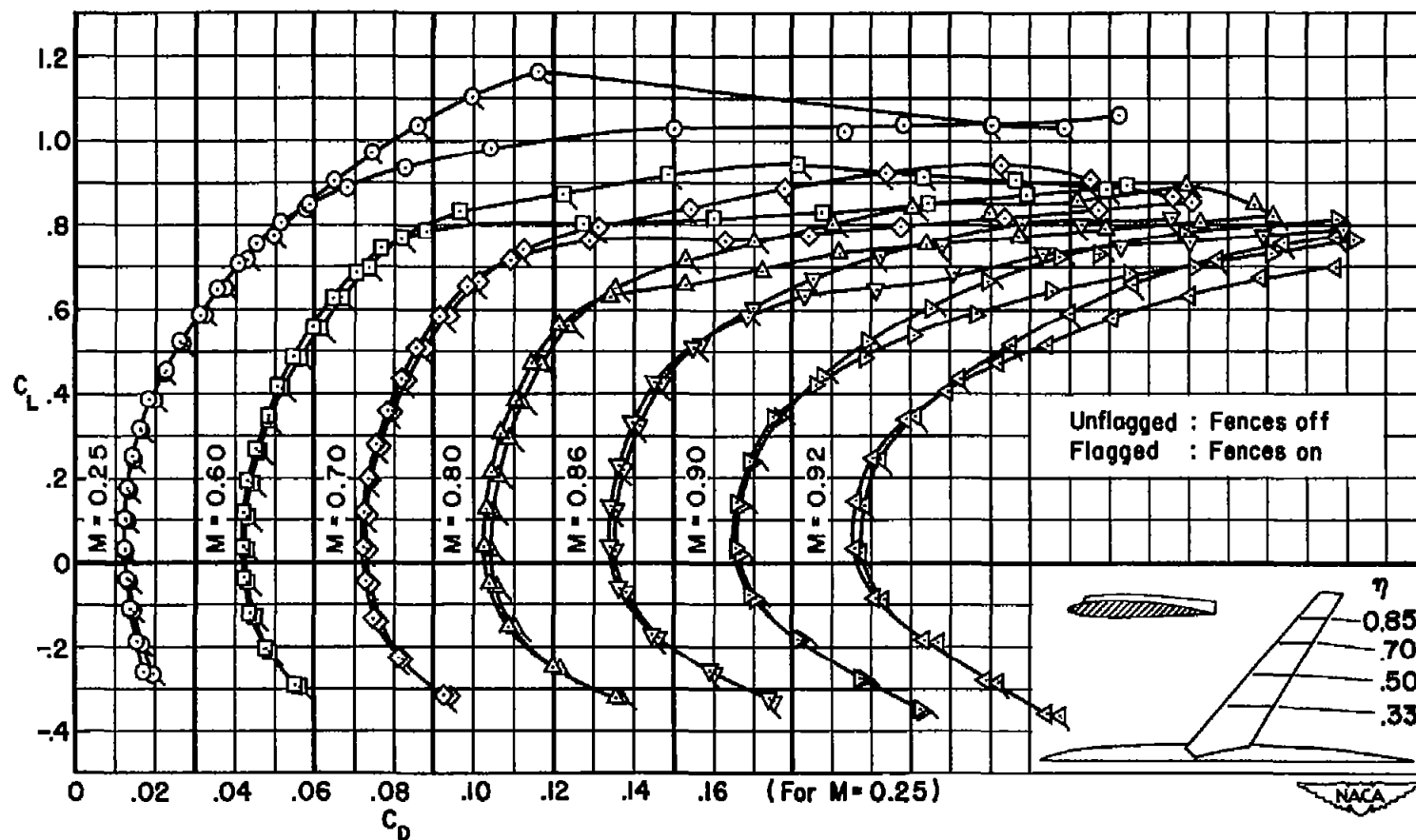
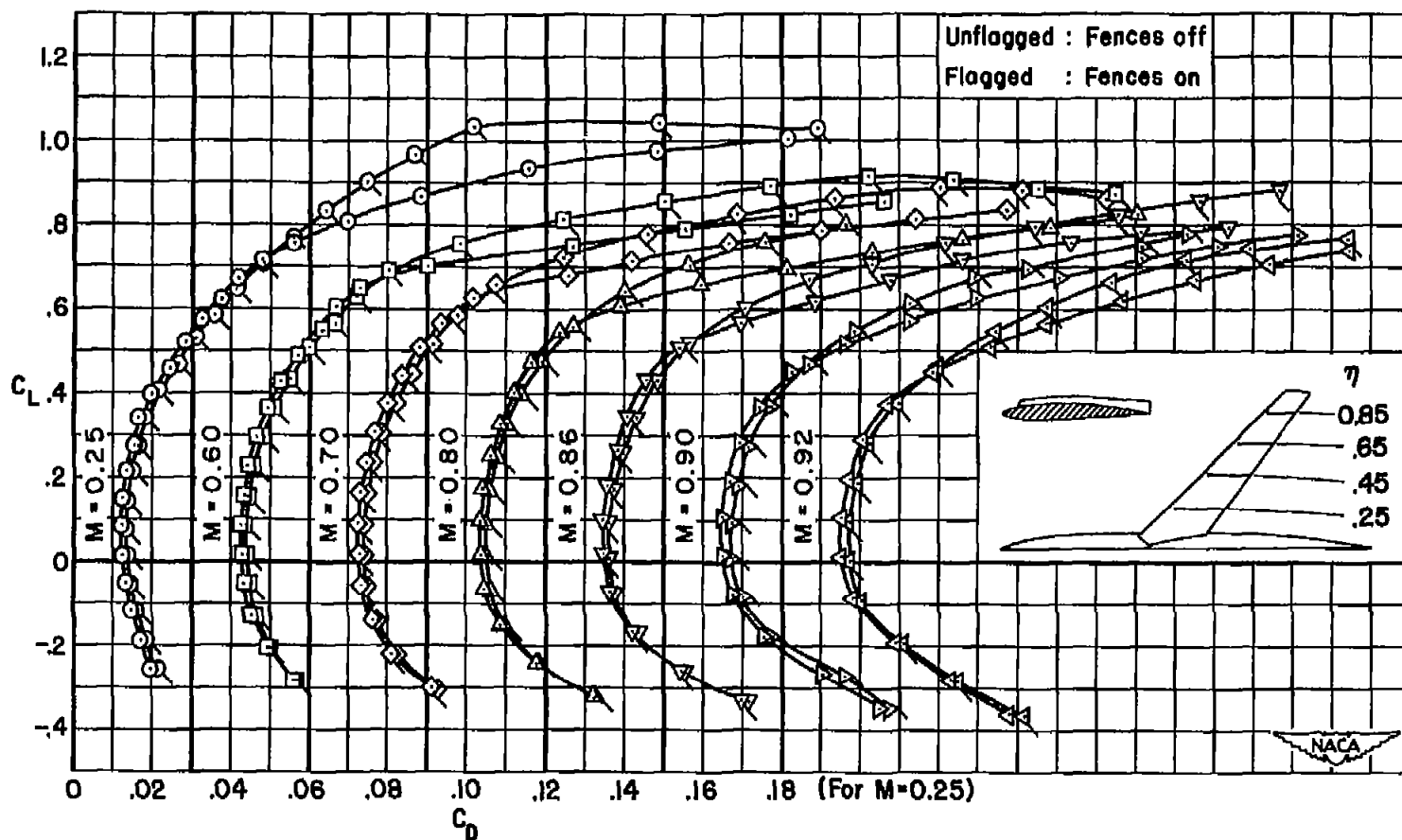
(c) $\Lambda = 50^\circ$

Figure 18.- Concluded.



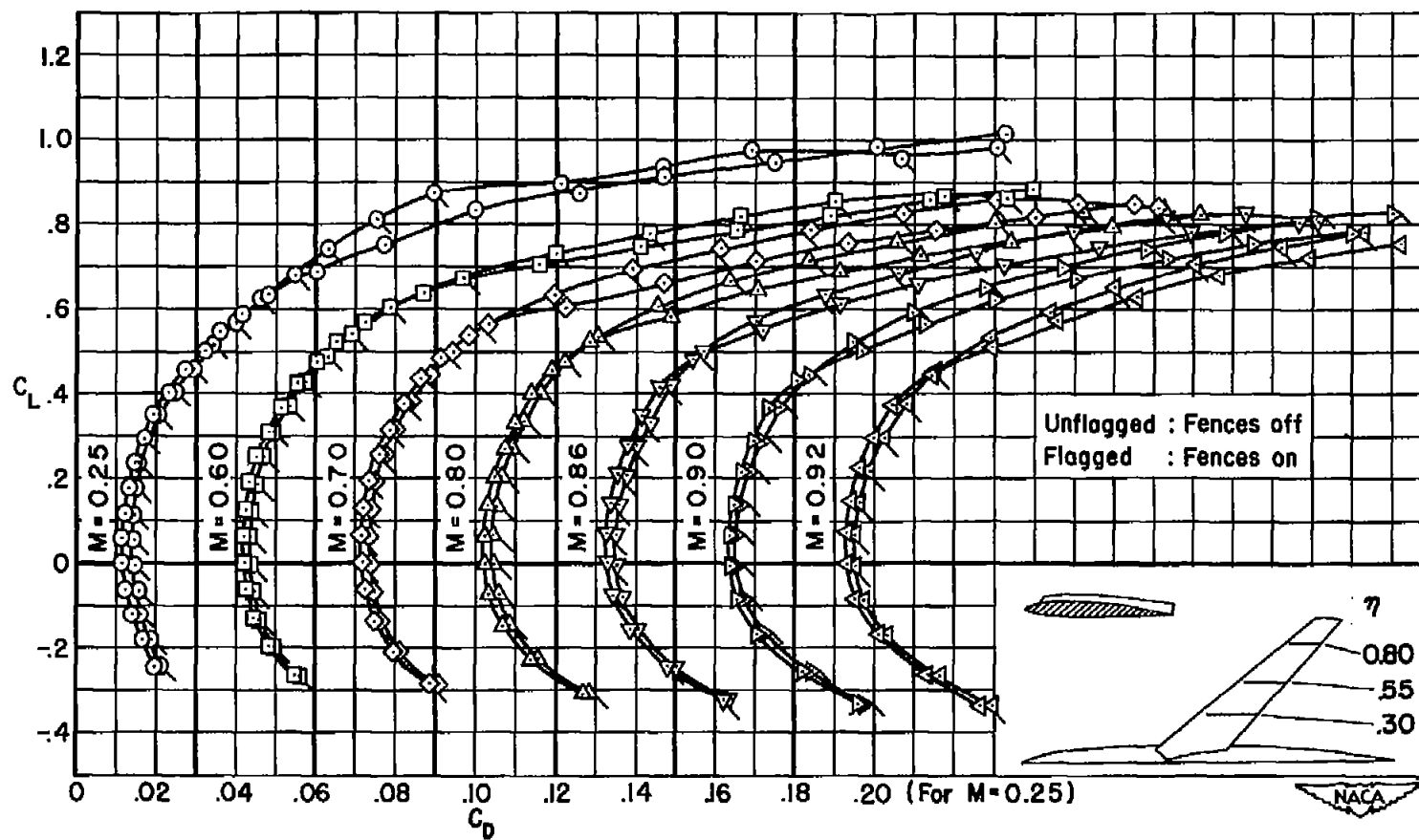
(a) $\Lambda = 40^\circ$

Figure 19.- The effect of wing fences at several Mach numbers on the drag characteristics of the wing-fuselage combinations; $R = 2,000,000$.



(b) $\Lambda = 45^\circ$

Figure 19.- Continued.



(c) $\Lambda = 50^\circ$

Figure 19.- Concluded.

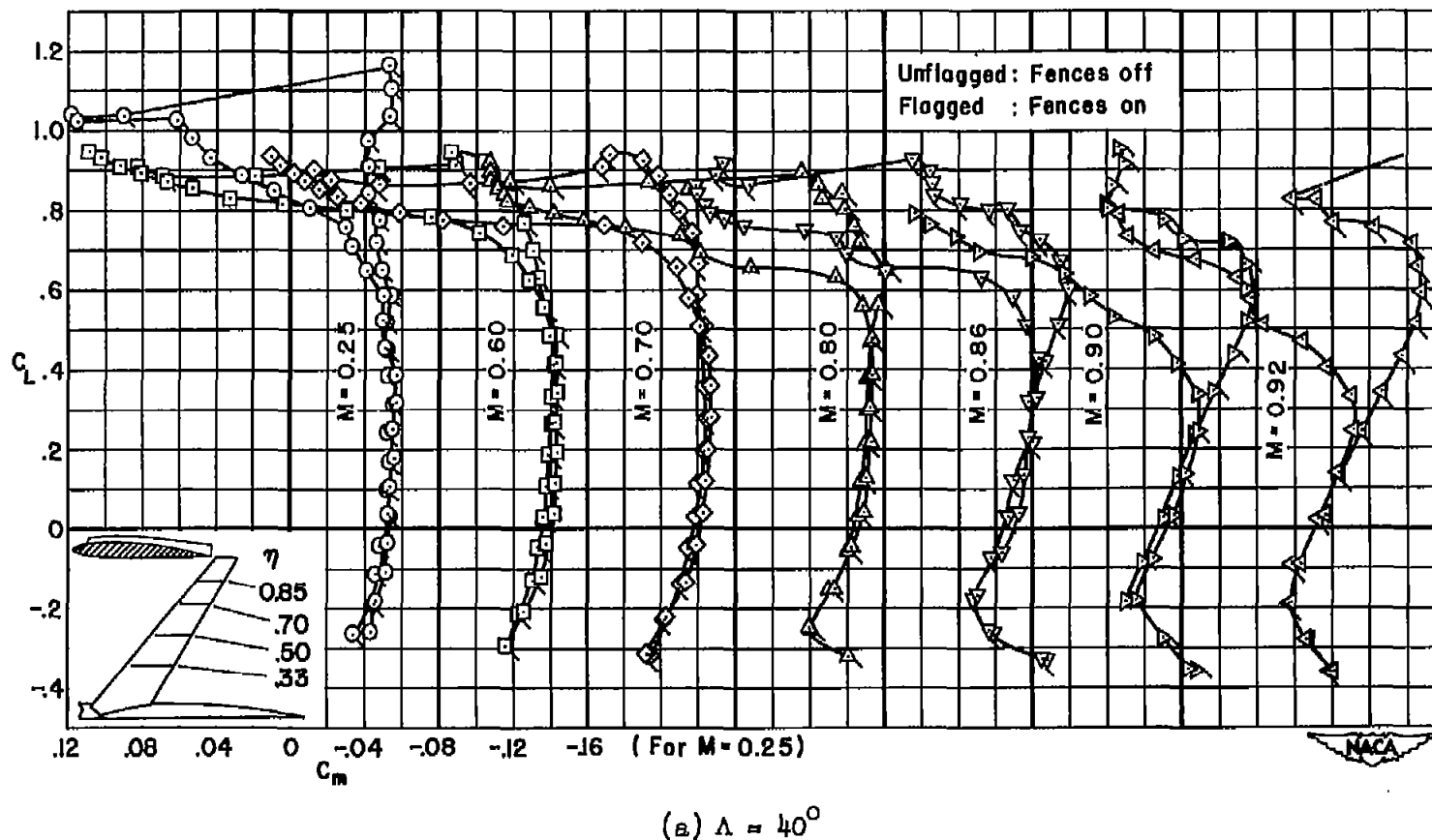
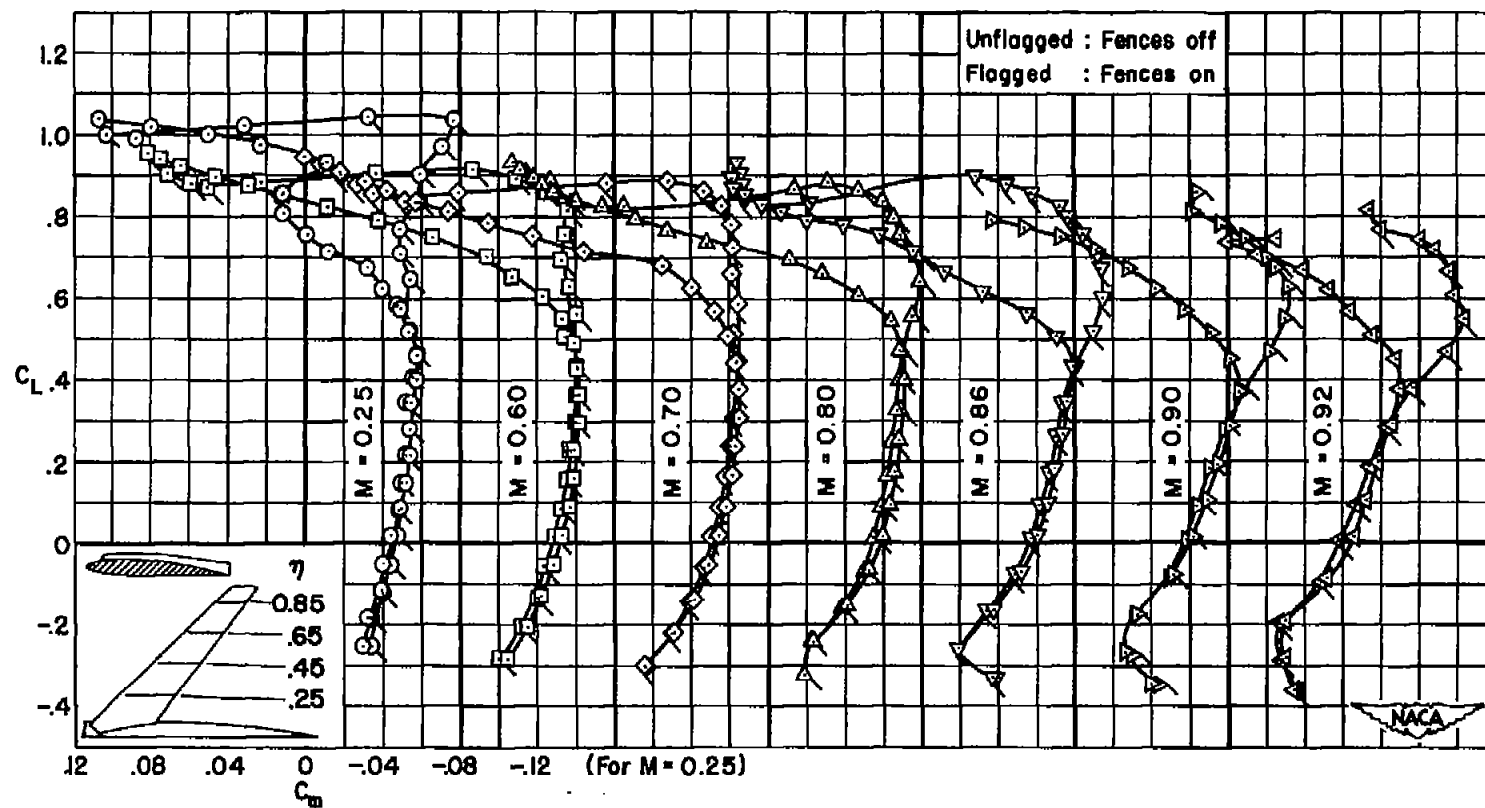
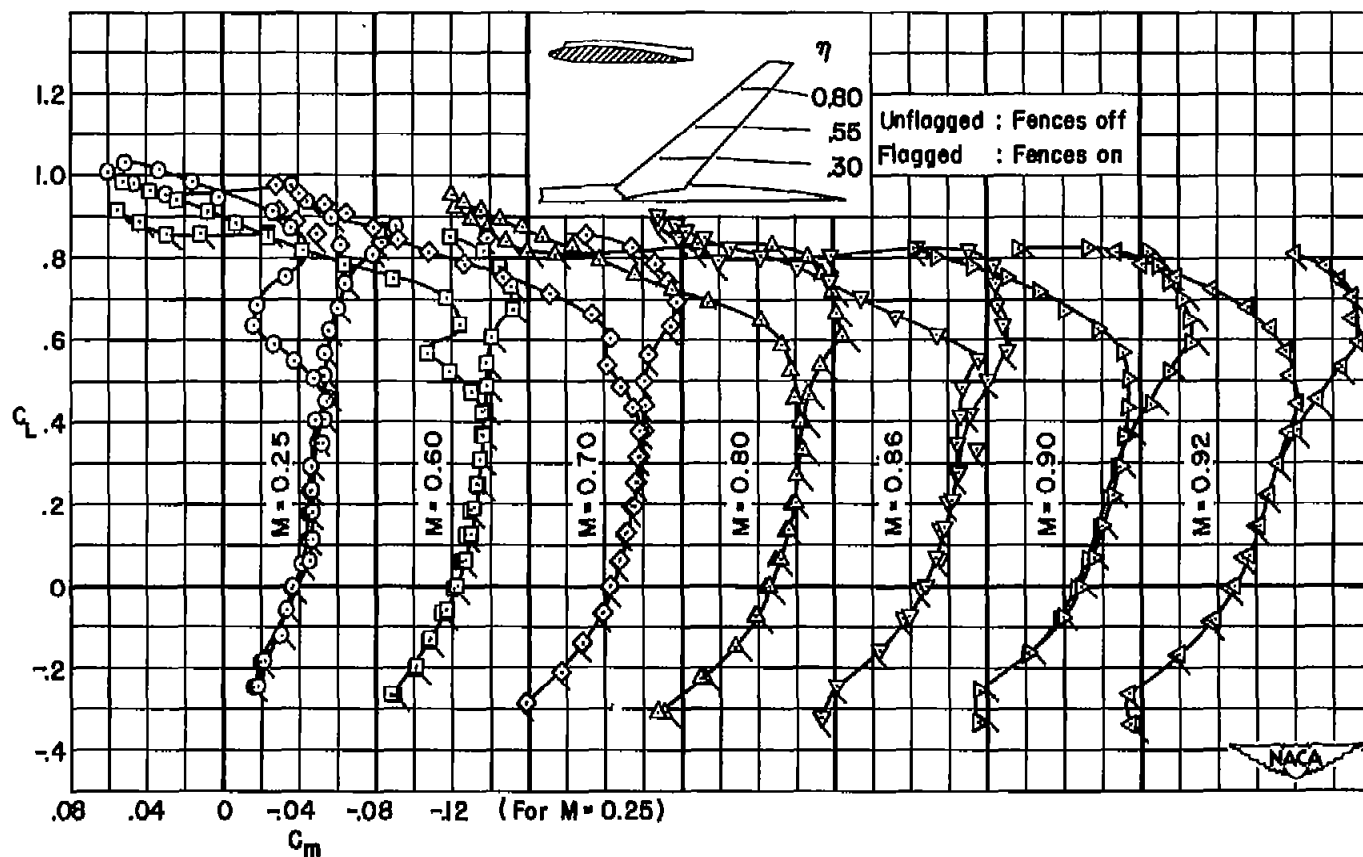


Figure 20.- The effect of wing fences at several Mach numbers on the pitching-moment characteristics of the wing-fuselage combinations; $R = 2,000,000$.



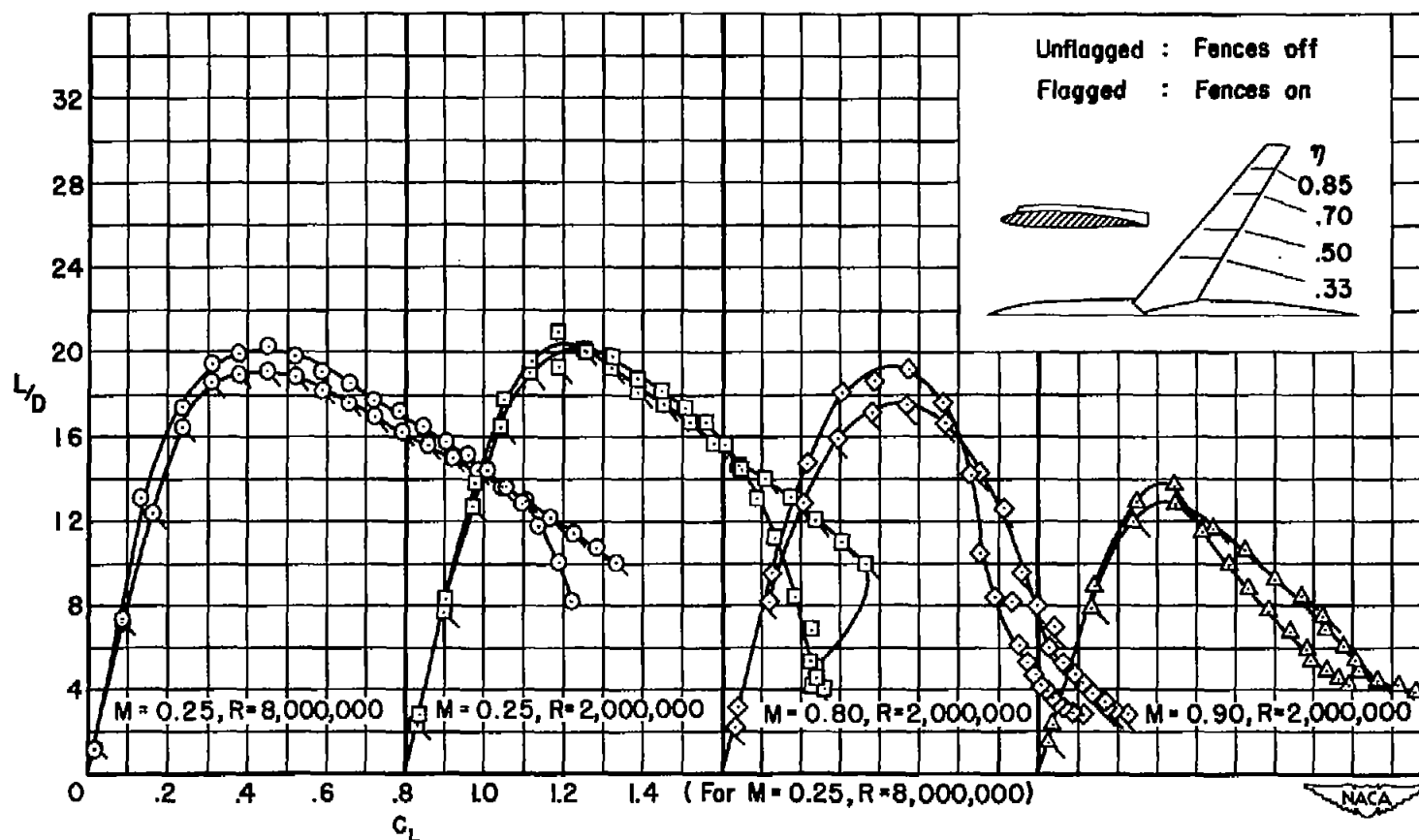
(b) $\Lambda = 45^\circ$

Figure 20.- Continued.



(c) $\Lambda = 50^\circ$

Figure 20.- Concluded.



(a) $\Lambda = 40^\circ$

Figure 21.- The effect of fences on the lift-drag ratios of the wing-fuselage combinations.

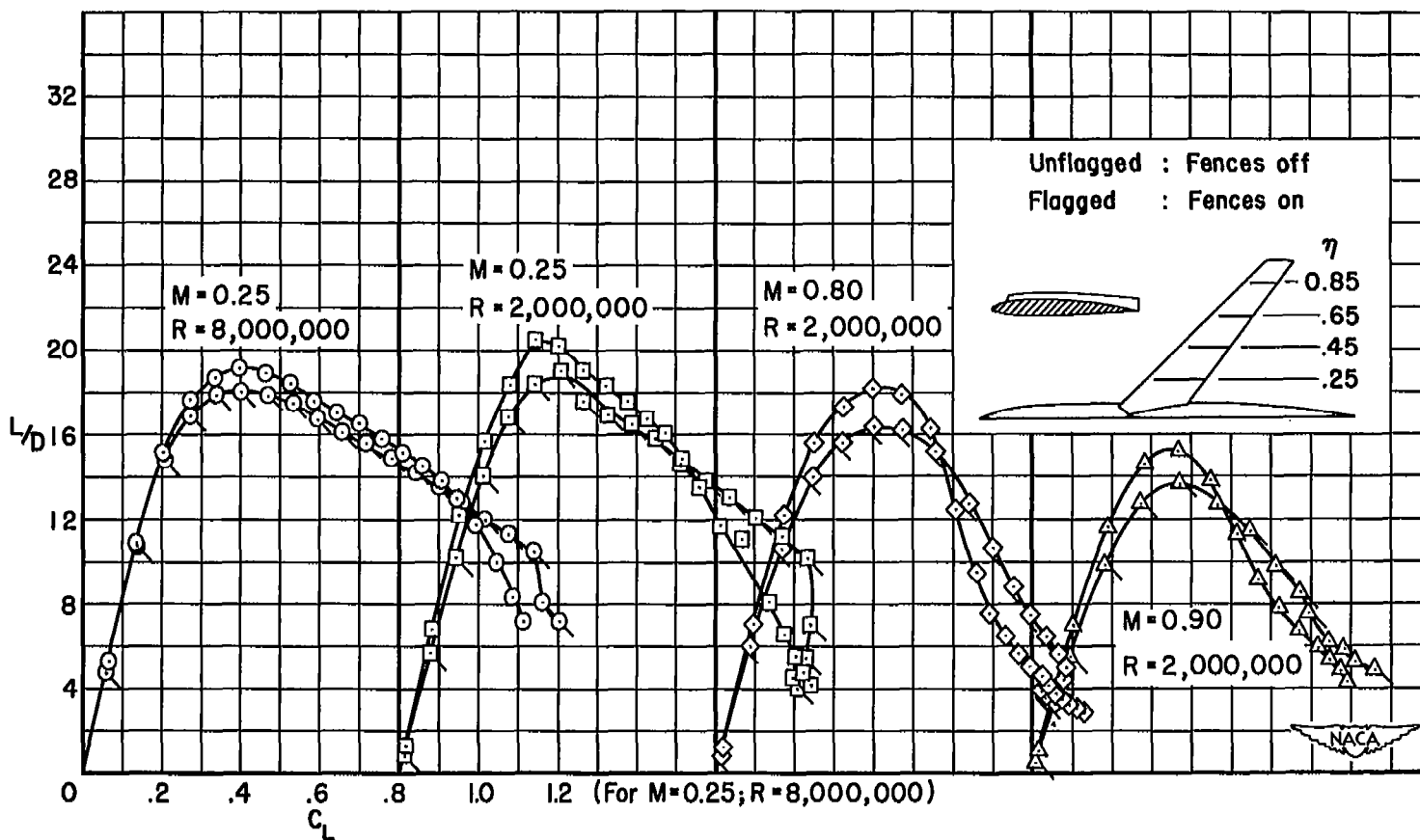
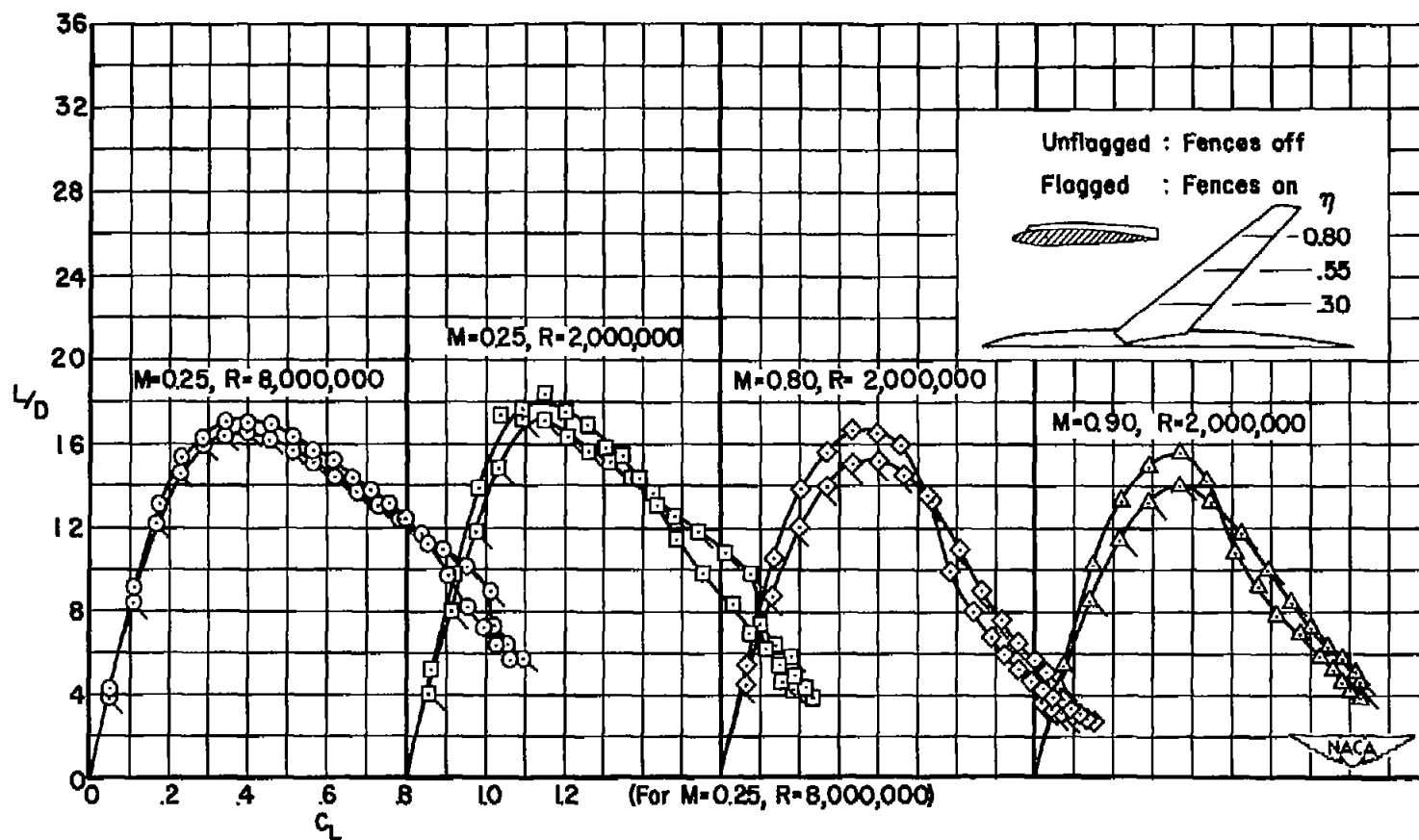
(b) $\Lambda = 45^\circ$

Figure 21.- Continued.



(c) $\Lambda = 50^\circ$

Figure 21.- Concluded.

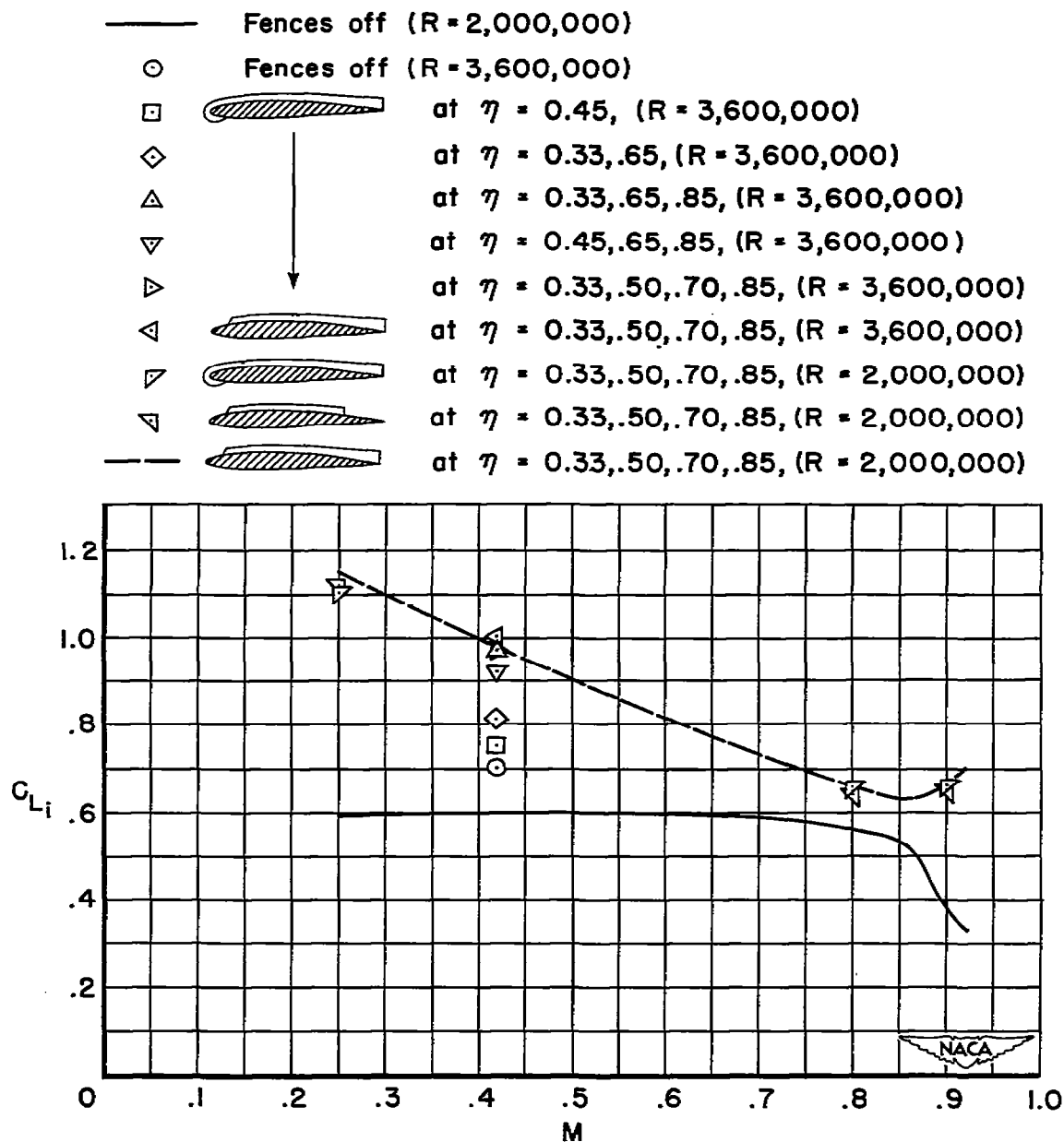
(a) $\Lambda = 40^\circ$

Figure 22.- The variation with Mach number of the inflection lift coefficients of the wing-fuselage combinations with and without wing fences.

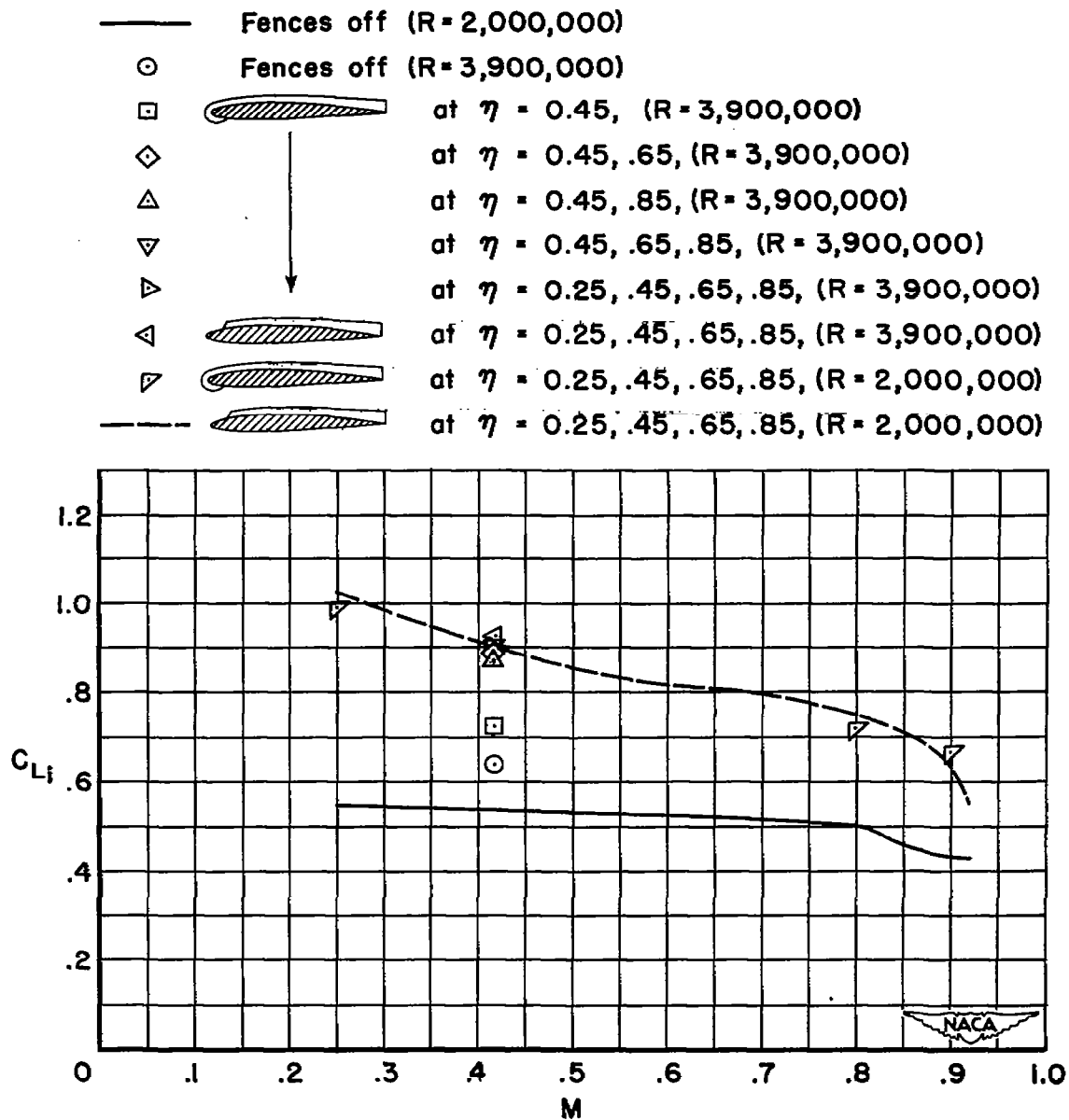


Figure 22.- Continued.

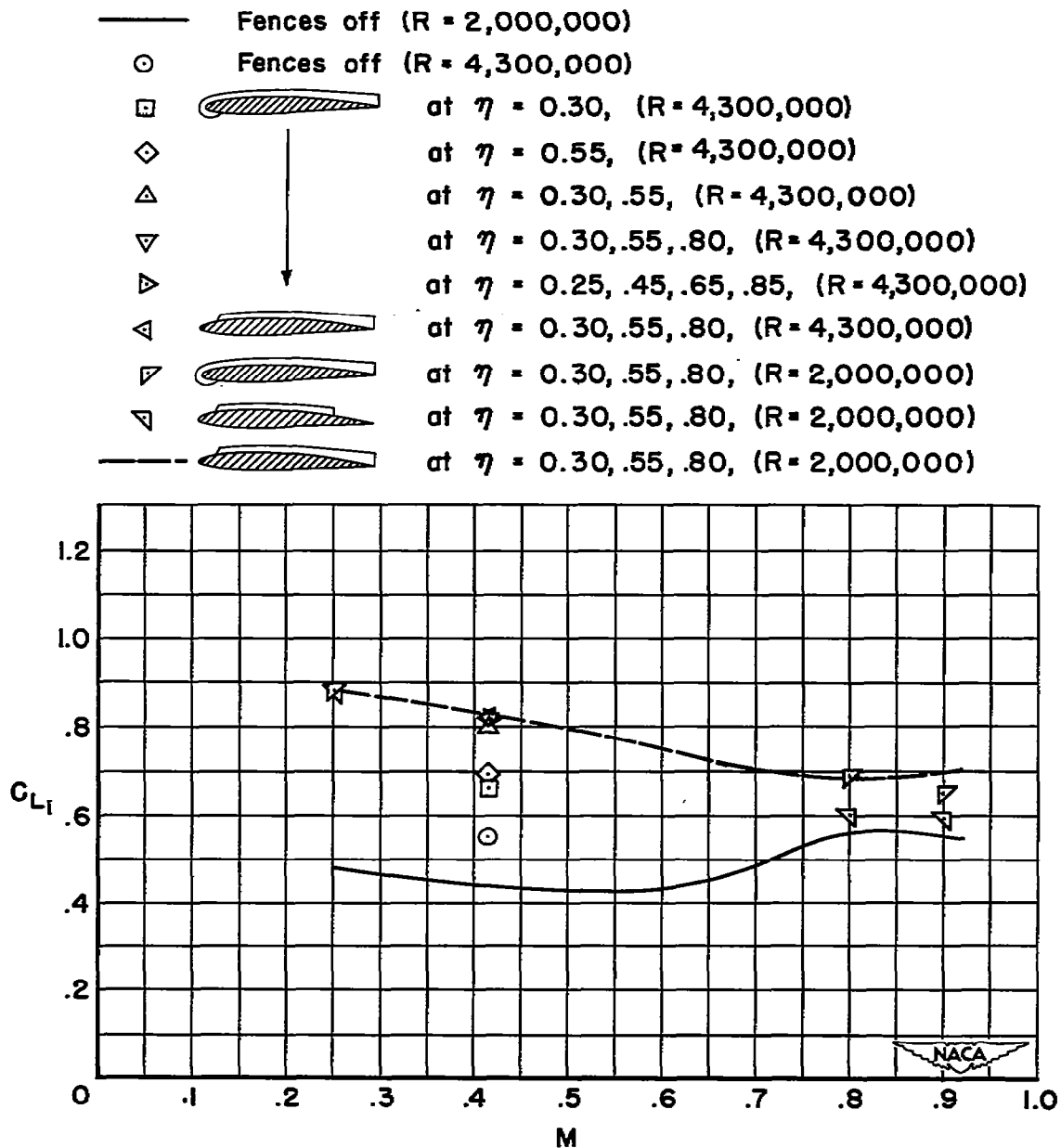
(c) $\Lambda = 50^\circ$

Figure 22.- Concluded.

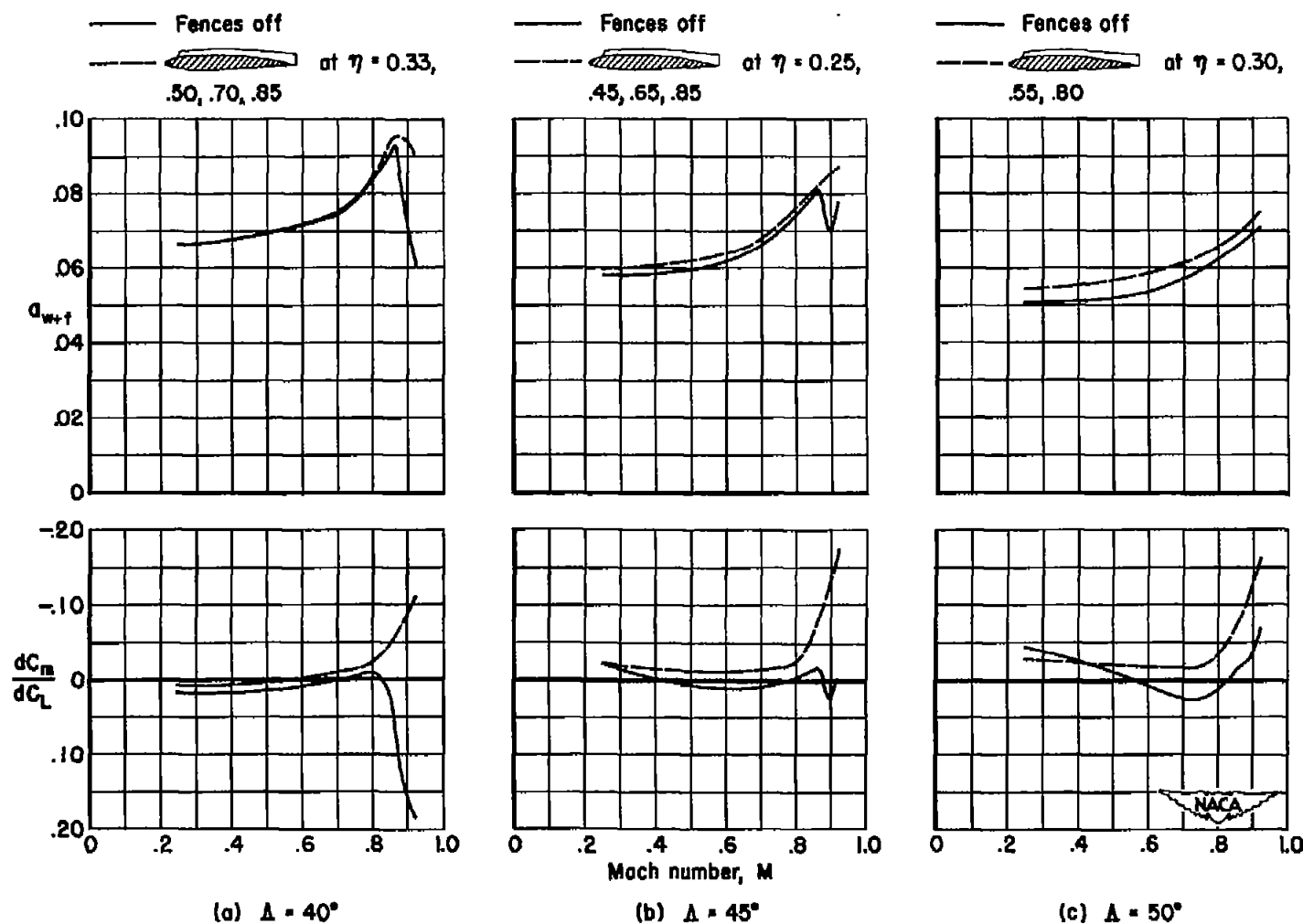


Figure 23.- The variations with Mach number of the slopes of the lift and pitching-moment curves of the wing-fuselage combinations with and without wing fences; $C_L = 0.40$; $R = 2,000,000$.

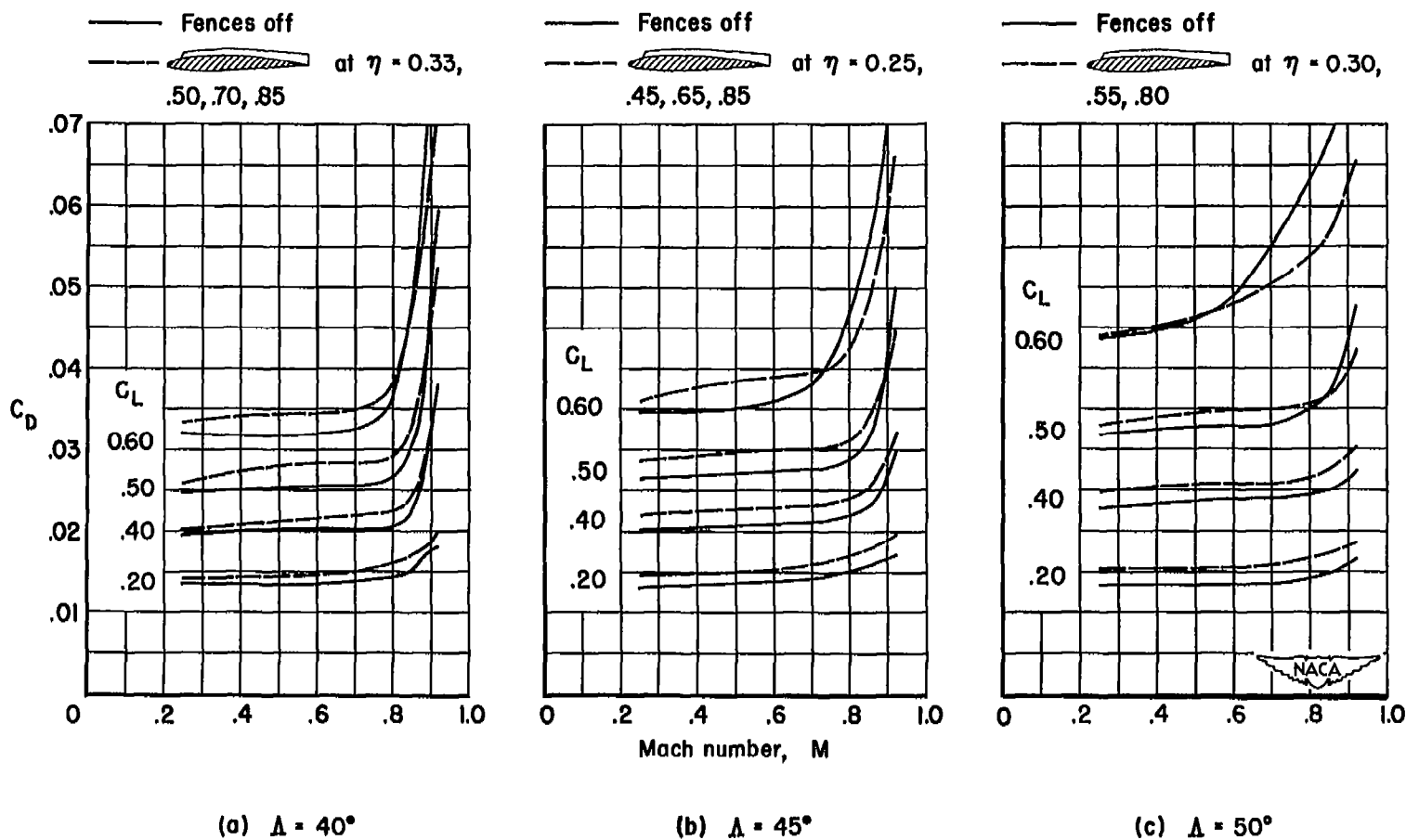
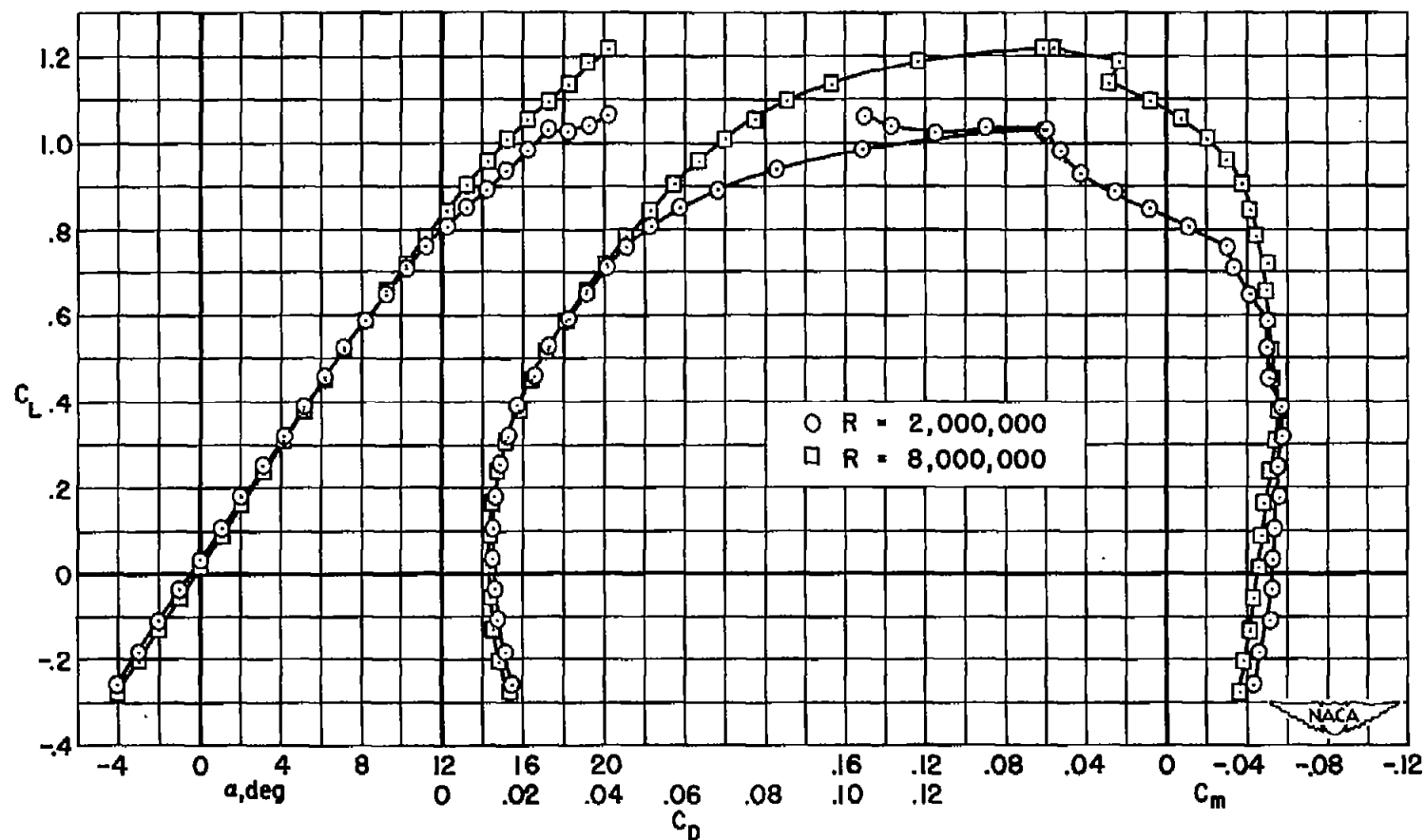
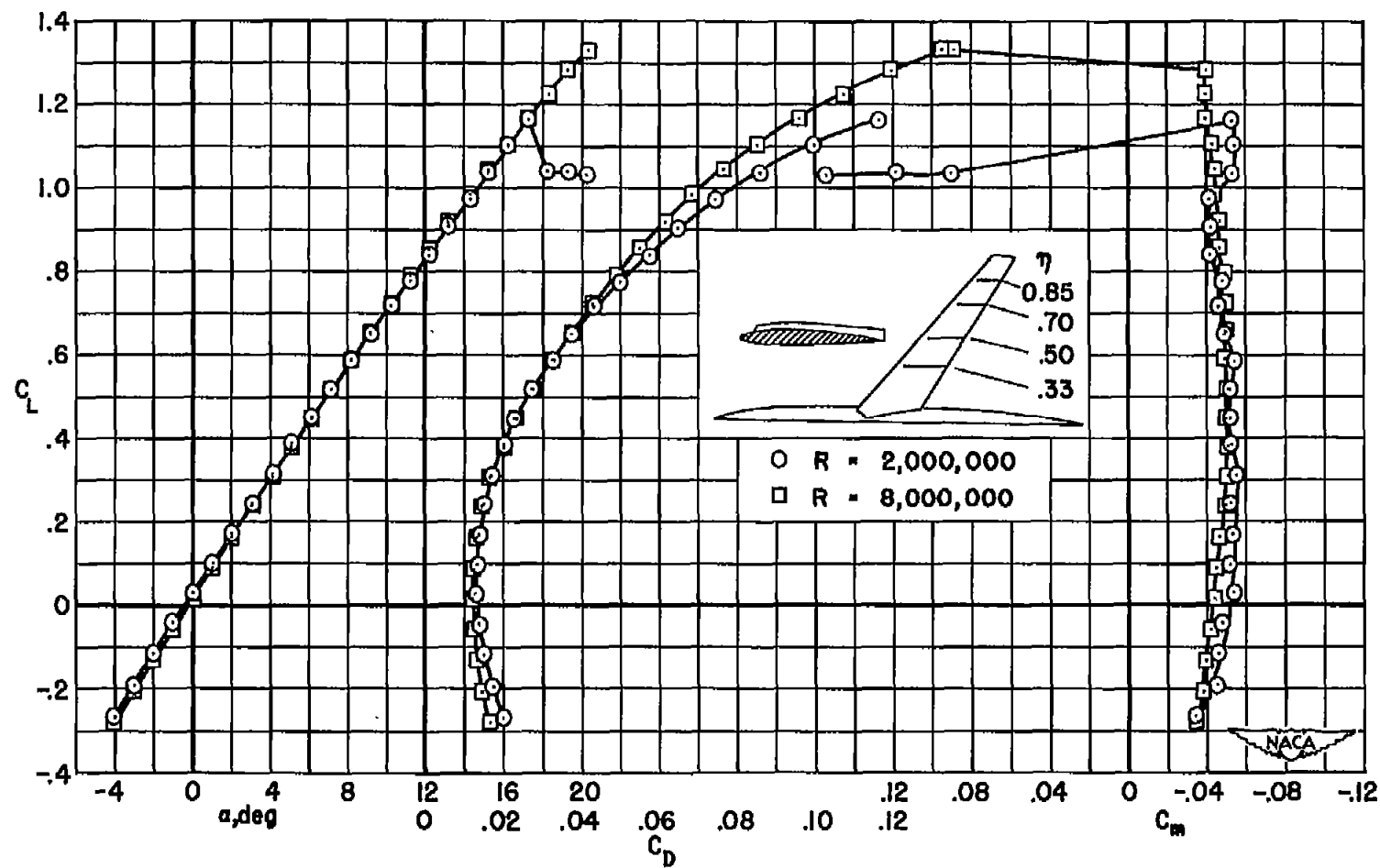


Figure 24.- The variation with Mach number of the drag coefficients of the wing-fuselage combinations with and without wing fences at several constant lift coefficients; $R = 2,000,000$.



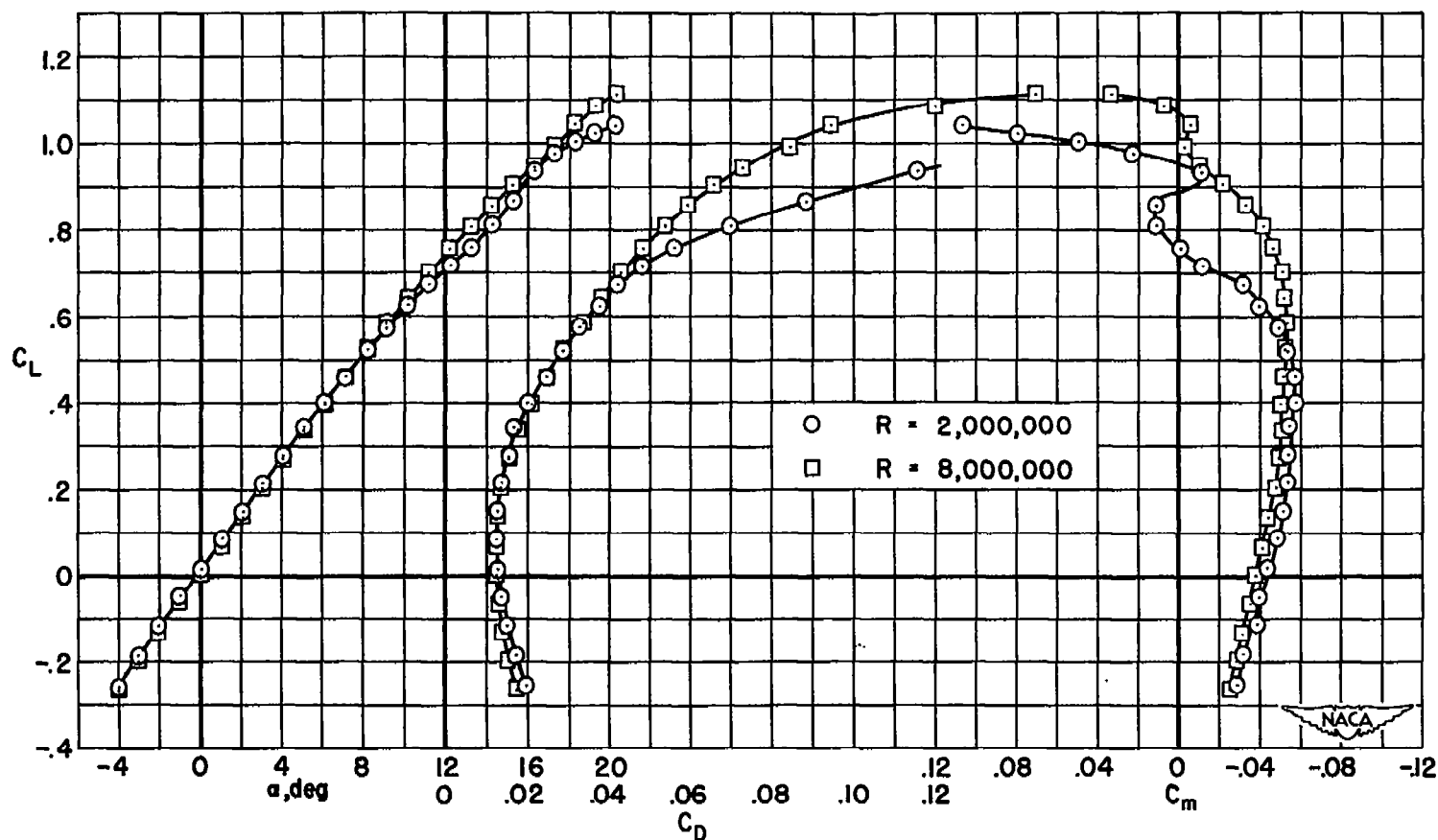
(a) Fences off.

Figure 25.- Effect of Reynolds number on the longitudinal characteristics of a wing-fuselage combination using a wing with 40° of sweepback and an aspect ratio of 7.00; $M = 0.25$.



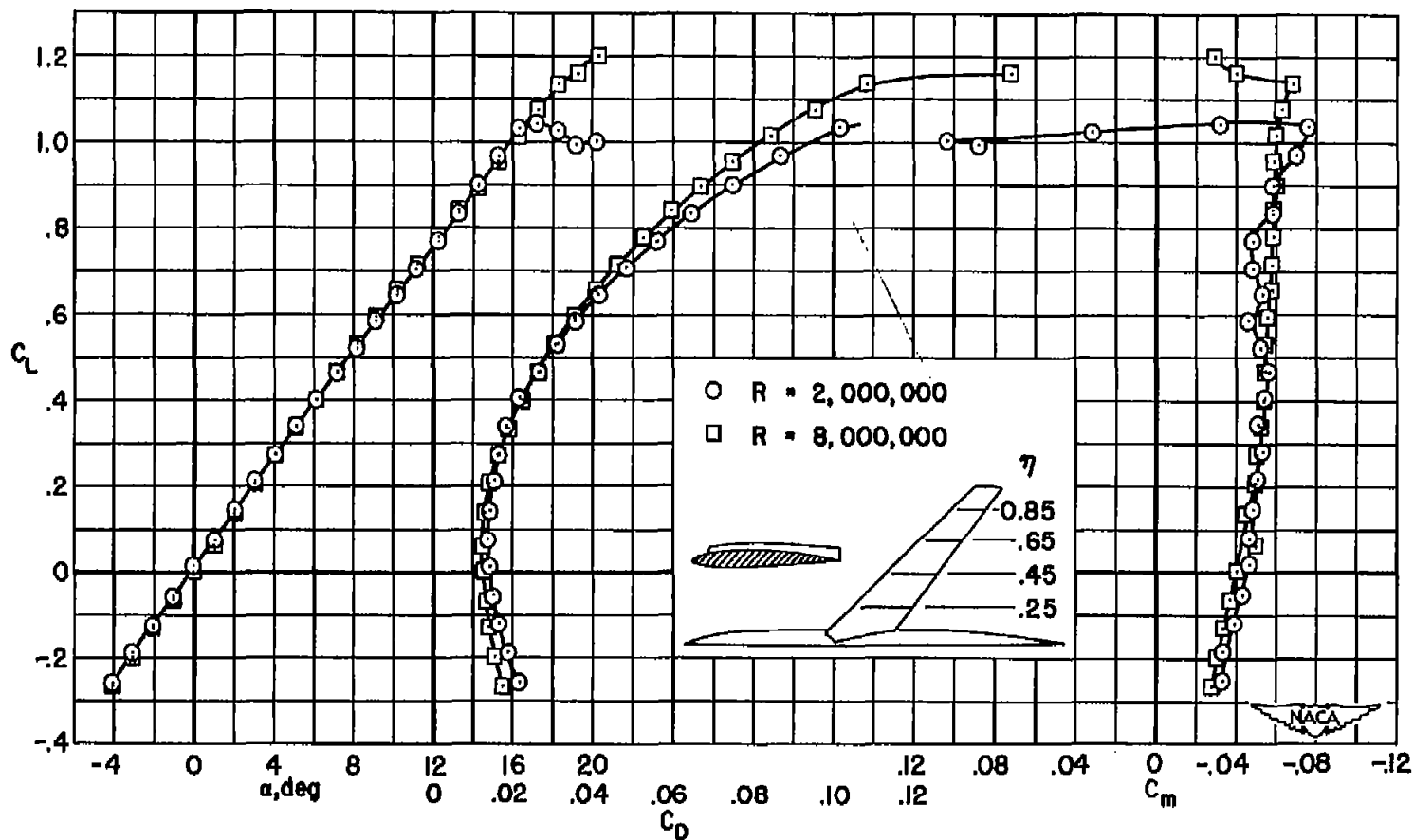
(b) Fences on.

Figure 25.- Concluded.



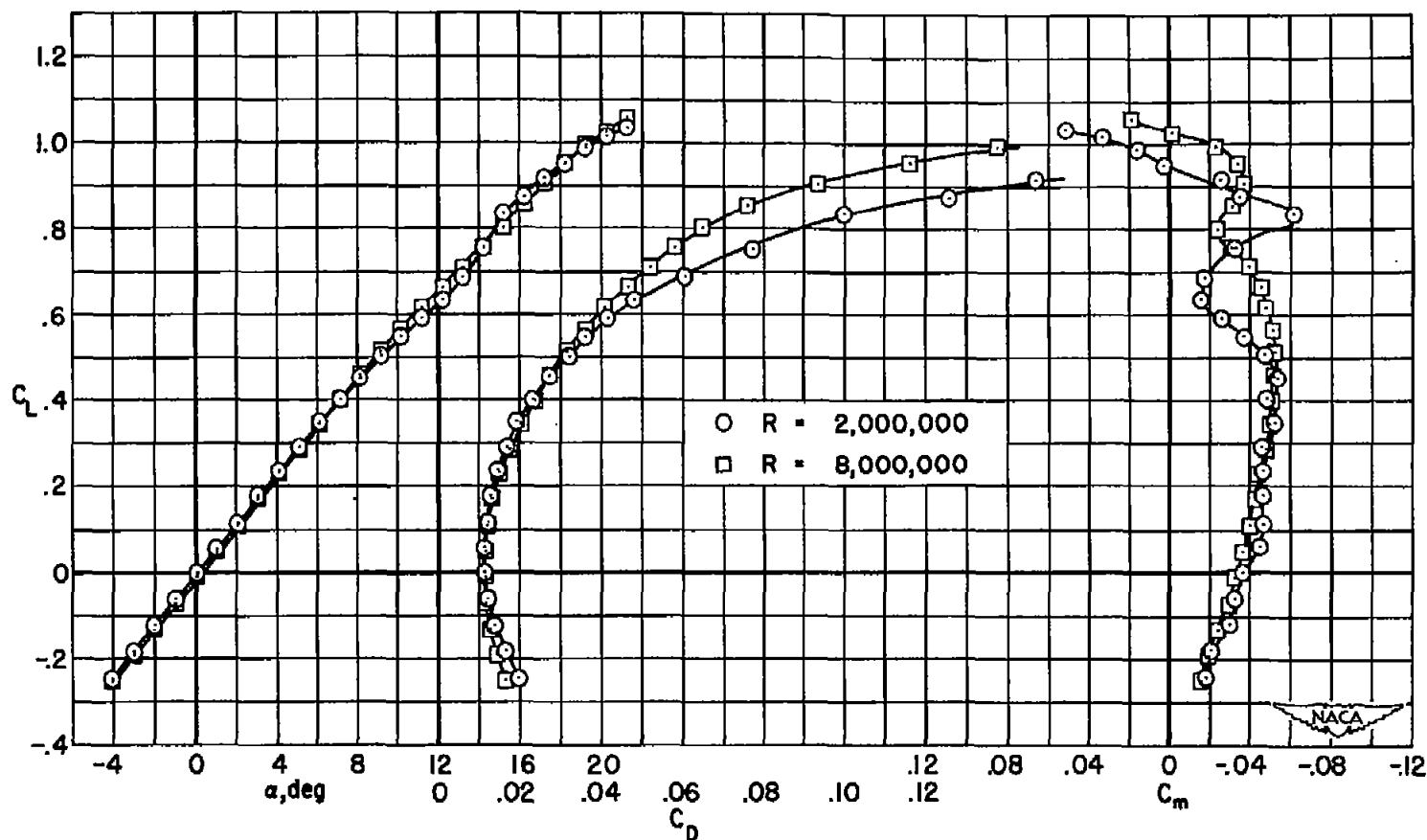
(a) Fences off.

Figure 26.- The effect of Reynolds number on the longitudinal characteristics of a wing-fuselage combination using a wing with 45° of sweepback and an aspect ratio of 6.03; $M = 0.25$.



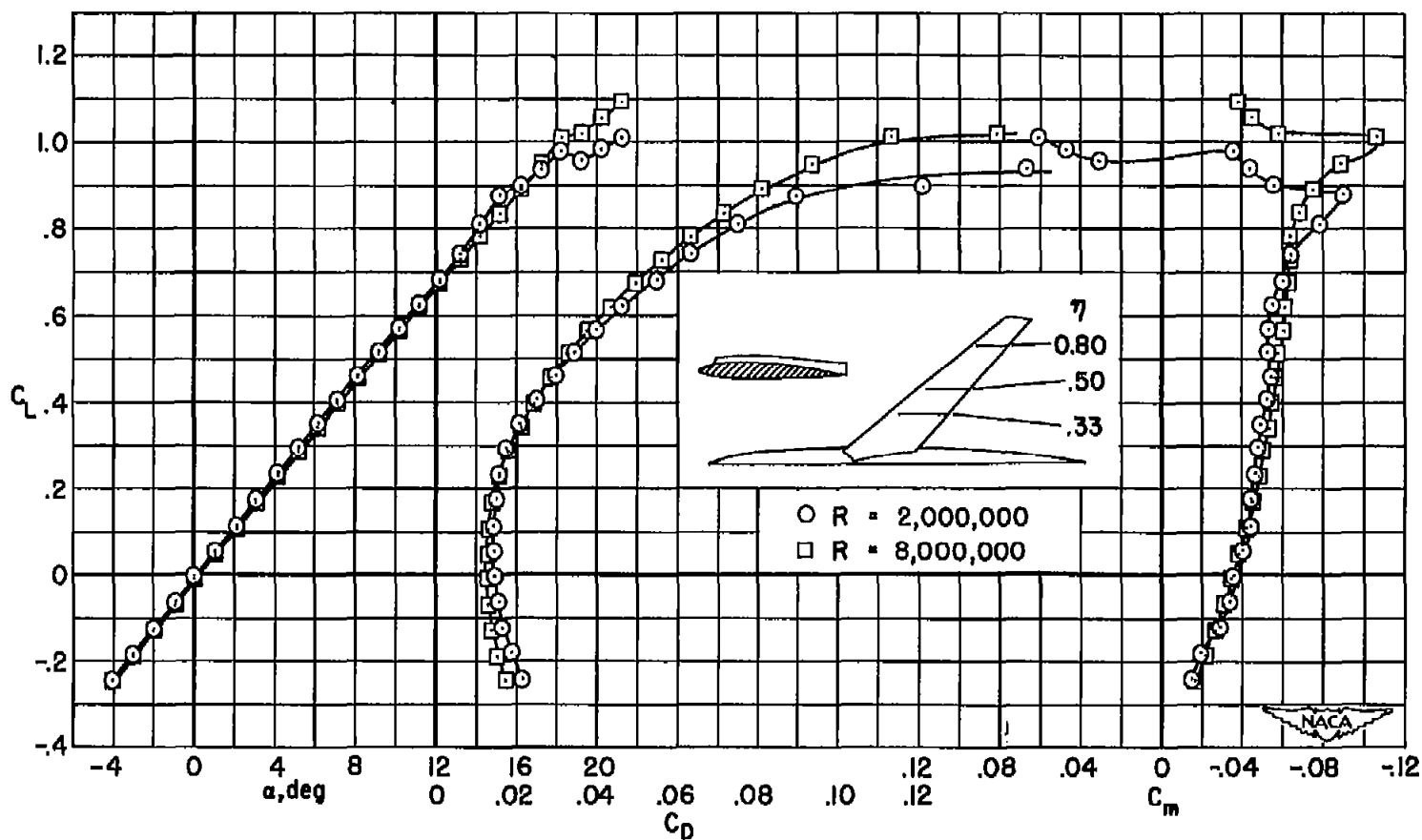
(b) Fences on.

Figure 26.- Concluded.



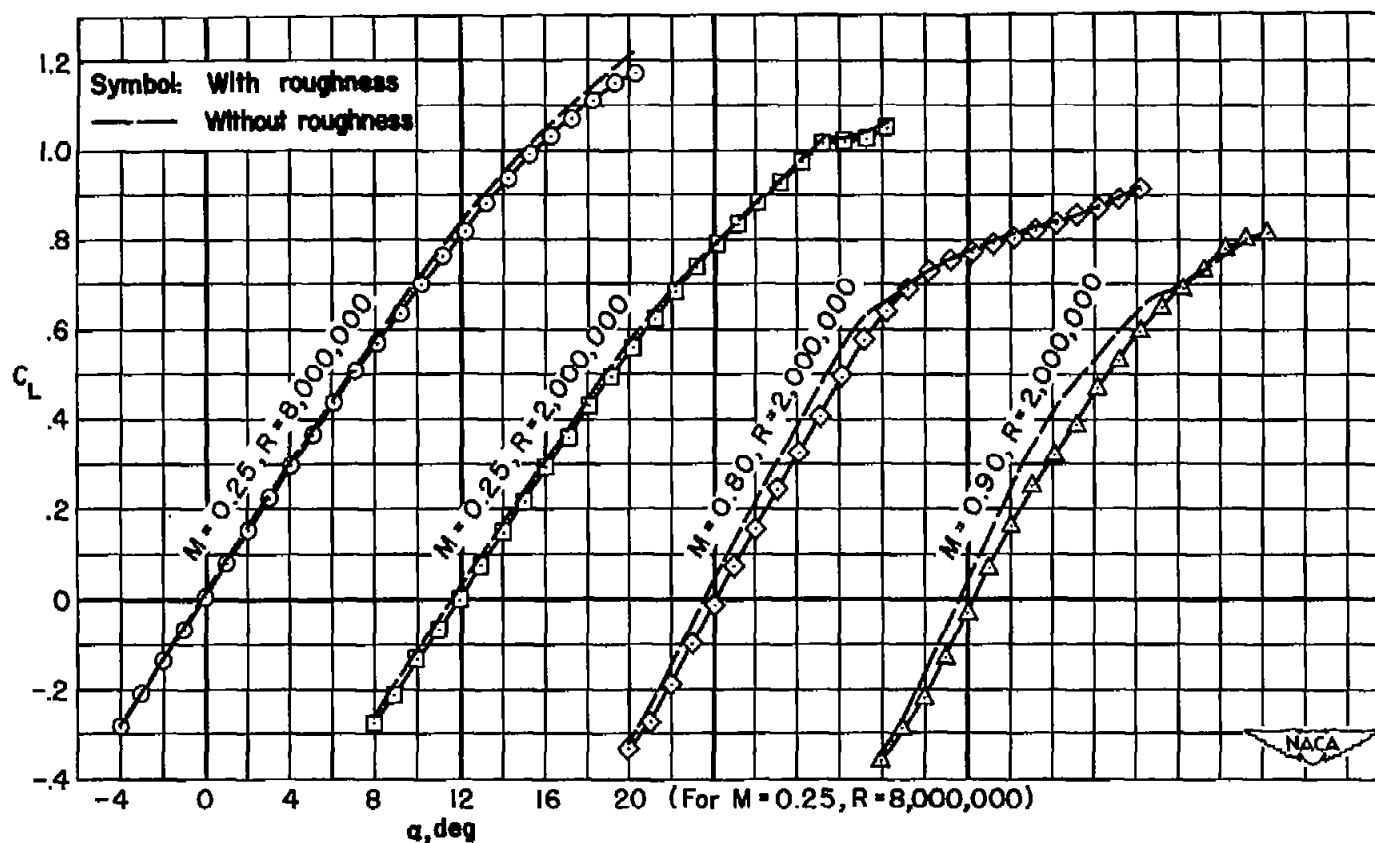
(a) Fences off.

Figure 27.- The effect of Reynolds number on the longitudinal characteristics of a wing-fuselage combination using a wing with 50° of sweepback and an aspect ratio of 5.04; $M = 0.25$.



(b) Fences on.

Figure 27.- Concluded.



(a) $\Lambda = 40^\circ$

Figure 28.- The effect of roughness at 0.10 chord on the lift characteristics of the wing-fuselage combinations.

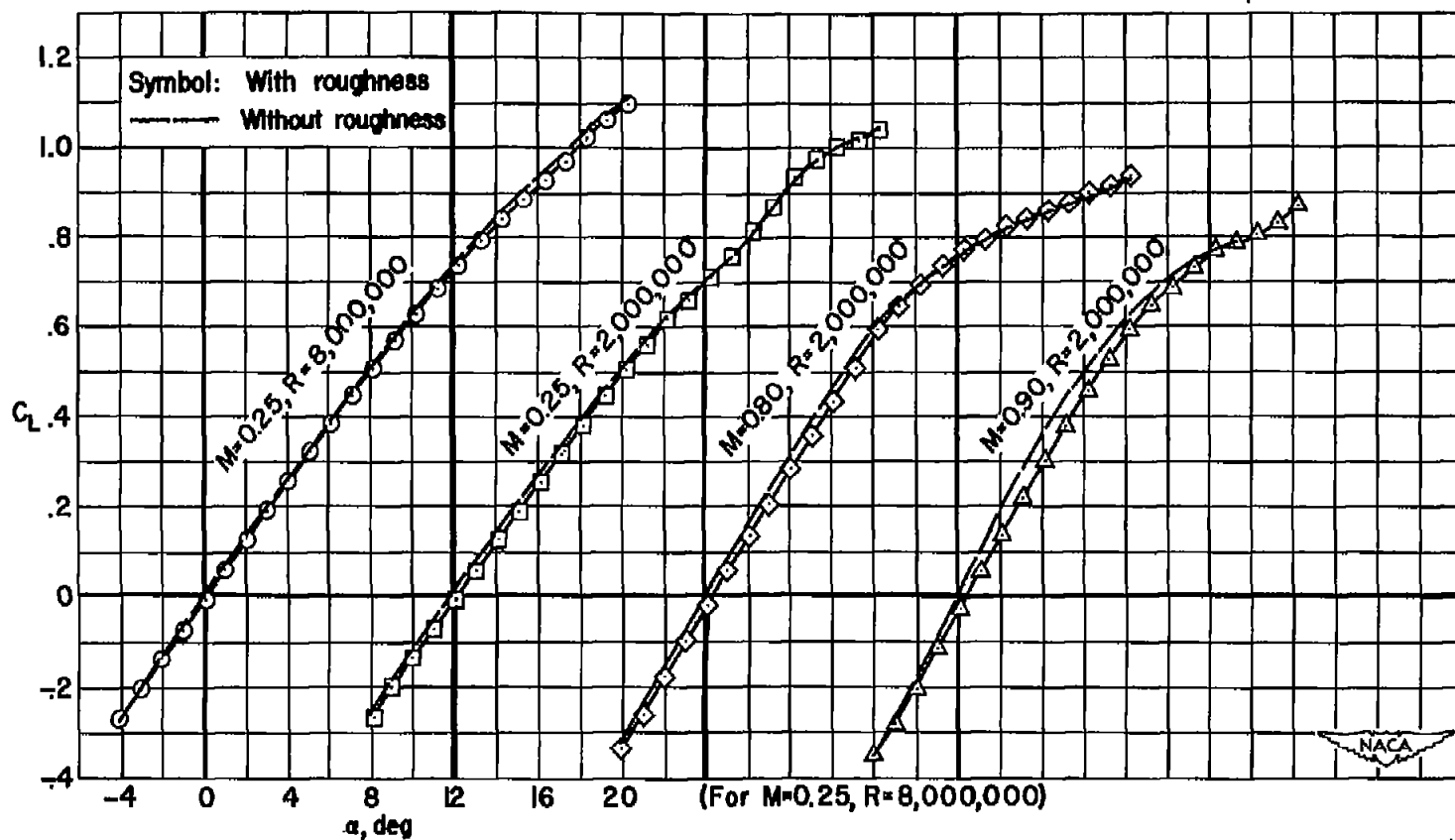
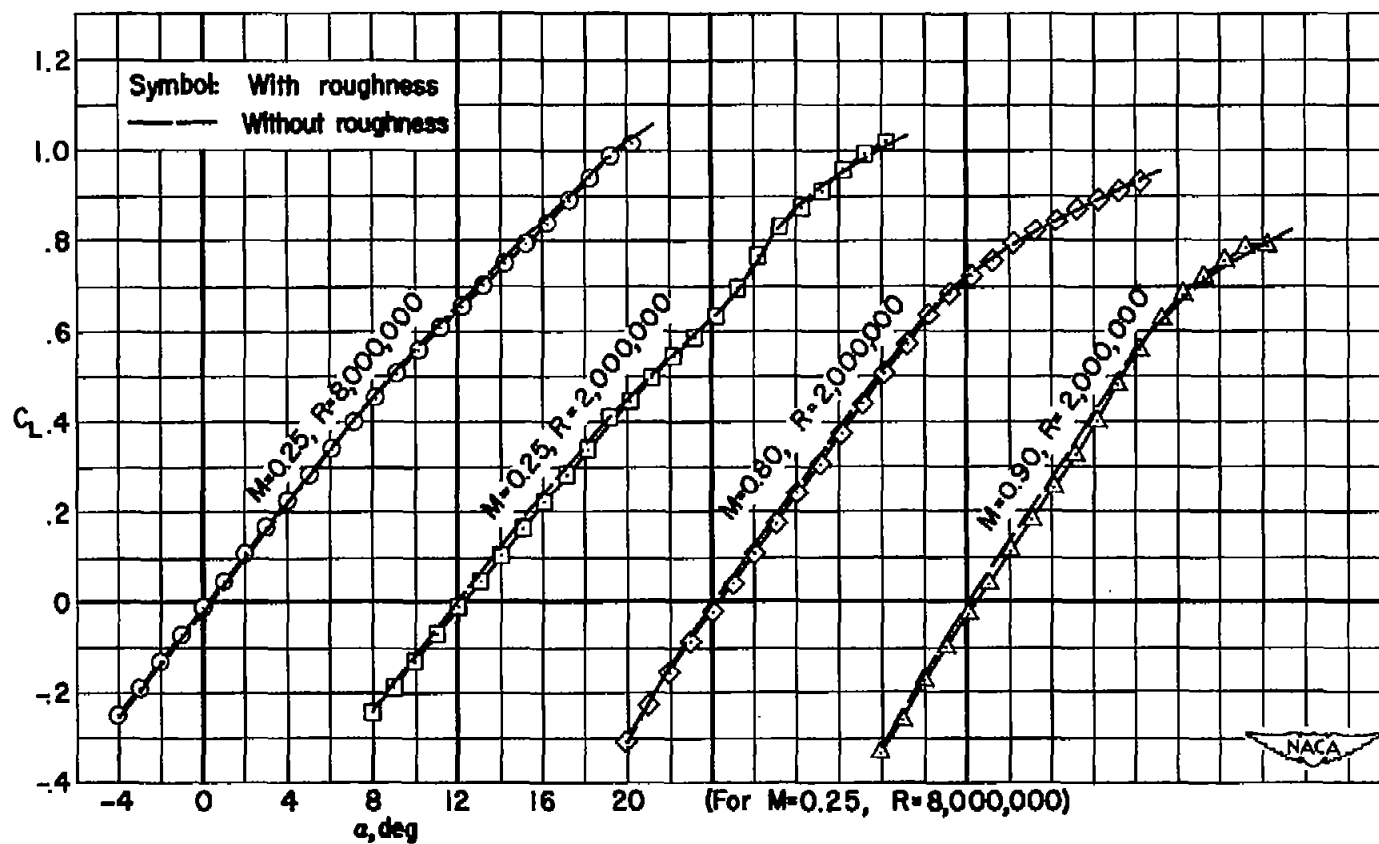
(b) $\Lambda = 45^\circ$

Figure 28.- Continued.



(c) $\Lambda = 50^\circ$

Figure 28.- Concluded.

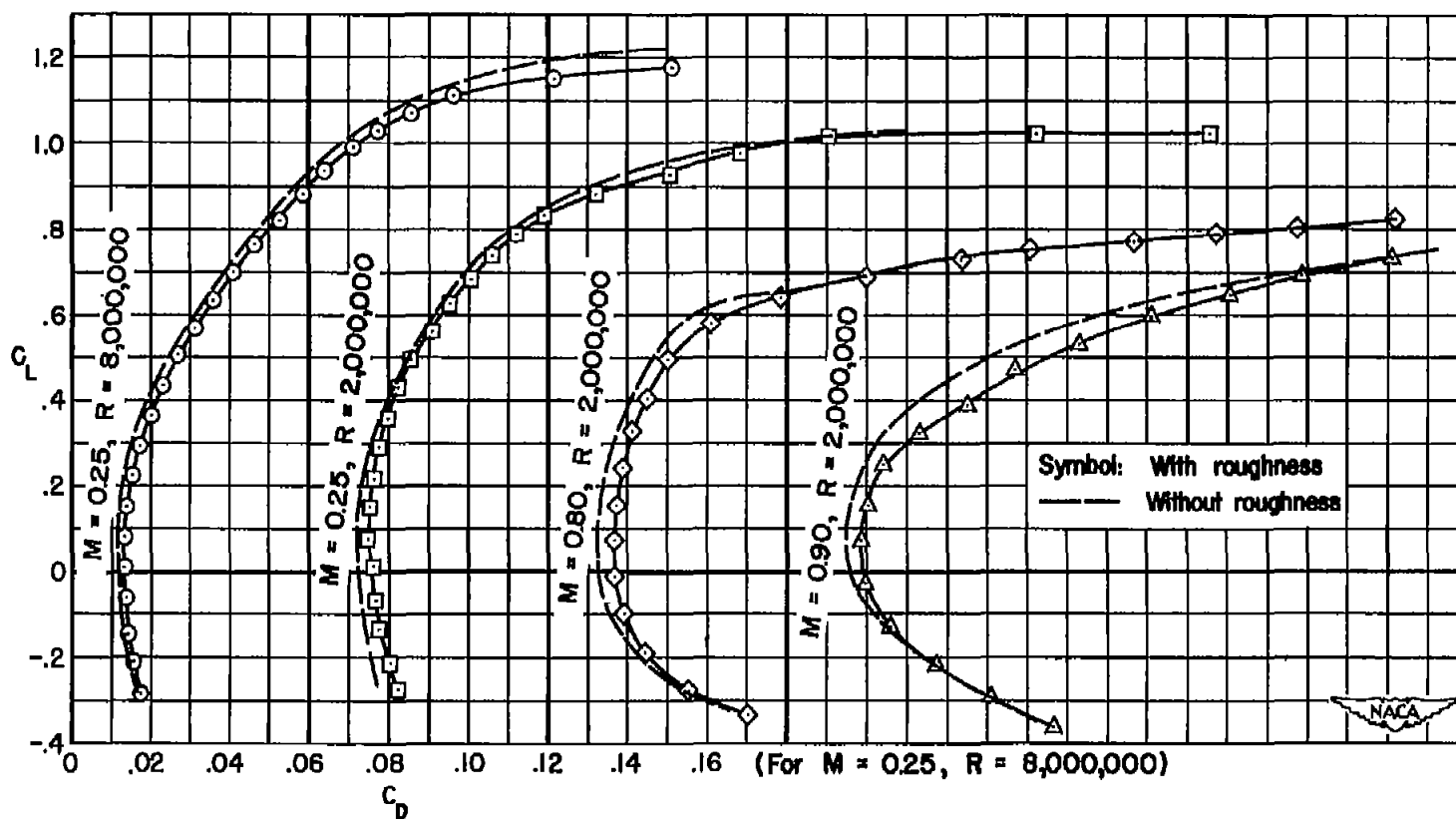
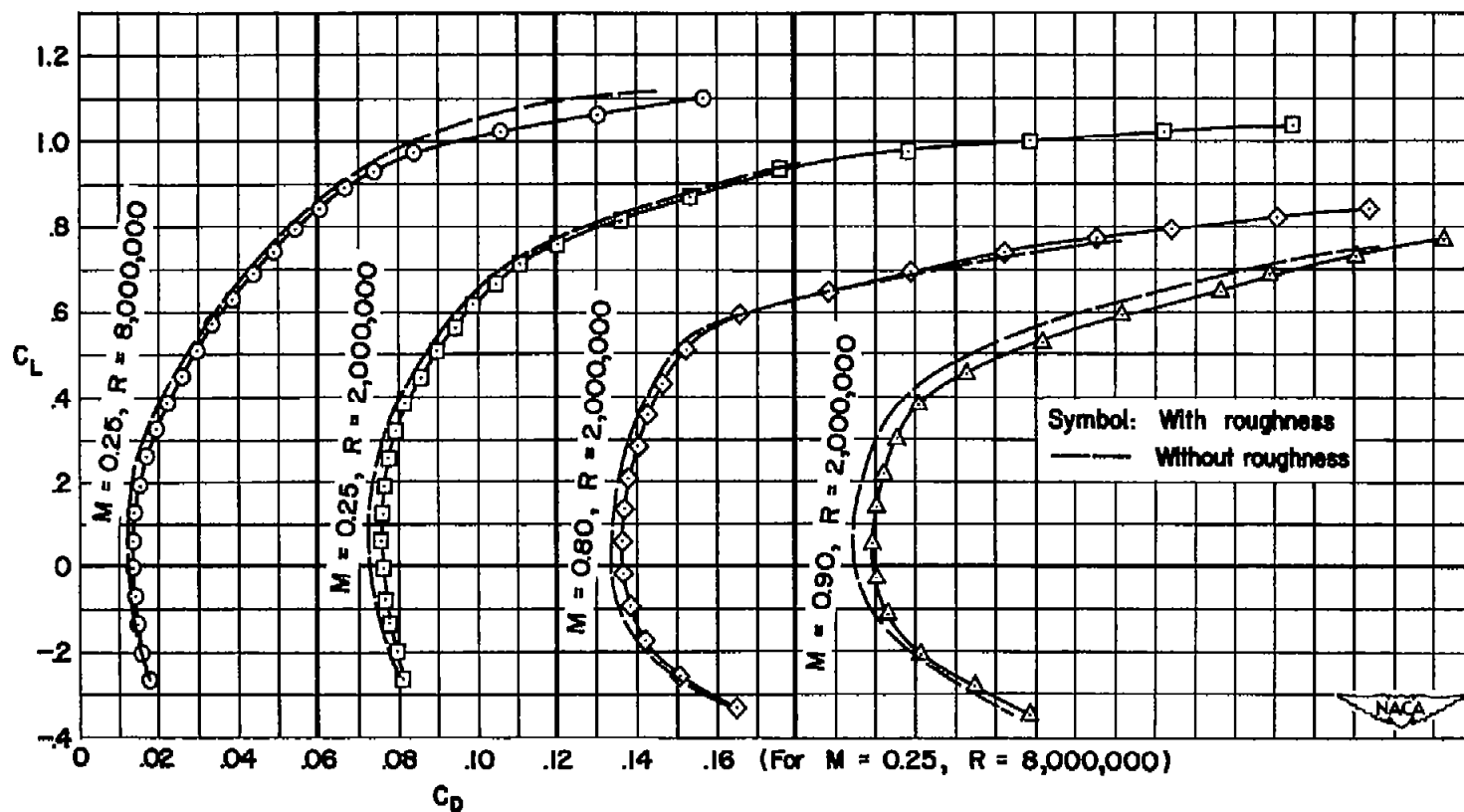
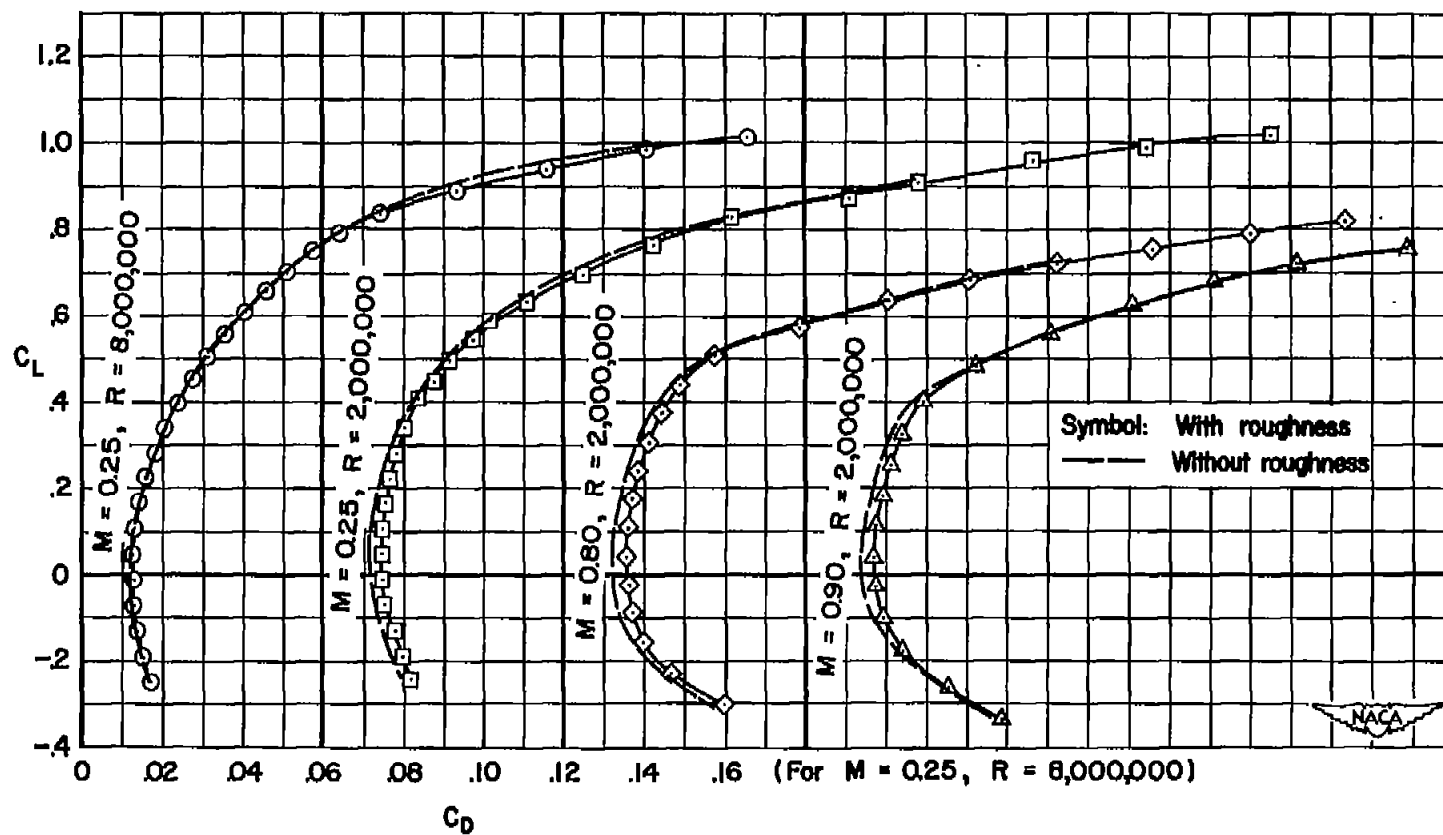
(a) $\Lambda = 40^\circ$

Figure 29.- The effect of roughness at 0.10 chord on the drag characteristics of the wing-fuselage combinations.



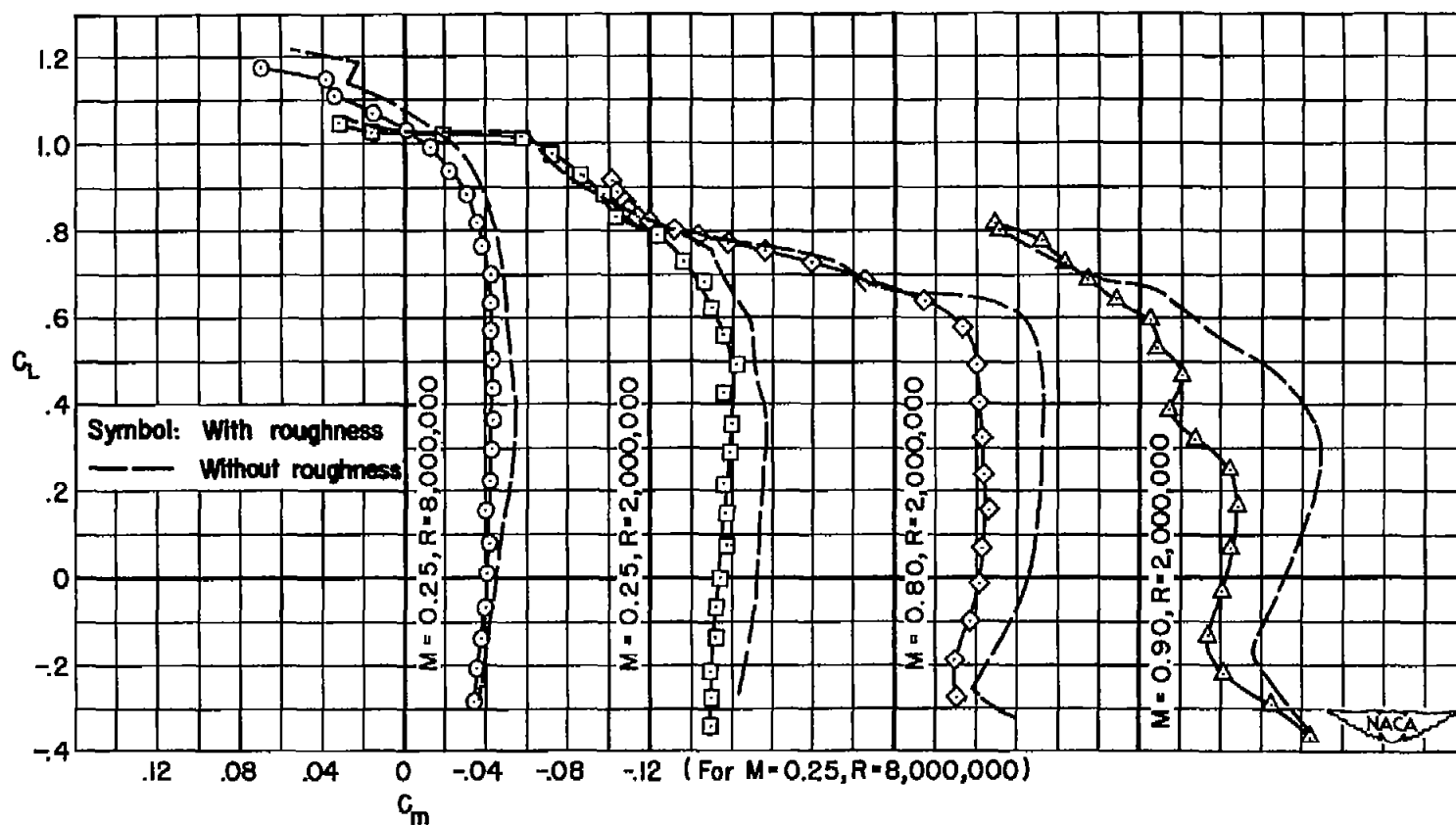
(b) $\Lambda = 45^\circ$

Figure 29.- Continued.



(c) $\Lambda = 50^\circ$

Figure 29.- Concluded.



(a) $\Lambda = 40^\circ$

Figure 30.- The effect of roughness at 0.10 chord on the pitching-moment characteristics of the wing-fuselage combinations.

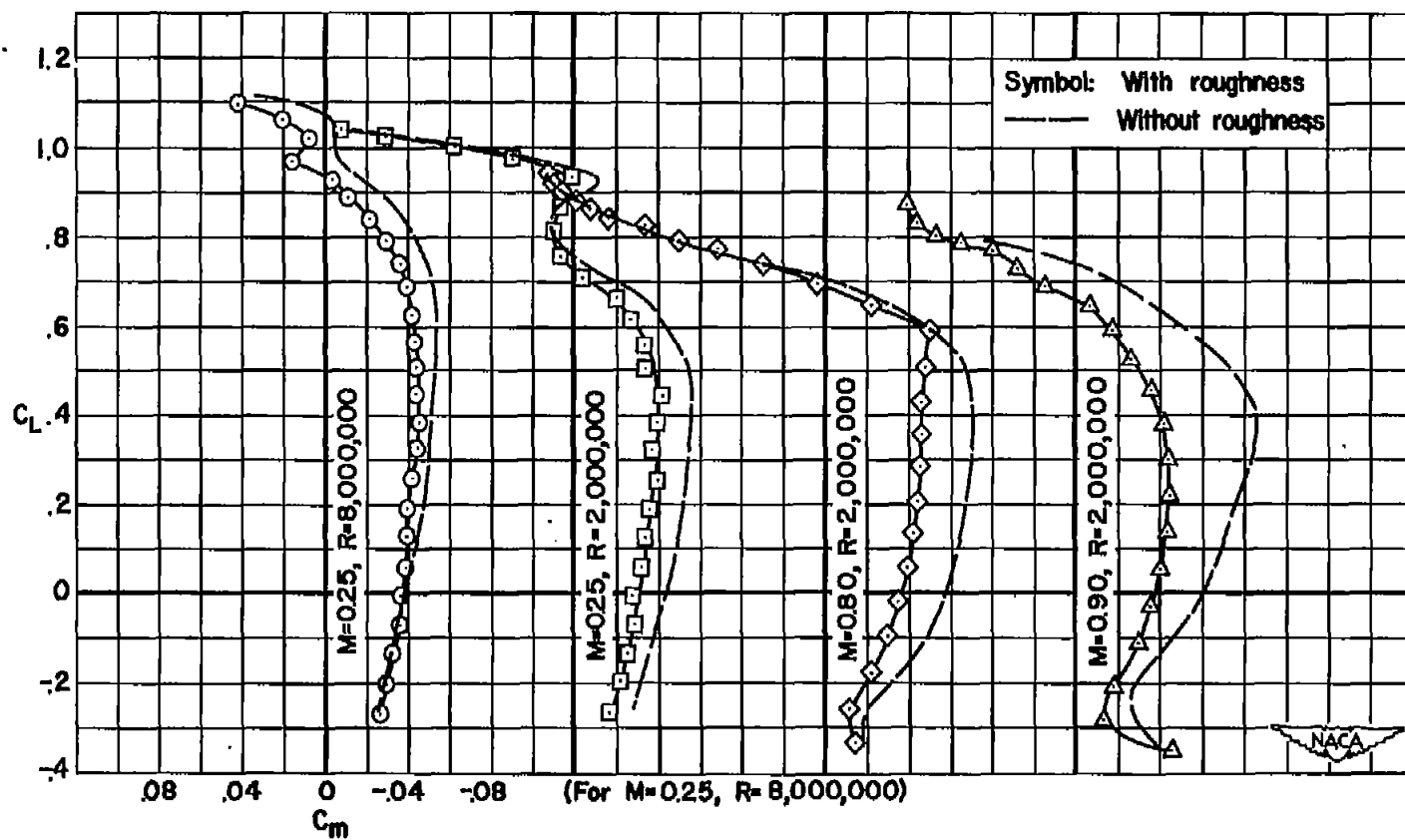
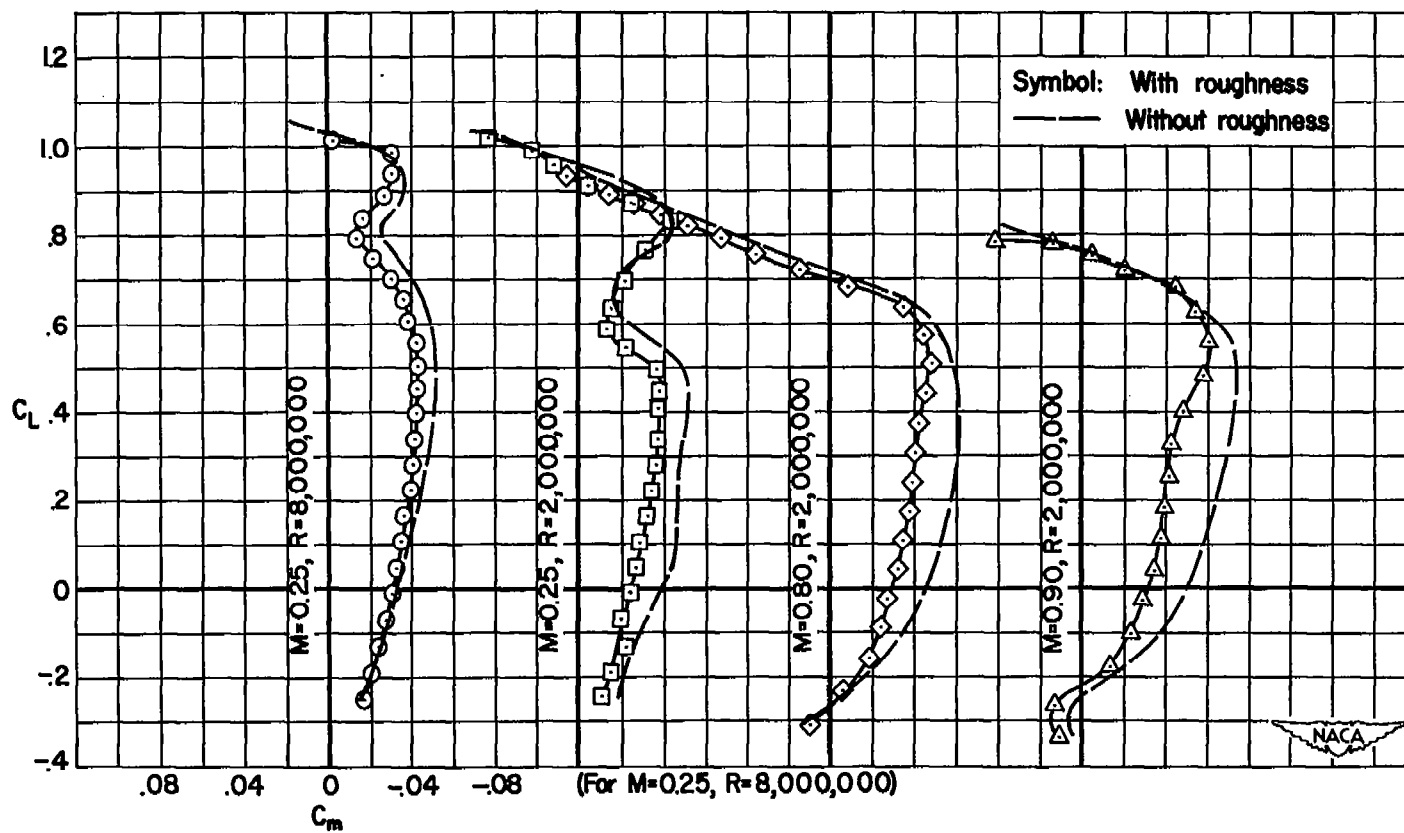
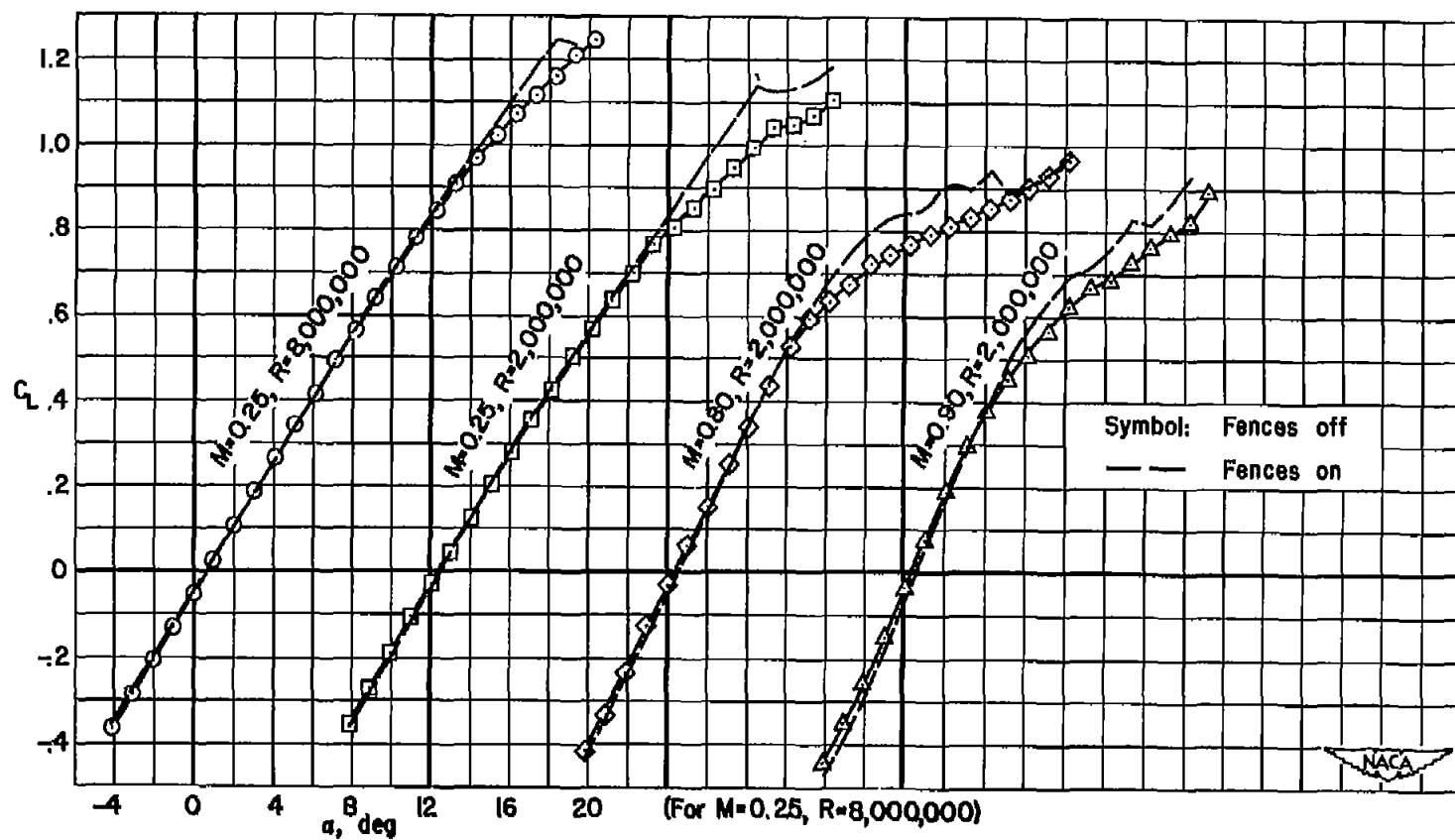
(b) $\Lambda = 45^\circ$

Figure 30.- Continued.



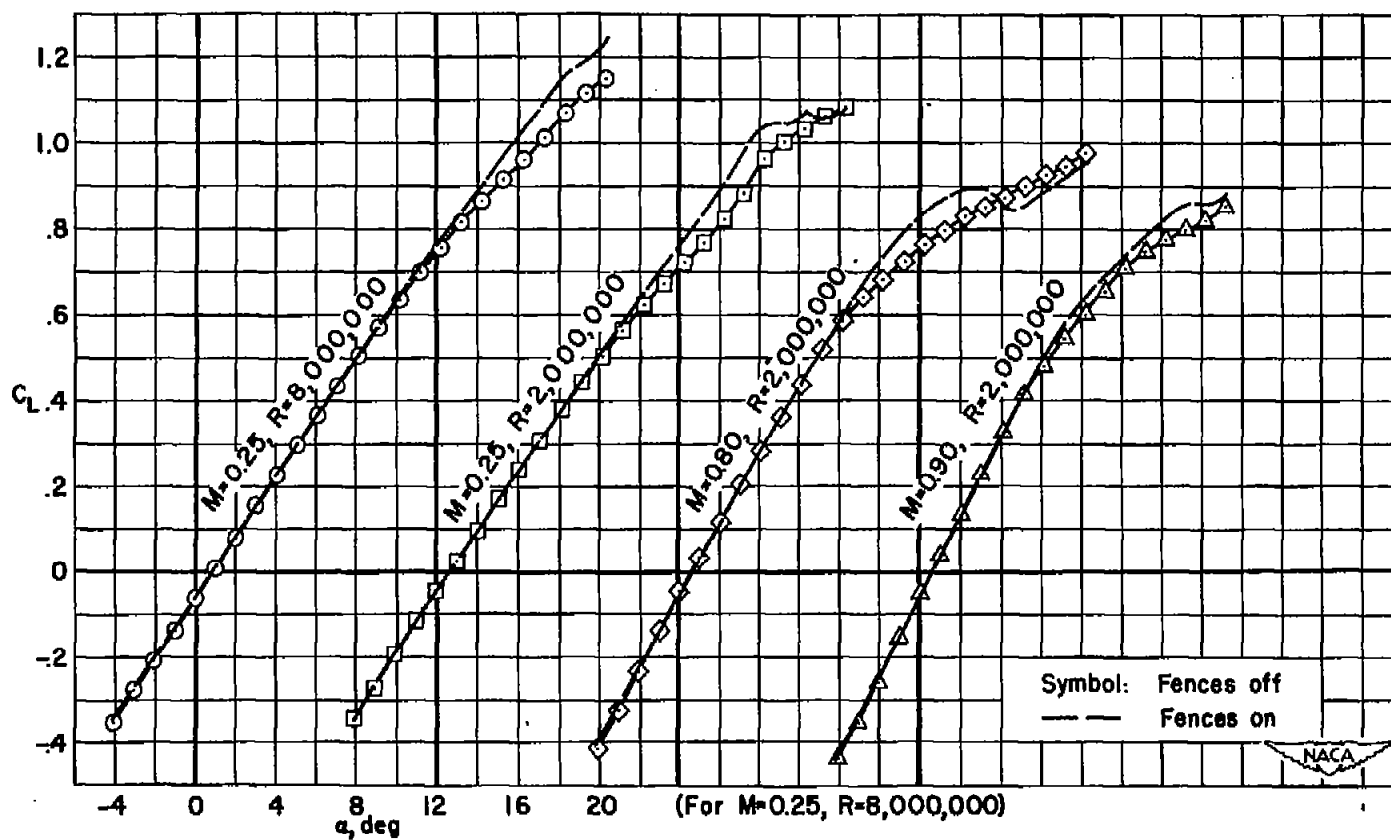
(c) $\Lambda = 50^\circ$

Figure 30.- Concluded.



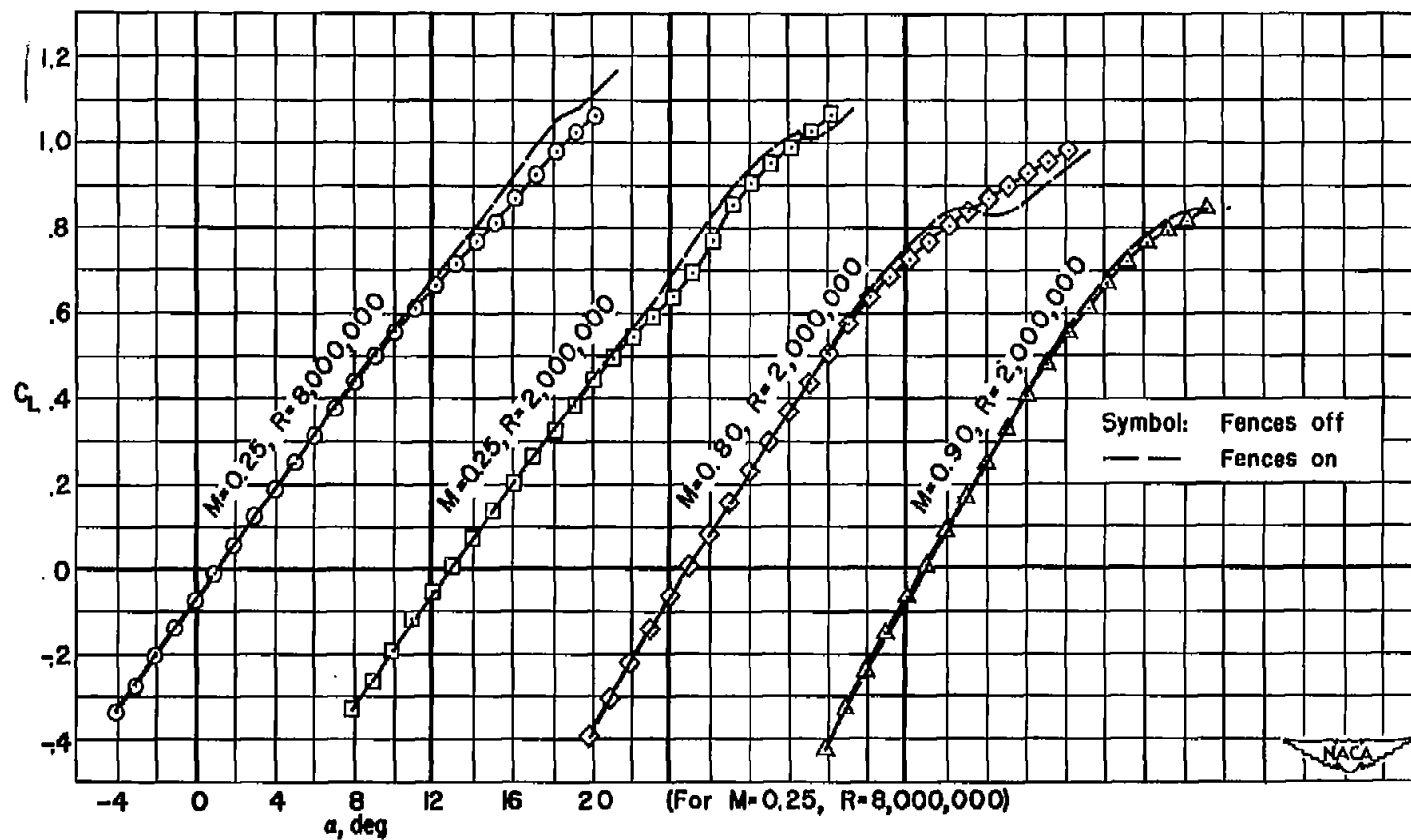
(a) $\Lambda = 40^\circ$

Figure 31.- The effect of wing fences on the lift characteristics of the combinations with a horizontal tail; tail height = $0.5 b/2$; $i_t = -8^\circ$.



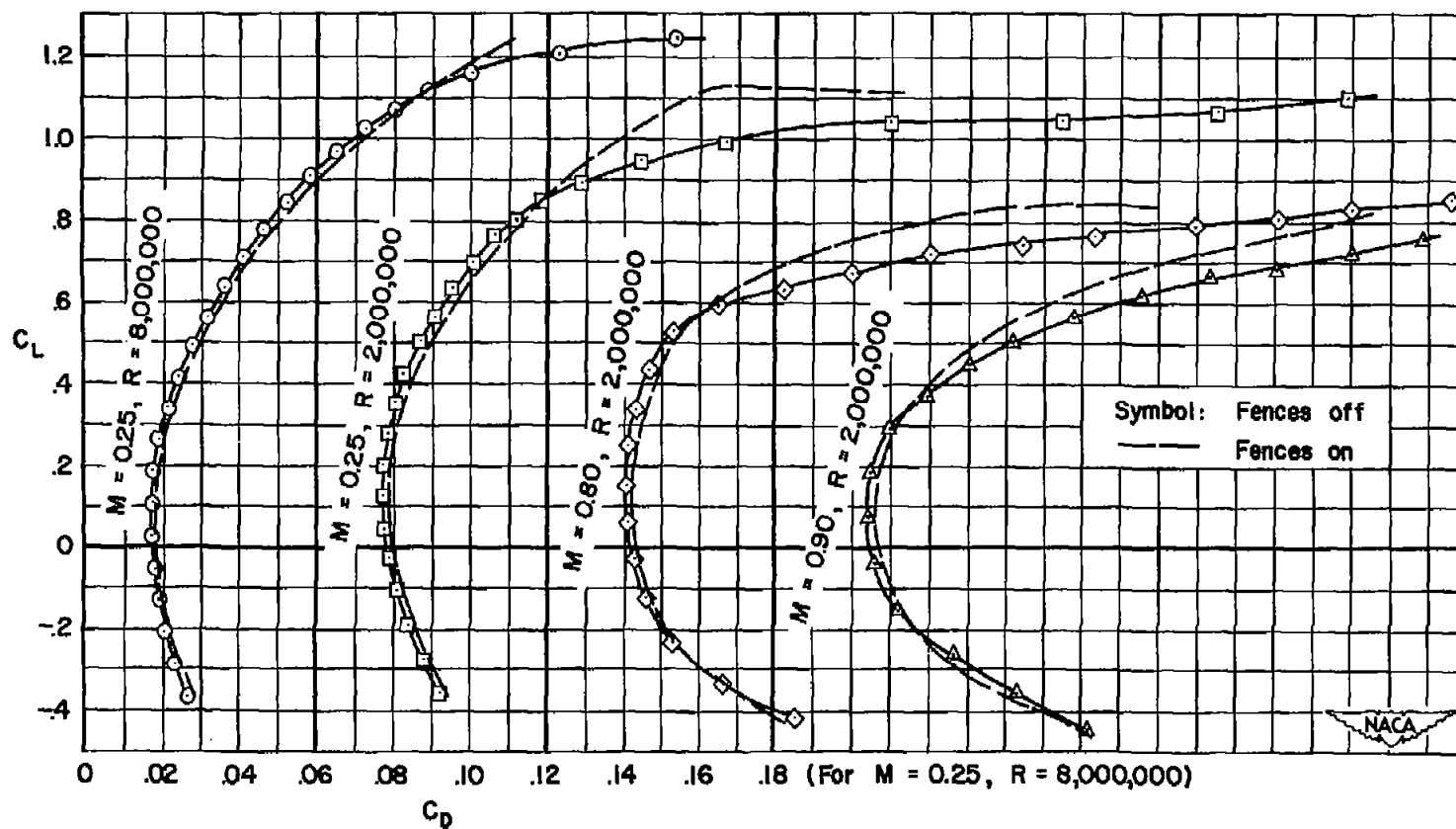
(b) $\Lambda = 45^\circ$

Figure 31.- Continued.



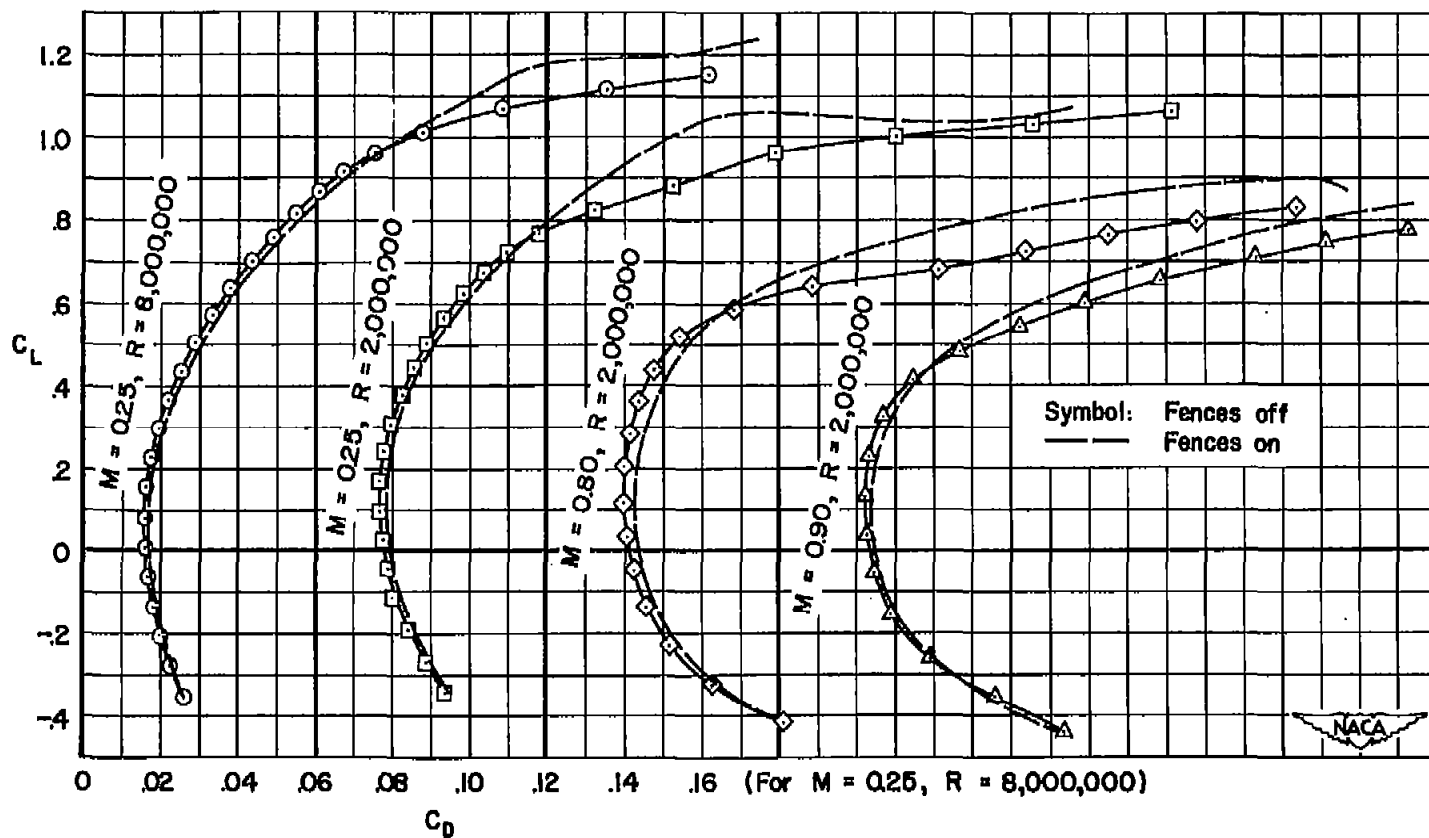
(c) $\Lambda = 50^\circ$

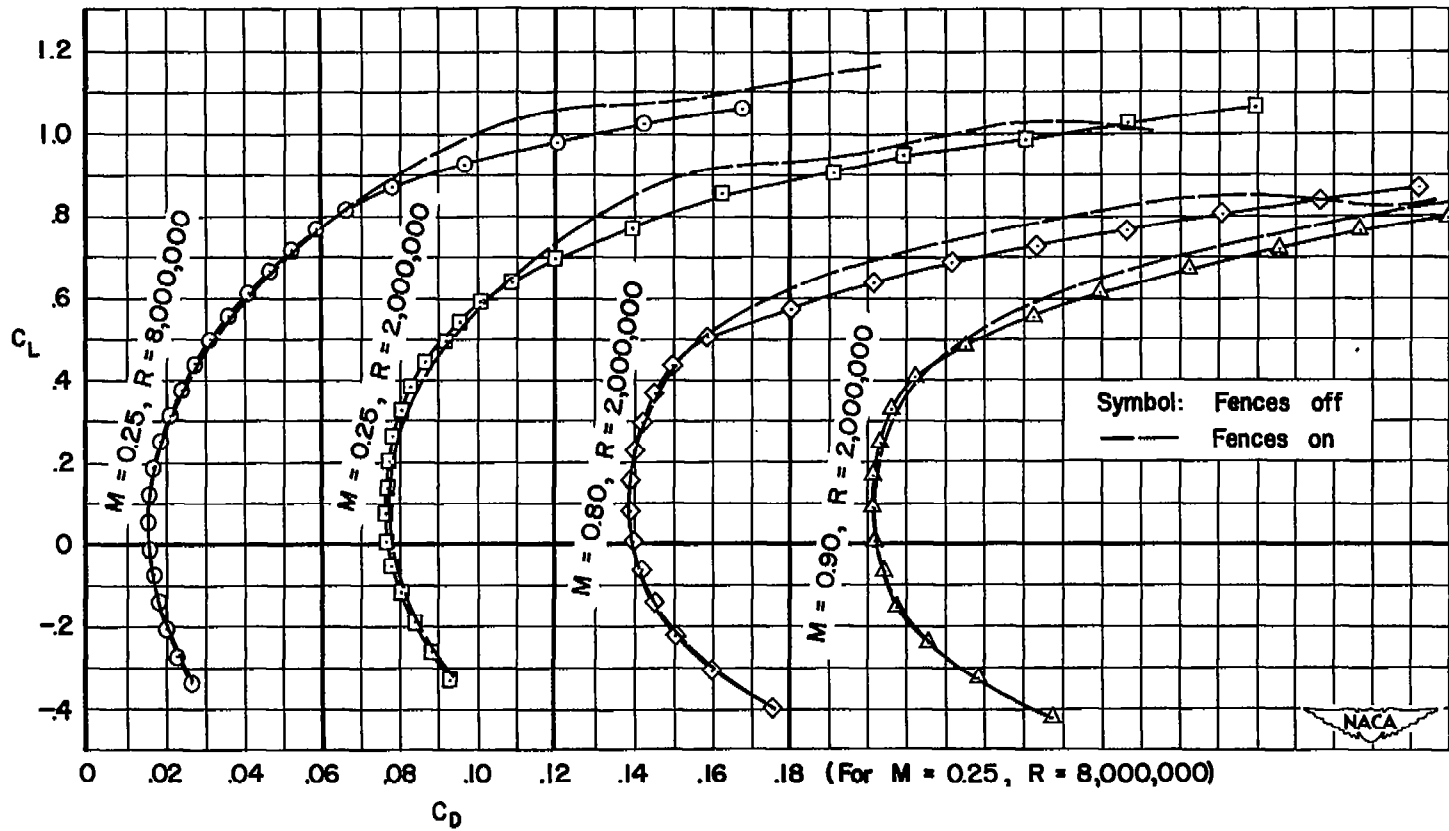
Figure 31.- Concluded.



(a) $\Lambda = 40^\circ$

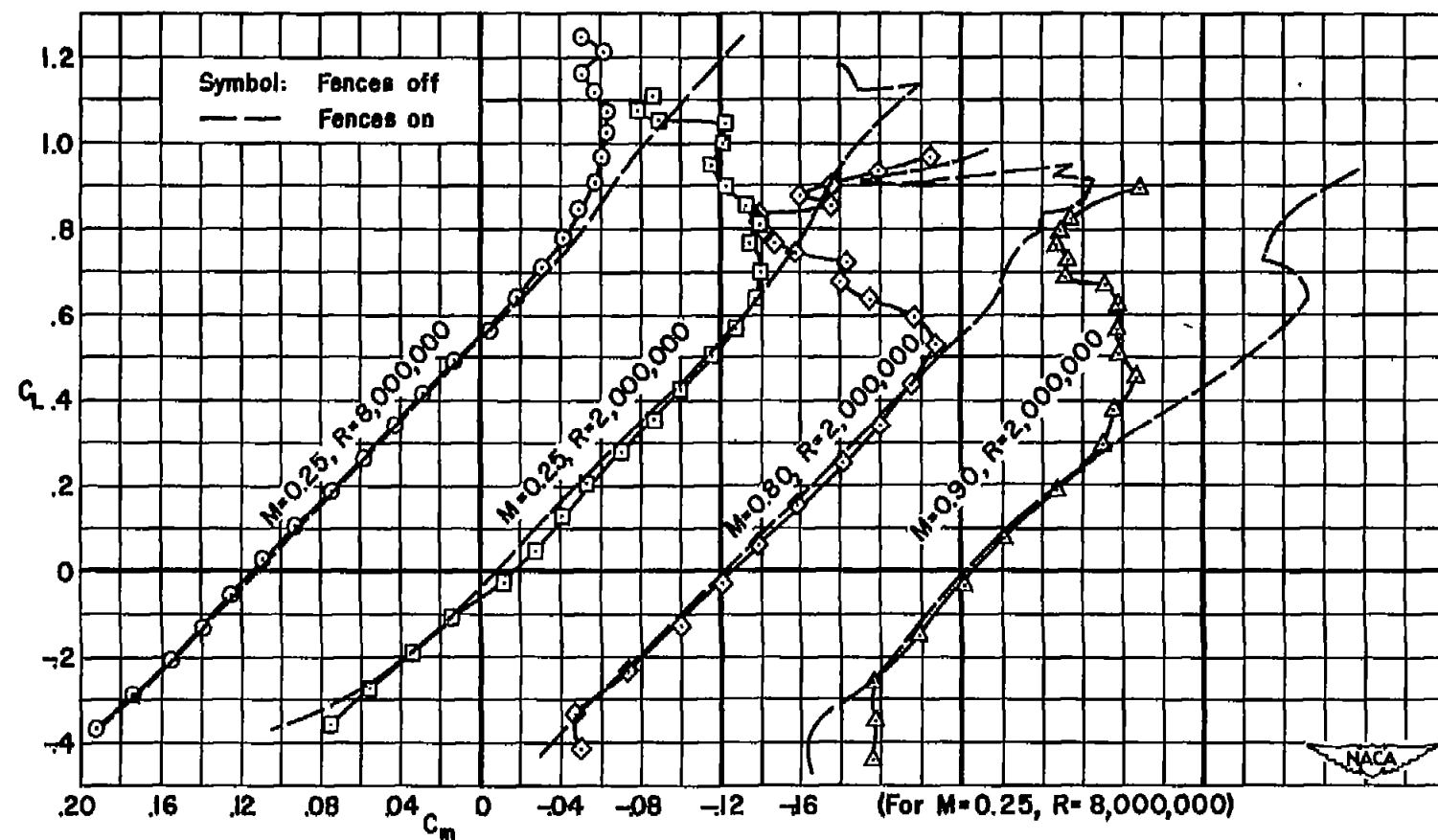
Figure 32.- The effect of wing fences on the drag characteristics of the combinations with a horizontal tail; tail height = $0.5b/2$; $i_t = -8^\circ$.





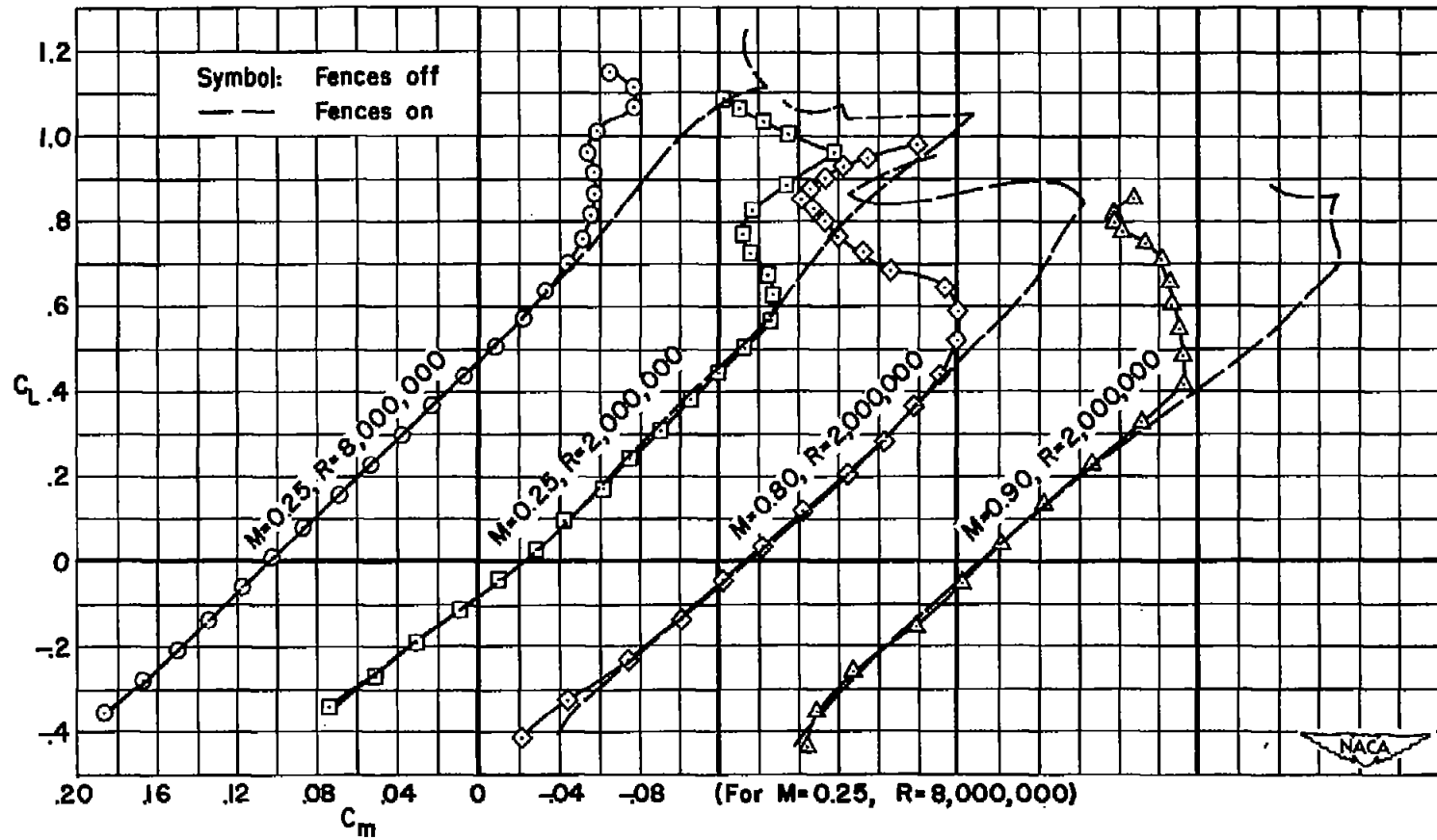
(c) $\Lambda = 50^\circ$

Figure 32.- Concluded.



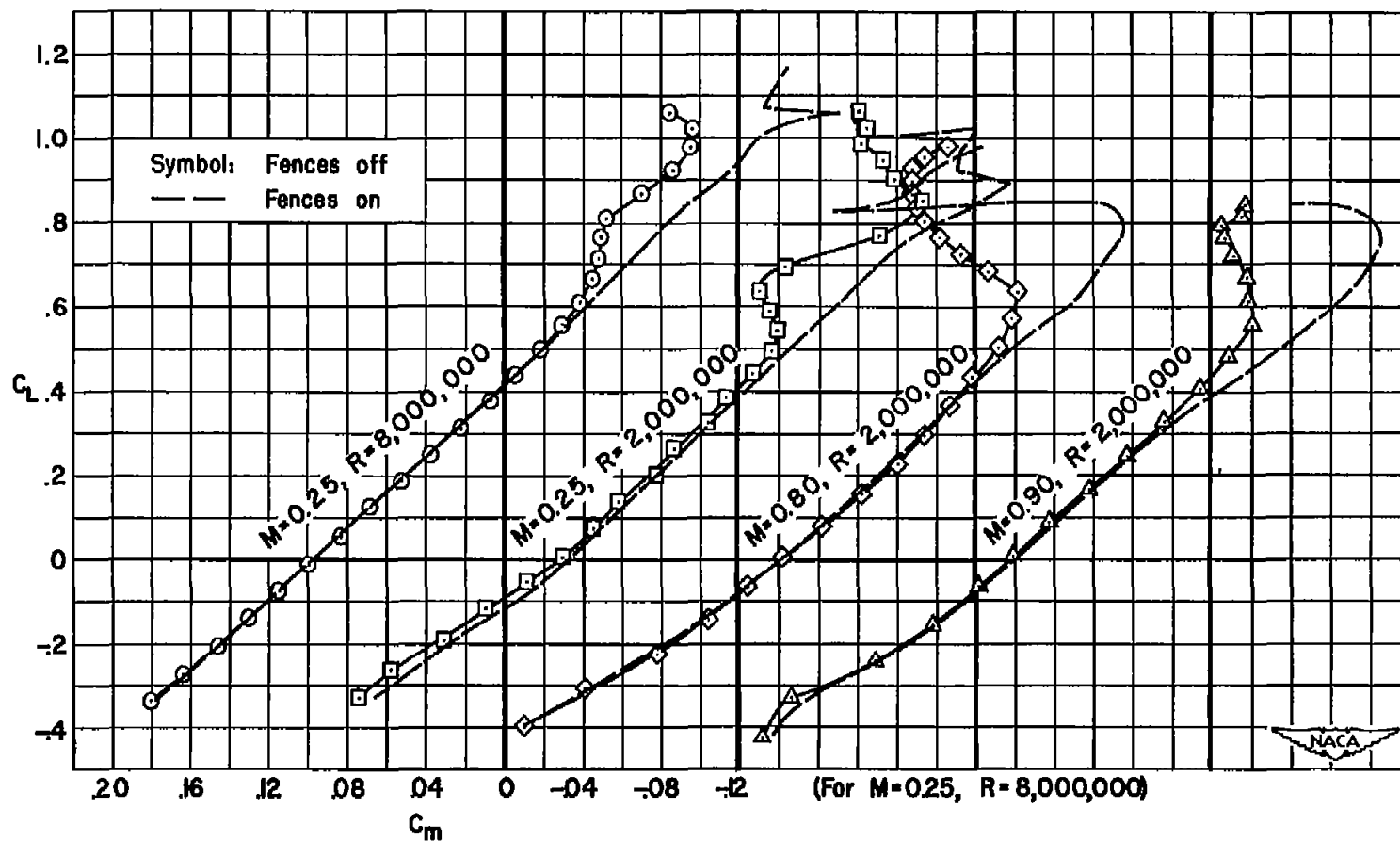
(a) $\Lambda = 40^\circ$

Figure 33.- The effect of wing fences on the pitching-moment characteristics of the combinations with a horizontal tail; tail height = $0.5b$; $i_t = -8^\circ$.



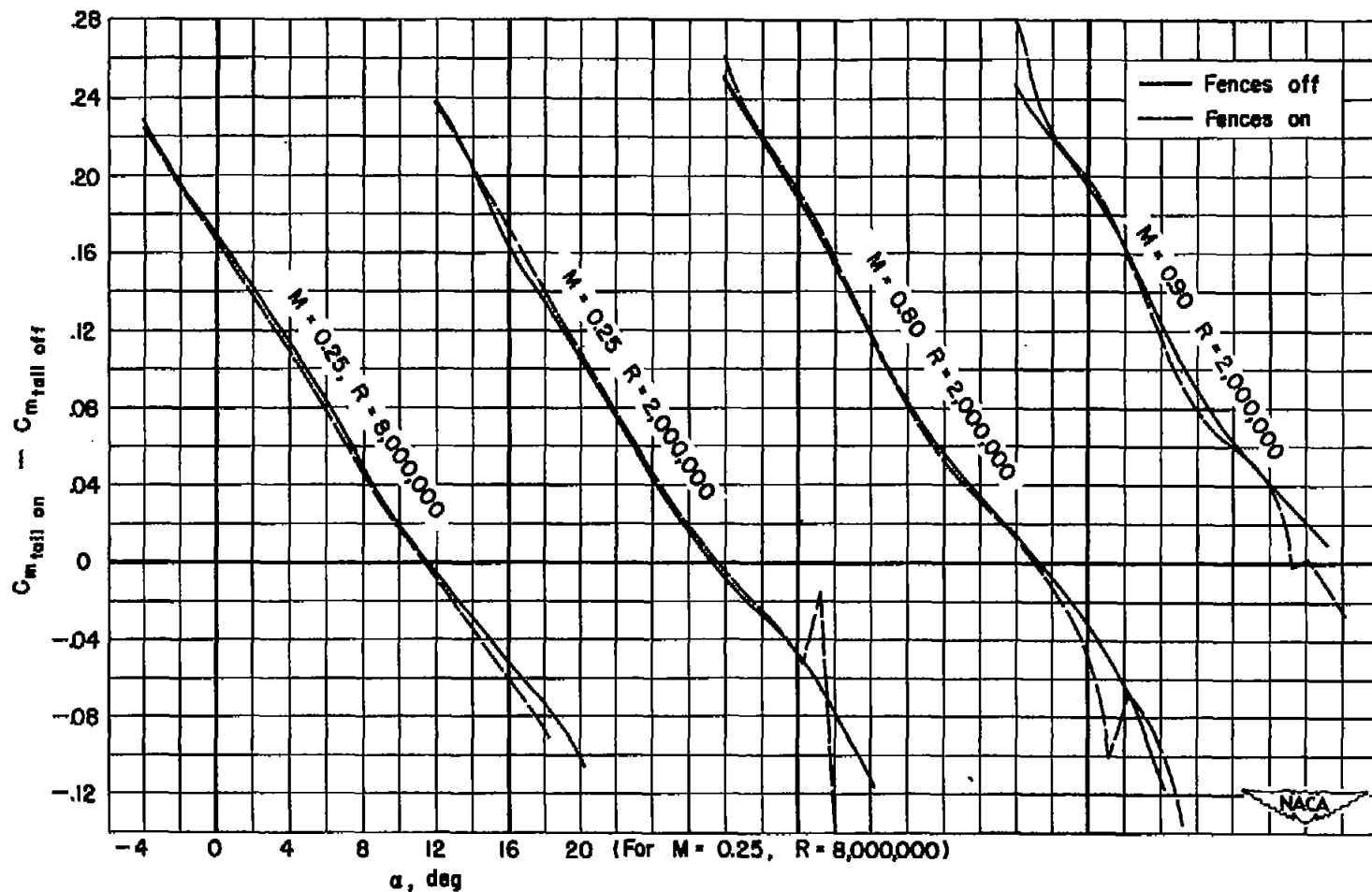
(b) $\Lambda = 45^\circ$

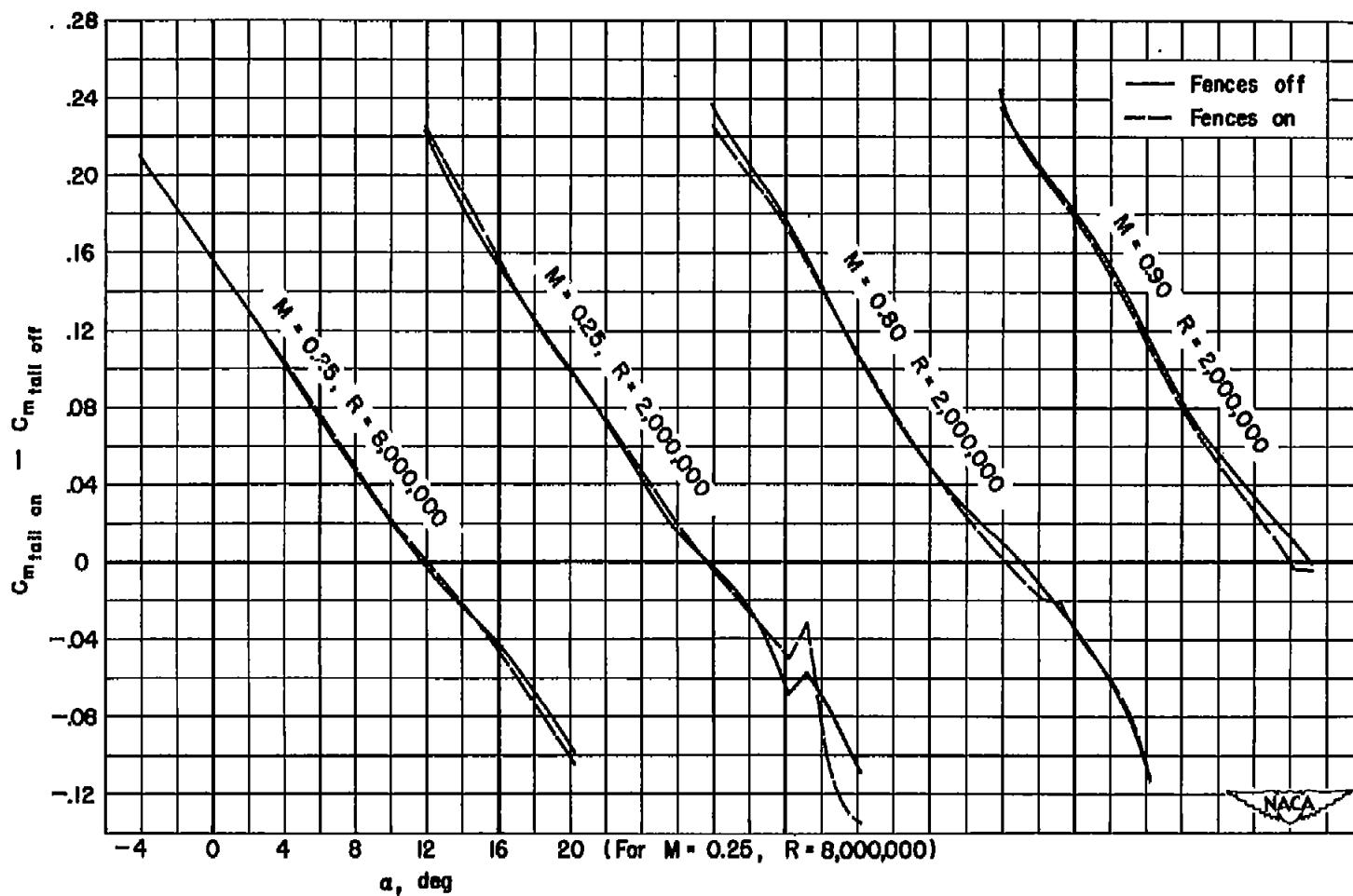
Figure 33.- Continued.



(c) $\Lambda = 50^\circ$

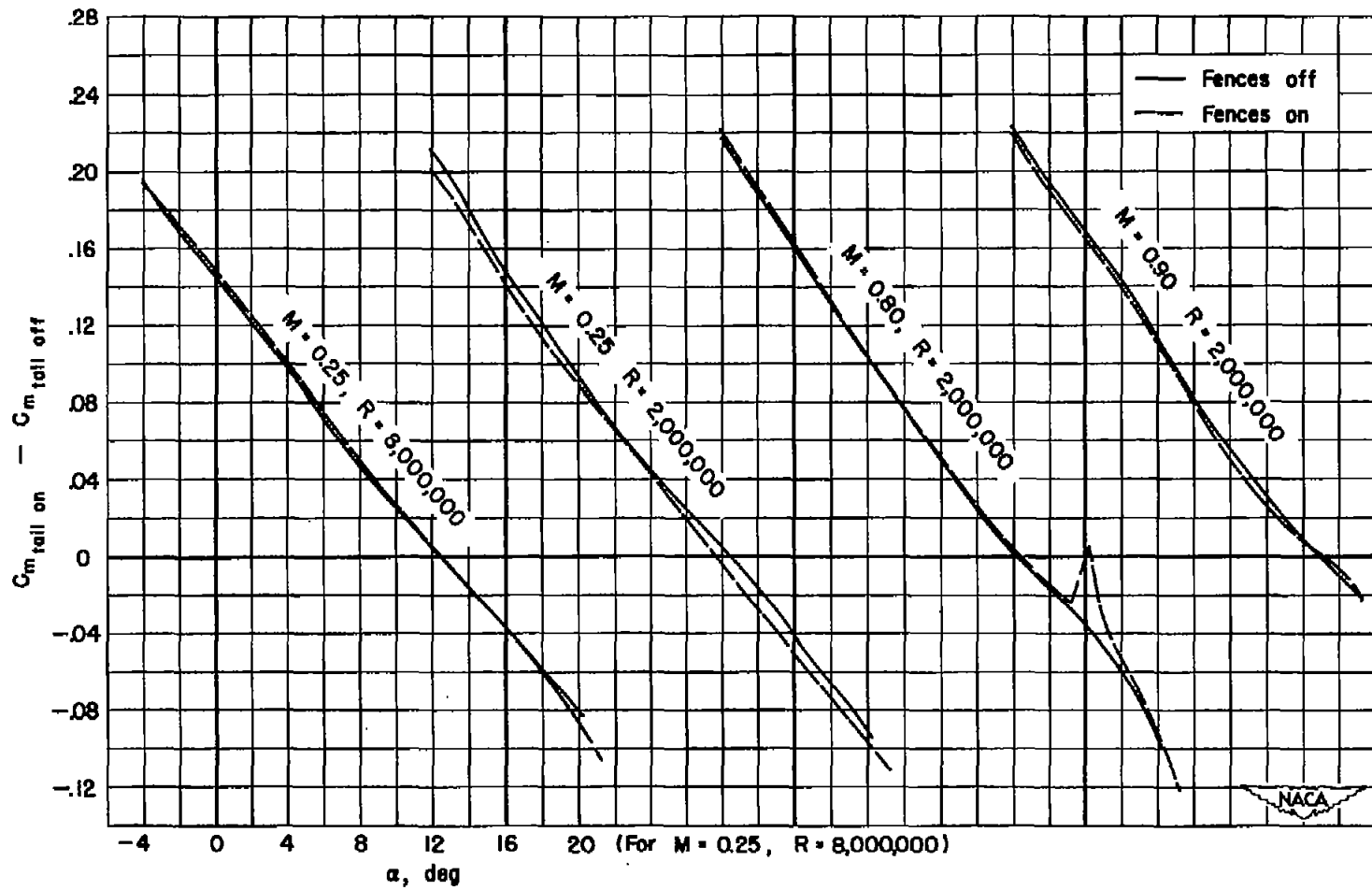
Figure 33.- Concluded.

(a) $\Lambda = 40^\circ$ Figure 34.- Pitching-moment coefficient due to the horizontal tail; tail height = $0.5 b/2$; $i_t = -8^\circ$.



(b) $\Lambda = 45^\circ$

Figure 34.- Continued.



(c) $\Lambda = 50^\circ$

Figure 34.- Concluded.

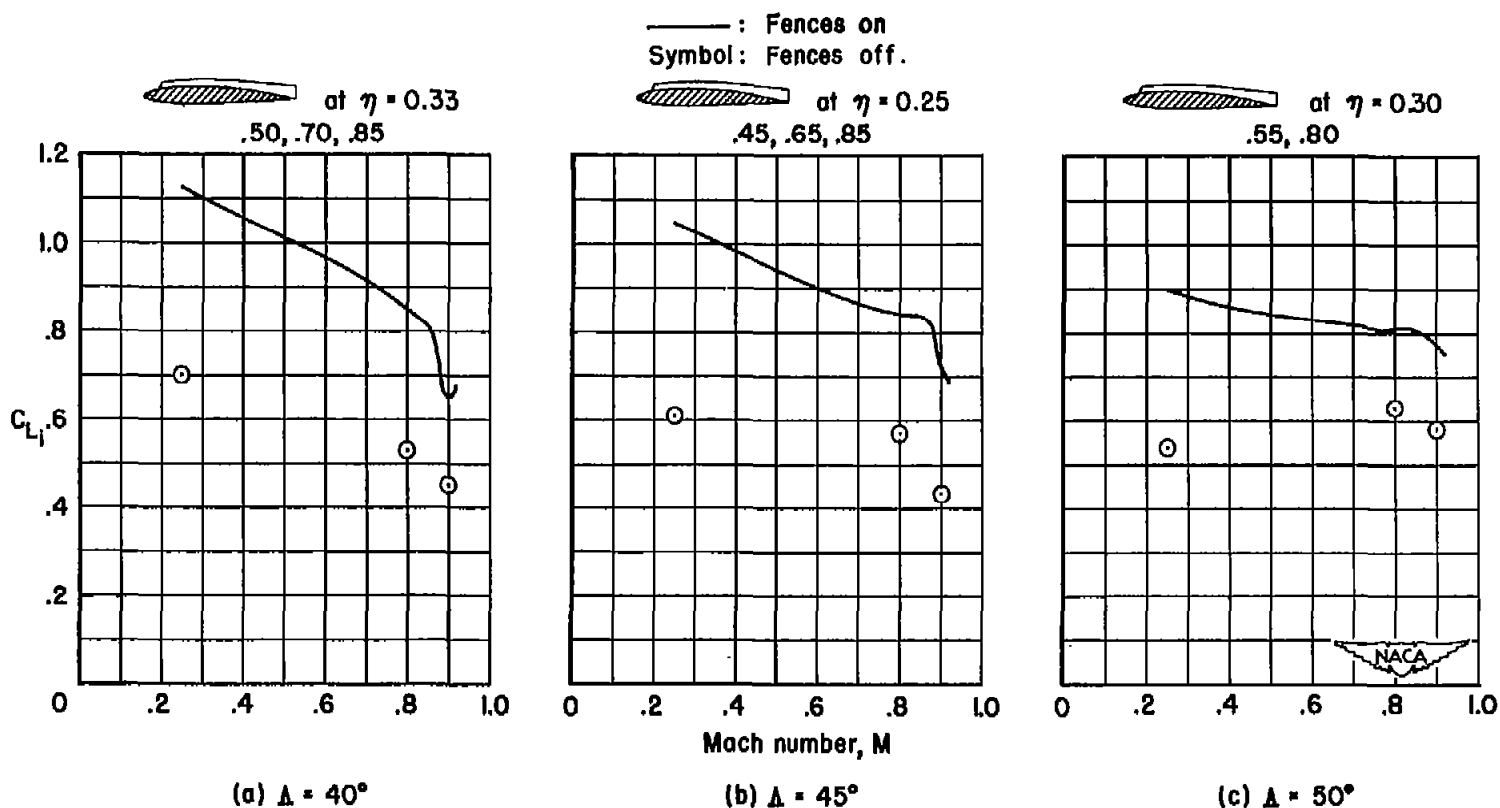


Figure 35.- The variation with Mach number of the inflection lift coefficients of the wing-fuselage-tail combinations; tail height = $0\ b/2$; $i_t = -8^\circ$; $R = 2,000,000$.

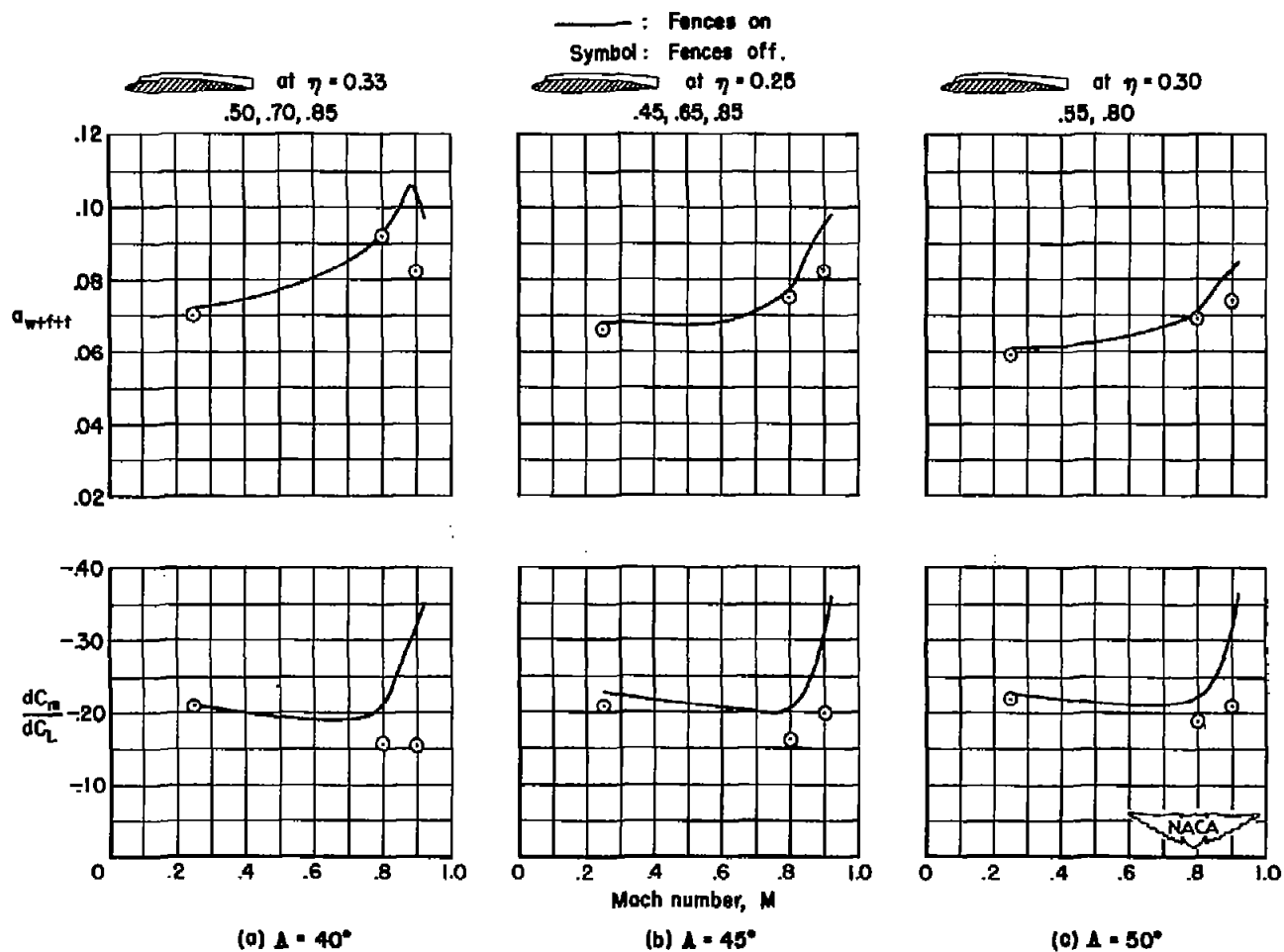


Figure 36.- The variations with Mach number of the slopes of the lift and pitching-moment curves of the wing-fuselage-tail combinations with and without wing fences; $C_L = 0.40$; tail height = $0.5b$; $i_t = -8^\circ$; $R = 2,000,000$.

CONFIDENTIAL

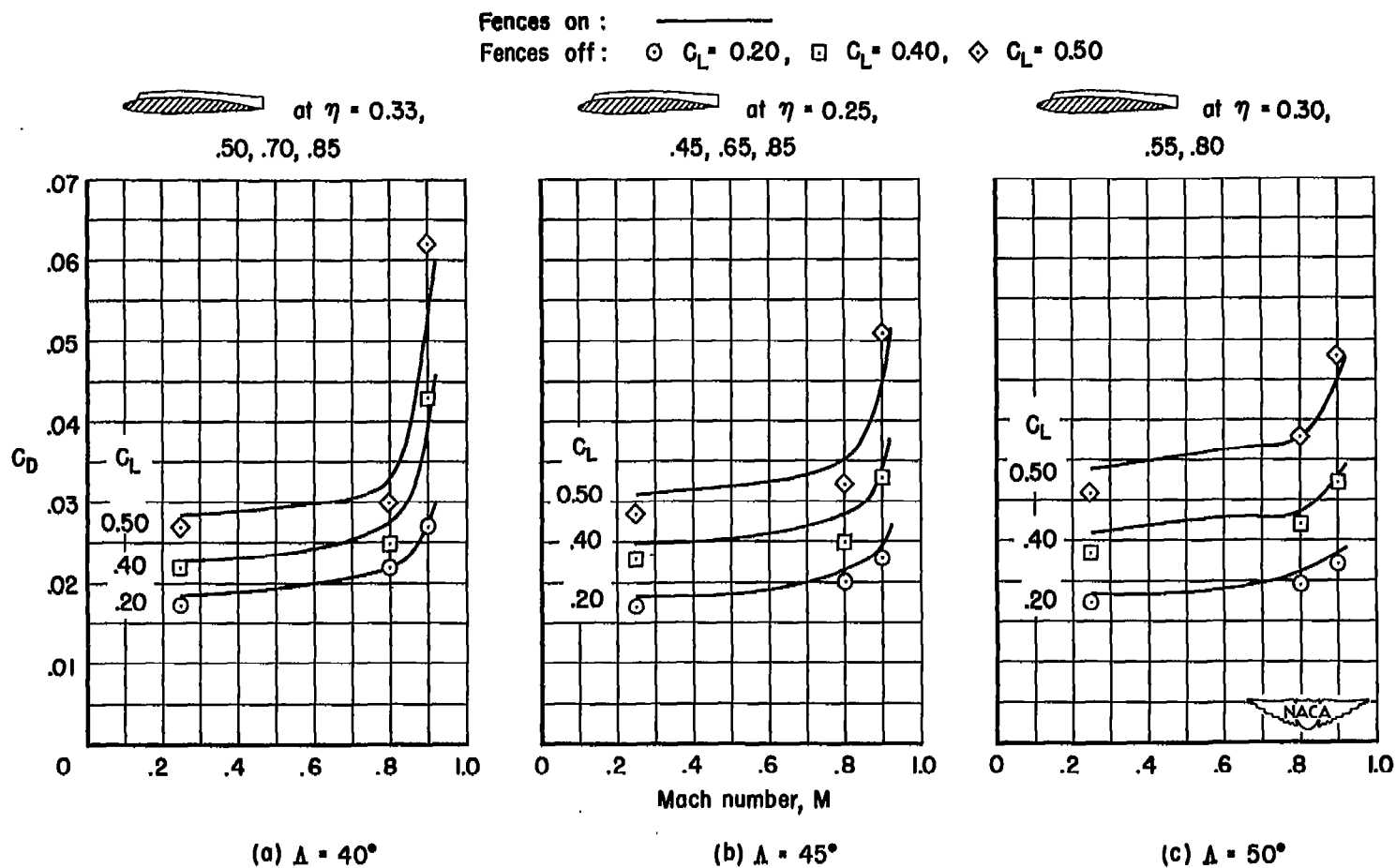
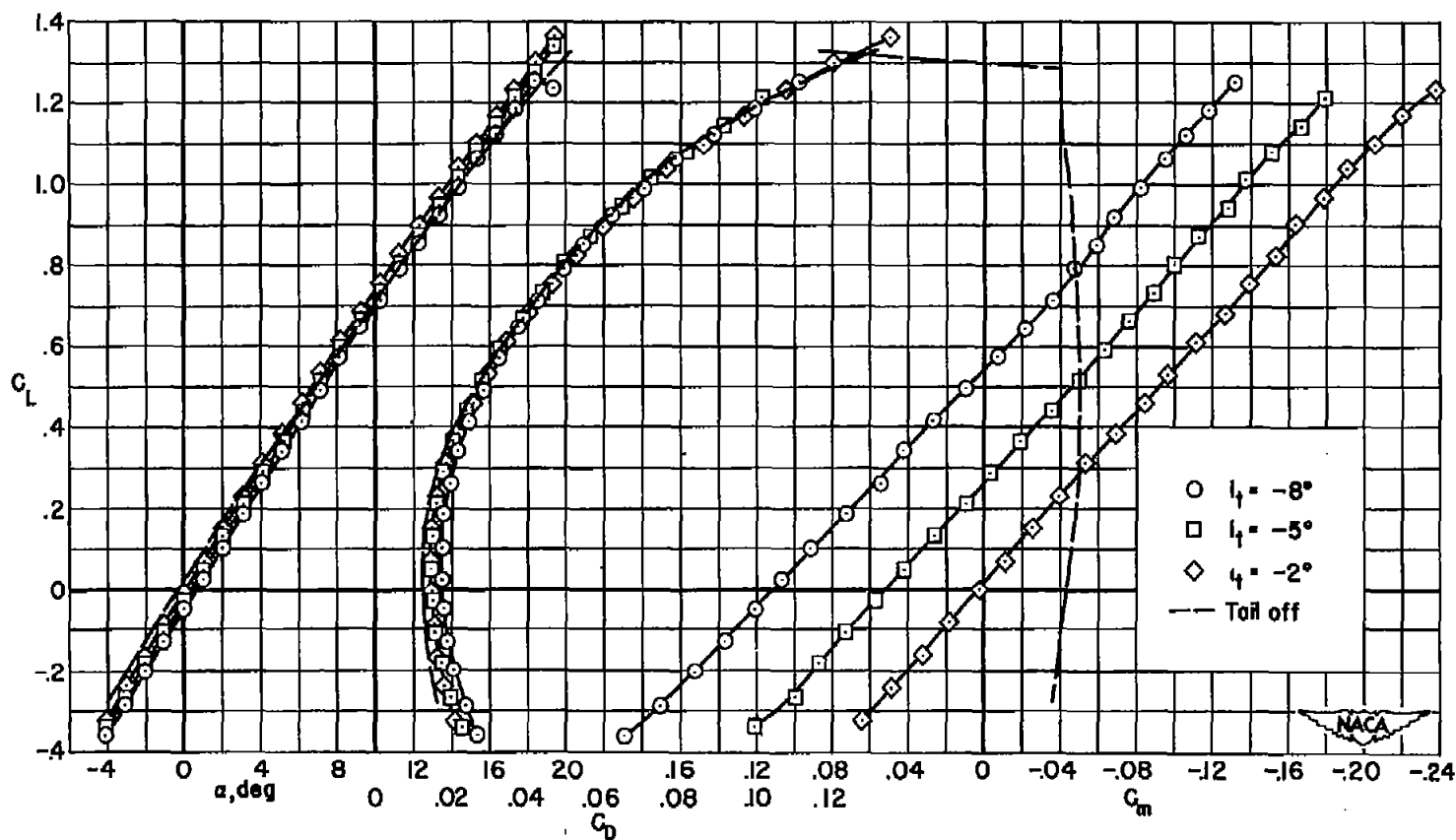
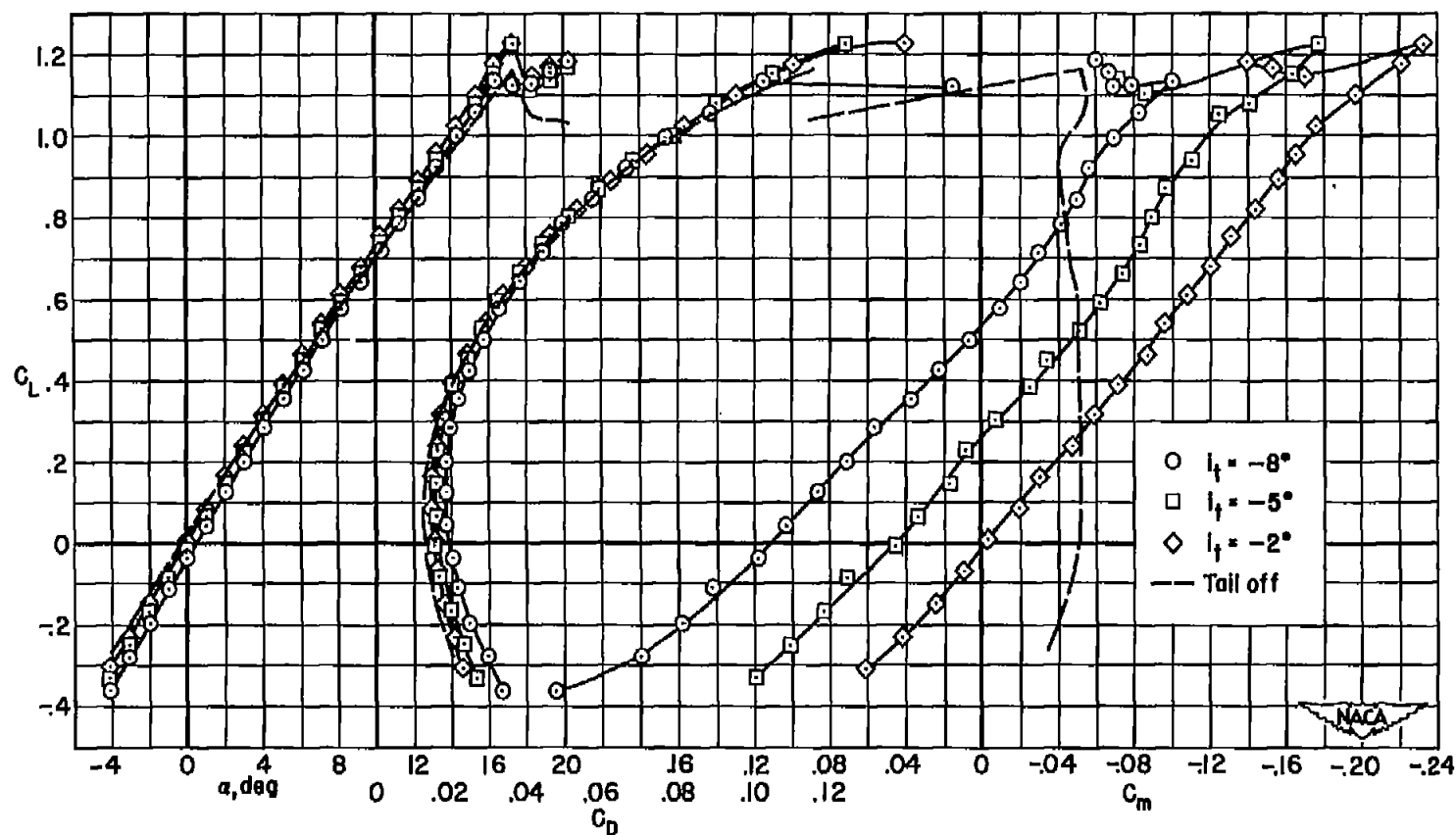


Figure 37.- The variation with Mach number of the drag coefficients of the wing-fuselage-tail combinations with and without fences at several constant lift coefficients; tail height = $0.5b$; $i_t = -8^\circ$; $R = 2,000,000$.



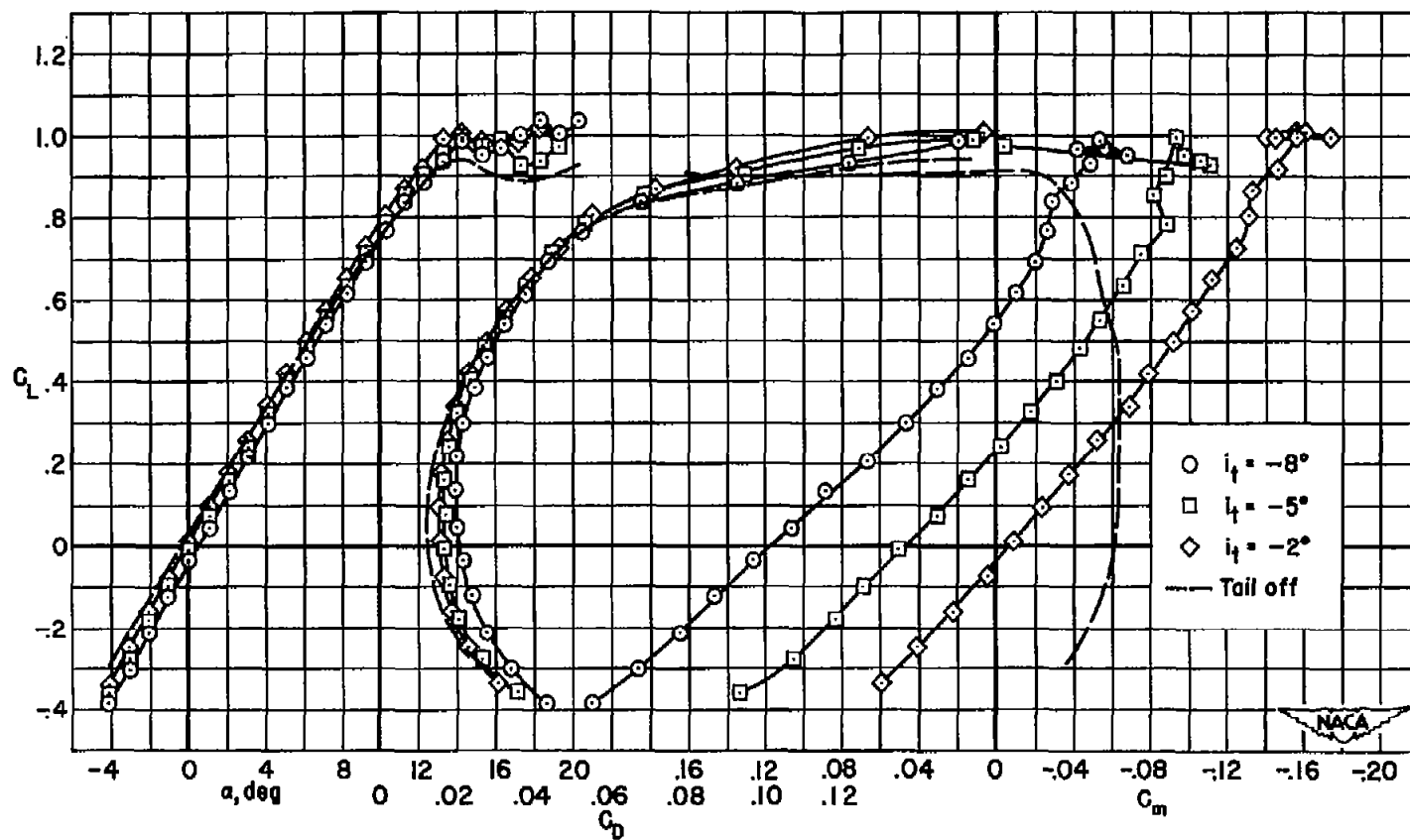
(a) $M = 0.25$; $R = 8,000,000$

Figure 38.- The longitudinal characteristics of the 40° combination with fences and a horizontal tail at several angles of incidence; tail height = $0.5b$.



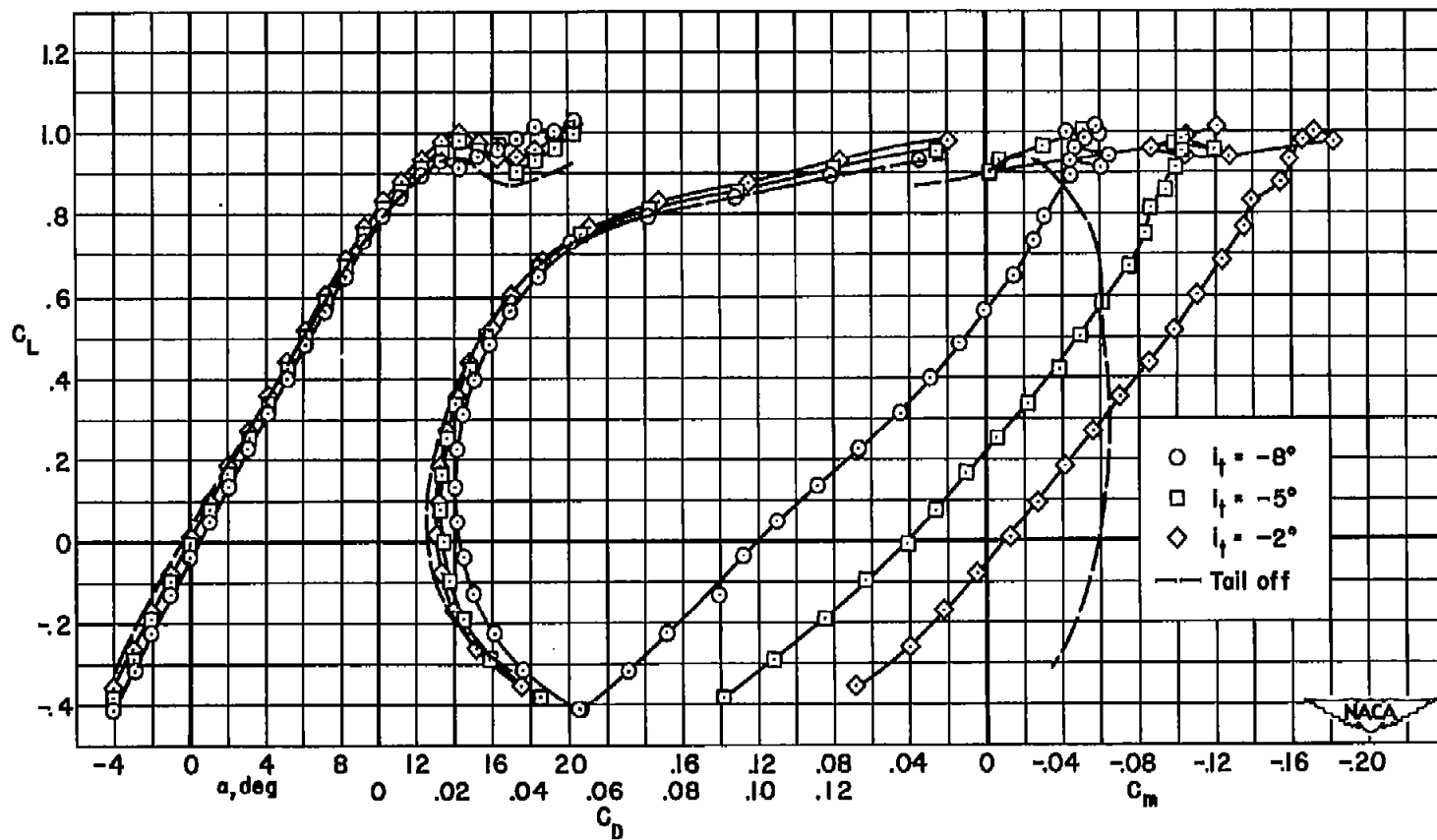
(b) $M = 0.25$; $R = 2,000,000$

Figure 38.- Continued.



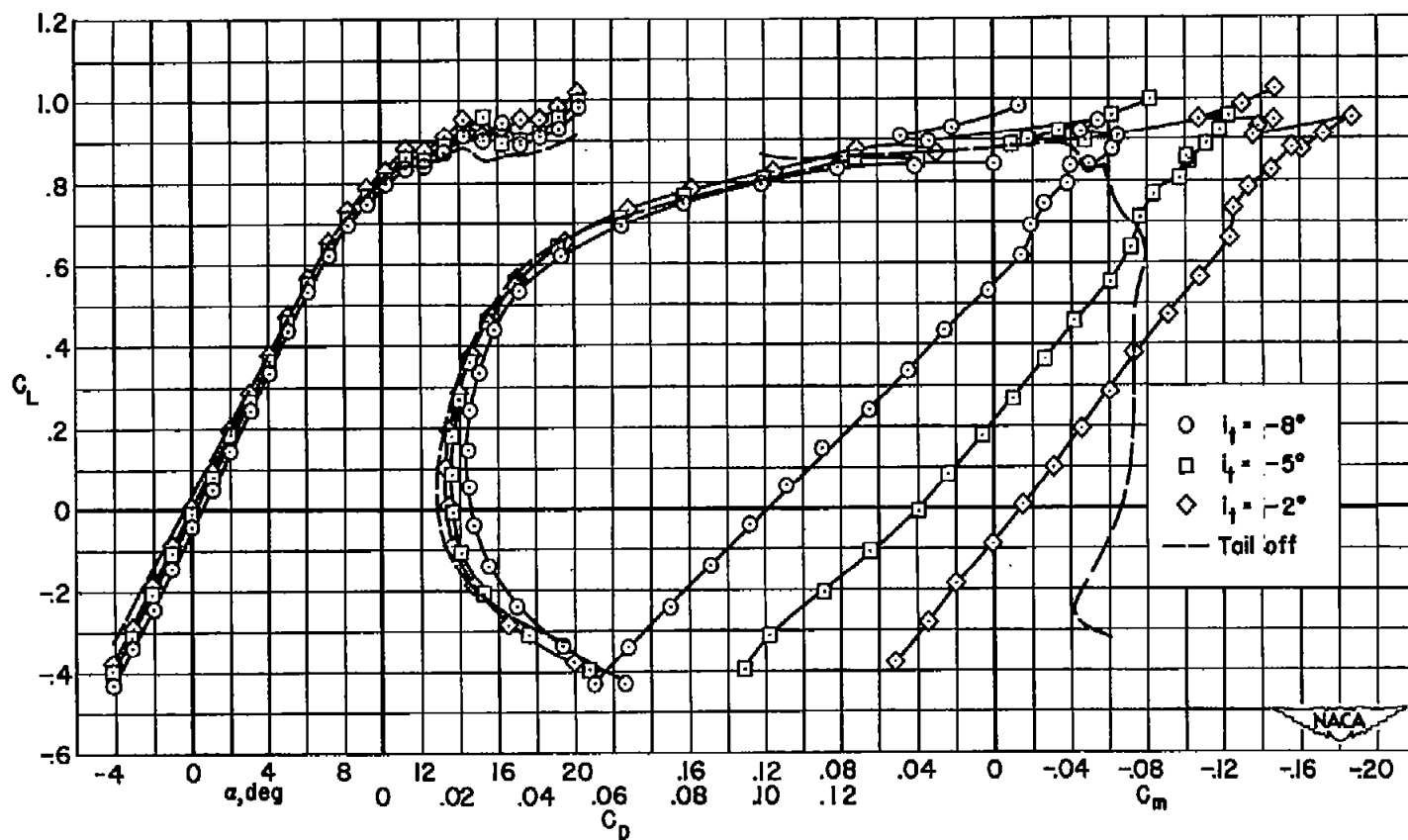
(c) $M = 0.60$; $R = 2,000,000$

Figure 38.- Continued.



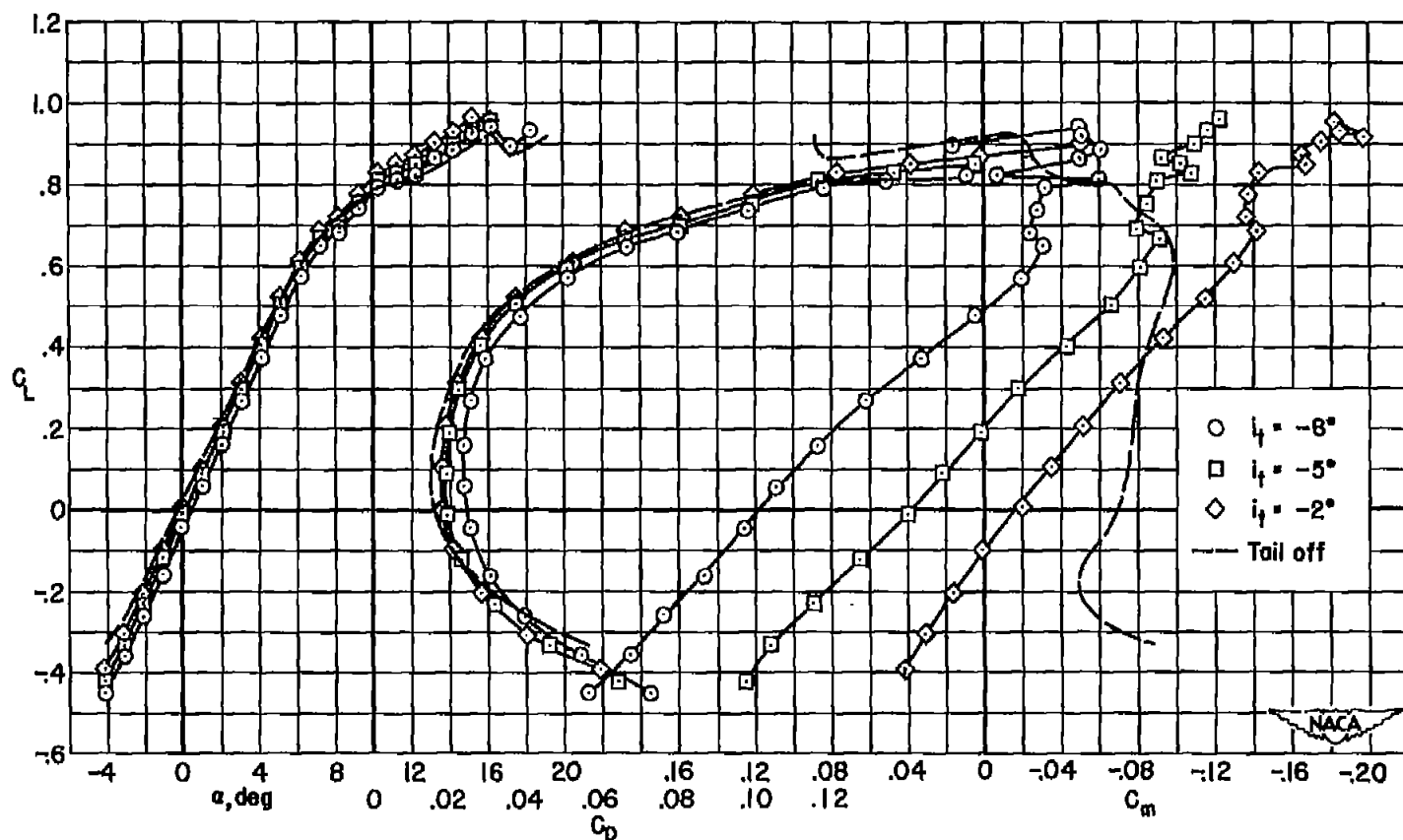
(d) $M = 0.70$; $R = 2,000,000$

Figure 38.- Continued.



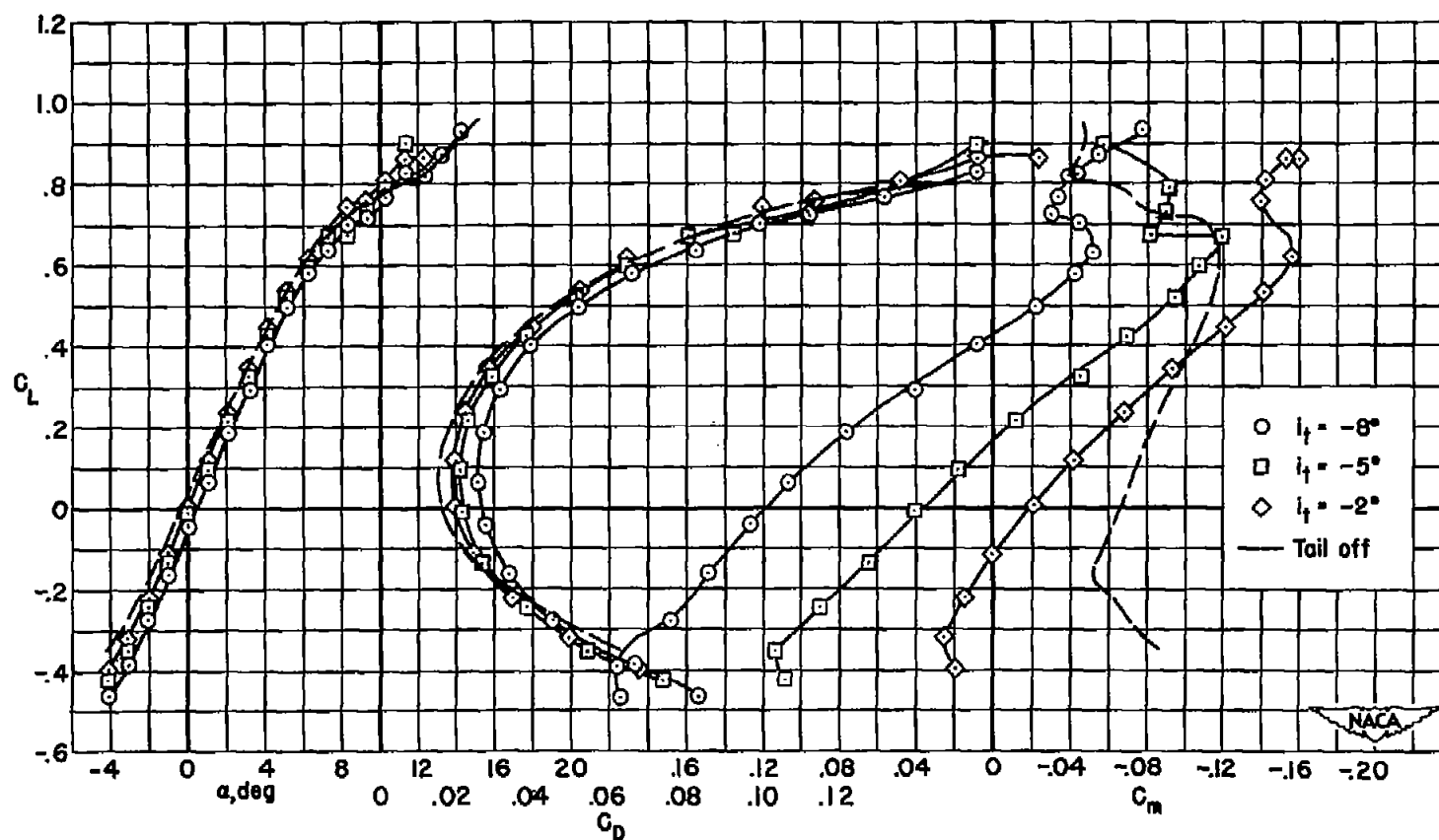
(e) $M = 0.80$; $R = 2,000,000$

Figure 38.- Continued.



(f) $M = 0.86$; $R = 2,000,000$

Figure 38.- Continued.



(g) $M = 0.90$; $R = 2,000,000$

Figure 38.- Continued.

CONFIDENTIAL

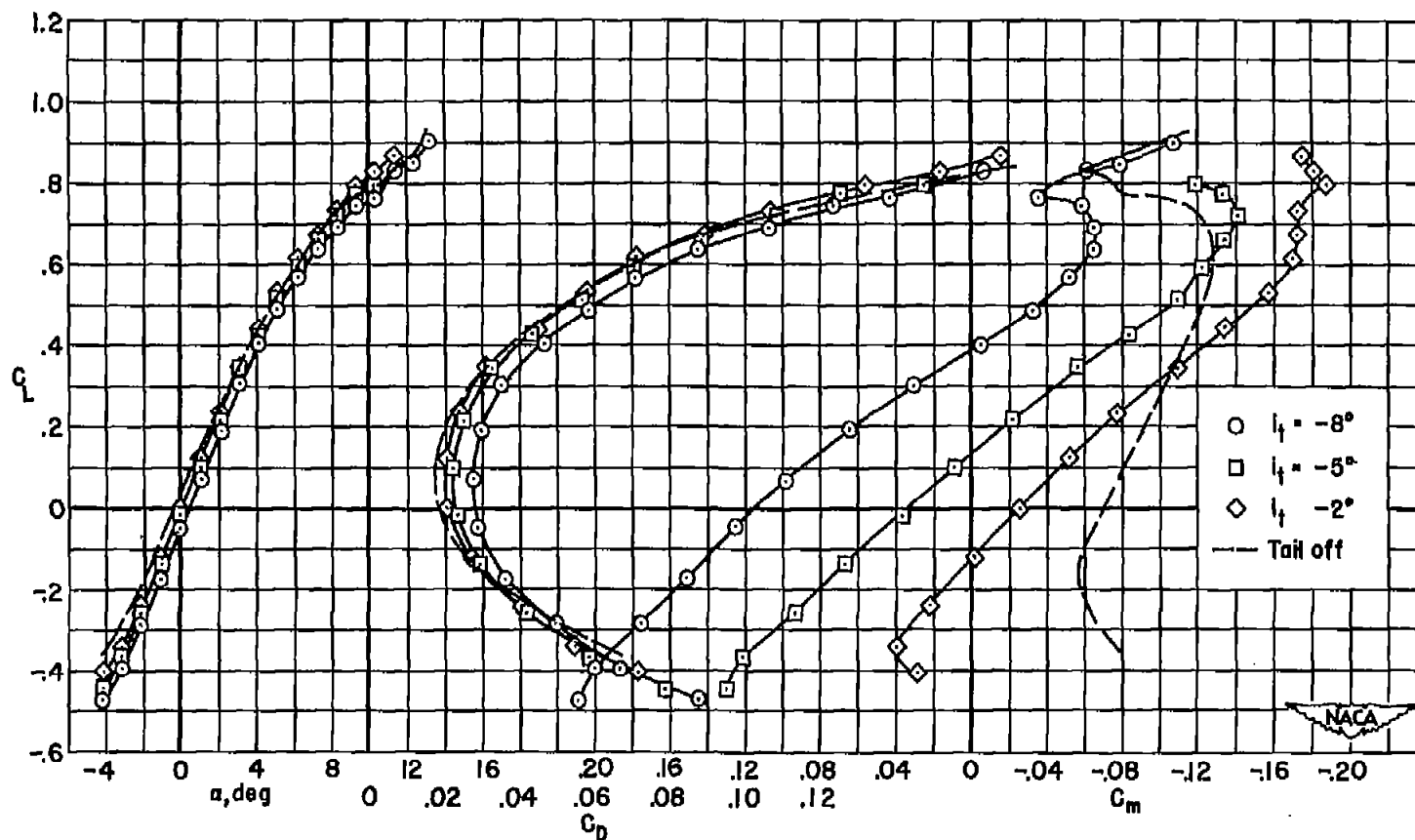
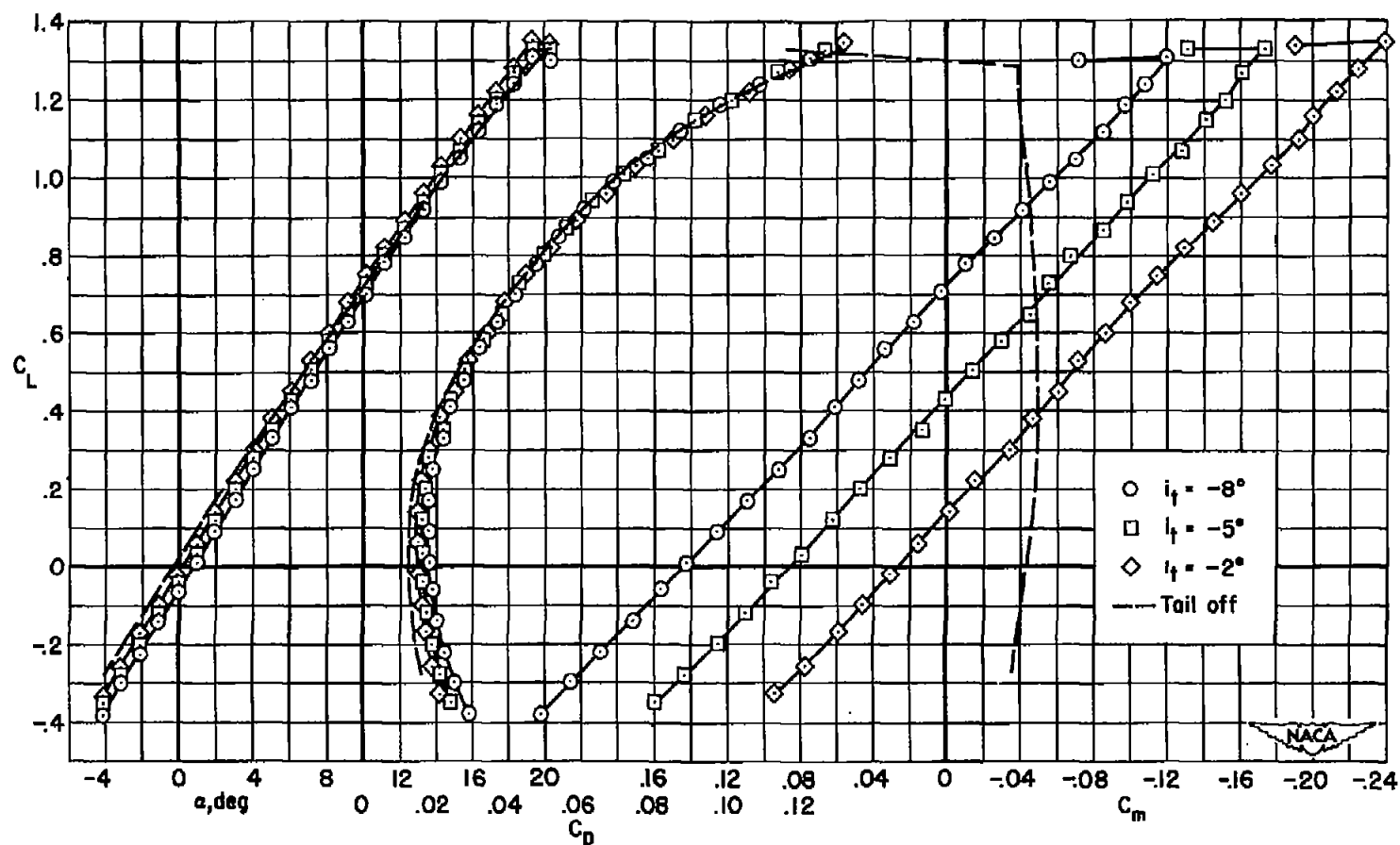
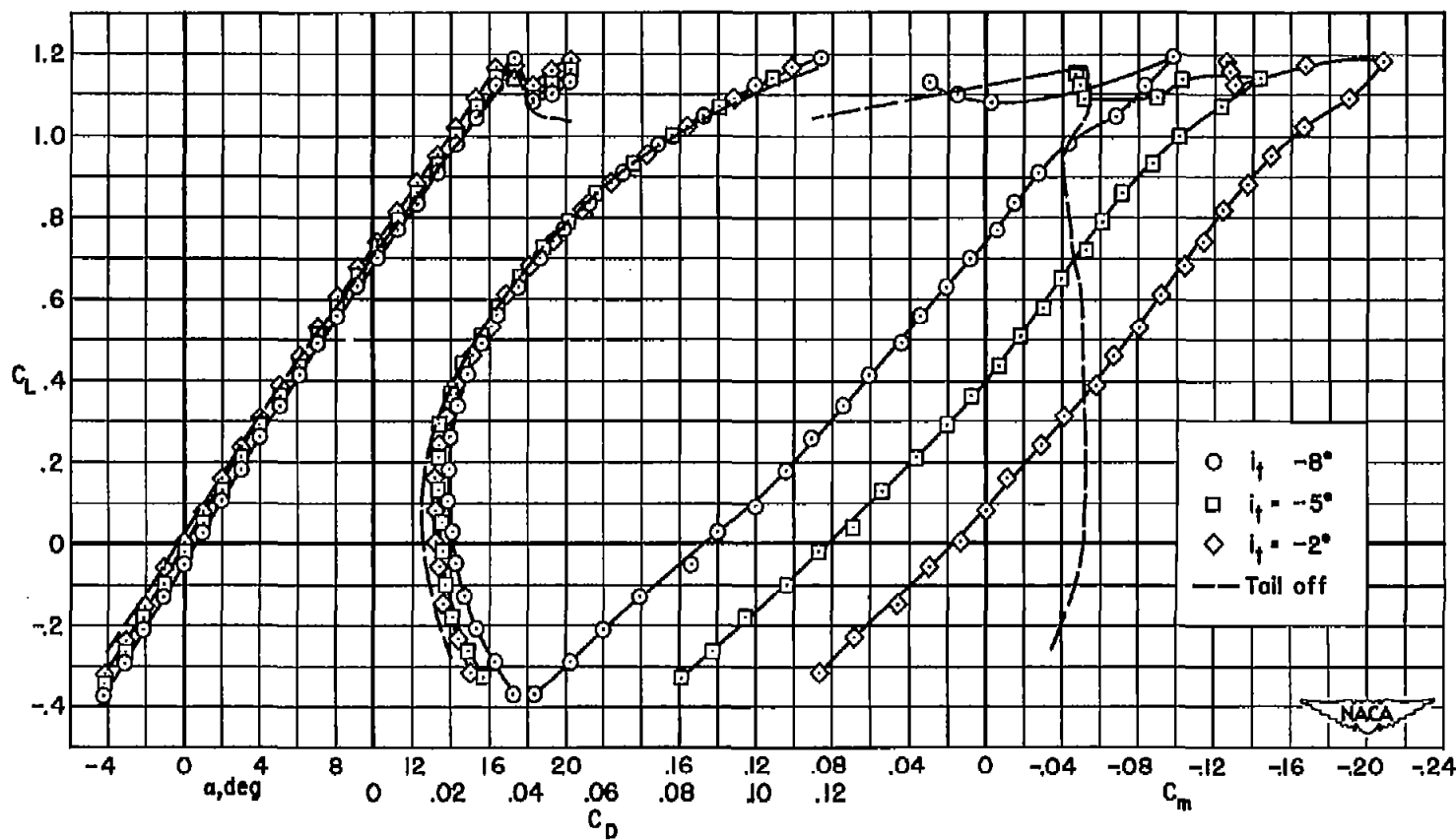
(h) $M = 0.92$; $R = 2,000,000$

Figure 38.- Concluded.



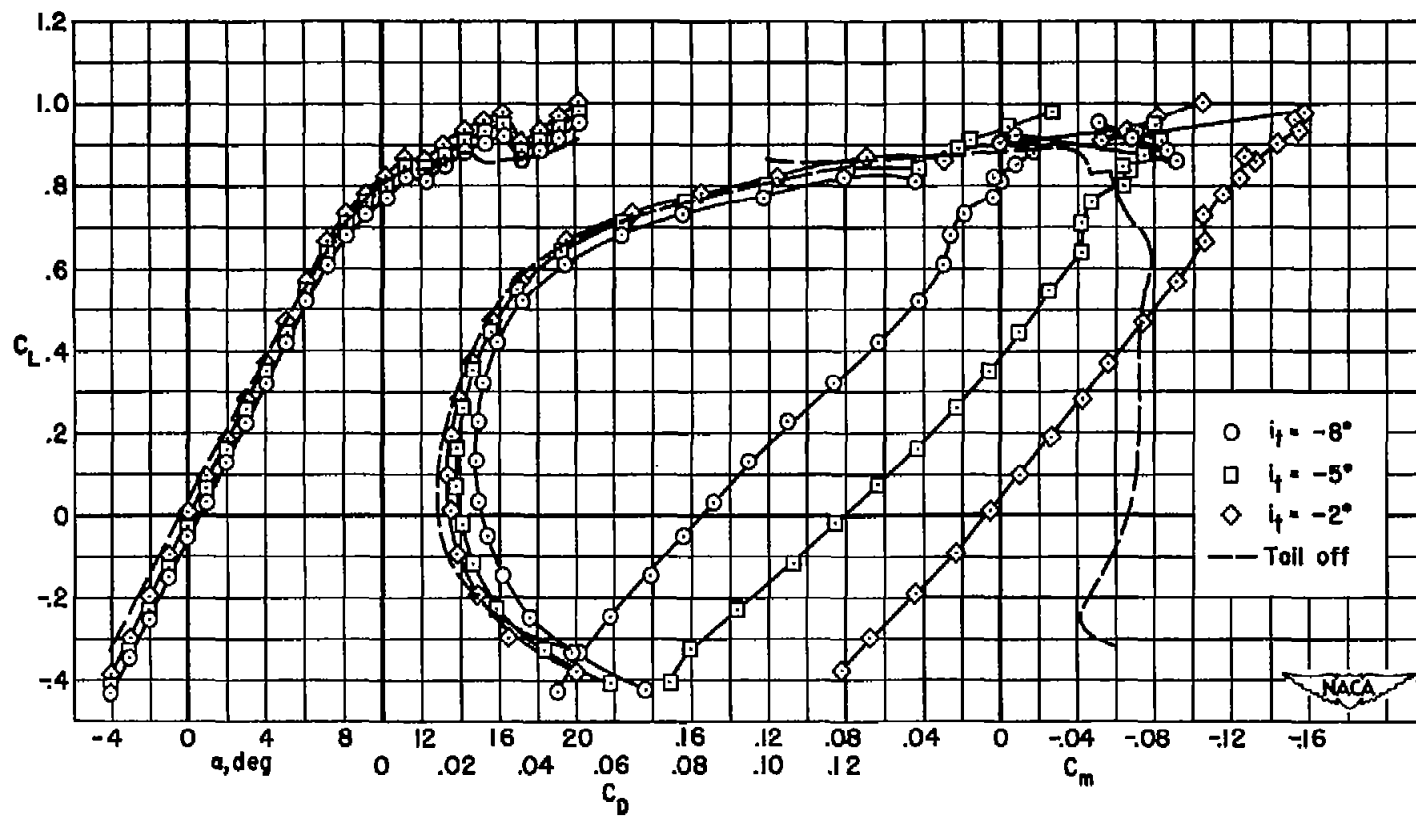
(a) $M = 0.25$; $R = 8,000,000$

Figure 39.- The longitudinal characteristics of the 40° combination with fences and a horizontal tail at several angles of incidence; tail height = $0.07 b/2$.



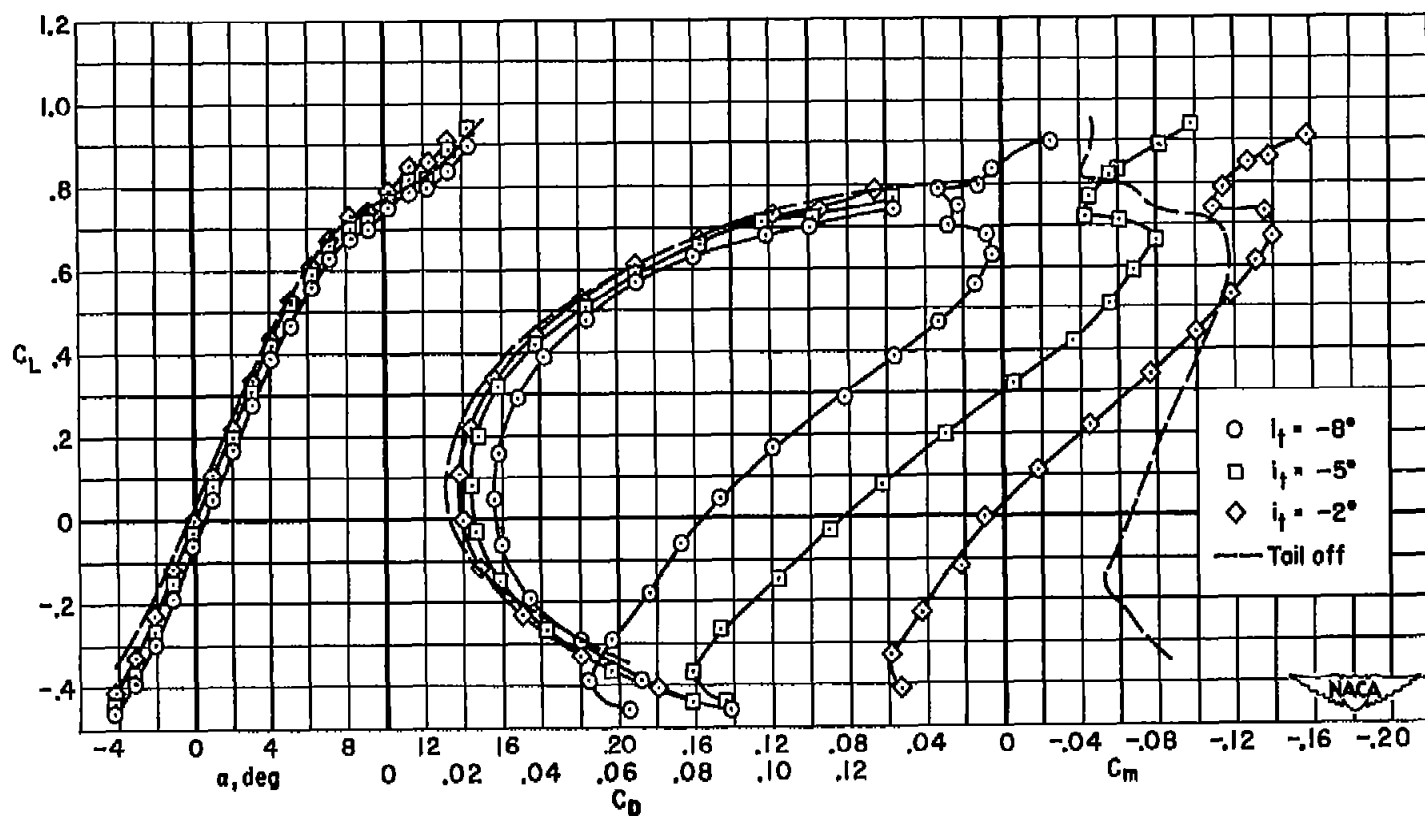
(b) $M = 0.25$; $R = 2,000,000$

Figure 39.- Continued.



(c) $M = 0.80$; $R = 2,000,000$

Figure 39.- Continued.



(d) $M = 0.90$; $R = 2,000,000$

Figure 39.- Concluded.

CONFIDENTIAL

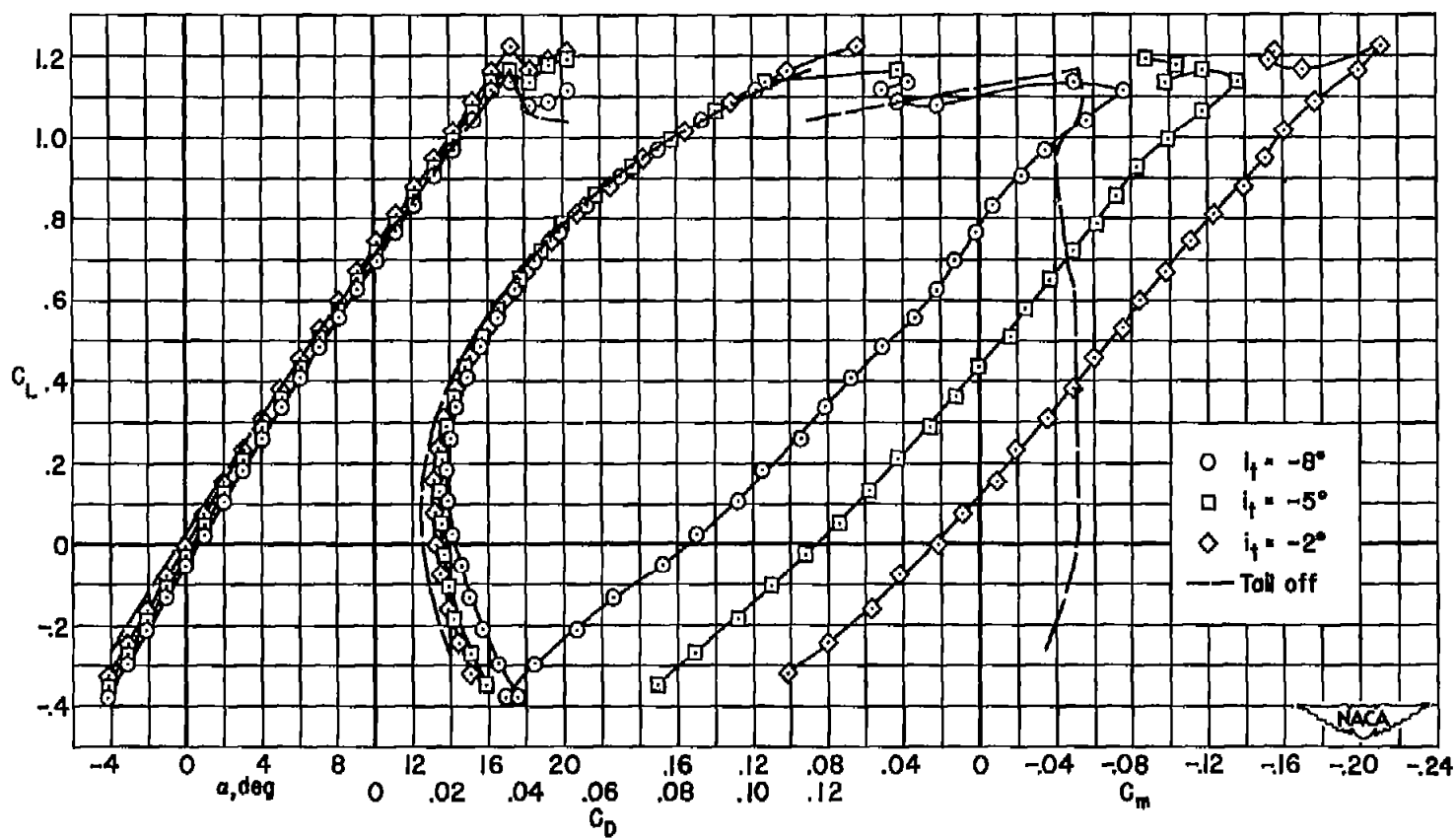
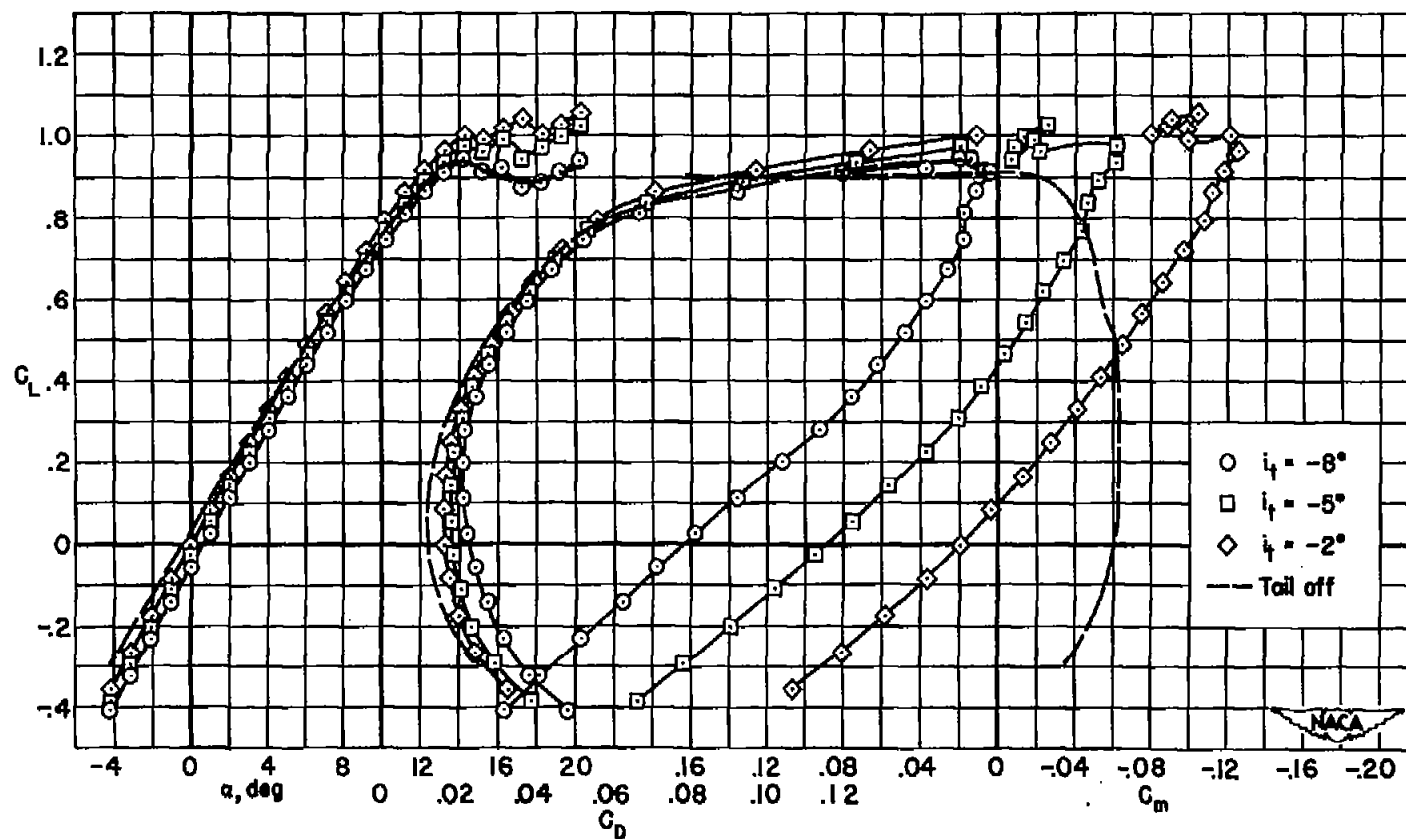
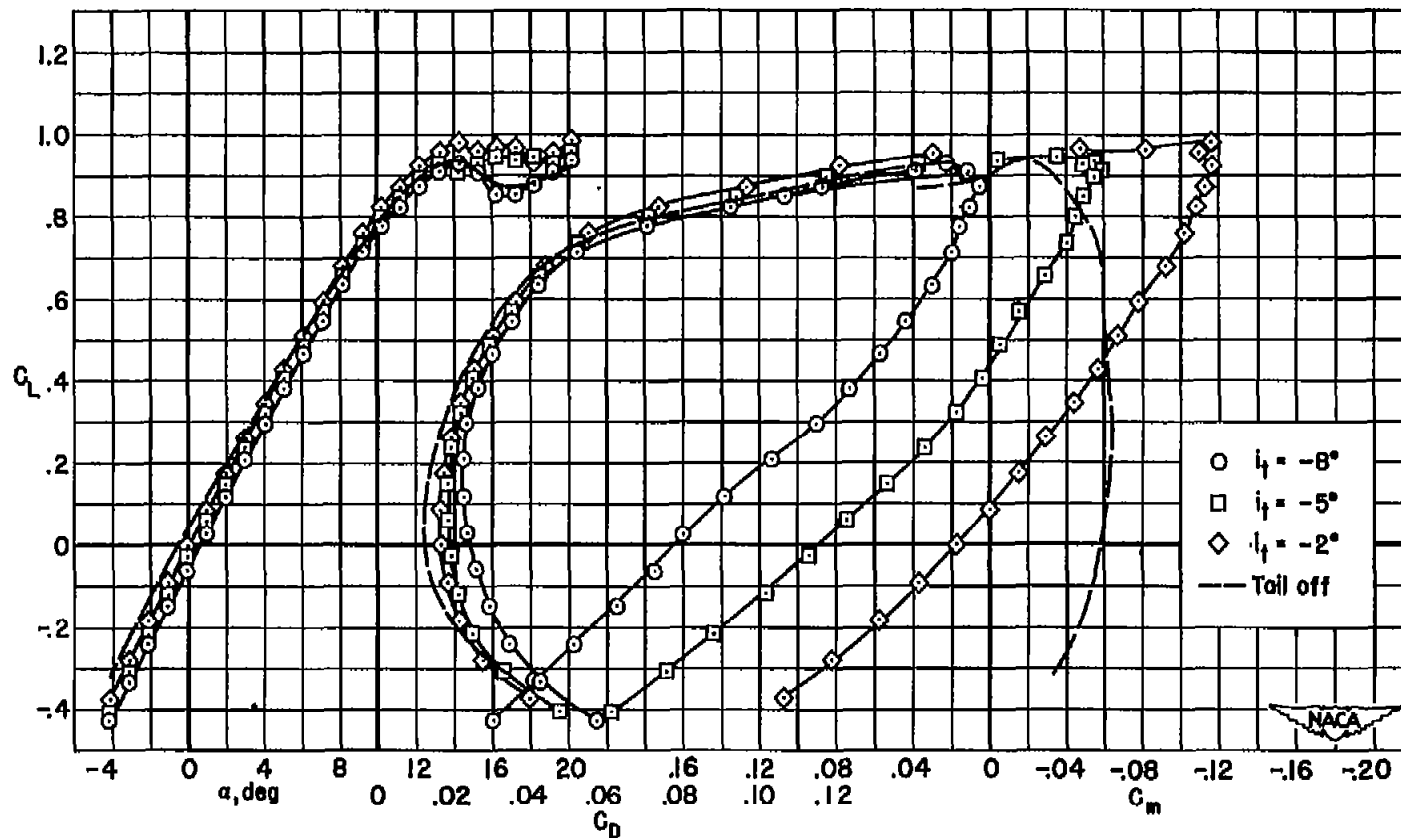
(b) $M = 0.25$; $R = 2,000,000$

Figure 40.- Continued.



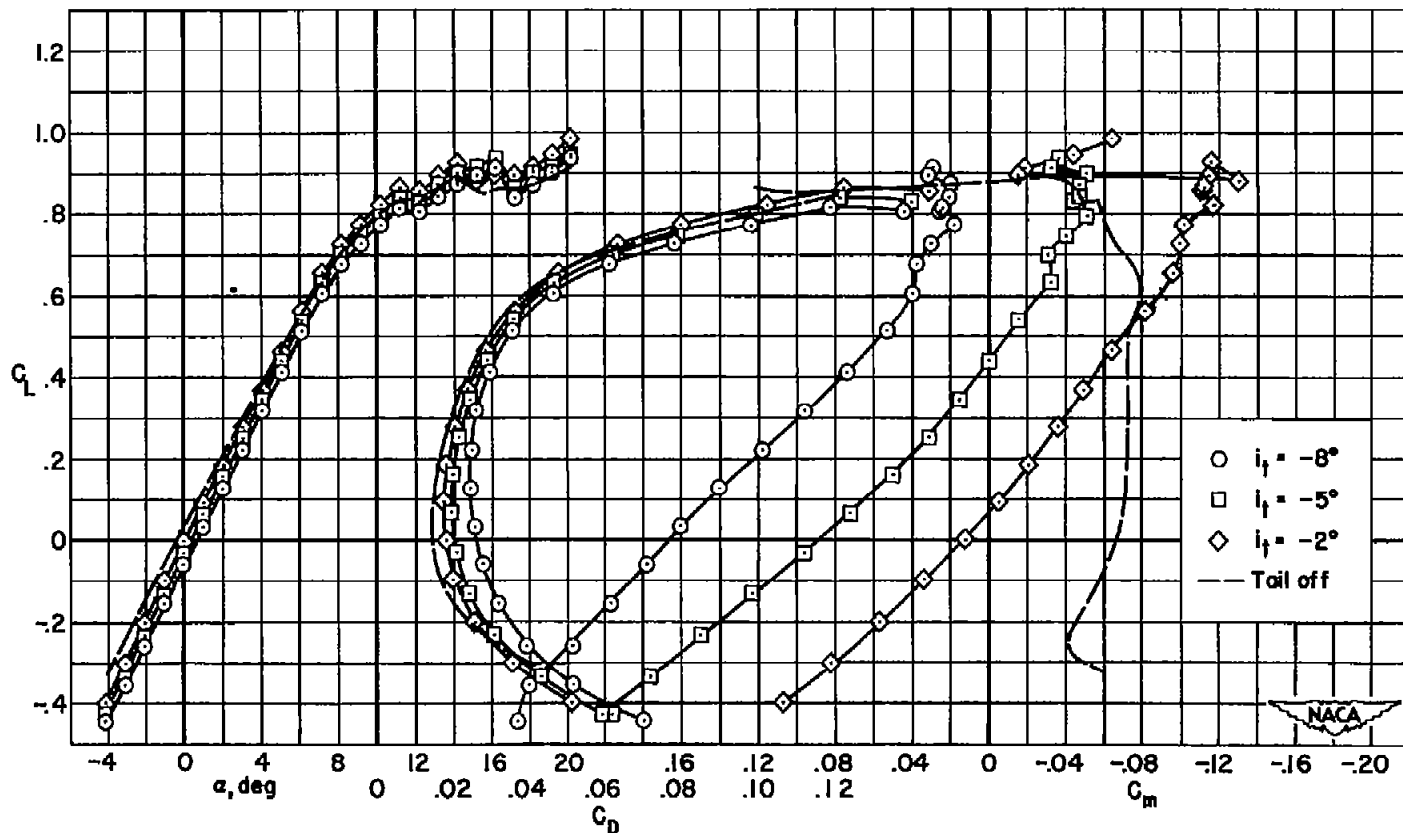
(c) $M = 0.60$; $R = 2,000,000$

Figure 40.- Continued.



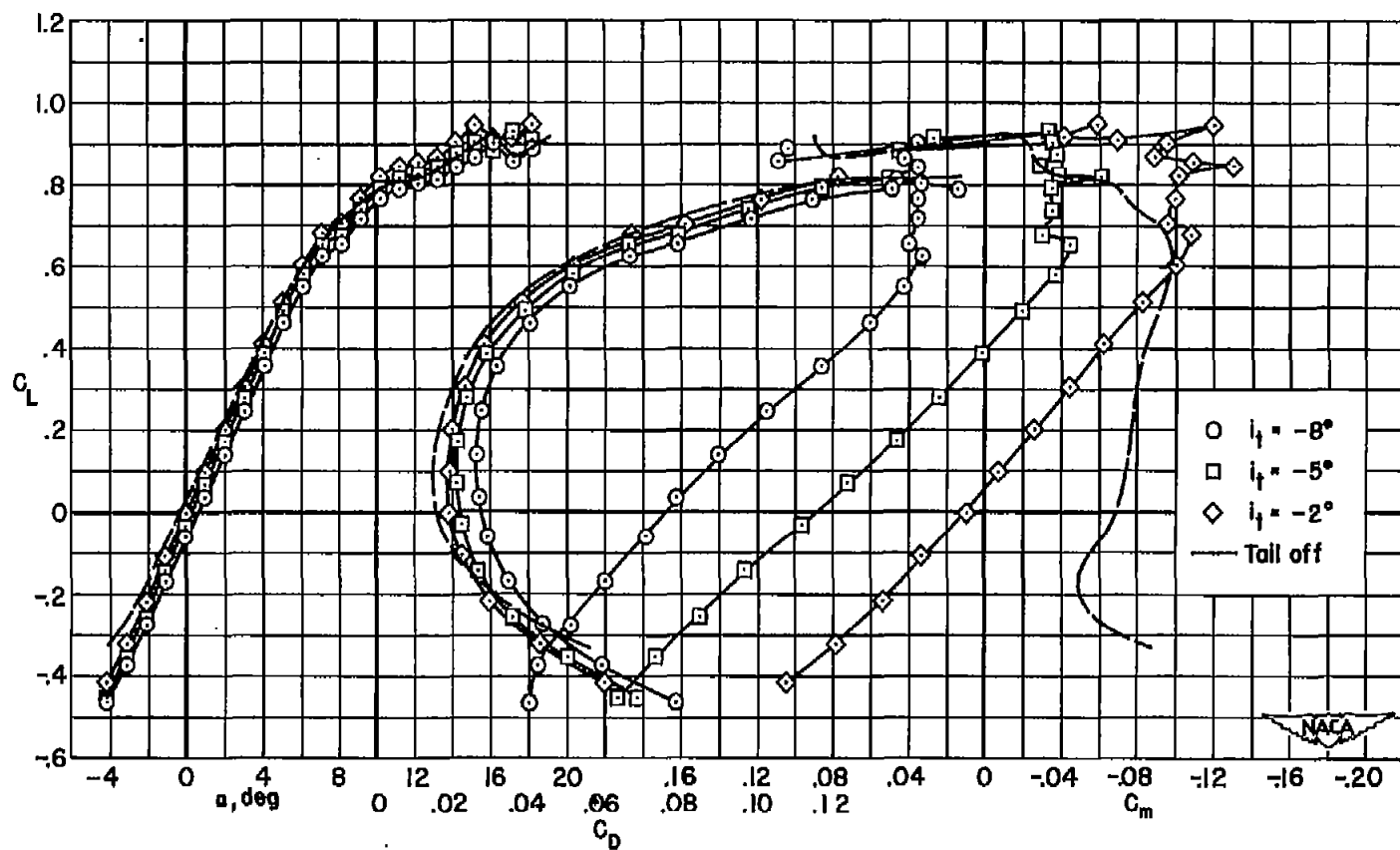
(d) $M = 0.70$; $R = 2,000,000$

Figure 40.- Continued.



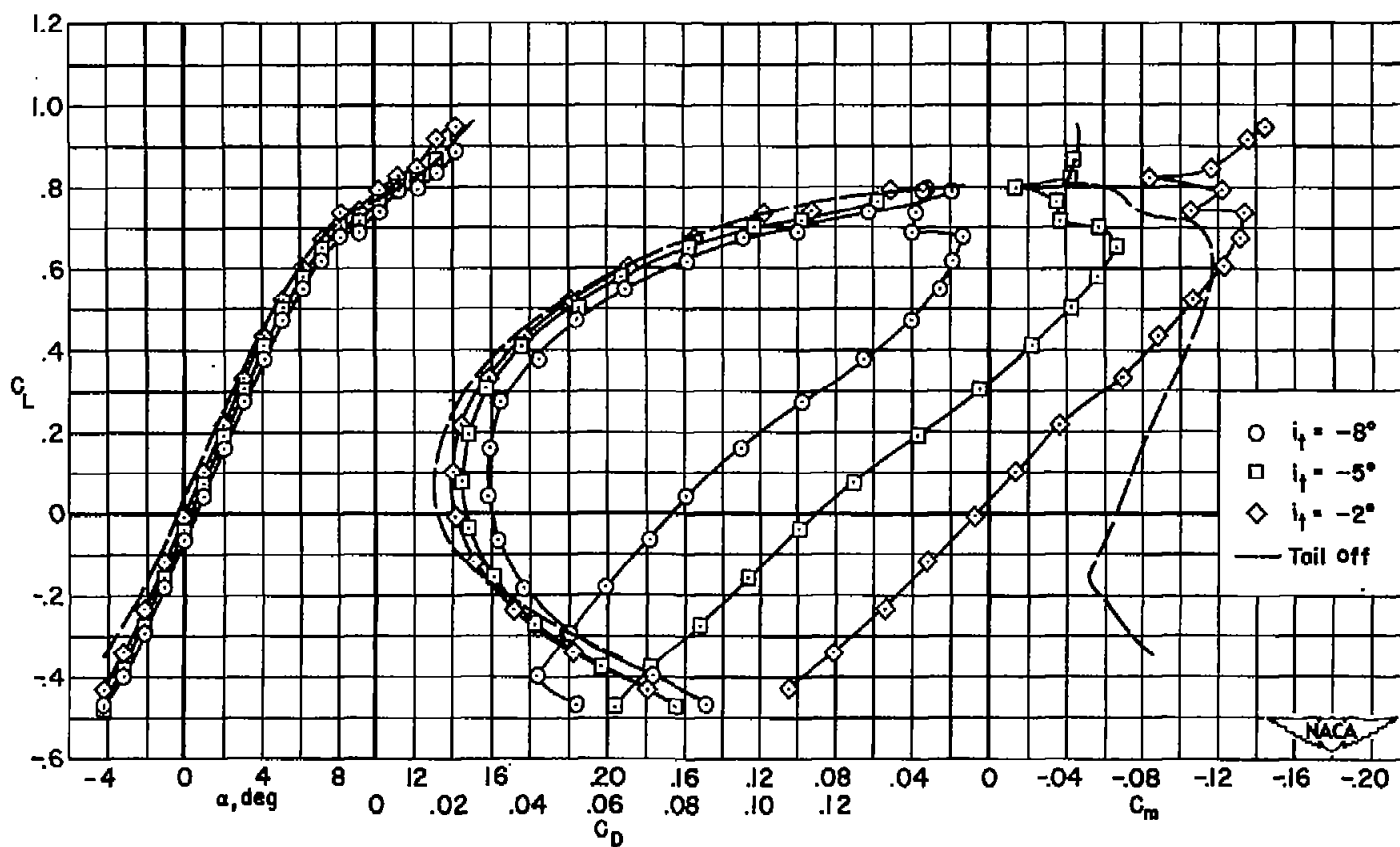
(e) $M = 0.80$; $R = 2,000,000$

Figure 40.- Continued.



(f) $M = 0.86$; $R = 2,000,000$

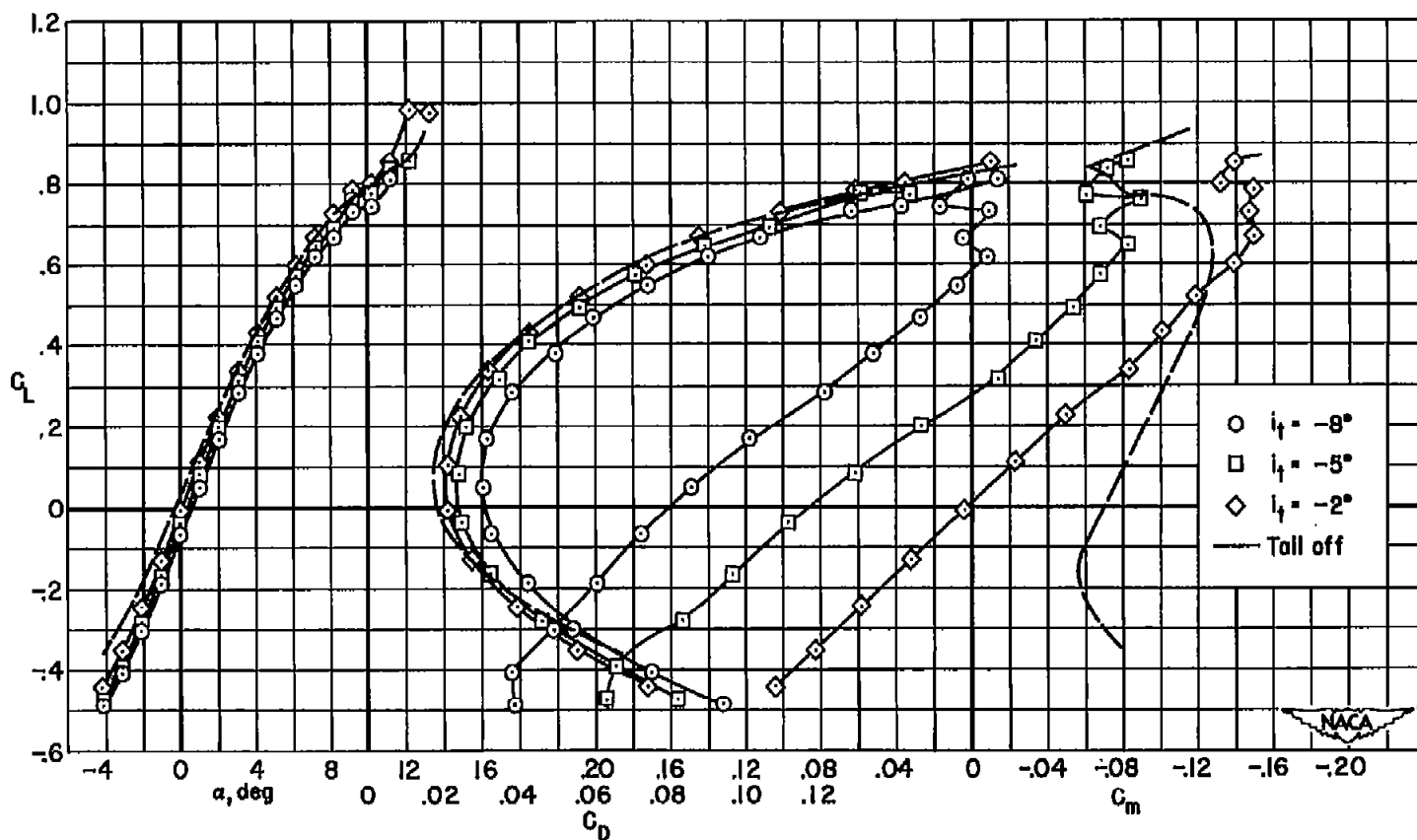
Figure 40.- Continued.



(g) $M = 0.90$; $R = 2,000,000$

Figure 40.- Continued

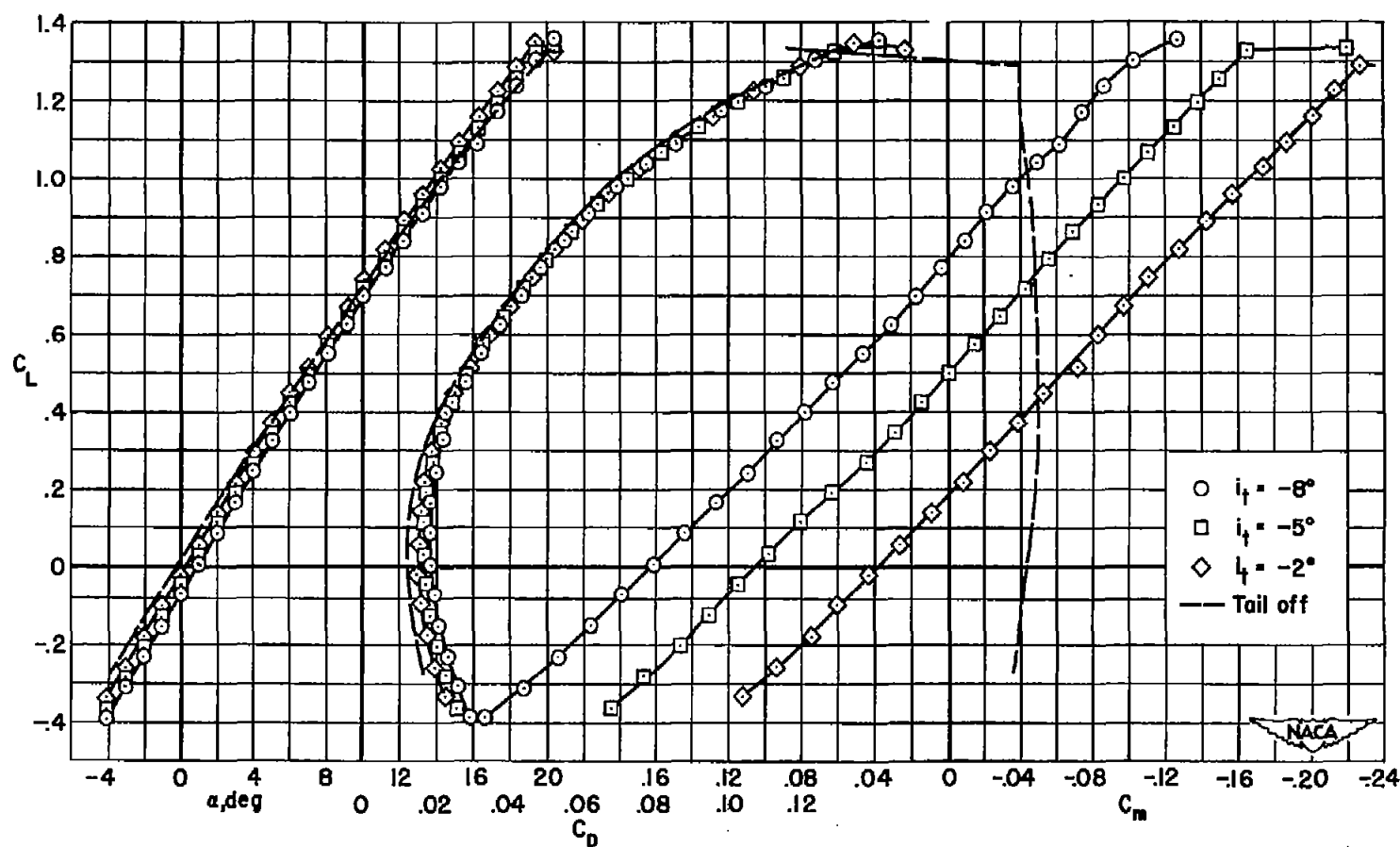
CONFIDENTIAL



(h) $M = 0.92$; $R = 2,000,000$

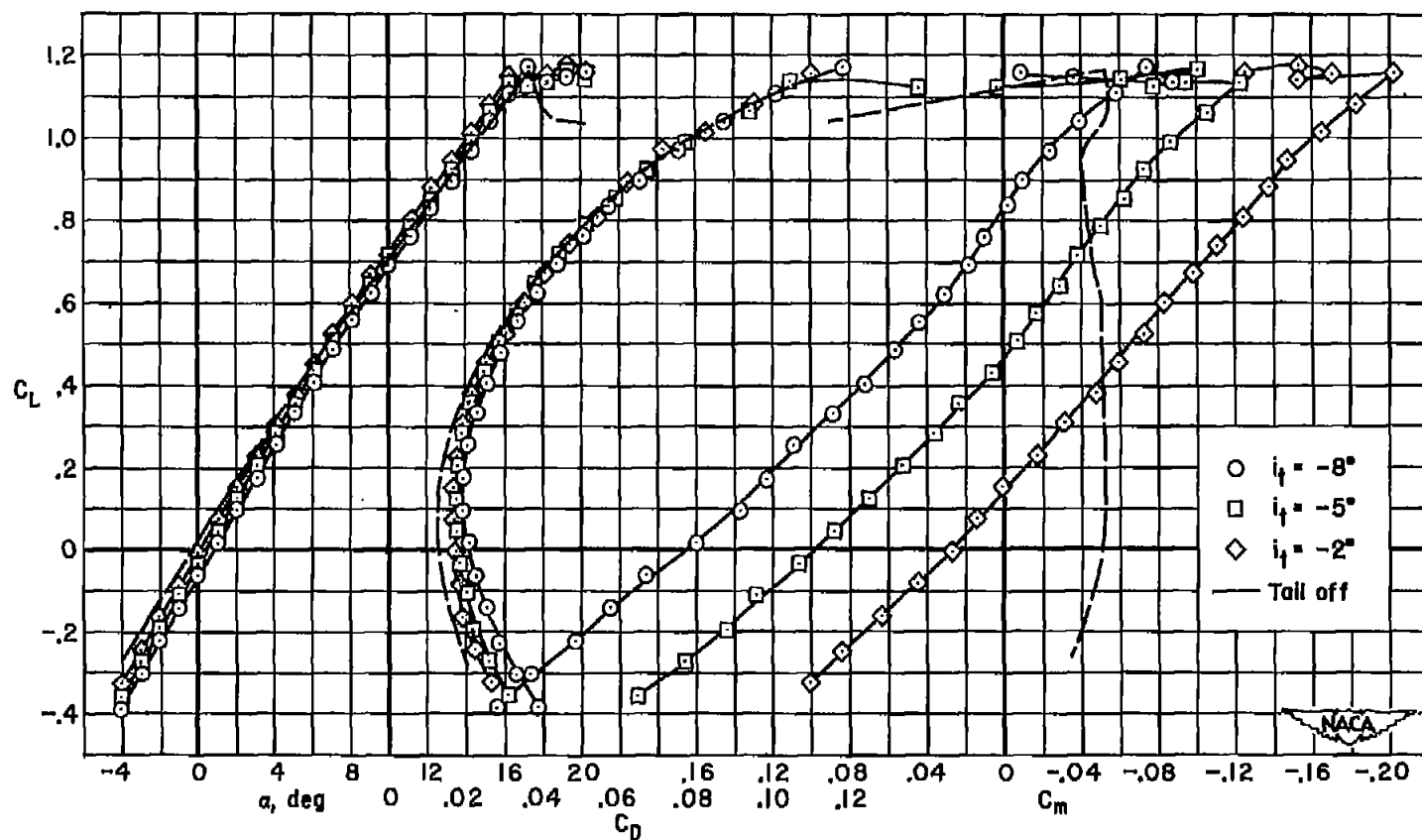
Figure 40.- Concluded.

CONFIDENTIAL



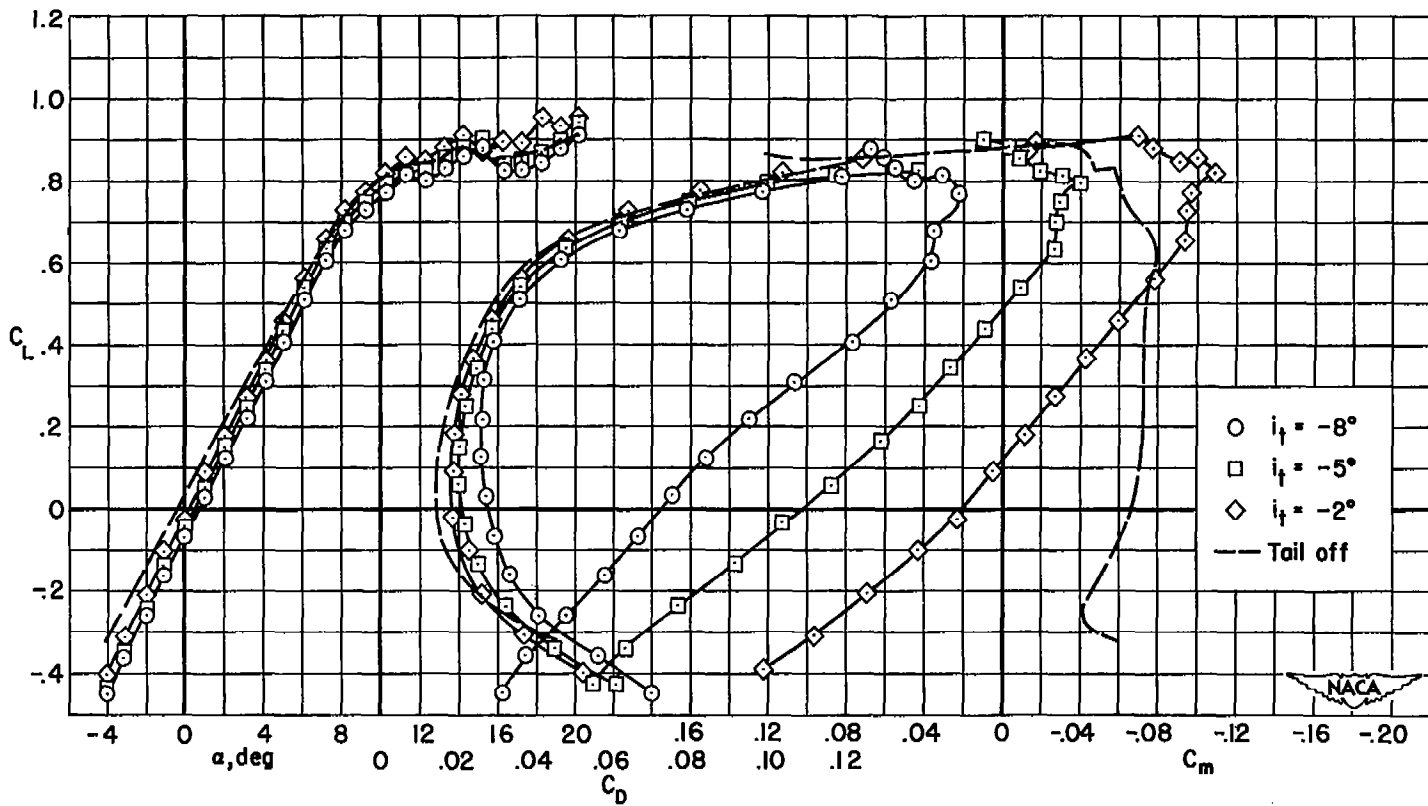
(a) $M = 0.25$; $R = 8,000,000$

Figure 41.- The longitudinal characteristics of the 40° combination with fences and a horizontal tail at several angles of incidence; tail height = $0.19 b/2$.



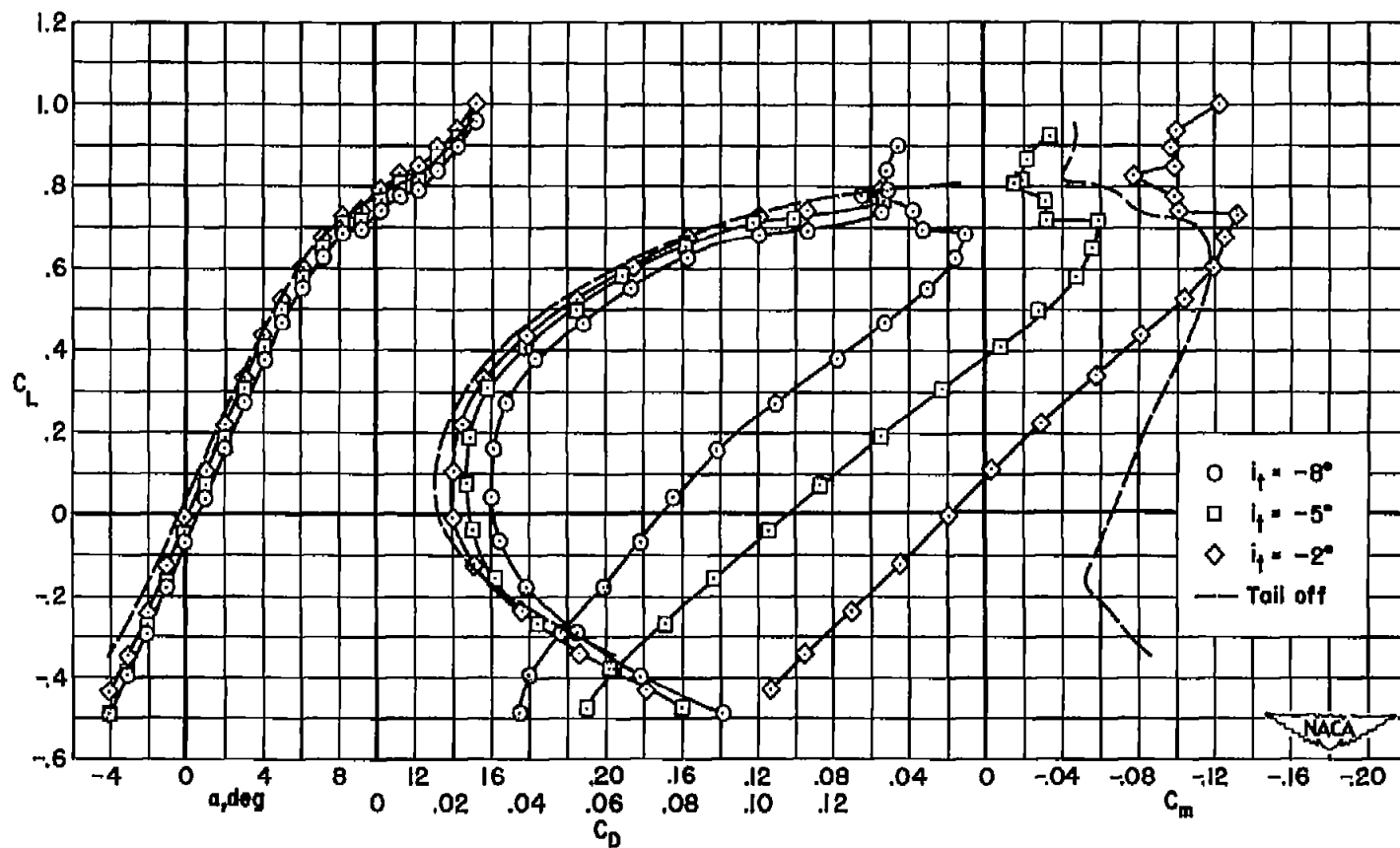
(b) $M = 0.25$; $R = 2,000,000$

Figure 41.- Continued.



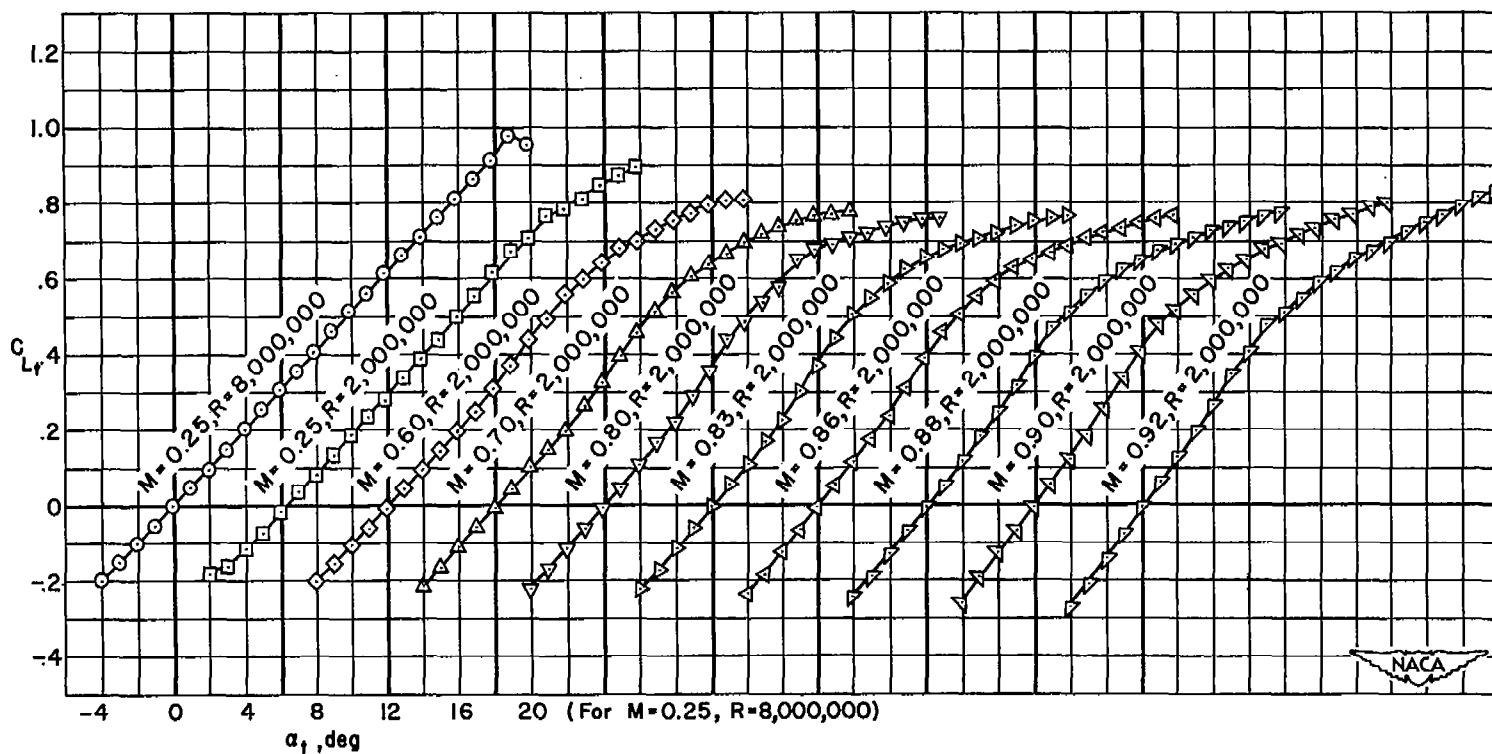
(c) $M = 0.80$; $R = 2,000,000$

Figure 41.- Continued.



(a) $M = 0.90$; $R = 2,000,000$

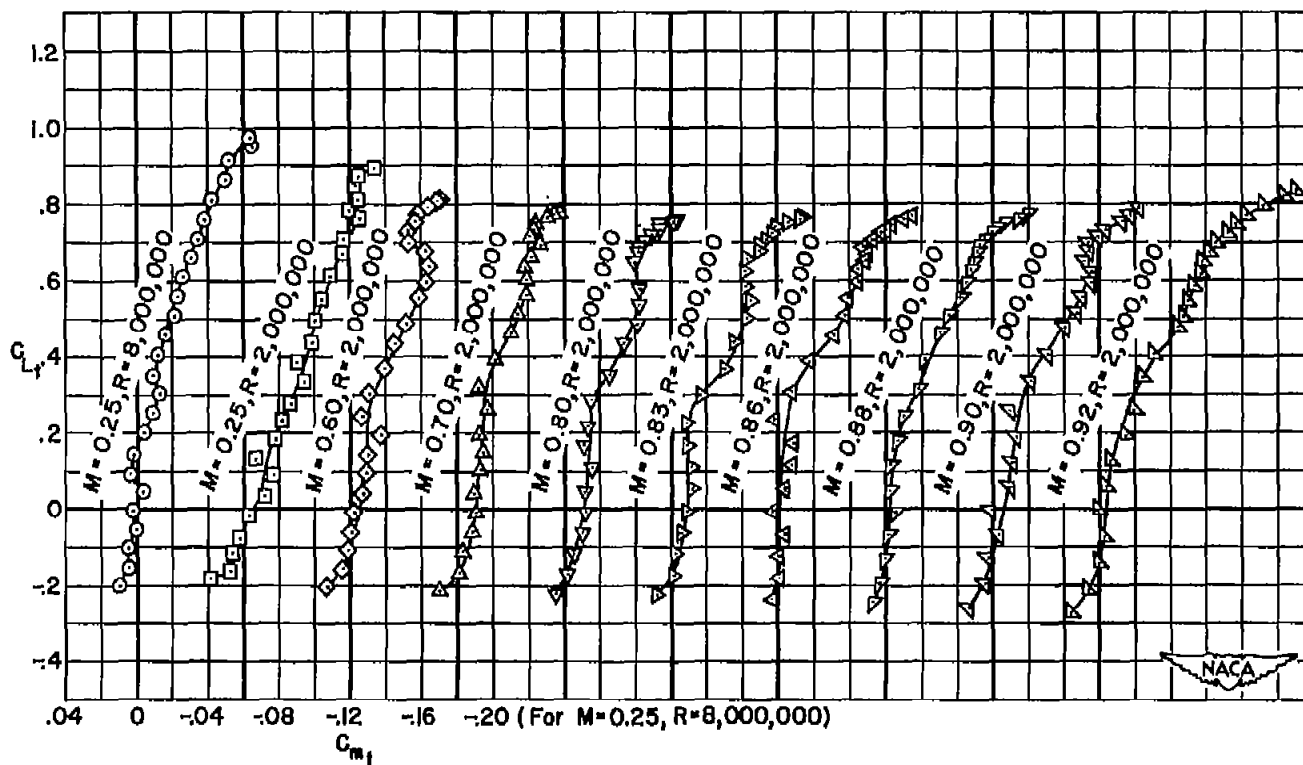
Figure 41.- Concluded.



(a) Lift.

Figure 42.- The lift and pitching-moment characteristics of the isolated horizontal tail.

CONFIDENTIAL



(b) Pitching moment.

Figure 42.- Concluded.

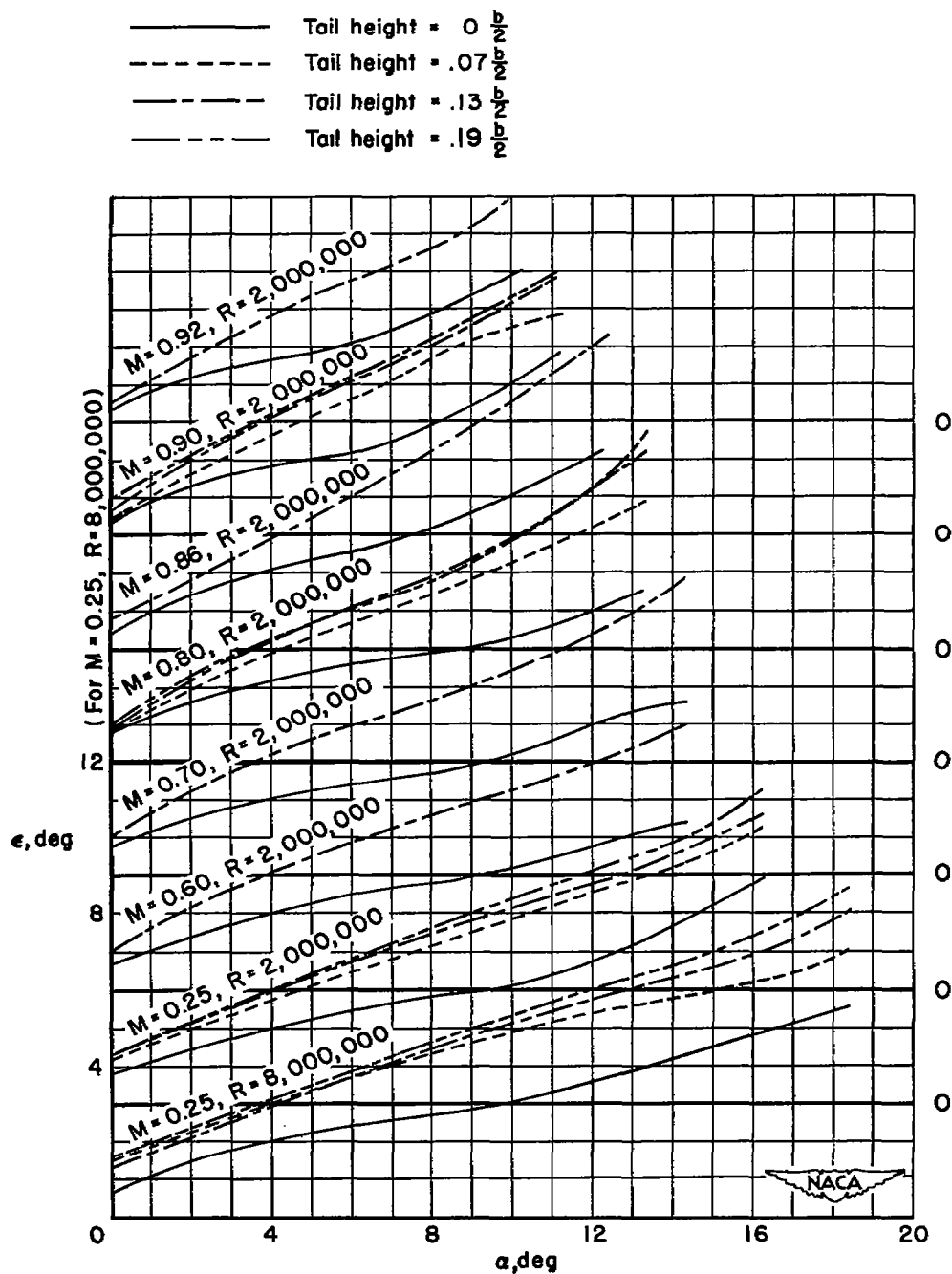
~~CONFIDENTIAL~~

Figure 43.- The factors affecting the stability contribution of the horizontal tail at several tail heights on the 40° combination.

~~CONFIDENTIAL~~

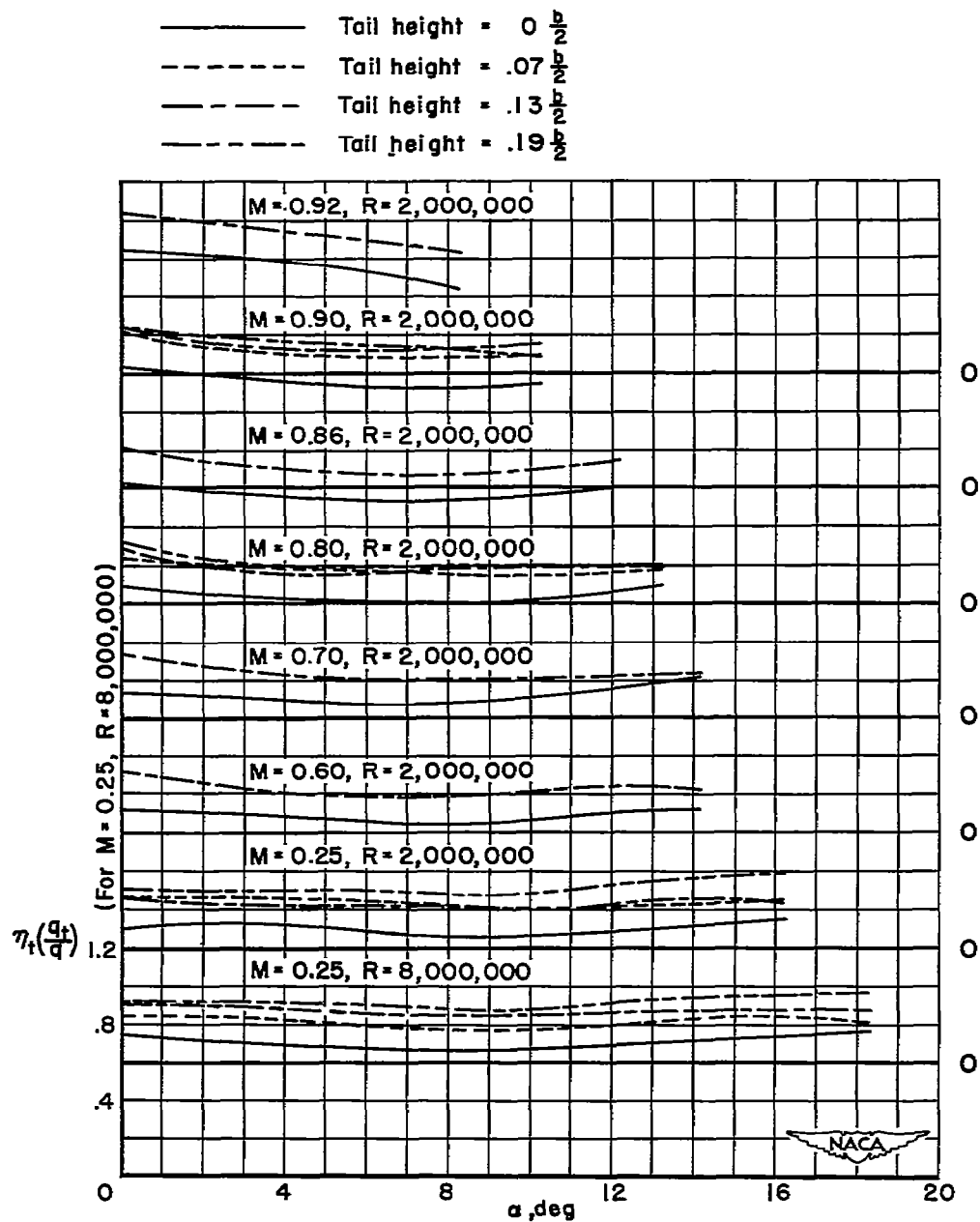
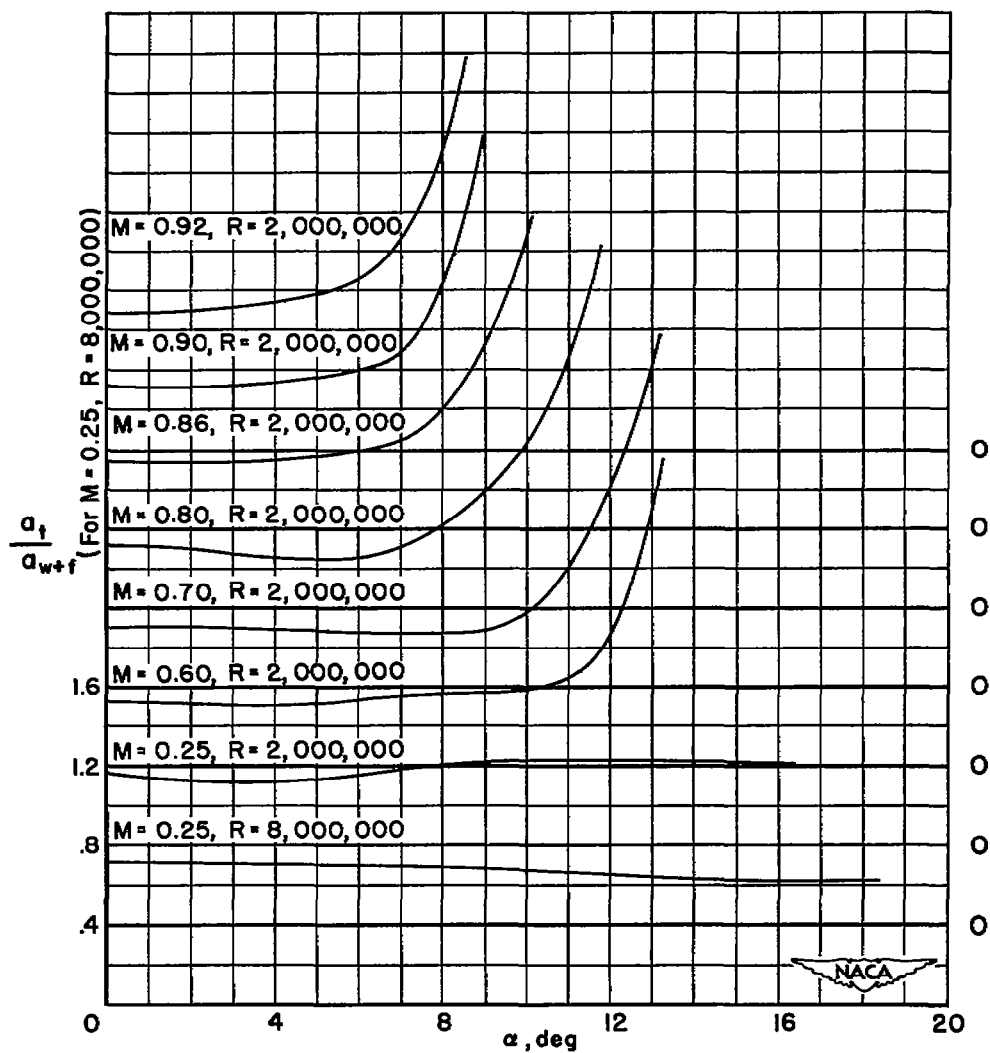
(b) $\eta_t(q_t/q)$ vs. α

Figure 43.- Continued.



(c) a_t/a_{w+f} vs. α

Figure 43.- Concluded.

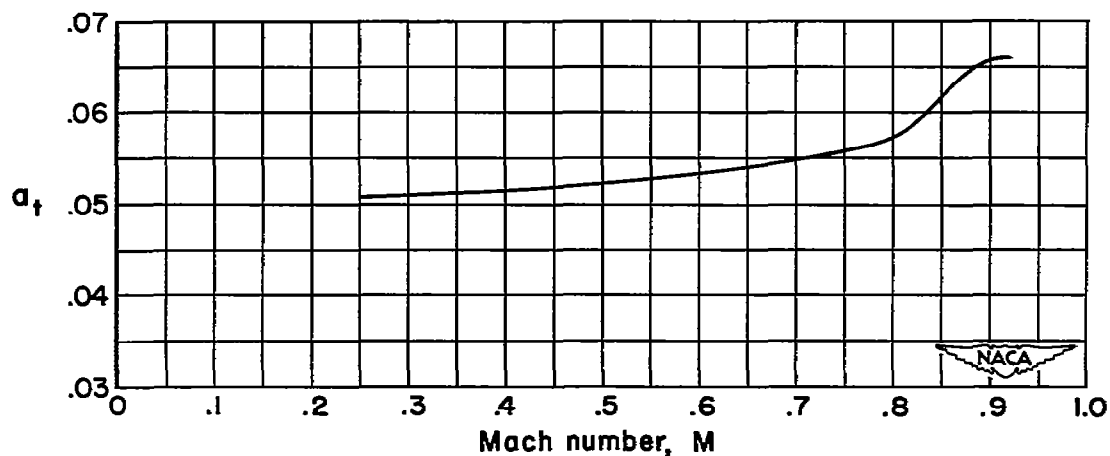


Figure 44.- The variation with Mach number of the lift-curve slope of the isolated horizontal tail; $\alpha_t = 4^\circ$; $R = 2,000,000$.

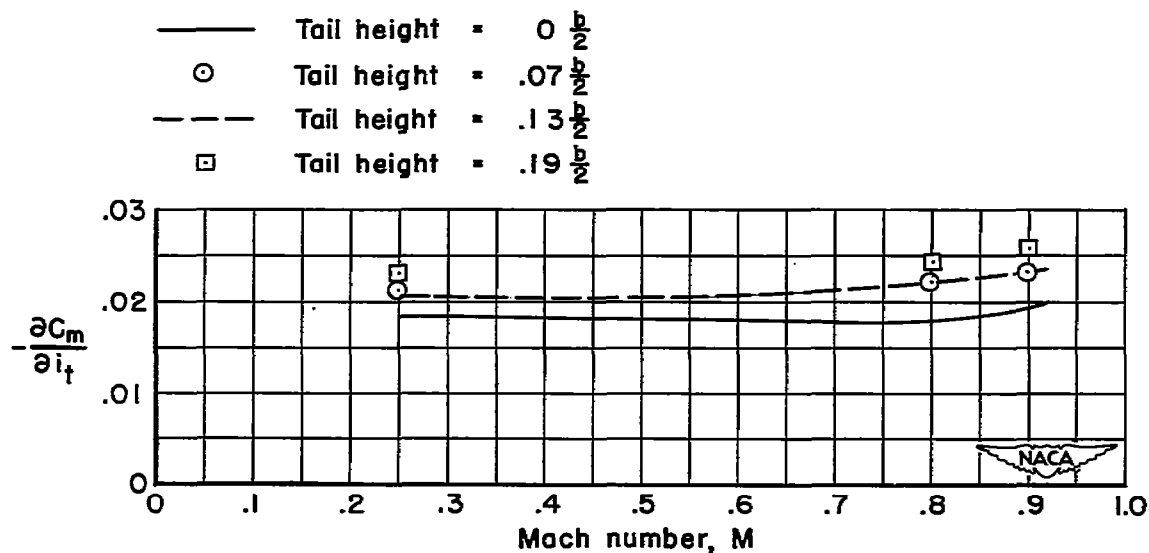


Figure 45.- The variation with Mach number of the control-effectiveness of the horizontal tail at several tail heights on the 40° combination; $\alpha = 4^\circ$; $R = 2,000,000$.

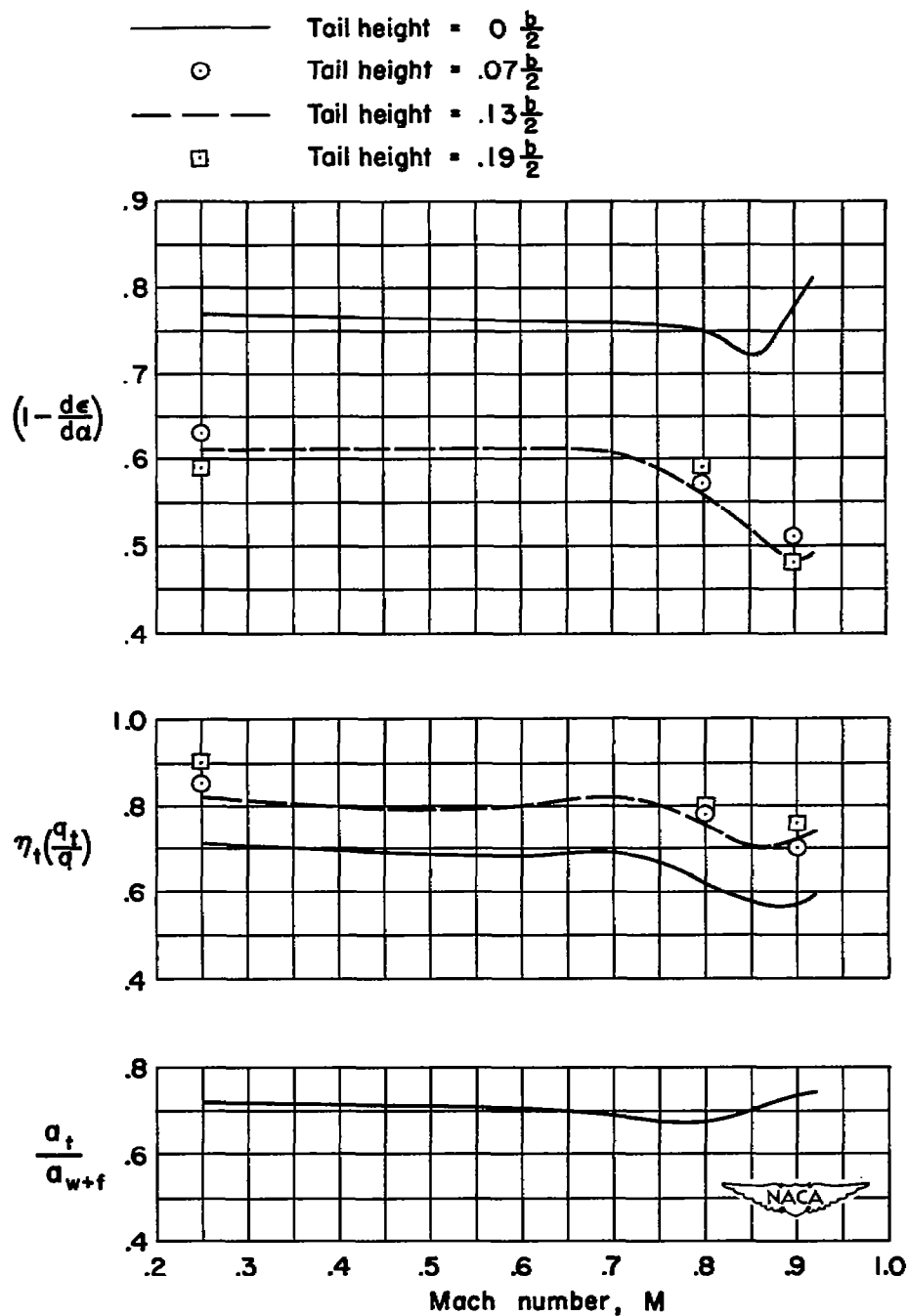


Figure 46.- The variation with Mach number of the factors affecting the stability contribution of the horizontal tail at several tail heights on the 40° combination; $\alpha = 4^\circ$; $R = 2,000,000$.

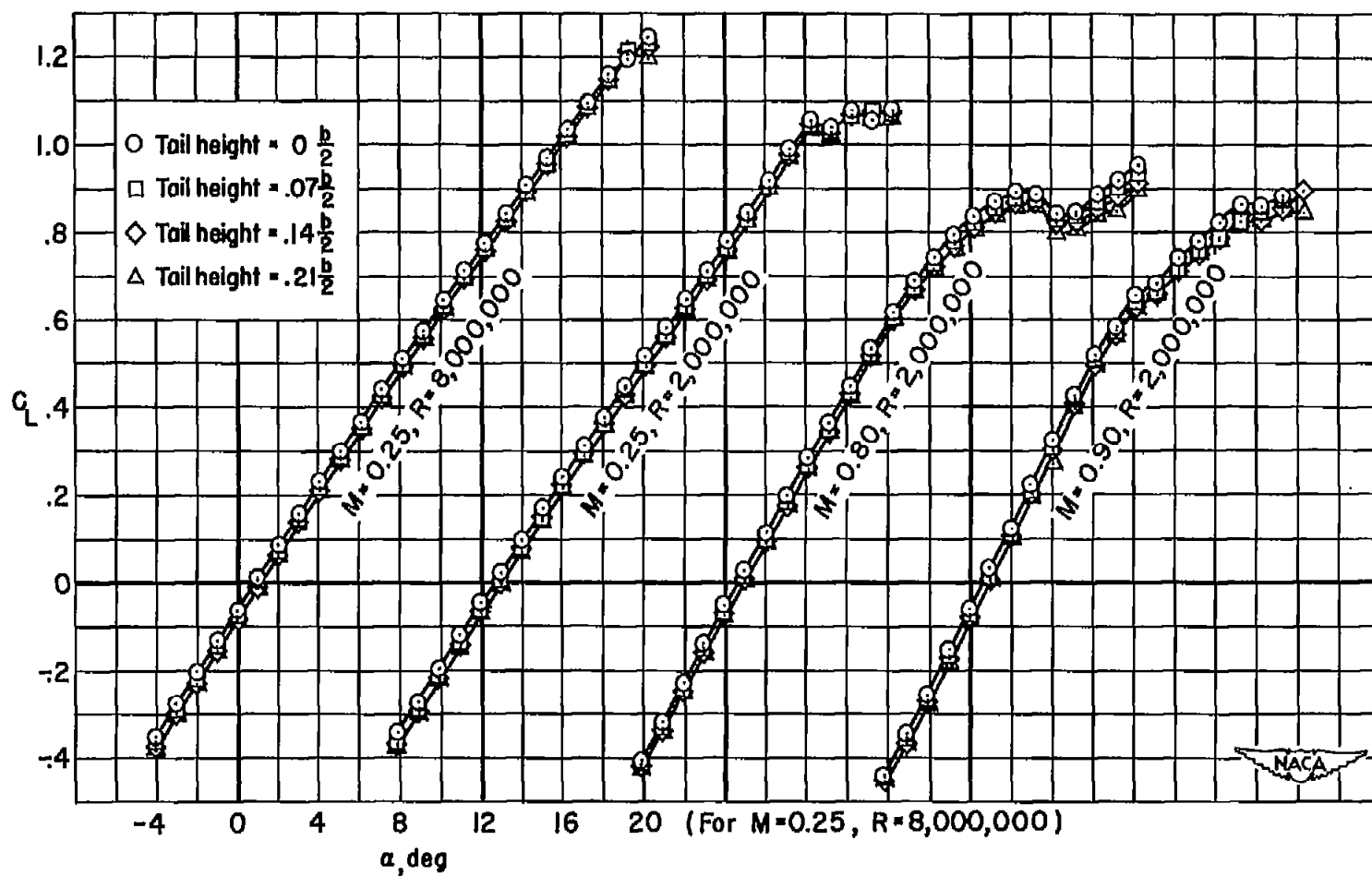
(a) $\Lambda = 45^\circ$

Figure 47.- The effect of tail height on the lift characteristics of the 45° and 50° combinations with fences; $i_t = -8^\circ$.

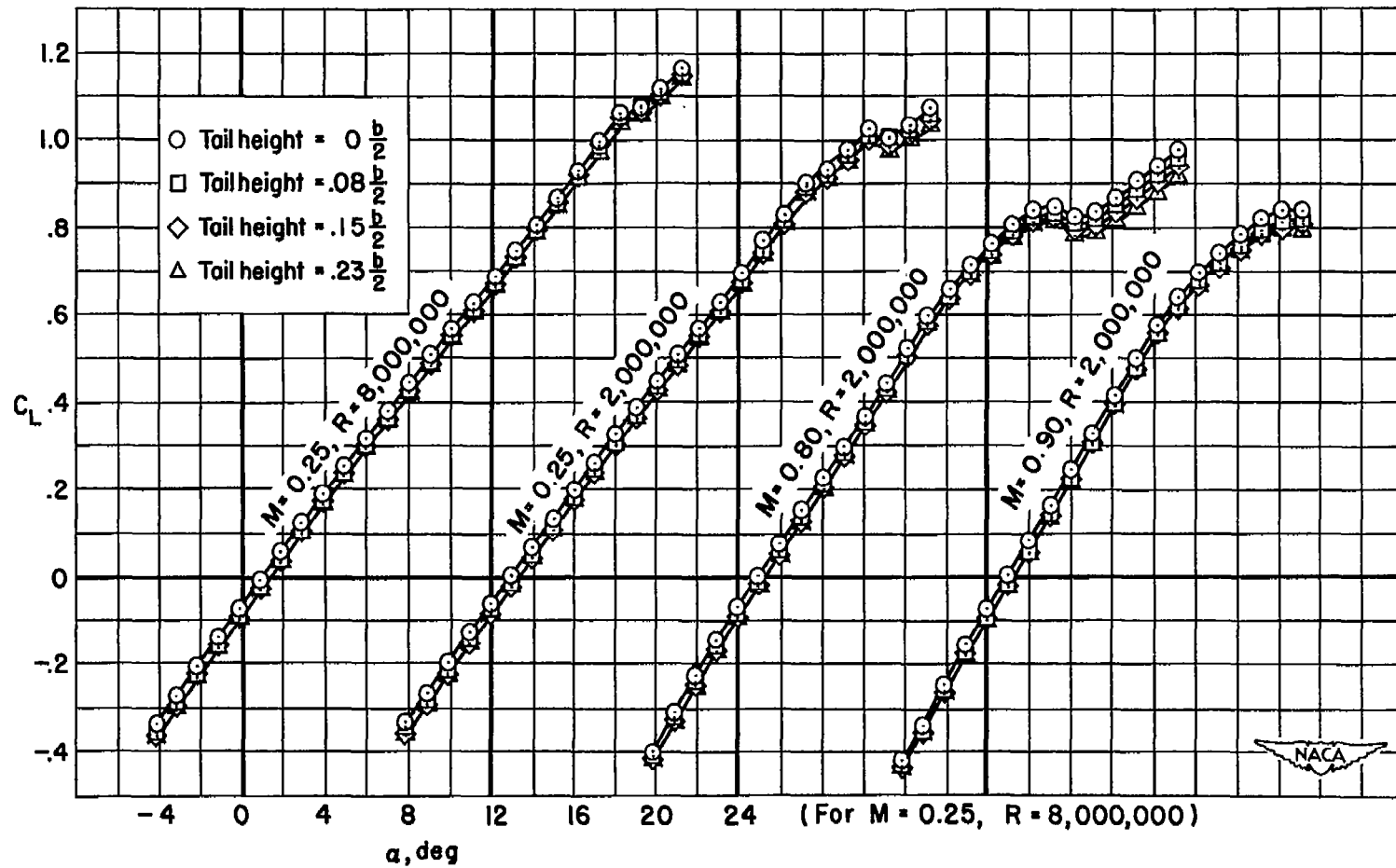
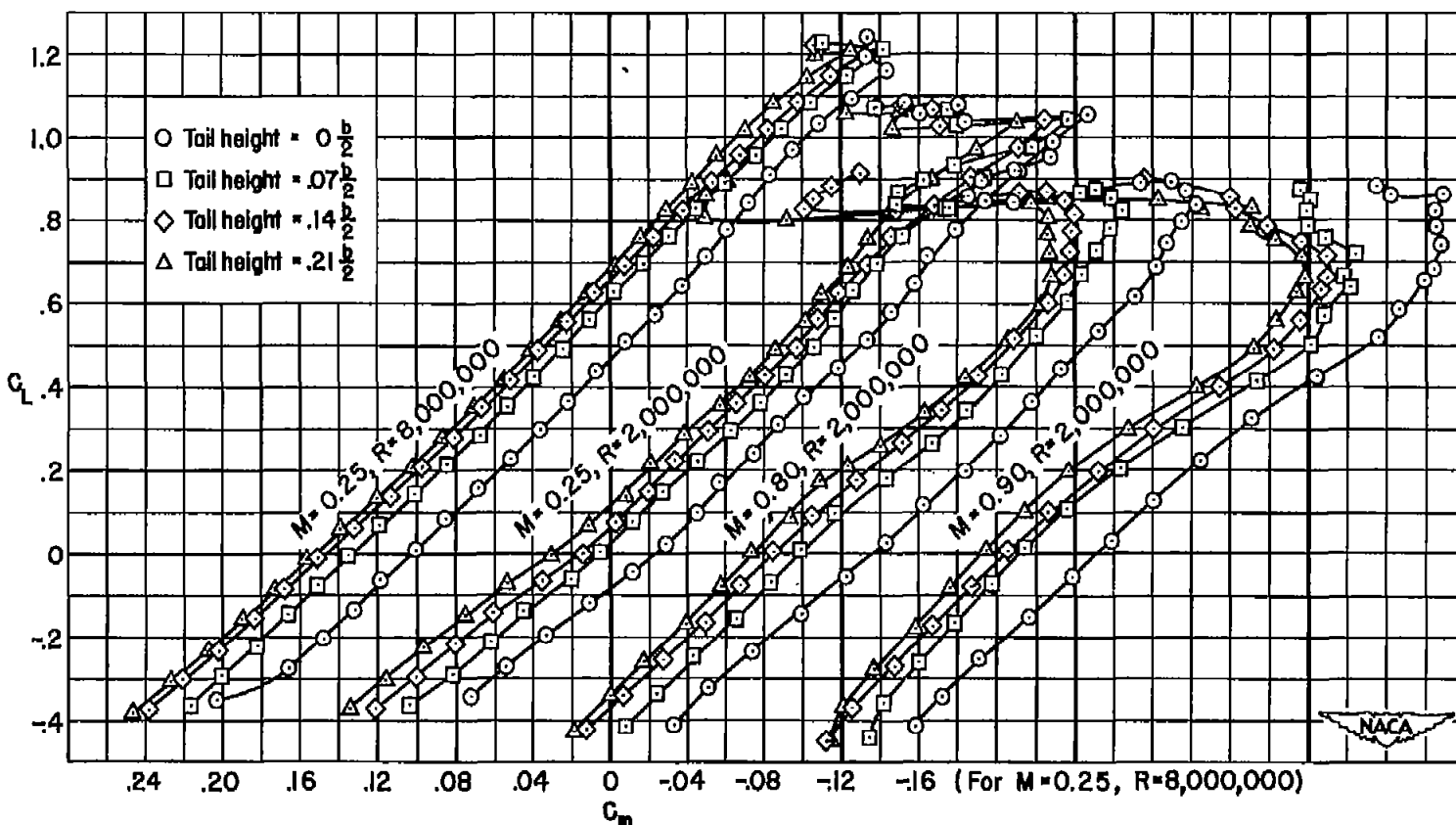
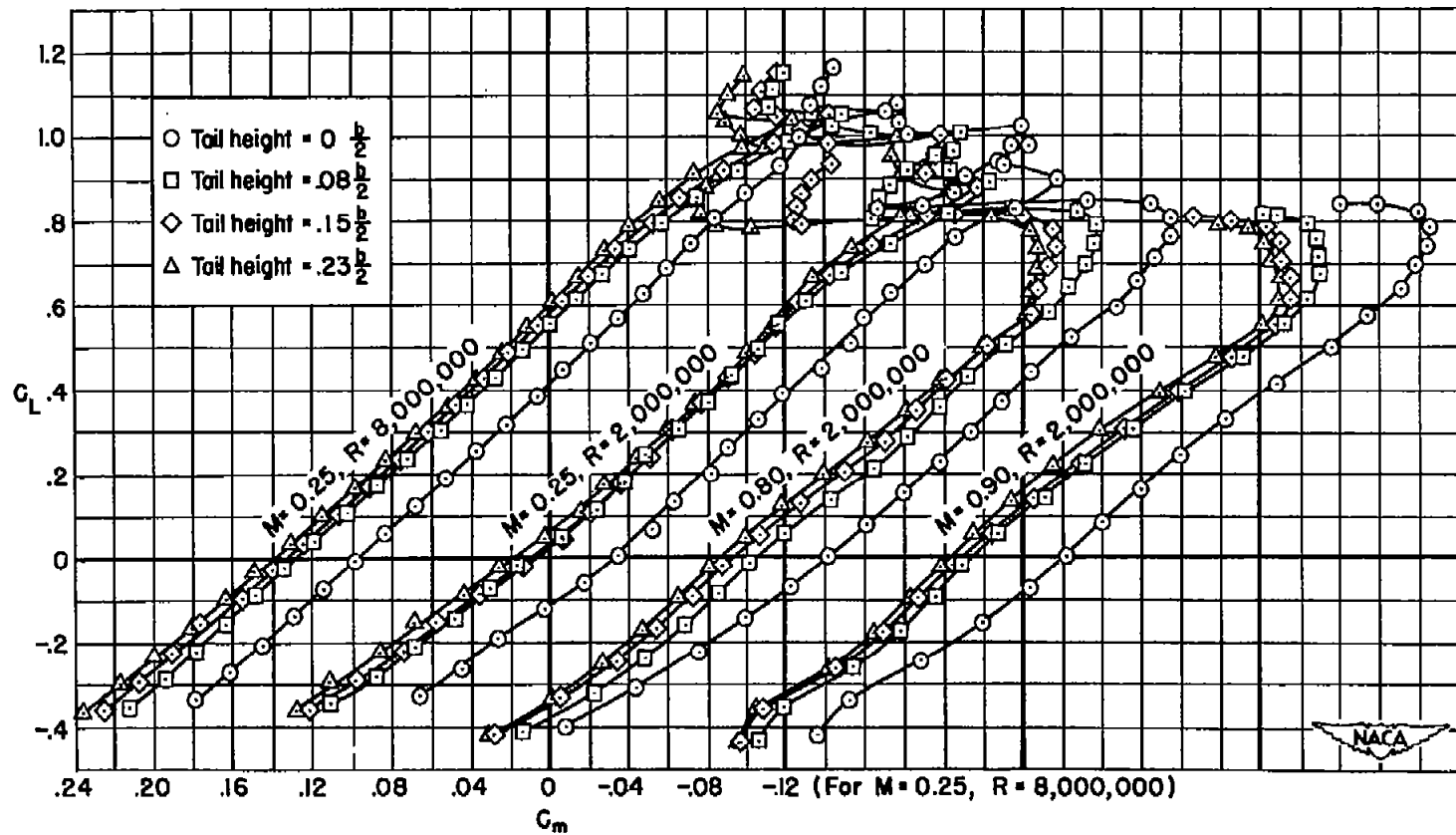
(b) $\Lambda = 50^\circ$

Figure 47.- Concluded.



(a) $\Lambda = 45^\circ$

Figure 48.- The effect of tail height on the pitching-moment characteristics of the 45° and 50° combinations with fences; $i_t = -8^\circ$.



(b) $\Lambda = 50^\circ$

Figure 48.- Concluded.

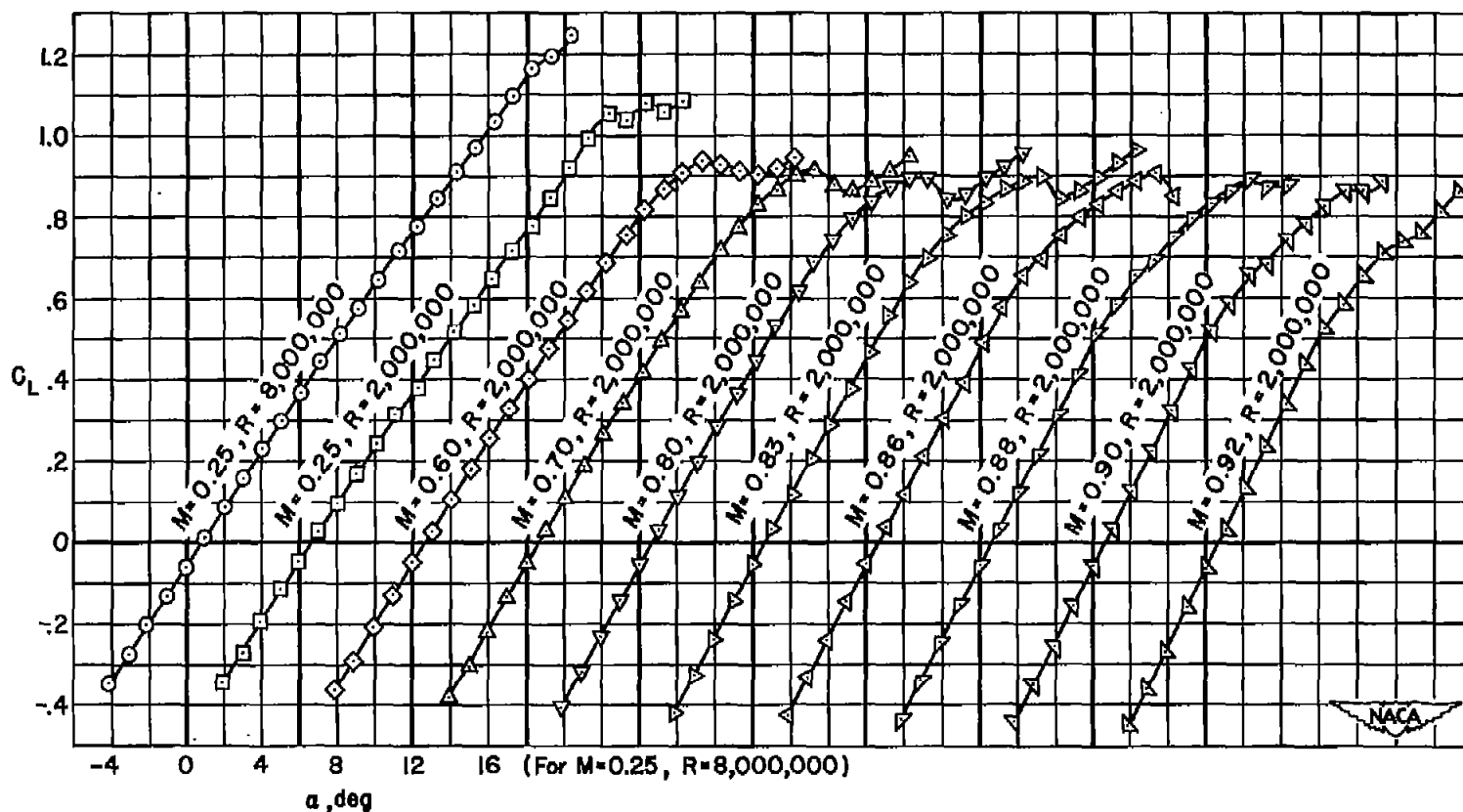
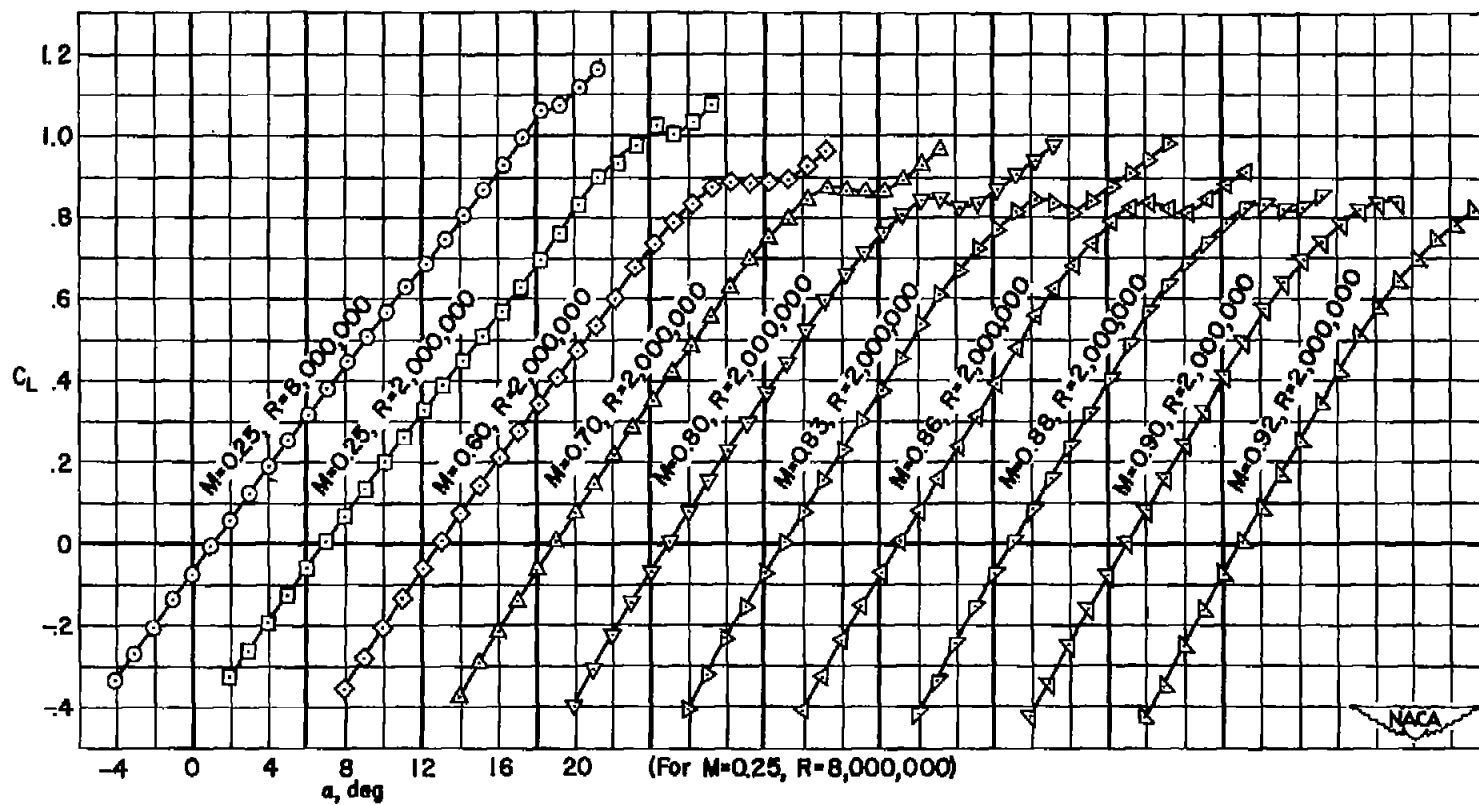
(a) $\Lambda = 45^\circ$

Figure 49.- The lift characteristics of the 45° and 50° combinations with fences and a horizontal tail; tail height = $0.5b/2$; $i_t = -8^\circ$.



(b) $\Lambda = 50^\circ$

Figure 49.- Concluded.

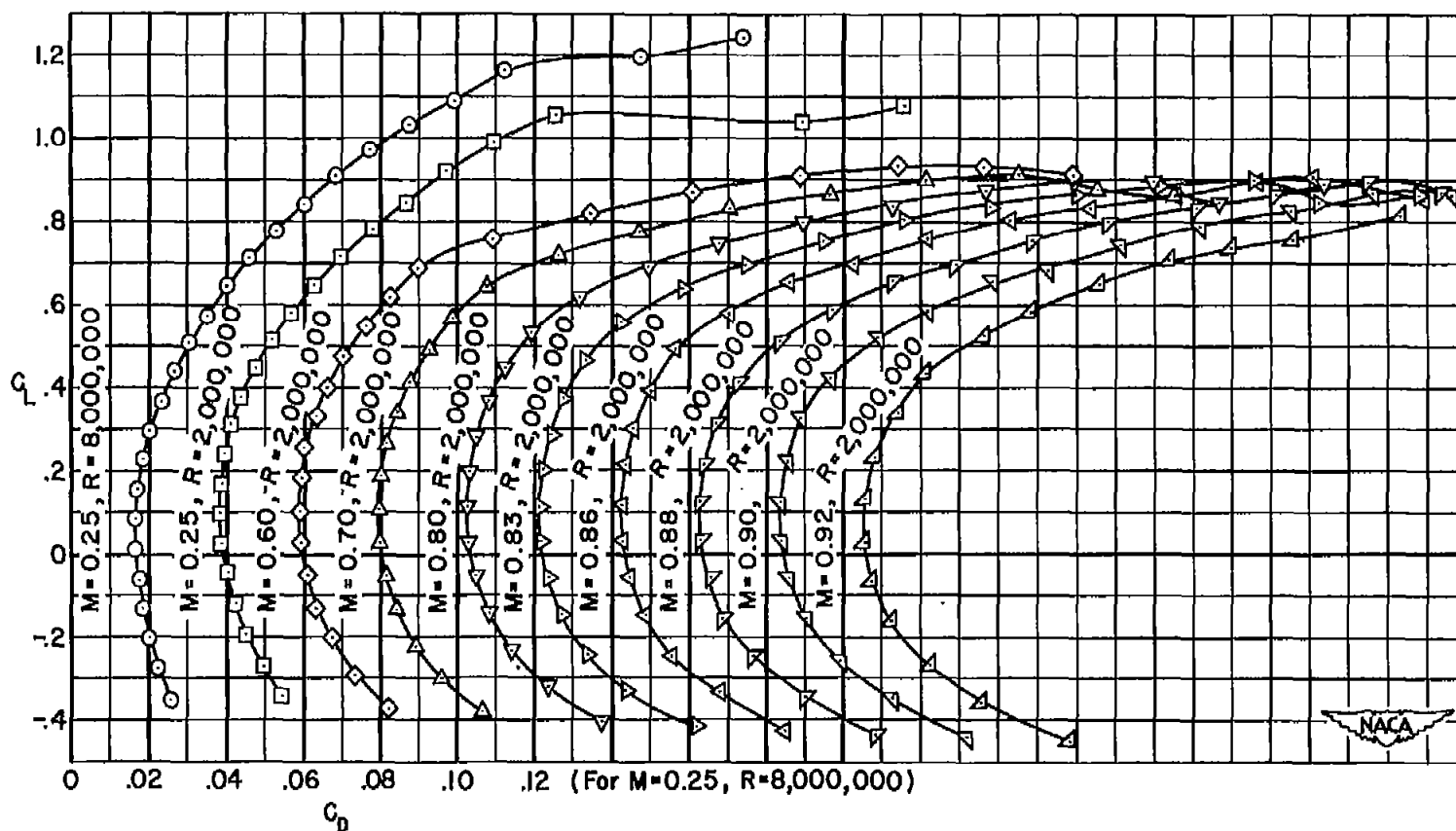
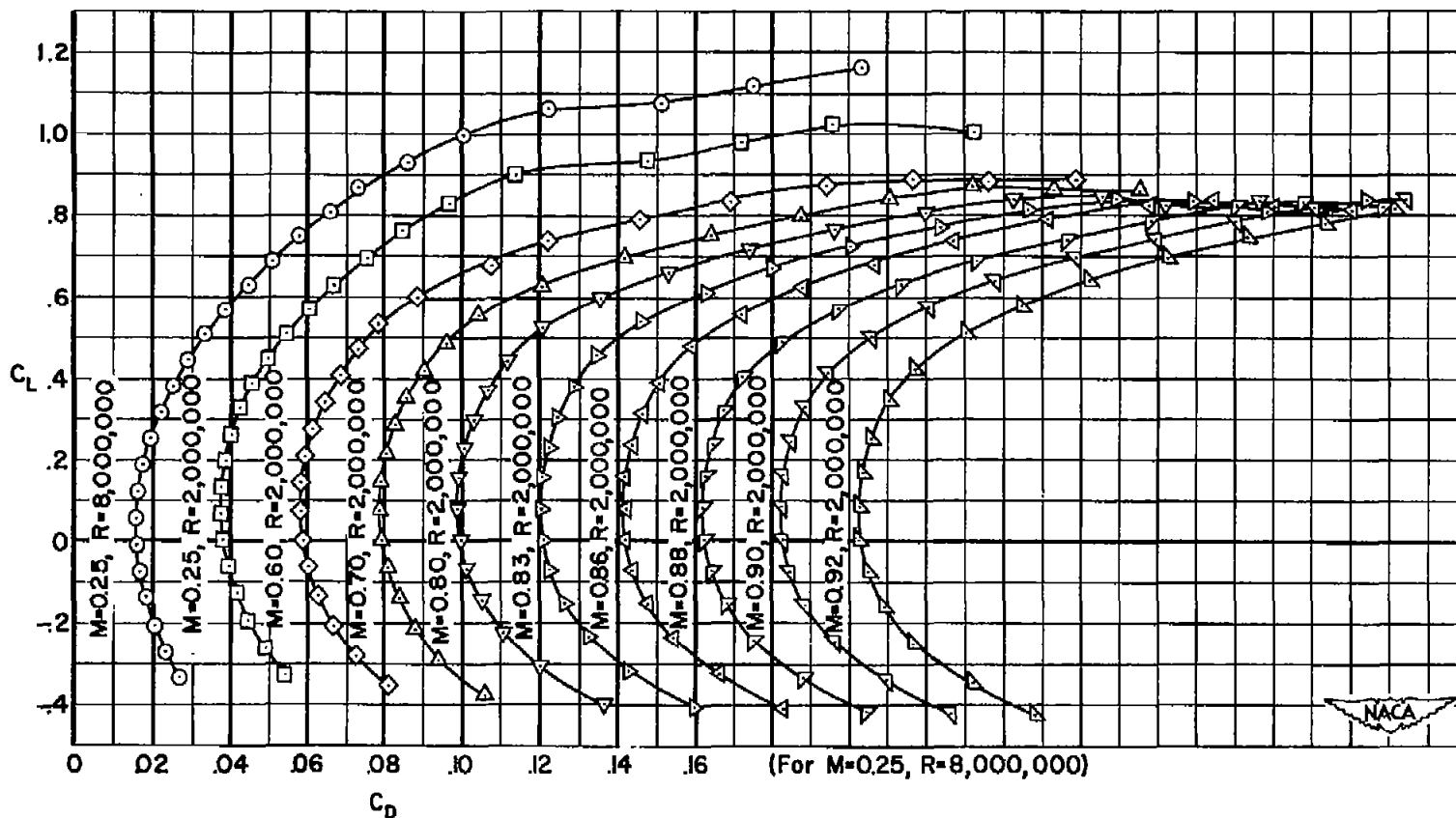
(a) $\Lambda = 45^\circ$

Figure 50.- The drag characteristics of the 45° and 50° combinations with fences and a horizontal tail; tail height = $0.5b/2$; $i_t = -8^\circ$.



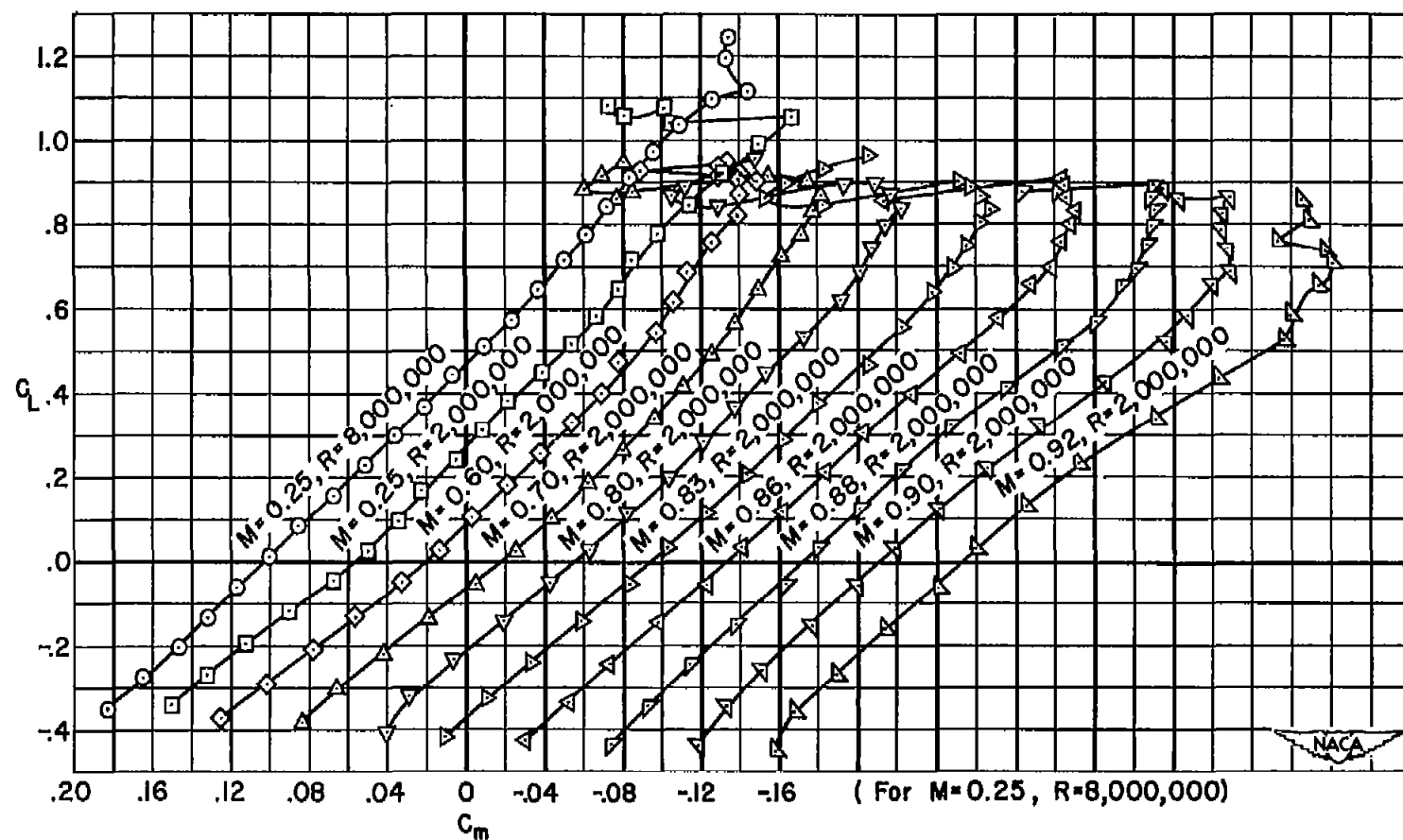
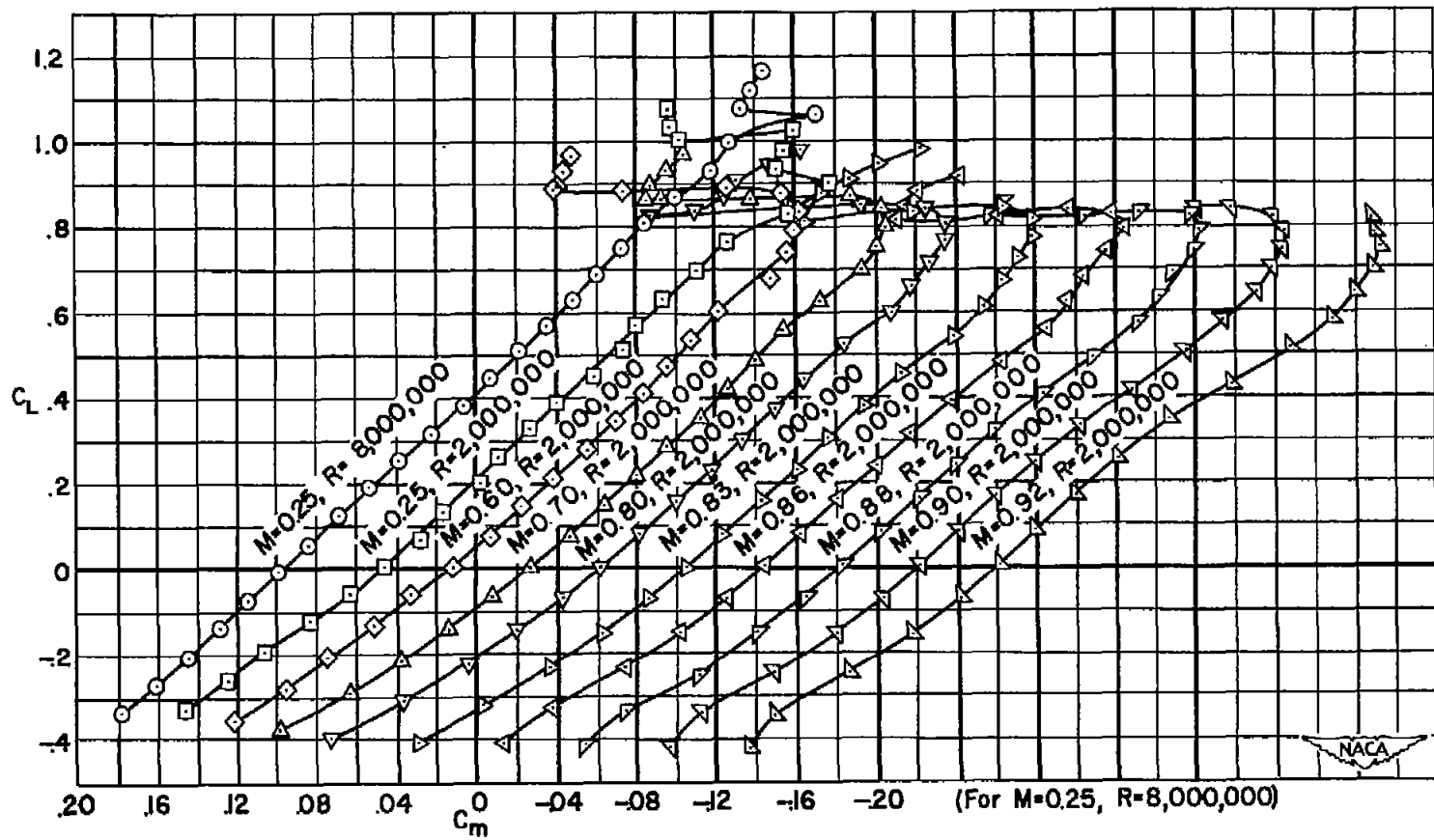
(a) $\Lambda = 45^\circ$

Figure 51.- The pitching-moment characteristics of the 45° and 50° combinations with fences and a horizontal tail; tail height = $0.5b$; $i_t = -8^\circ$.



(b) $\Lambda = 50^\circ$

Figure 51.- Concluded.